UNIVERSIDADE ESTADUAL DE CAMPINAS
INSTITUTO DE BIOLOGIA

BRUNA OLIVEIRA E CARVALHO

ANÁLISE DAS CAPACIDADES CITOADESIVAS DE *Plasmodium vivax* DE PACIENTES DA AMAZÔNIA BRASILEIRA

Tese apresentada ao Instituto de Biologia da Universidade Estadual de Campinas visando à obtenção do título de Doutor em Genética e Biologia Molecular

Orientador: Fabio Trindade Maranhão Costa

CAMPINAS, 2010

FICHA CATALOGRÁFICA ELABORADA PELA
BIBLIOTECA DO INSTITUTO DE BIOLOGIA – UNICAMP

C253a

Carvalho, Bruna Oliveira
Análise das capacidades citoadesivas de *Plasmodium vivax* de pacientes da Amazônia brasileira / Bruna Oliveira e Carvalho. – Campinas, SP: [s.n.], 2010.

Orientador: Fabio Trindade Maranhão Costa.
Tese (doutorado) – Universidade Estadual de Campinas, Instituto de Biologia.

1. Malária. 2. *Plasmodium vivax*. 3. Aderência celular. 4. Endotélio. I. Costa, Fabio Trindade Maranhão, 1972-. II. Universidade Estadual de Campinas. Instituto de Biologia. III. Título.

(rcdt/ib)

Título em inglês: Evaluation of cytoadhesive capacities of *Plasmodium vivax* from Brazilian Amazon patients.
Palavras-chave em inglês: Malaria; *Plasmodium vivax*; Cell adhesion; Endothelium.
Área de concentração: Imunologia.
Titulação: Doutora em Genética e Biologia Molecular.
Banca examinadora: Fabio Trindade Maranhão Costa, Cláudio Chrysostomo Werneck, Cláudio Romero Farias Marinho, Sabrina Epiphanio, Selma Giorgio.
Data da defesa: 28/05/2010.
Programa de Pós-Graduação: Genética e Biologia Molecular.

BANCA EXAMINADORA

Prof. Dr. Fabio Trindade Maranhão Costa

(Orientador)

Prof. Dr. Claudio Chrysostomo Werneck

Prof. Dr. Claudio Romero Farias Marinho

Profa. Dra. Irene da Silva Soares

Profa. Dra. Leonilda M. Barbosa dos Santos

Prof. Dr. Marcelo Brocchi

Profa. Dra. Sabrina Epiphanio

Profa. Dra. Selma Giorgio

DECLARAÇÃO

Declaro para os devidos fins que o conteúdo de minha tese de Doutorado intitulada "Análise das Capacidades Citoadesivas de *Plasmodium vivax* de pacientes da Amazônia Brasileira"

( ) não se enquadra no § 3º do Artigo 1º da Informação CCPG 01/08, referente a bioética e biossegurança.

(X) tem autorização da seguinte Comissão de Bioética ou Biossegurança*:
"Comitê de Ética em Pesquisa em Seres Humanos/ Fundação de Medicina Tropical do Amazonas- Manaus", sob Protocolo nº **2758/08**.

** Caso a Comissão seja externa à UNICAMP, anexar o comprovante de autorização dada ao trabalho. Se a autorização não tiver sido dada diretamente ao trabalho de tese ou dissertação, deverá ser anexado também um comprovante do vínculo do trabalho do aluno com o que constar no documento de autorização apresentado.*

Aluna: Bruna Oliveira e Carvalho

Orientador: Fabio Trindade Maranhão Costa

Para uso da Comissão ou Comitê pertinente:
(X) Deferido ( ) Indeferido

Nome: *Profa. Dra. Carmen Silvia Bertuzzo*
Função: Vice-Presidente do
Comitê de Ética em Pesquisa
FCM/UNICAMP
Matrícula: 28856-6

Fundação de Medicina Tropical do Amazonas
Comitê de Ética em Pesquisa em Seres Humanos
Av. Pedro Teixeira, 25 – Dom Pedro
Cep: 69040-000
Manaus – Amazonas - Brasil

CEP
COMITE DE ETICA EM PESQUISA
EM SERES HUMANOS

APROVAÇAO Nº 1943

Registro CEP Nº 2758-08

CAAE – 0054.1.114.000-08 **Processo: 2758/2008-FMT-AM**

Projeto de Pesquisa: Caracterização Clinica da Malária Complicada por Plasmodium vivax
Pesquisador responsável: Marcus Vinicius G. Lacerda
Instituição Sediadora: FMT-AM
Instituição Vinculada: Não se aplica
Área Temática Especial: Pesquisa com cooperação estrangeira
Patrocinador: Centre de Recerca de Salut Internacional de Barcelona
Registro para armaz. de mat. Biológico humano: Não se aplica

Ao se proceder à análise relativo do Projeto em questão, o Comitê de Ética em Pesquisa em Seres Humanos (CEP) da Fundação de Medicina Tropical do Amazonas (FMT-AM), em sessão ordinária do dia 10 de Novembro de 2008 e de acordo com as atribuições definidas na Resolução CNS 196/96, manifesta-se pela aprovação do projeto de pesquisa proposto, bem como o Termo de Consentimento Livre e Esclarecido.

Situação do Protocolo: Como se trata de área especial "Cooperação Estrangeira" item VIII. 5-IX.5 da resolução MS 196/96, o projeto será enviado à CONEP-Comissão Nacional de Ética em Pesquisa que dará aprovação final.

Manaus, 10 de Novembro de 2008.

NÃO CONTÉM RASURA

Luiz Carlos de Lima Ferreira
Coordenador de Ética em Pesquisa
FMT-AM

Obs: Cabe ao pesquisador elaborar e apresentar ao CEP, os relatórios parciais e final sobre a pesquisa (Resolução do Conselho Nacional de Saúde nº196, de 10.10.1996, inciso IX.2, letra "c") conforme o Formulário de acompanhamento dos Projetos aprovados no CEP, disponível em nossa home Page.

TERMO DE CONSENTIMENTO LIVRE E ESCLARECIDO

Você está sendo convidado para participar da pesquisa de **Caracterização da Malária Grave por *Plasmodium vivax* na Fundação de Medicina Tropical do Amazonas, Brasil.** Você foi selecionado por ter sido visitado ou estar internado na FMT-AM, hospital de referência para o tratamento da malária em Manaus. A qualquer momento você pode desistir de participar e retirar seu consentimento. Sua recusa não trará nenhum prejuízo em sua relação com o pesquisador ou com a instituição. O acompanhamento da sua doença e tratamento continuará sendo realizado independentemente de você estar na pesquisa ou não. Você será retirado do estudo caso você deixe de seguir as orientações para a participação no estudo.

A Cidade de Manaus apresenta, anualmente, um grande número de pessoas acometidas com malária vivax, sendo que parte destas pessoas necessitam de tratamento em ambiente hospitalar por apresentarem algumas complicações decorrentes da malária e/ou do seu tratamento. Para nos ajudar a entender melhor isto, a fim de estabelecer a melhor forma de controle e tratamento, nós estamos convidando você a considerar a participação neste estudo. Precisamos do maior número possível de pessoas.

Trata-se de um estudo observacional sobre malária vivax em pacientes internados na unidade hospitalar da FMT-AM e terá duração de ***24 meses***. Você não precisa fazer qualquer coisa especial para participar desse projeto e receberá o mesmo tratamento e acompanhamento estabelecido de acordo com as normas do Ministério da Saúde.

Como parte do estudo, nós vamos estabelecer um sistema de monitoramento para malária durante sua internação até o momento em que você puder receber alta hospitalar. Quando você for internado, nós coletaremos além de várias informações clínicas, uma amostra de sangue (10 ml) através de uma agulha (venopunção) para fazer o teste de malária (gota espessa) e outros exames laboratoriais. Em alguns casos usaremos apenas o sangue coletado do dedo para avaliar a infecção pela malária, sem que o paciente esteja internado ou se submeta a outros exames.

Nós gostaríamos de sua permissão para fazer testes com as parasitas de malária nas amostras de sangue coletadas e para guardar o restante do sangue para ser usado em estudos sobre malária no futuro. Isto pode exigir o armazenamento mais prolongado de seu sangue em laboratórios da FMT-AM. Para isso, seu sangue será guardado com um código e não deverá identificar seu nome.

Além do exame para malária, o sangue será analisado em nossos laboratórios para entendermos as alterações ocorridas em outros órgãos e sistemas durante o tratamento da malária. A sua participação também nos ajudará a avaliar quantas pessoas acometidas de malária vivax necessitam de internação hospitalar.

Você pode sentir alguma dor por causa da picada no dedo ou pela coleta de amostra de sangue na veia do braço. Mas qualquer dor deve durar apenas alguns instantes. Existe um risco muito pequeno de infecção onde o sangue for coletado, mas qualquer infecção será monitorada e tratada pela equipe médica. A amostra de sangue colhida é muito pequena e não representa nenhum risco à sua saúde.

O benefício em estar participando deste estudo será um aumento de informações sobre malária vivax e seus riscos na nossa cidade, mas você não será pago nem receberá incentivo financeiro durante o acompanhamento.

Se você concordar em participar, todas as informações coletadas serão confidenciais, usadas somente no estudo. Nós não compartilharemos suas informações, e um código será usado para identificar você em vez de seu nome. Nós não tornaremos público qualquer detalhe sobre você. No caso de algum pesquisador tirar uma foto sua, ele cuidará para que você não seja identificado. Esta imagem sua será publicada apenas em revistas para médicos.

Pessoas para contato

Se você tiver qualquer pergunta ou preocupação sobre o estudo, por favor, vamos esclarecer isso agora. Mesmo assim, se depois você desejar esclarecer suas dúvidas sobre a pesquisa ou sobre ser um sujeito de pesquisa, por favor, sinta-se à vontade para contatar ***Dr. Marcus Vinícius Guimarães de Lacerda,*** pesquisador principal do projeto na ***Fundação de Medicina Tropical do Amazonas.*** O endereço do hospital é **Av. Pedro Teixeira, nº 25, Dom Pedro** e o número do telefone é (92) 3656 0620. *O endereço do Comitê de Ética em Pesquisa da FMT-AM (que é um grupo de pessoas que avaliam este projeto e acompanham a pesquisa) é também na Av. Pedro Teixeira, n° 25, Bairro Dom Pedro, e o telefone para contato é o (92) 2127 3432. O presidente deste comitê é o Dr. Luiz Carlos de Lima Ferreira.*

Eu, Flávia Raquel Ramos Batista, participante desse estudo ou responsável pelo paciente Flávia Alexandra Batista Rocha, entendi todas as informações dadas a mim sobre o estudo **Caracterização da Malária Grave por *Plasmodium vivax* na Fundação de Medicina Tropical do Amazonas, Brasil**, inclusive o seu propósito e a forma como será executado. Eu tive a chance de fazer perguntas sobre o estudo e concordo em participar do mesmo.

Elania Raquel R. Batista
Assinatura do participante ou responsável
ou impressão do polegar direito

Data 23/09/09

Maila C. Alves Rojas
Nome do entrevistador

Assinatura do entrevistador

Data 23/09/09

MARCUS V. G. LACERDA
Nome do pesquisador responsável

Assinatura do pesquisador responsável

Data 23/4/9

Versão final: 16 de Julho de 2008
Emenda 1: 30 de Março de 2009

Trabalho realizado com apoio da

Fundação de Amparo à Pesquisa do Estado de São Paulo

Aos meus pais, Ana e Beto, e irmão, Égas,

responsáveis por minha sólida formação

e que, com carinho e dedicação, me prepararam para a vida;

Ao Bruno,

pelo amor

e pelo privilégio de caminharmos juntos em situações diversas

e adversas.

A eles, dedico esta tese.

AGRADECIMENTOS

Ao Prof. Dr. Fabio Trindade Maranhão Costa, pela orientação e por tudo que me ensinou. E ao amigo Fabio, agradeço principalmente a compreensão.

Aos membros da banca examinadora, pela atenção e pelas correções.

Às companheiras (e amigas!) do laboratório em Campinas: Stefanie, Juliana e Yara, por tanta coisa... Pela inestimável ajuda na realização dos experimentos, meus sinceros agradecimentos e reconhecimento. Pelos almoços no bandejão, pelas conversas no banquinho do IB, pelas discussões filosóficas, enfim, sou grata pela amizade.

Às (a meu ver) recém chegadas colegas do laboratório em Campinas, Carol e Marcele, com as quais não tive tanto tempo de convivência, mas que sempre me foram muito prestativas e amigas.

Aos colegas do laboratório em Manaus, principalmente à Leidiane, amiga e confidente, e ao André, exemplo de pessoa e pesquisador, obrigada pelas agradáveis companhias madrugada afora, seja no laboratório mal assombrado ou em qualquer outro lugar.

Aos amigos Dr. Paulo Nogueira e Dra. Patrícia Orlandi, por me abrirem as portas não só do laboratório da Fiocruz em Manaus, mas também de sua casa. Pelas conversas e pelo muito que aprendi.

À Dra. Joycenea Matsuda, pela imensa atenção a mim dedicada.

Ao Dr. Marcus Vinícius Lacerda, que me abriu as portas da Fundação de Medicina Tropical do Amazonas, em Manaus.

Ao Dr.Gerhard Wunderlich, pelo apoio fundamental.

A colegas como Tatiana Amabile, Carla Claser e Uta Goelnitz, pela paciência e por tudo que me ensinaram.

A todos os participantes do Seminário Laveran & Deane no ano de 2007, pelas sugestões, críticas, pelo ambiente de debate científico tão estimulante e que tanto me acrescentou.

Mais uma vez ao Seminário Laveran & Deane, que me trouxe amizades inesperadas e indescritíveis, como a da Fernanda e da Bianca.

Aos amigos de perto, de longe, de infância ou quase virtuais, em especial à Alê e à Mari Lazarini, pelo carinho, companheirismo e por tantos momentos inesquecíveis. À Mari Stanton, minha "filha" da Biologia, pela convivência e por me abrir tanto a mente. À Lyvia, amiga desde a barriga e companheira de casa em Campinas, pela serenidade (essencial) e pelos 27 anos de convivência.

E à Unicamp, por momentos tão felizes.

Lista de Abreviaturas

ARDS	Síndrome do Desconforto Respiratório Agudo
CD36	*Cluster* de Diferenciação 36
CHO	Células de Ovário de Hamster Chinês
CSA	Condroitina-Sulfato-A
CSB	Condroitina-Sulfato-B
DAPI	4',6-Diamidino-2-Phenylindole
DDT	Dicloro-Difenil-Tricloroetano
DTT	Dithiothreitol
ECGS	Suplemento para Crescimento de Células Endoteliais
EI	Eritrócitos Infectados
FITC	Fluoresceína Isothiocianato
GST	Glutationa S-Transferase
HLEC	Células Endoteliais de Pulmão Humano
ICAM-1	Molécula de Adesão Intercelular -1
IFA	Ensaio de Imunofluorescência Indireta
MAb	Anticorpo Monoclonal
MSP-1	Proteína 1 da Superfície do Merozoíta
OMS	Organização Mundial de Saúde
PfEMP-1	Proteína 1 da Membrana do Eritrócito Infectado por *P. falciparum*
Pf-EI	Eritrócitos Infectados por *Plasmodium falciparum*
Pv-EI	Eritrócitos Infectados por *Plasmodium vivax*
SBEC	Células Endoteliais de Cérebro de Macaco *Saimiri*
SIVEP	Sistema de Informação em Vigilância Epidemiológica

Resumo

Malária vivax foi por muito tempo considerada uma infecção benigna, porém, complicações frequentes nas infecções por *P. falciparum*, como a malária cerebral, síndrome respiratória aguda (ARDS), disfunção hepática, trombocitopenia grave e baixo peso ao nascer devido à infecção placentária, também têm sido observadas em pacientes infectados por *P. vivax.* Na malária falciparum, estes sintomas estão associados à adesão de eritrócitos infectados por *P. falciparum* (Pf-IE) que se ligam a diversos receptores do hospedeiro, incluindo CD36, ICAM-1 e CSA. No entanto, não há evidência direta do seqüestro de eritrócitos infectados por *P. vivax* (Pv-IE) e uma possível capacidade citoadesiva permanecia por ser demonstrada. Pv-IE coletados de pacientes da Amazônia brasileira foram enriquecidos por gradiente de *Percoll* ® e a capacidade de citoadesão parasitária foi testada em um grupo de células que expressam receptores endoteliais sabidamente envolvidos na citoadesão de *P. falciparum*, em condições estáticas e em um sistema que mimetiza o fluxo sanguíneo. Mostramos que Pv-IE citoaderem sob condições estáticas e de fluxo, embora em níveis cerca de 10 vezes inferiores aos observado para *P. falciparum*. Demonstramos ainda que a citoadesão de *P. vivax* pode ser mediada por membros da família VIR, proteínas expressas na superfície de eritrócitos infectados e codificadas por uma superfamília de genes variantes (vir). Estes dados abrem perspectivas para uma melhor compreensão do fenômeno patológico relacionado com a malária vivax grave incluindo a descoberta de ligantes parasitários e receptores do hospedeiro.

ABSTRACT

Vivax malaria has been considered for a long time a benign infection; however severe complications, as observed in *P. falciparum*, such as cerebral malaria, acute respiratory distress syndrome (ARDS), liver dysfunction, severe thrombocytopenia and low birth weight due placental infection have also been reported worldwide for *P. vivax*-infected patients. In falciparum malaria, these symptoms are associated to sequestration of *P. falciparum*-infected erythrocytes (Pf-IE) that bind to several host receptors, including CD36, ICAM-1 and CSA. Nonetheless, direct evidence of *P. vivax*-infected erythrocytes (Pv-IE) sequestration is missing and binding analyzes of this species is lacking. Pv-IE obtained from patients in the Brazilian Amazon were enriched by *Percoll*® gradient and parasite adherence was tested to a panel of cells expressing endothelial receptors known to mediate cytoadhesion of *P. falciparum*, in static and flow conditions. Here we show that mature Pv-IE cytoadhere both under static and flow conditions, albeit at levels about 10-fold lower than those observed for *P. falciparum*. We further demonstrate that cytoadhesion by *P. vivax* was in part mediated by members of the VIR family, parasite-derived proteins expressed at the infected erythrocyte surface and encoded by a superfamily of variant genes (*vir*). These data open perspectives for a better understanding of the pathological phenomenon related to severe *P. vivax* malaria, including the discovery of novel parasite ligand(s) and host receptor(s).

SUMÁRIO

ANEXOS

Introdução

A Malária, infecção por protozoários do gênero *Plasmodium*, continua sendo a principal doença parasitária do mundo e afeta mais de 100 países em regiões tropicais e subtropicais. Segundo a Organização Mundial de Saúde (OMS), metade da população mundial vive em áreas de exposição à infecção malárica, com 300 a 500 milhões de casos diagnosticados todos os anos e aproximadamente 1,7 a 2,5 milhões de mortes. Segundo dados do Sistema de Informação de Vigilância Epidemiológica (SIVEP), vinculado ao Ministério da Saúde, o Brasil apresenta cerca de 500 mil infecções anuais, 80% delas causadas pelo *Plasmodium vivax.* Foi constatado que 36% dos casos reportados nas Américas referem-se à Região da Amazônia Legal, principalmente nos estados do Amazonas, Rondônia e Pará.

Acreditava-se que quatro espécies eram responsáveis pelas infecções em humanos: *Plasmodium falciparum*, *Plasmodium vivax*, *Plasmodium malariae* e *Plasmodium ovale*. No entanto, foi demonstrado recentemente que o *Plasmodium knowlesi,* antes considerado um parasita de primatas não humanos, também pode causar infecções naturais em humanos (Singh *et al*., 2004). As espécies responsáveis pela grande maioria dos casos de malaria no mundo são *P. vivax* e *P. falciparum*. As infecções por *P. falciparum* concentram-se principalmente na África Subsaariana, enquanto que o *P. vivax* é uma espécie globalmente distribuída.

O ciclo de vida é essencialmente o mesmo em todas as espécies do gênero. Como mostrado na Figura 1, a infecção do hospedeiro vertebrado inicia-se com a picada do mosquito do gênero *Anopheles* infectado, inoculação de esporozoítos que penetram ativamente na derme e em vasos sanguíneos (Amino *et al*., 2006) e migram, principalmente através da corrente sanguínea, para o fígado, invadem hepatócitos onde se reproduzem assexuadamente (fase hepática). Novas formas do parasita livre, denominados merozoítos, são então liberadas, inicialmente em vesículas (merossomos) e posteriormente atingem a corrente sanguínea (Thiberge *et al.*, 2007). Nesta etapa do ciclo

(fase eritrocítica), os merozoítos livres invadem ativamente os eritrócitos, onde se desenvolvem para formas conhecidas como “anéis” ou trofozoítos jovens. Estas formas amadurecem e então se reproduzem por esquizogonia, sendo tal estágio conhecido como esquizonte, culminando com o rompimento do eritrócito e liberação de novos merozoítos na corrente sanguínea (Figuras 2 e 3). O sintoma clássico da malária é a febre intensa e intermitente, que ocorre a cada 48h, coincidindo com a ruptura dos eritrócitos infectados e liberação dos merozoítos. Alguns trofozoítos diferenciam-se em gametócitos femininos ou masculinos, que darão continuidade ao ciclo no hospedeiro invertebrado.

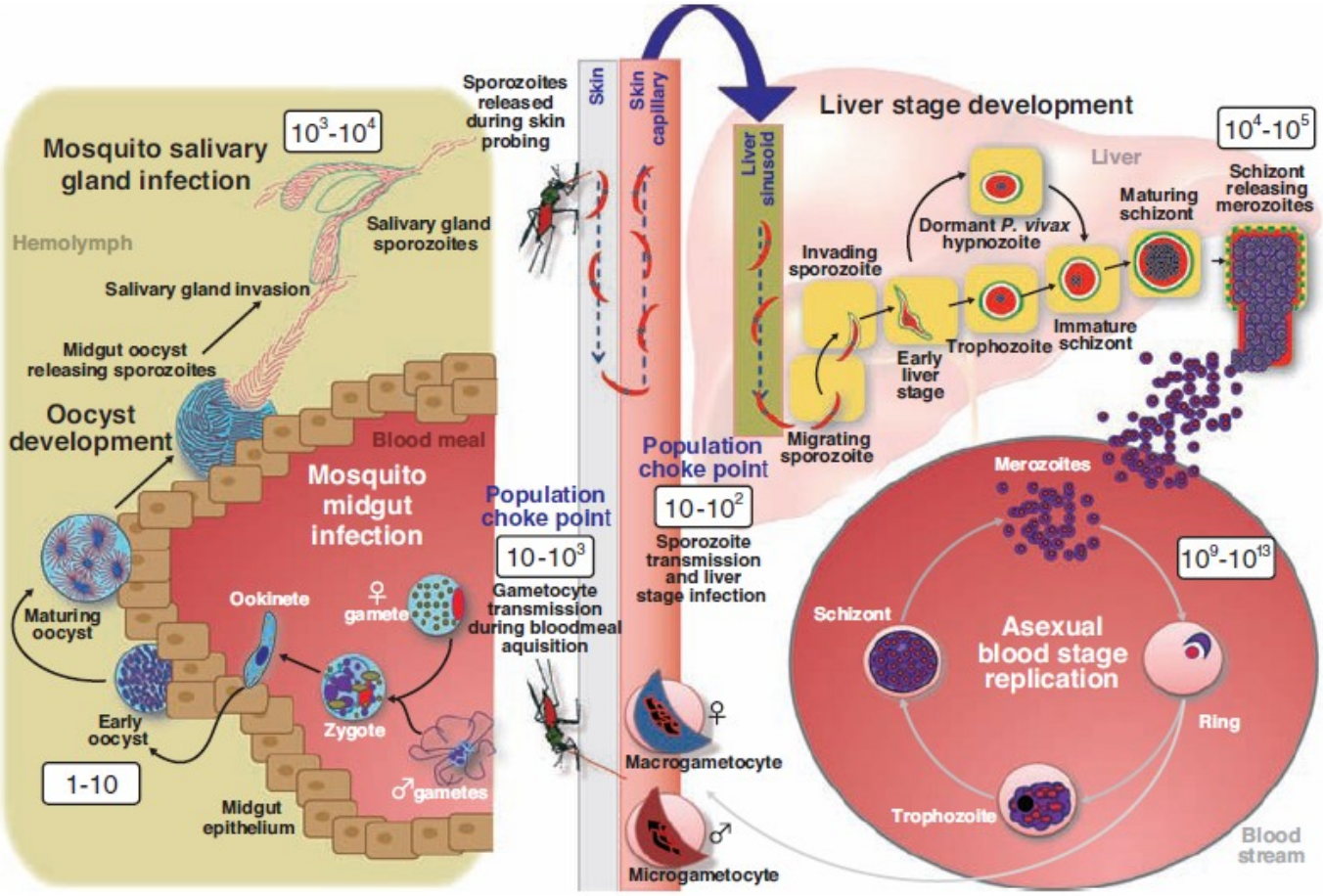

Figura 1. Ciclo de vida *Plasmodium* spp. Os números mostrados indicam o tamanho da população de parasitas durante a progressão do ciclo de vida. Fonte: Kappe *et al.* Science, 2010.

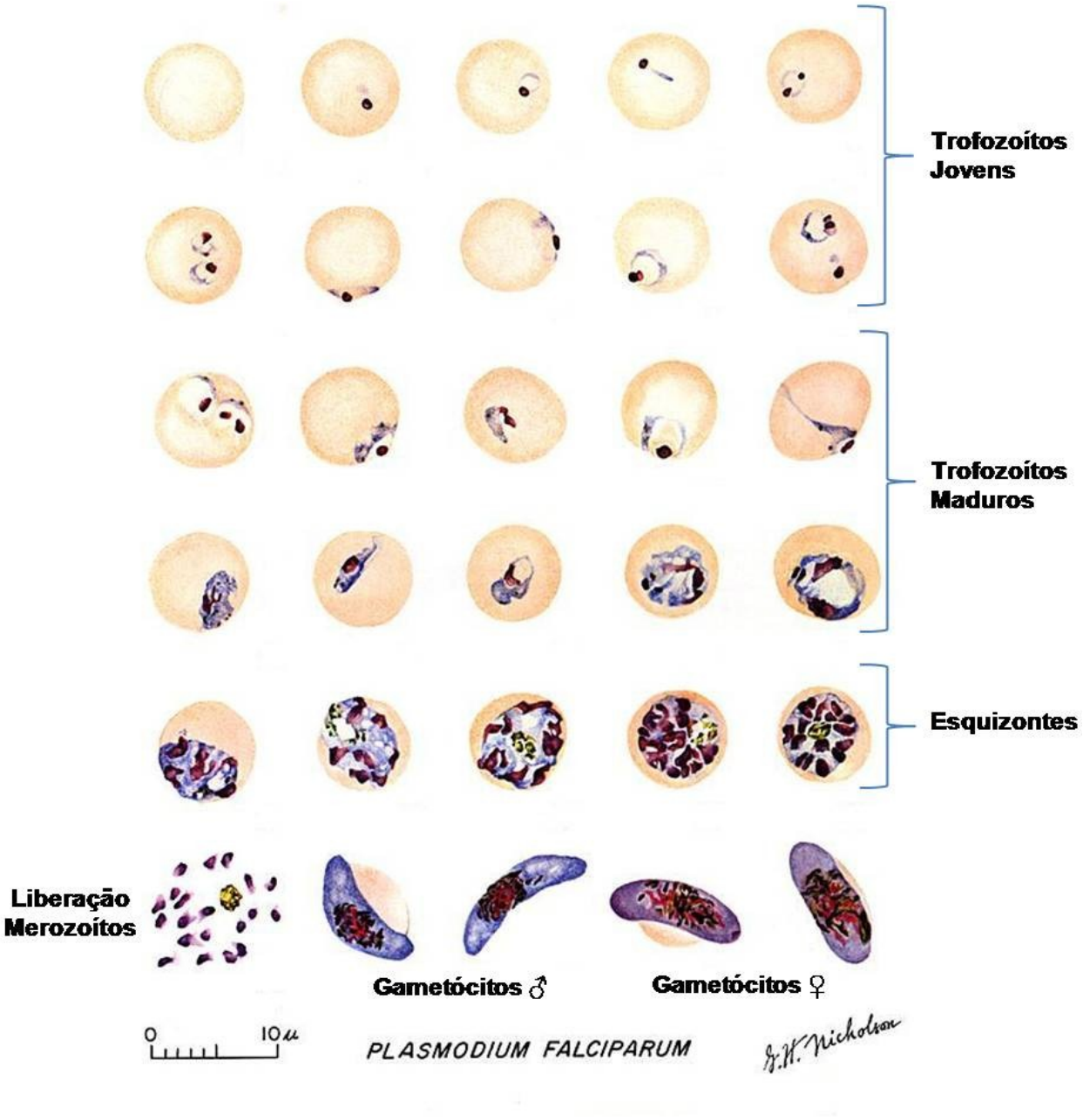

Figura 2. Desenvolvimento intra-eritrocítico *P. falciparum*. Fonte: *The Primate Malarias*. Bethesda: U.S. Department of Health, Education and Welfare; 1971. Autores: Coatney GR, Collins WE, Warren M, Contacos PG.

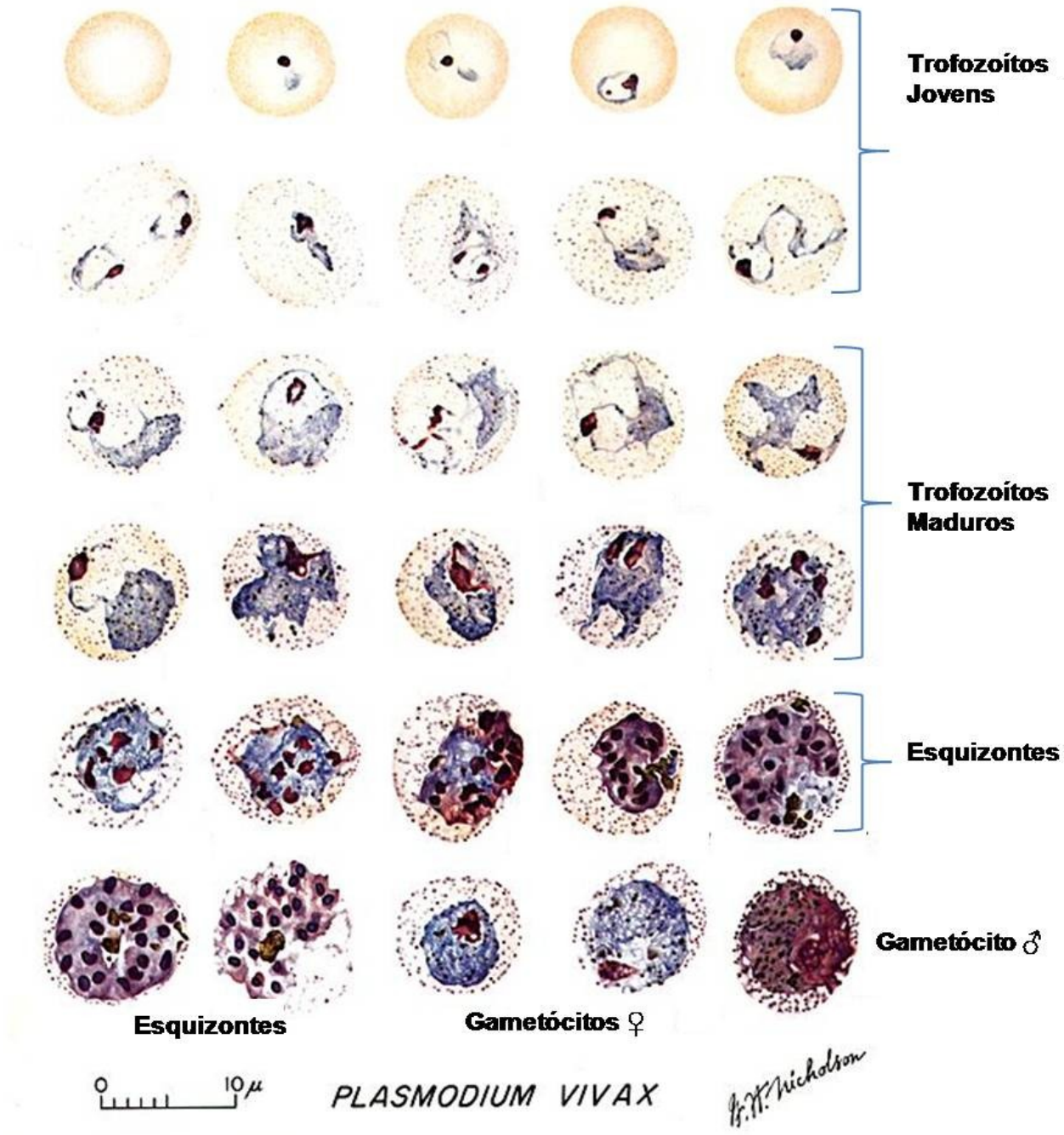

Figura 3. Desenvolvimento intra-eritrocítico *P. vivax*. Fonte: *The Primate Malarias*. Bethesda: U.S. Department of Health, Education and Welfare; 1971. Autores: Coatney GR, Collins WE, Warren M, Contacos PG.

Durante décadas a malária vem sendo alvo de campanhas de erradicação da transmissão por meio de inseticidas e quimioterapia. As estratégias de controle empregadas principalmente durante a década de 50 reduziram a distribuição global da doença, mas não foram plenamente eficazes devido a diversos fatores, dentre eles fenômenos de resistência às drogas convencionalmente utilizadas (Wernsdorfer & Payne, 1991) e a inexistência de uma vacina eficaz. A redução drástica da eficácia de drogas como cloroquina, primaquina e pirimetamina contra infecções maláricas, têm sido reportadas em várias áreas há algumas décadas, contribuindo para o agravamento dos sinais clínicos (Le Bras & Durand, 2003). Cabe ressaltar que, como evidenciado na Figura 4, a prevalência da malária está nitidamente associada a um baixo desenvolvimento socioeconômico, sendo um problema de dimensão político-social.

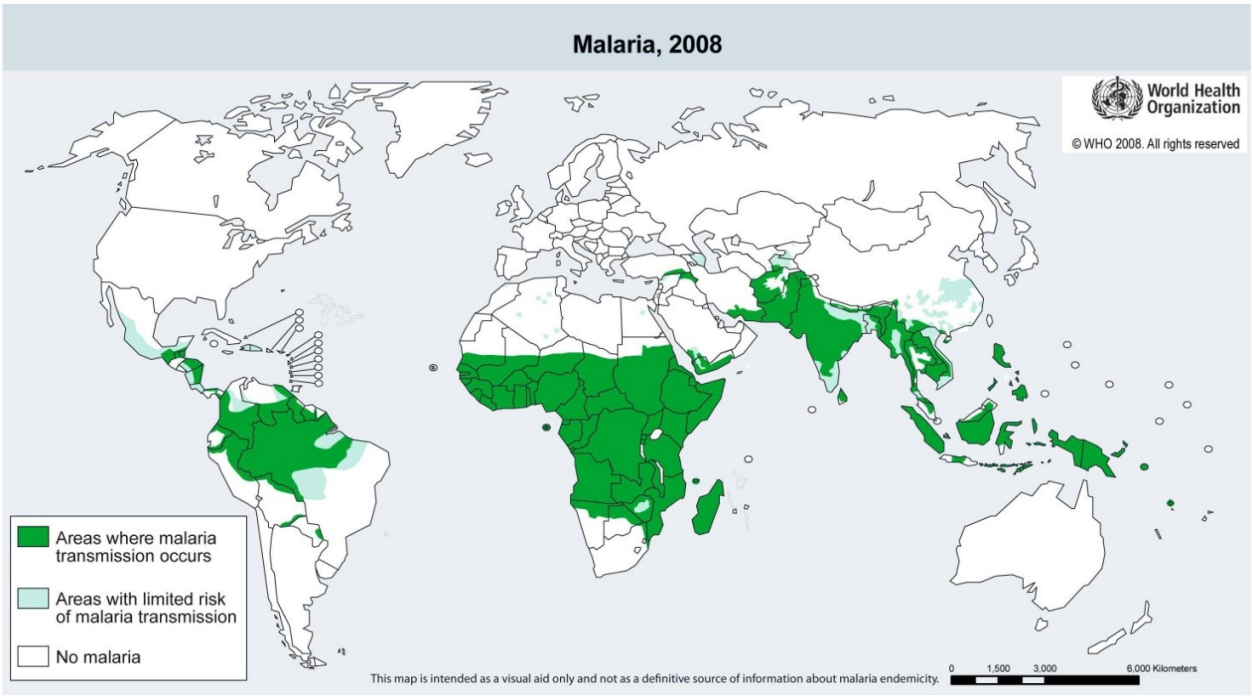

Figura 4. Distribuição global da malária. Fonte: Organização Mundial de Saúde, 2008.

A OMS recomenda fortemente que o tratamento antimalárico seja administrado através de um coquetel de drogas que, agindo sinergicamente, buscam a redução da doença e previnem o aparecimento da resistência. Ainda, apesar de a Artemisinina ser o único medicamento contra o qual não houve relatos de resistência, Jambou e colaboradores, em 2005, mostraram que parasitas cultivados *in vitro* foram capazes de apresentar resistência também contra esse composto. Sendo assim, a luta pelo controle da malária pode entrar em uma fase ainda mais complicada e, por isso, o desenvolvimento de novas drogas e de vacinas eficientes contra malária é prioridade para OMS.

A emergência da resistência tem contribuído para a ressurgência global da malária (Marsh, 1998). Mas além do aumento do número de casos, tem sido relatado um aparente aumento das complicações decorrentes da infecção malárica em diferentes regiões do mundo. Neste sentido, foi mostrado que a resistência à cloroquina parece estar associada com taxas mais elevadas de reprodução de *P. falciparum* e *P. vivax* (Chotivanich *et al*., 2000). Como este fenótipo foi associado com malária falciparum grave, maiores taxas de crescimento em *P. vivax* resistentes à cloroquina podem similarmente contribuir para o surgimento de complicações clínicas (Russell *et al.*, 2008). Porém, no caso da malária vivax, antes considerada “malária benigna”, não se sabe o quanto o aumento das complicações é causado por uma mudança na prevalência de fenótipos parasitários, ou se estes casos eram simplesmente ignorados. De fato, a disseminação de fenótipos resistentes e o aparente aumento das complicações decorrentes de infecções por *P. falciparum* como por *P. vivax* são hoje um desafio para a saúde pública mundial.

Evolução e Virulência

O objetivo principal dos programas de controle da malária é inibir o desenvolvimento do parasita, com administração de drogas que agem pontualmente sobre determinada característica parasitária. O sucesso de tais programas depende do quão essencial essa característica é para o parasita; e também está ligado com a forma de interação parasita-hospedeiro. Porém, tais programas acabam fazendo mais do que apenas reduzir doenças. Do ponto de vista evolutivo, as intervenções medicamentosas, assim como outras tentativas de controle, são efetivas formas de pressão seletiva, direcionando o processo evolutivo parasitário e causando drásticas mudanças fenotípicas na população do parasita. A pressão seletiva causada pela interferência humana impacta consideravelmente as populações de organismos com curto ciclo de vida, como os parasitas unicelulares e até mesmo o vetor invertebrado. Em um curto prazo, são direcionadas mudanças significativas e preocupantes em populações de diversos organismos. A título de exemplo, o uso indiscriminado do DDT (Dicloro-Difenil-Tricloroetano) favoreceu a prevalência de insetos resistentes (Greenwood *et al.*, 2005). No caso específico da malária, a constante pressão ocasionada pelo uso inadequado das drogas combinada com o curto ciclo de vida do parasita possibilitam a rápida seleção de fenótipos resistentes (Daily, 2006).

Ainda, não podemos deixar de pensar nas co-infecções ou mesmo nas interações entre diferentes populações de uma mesma espécie, como os casos de infecção por múltiplos clones de *P. vivax,* que são comumente detectados em áreas com diferentes índices de transmissão da malária. Um estudo recente sugere que quando dois ou mais clones, geneticamente distintos, infectam o mesmo hospedeiro, ocorre uma limitação de recursos capaz de direcionar a seleção de fenótipos de *P. vivax* com maior virulência, transmissibilidade e resistência medicamentosa (Havryliuk & Ferreira, 2009).

Em relação ao processo evolutivo parasitário, o aumento da taxa de transmissão é o principal benefício atribuído a uma maior virulência: por extrair mais recursos do hospedeiro, o parasita é capaz de gerar mais formas transmissíveis por unidade de tempo. Assim, a dificuldade do hospedeiro em efetuar o *clearance* parasitário, com o consequente aumento da duração da infecção, possibilita uma maior taxa de transmissão. Relação positiva entre a taxa de transmissão e virulência foi demonstrada para tripanosomas murinos (Turner *et al.*, 1995), assim como na malária murina (Mackinnon & Read, 1999; Ferguson *et al*., 2003). No entanto, o custo da virulência é a morte prematura do hospedeiro, encurtando a duração da infecção. É válido ressaltar que a virulência é resultado da interação entre parasita, hospedeiro e fatores ambientais, embora geralmente empreguemos tal termo como característica exclusiva do parasita.

A intervenção humana, assim como a competição intra ou interespecífica podem ser explicações para o aparente aumento da virulência e das complicações clínicas decorrentes da infecção malárica. No entanto, ainda pouco se discute sobre as eventuais consequências evolutivas e epidemiológicas dessas diferentes formas de pressão seletiva.

Citoaderência Parasitária e Manifestações Clínicas Graves

No caso do Gênero *Plasmodium*, um fenômeno relacionado à virulência e bastante descrito é a "citoaderência", que está fortemente associada às manifestações clínicas graves da malária (MacPherson *et al.* 1985; Treutiger *et al.* 1992; Ringwald *et al.* 1993; Rowe *et al.* 1995; Newbold *et al.* 1999; Kun *et al.* 1998; Roberts *et al.* 2000; Pain *et al.* 2001). O fenômeno da citoaderência refere-se a um grupo de mecanismos pelos quais eritrócitos infectados se ligam a receptores de diferentes células do hospedeiro, através de antígenos parasitários expressos na superfície do eritrócito. Podemos diferenciar três tipos de citoaderência observados no gênero *Plasmodium*: a formação de rosetas, que é a capacidade de eritrócitos infectados aderirem a outros não infectados; autoaglutinação, ou adesão entre eritrócitos infectados; e a capacidade de aderir diretamente ao endotélio, fenômeno denominado sequestração. Quando o parasita da malária invade o eritrócito, a célula hospedeira sofre modificações (Aikawa, 1988), o baço, por sua vez, reconhece eritrócitos anormais e os remove de circulação juntamente com o parasita intracelular (Wyler, 1983). Acredita-se que a adesão de eritrócitos infectados nos microcapilares impeça a destruição no baço. Entende-se ainda que, além de diminuir a destruição do parasita pelo sistema imunológico do hospedeiro, a citoaderência também possa aumentar a taxa de reinvasão de eritrócitos, impactando positivamente na densidade populacional parasitária. Neste sentido, várias hipóteses têm sido propostas há algum tempo: rosetas e sequestração aumentam o contato entre eritrócitos não infectados e os recém liberados merozoítas, aumentando a eficiência de reinvasão (Handunetti *et al*. 1989; Wahlgren *et al*. 1989); o sequestro pode garantir um ambiente mais favorável à maturação parasitária (Ho & White 1999); rosetas protegem as células infectadas de opsonização e fagocitose (revisto por Anders & Brown 1990).

Diversos estudos utilizando modelos animais indicam que antígenos parasitários relacionados à citoadesão têm expressão reduzida em animais esplenectomizados,

sugerindo que, na ausência do baço, a expressão torna-se onerosa para o parasita; mas é mantida em animais com o baço intacto, devido à vantagem que esses antígenos garantem (Hommel *et al*. 1983, David *et al*. 1983; Barnwell *et al*. 1983; Langreth & Peterson 1985; Handunetti *et al*. 1987; Gilks *et al*. 1990).

A ausência do baço, por outro lado, inviabiliza uma resposta imune adequada. A infecção aguda desencadeada seria, por sua vez, inviável para a transmissibilidade do parasita, devido às altas taxas de mortalidade. Do mesmo modo, os mecanismos de escape parasitário, embora garantam maiores taxas de reprodução, são regulados negativamente pelo aumento da virulência. Firma-se então um equilíbrio, entre capacidade de manutenção da infecção crônica e significativas taxas de transmissão.

No caso do *P. falciparum*, de cuja infecção decorrem altas taxas de parasitemia e mortalidade, é intrigante observar sua alta prevalência durante toda a história da humanidade. Algumas hipóteses sugerem que variações hematológicas humanas como a Anemia Falciforme e as Talassemias foram selecionadas na África e na região do Mar Mediterrâneo por garantirem proteção à malária, estabelecendo simultaneamente o equilíbrio necessário para a existência de um parasita altamente patogênico como o *P. falciparum* (Allison *et al.*, 1954).

Portanto, a citoaderência não parece ser um simples mecanismo de escape parasitário. O agravamento dos sintomas culminando com a morte do hospedeiro acaba representando um alto custo para a transmissibilidade da infecção. Ainda assim, fenômenos de citoaderência são comuns nas espécies de *Plasmodium*: a formação de rosetas é descrita na grande maioria das espécies estudadas (David *et al*., 1988; Handunetti *et al*., 1989; Udomsangpetch *et al*., 1991, 1995; Angus *et al*. 1996). A autoaglutinação foi descrita em *P. falciparum* (Roberts *et al*., 1992) e *P.knowlesi* (Knisely *et al*., 1941). Dentre as espécies de plasmódios que infectam o homem, a sequestração foi descrita apenas para *P. falciparum*, embora mecanismos semelhantes estejam

descritos para espécies que têm como hospedeiro outros vertebrados (Alger 1963; Miller 1969; Desowitz *et al*., 1969; Yoeli & Hargreaves, 1974; Cox *et al*., 1987; David *et al*., 1988; Gilks *et al*., 1990; Kaul *et al.*, 1994; Coquelin *et al.*, 1999; Mota *et al*., 2000; Neres *et al*., 2008). Ainda, acredita-se que gametócitos imaturos de *P. falciparum* são capazes de aderir ao endotélio vascular, voltando a circular apenas quando estão maduros (Thomson & Robertson, 1935; Smalley *et al*., 1980).

Em casos graves de infecções por *P. falciparum,* as complicações clínicas estão fortemente associadas ao sequestro de eritrócitos infectados na microvasculatura de diversos órgãos. De fato, formas maduras de eritrócitos infectados pelo *Plasmodium falciparum* (Pf-EI) são capazes de aderir maciçamente a moléculas presentes na superfície endotelial, desaparecendo da circulação periférica (Pasloske & Howard, 1994). Acredita-se que as complicações clínicas da malária falciparum sejam decorrentes de processo multifatorial envolvendo o sequestro maciço de eritrócitos infectados nos endotélios vasculares e a produção de citocinas inflamatórias como TNF-α e IFN-γ, causando necrose tecidual e falência de diversos órgãos (revisto por Schofield & Grau, 2005). Entre as formas graves da doença estão a malária gestacional, malária cerebral, síndrome do desconforto respiratório agudo e anemia profunda. A malária gestacional representa um modelo imunologicamente interessante, por ser a placenta um órgão que surge já na idade adulta. É sabido que indivíduos de áreas onde a transmissão de *P. falciparum* é intensa, frequentemente desenvolvem imunidade à doença. Apesar desta imunidade adquirida, mulheres se tornam novamente susceptíveis à infecção malárica durante a primeira gravidez (Brabin *et al*., 1983). Isto ocorre devido à seleção, na placenta, de um fenótipo antigenicamente distinto (Fried & Duffy, 1996). Foi mostrado que a população de parasitas selecionada na placenta é capaz de aderir à condroitina-sulfato-A (CSA; Fried & Duffy, 1996), um glicosaminoglicano presente na matriz extracelular que pode ser parte constitutiva de vários proteoglicanos, como a trombomodulina.

Modificações na Membrana do Eritrócito e Alguns Mitos

A infecção do eritrócito por *P. falciparum* acarreta em modificações morfológicas e estruturais da membrana eritrocítica, com o aparecimento de protuberâncias elétron-densas denominadas *knobs*. Estas protuberâncias foram descritas como sendo os locais pelos quais os Pf-EI aderem a superfícies endoteliais (revisto por Sharma, 1991). Os *knobs* são constituídos por diversos polipeptídios, tais como a proteína de membrana 1 do eritrócito infectado por *P. falciparum* (PfEMP-1). Esta proteína é expressa a partir de 60 genes variáveis (*var*) por genoma haplóide do parasita. A porção extracelular da PfEMP-1 é composta por uma série de domínios *Duffy-Binding Like* (DBL), intercalados por domínios ricos em cisteínas (CIDR), ambos responsáveis pela citoaderência do parasita e alvos do sistema imune do hospedeiro (Smith *et al*., 2000). Devido à recombinação ectópica que ocorre entre regiões teloméricas que contém os genes *var,* o número de alelos é muito grande. Entretanto, apesar desta variabilidade, apenas uma variante antigênica é expressa na superfície dos Pf-EI de cada vez (Craig & Scherf, 2001). Isto possibilita um constante e eficiente escape da resposta imune antes que sejam formados novos anticorpos que revertam a citoadesão. Por este mecanismo, a PfEMP-1 é capaz de mediar uma ampla gama de interações adesivas a diversos receptores endoteliais, incluindo o CD36 (*Cluster of Differentiation 36*; Ockenhouse *et al.,* 1989), a ICAM-1 (*Inter-Cellular Adhesion Molecule 1*; Berendt *et al.,* 1989), e a CSA (*Chondroitin Sulfate A;* Robert *et al.,* 1995; Rogerson *et al*., 1995). Muitas das interações adesivas entre Pf-EI e receptores do hospedeiro têm sido investigados *in vitro* utilizando células endoteliais como as da veia umbilical humana (Udeinya *et al*., 1981; Udeinya *et al*., 1989), as células endoteliais do cérebro humano (Smith *et al*., 1992), células de melanoma C32 (Schmidt *et al*., 1982), células endoteliais de pulmão humano (Muanza *et al*., 1996), células endoteliais do cérebro de Saimiri (Gay *et al*., 1995), e células de ovário de hamster chinês (Rogerson *et al*., 1995). Estes modelos para citoadesão *in vitro* são rotineiramente

empregadas para melhor compreender as interações parasita-hospedeiro e avaliar fenótipos adesivos de isolados clínicos.

A infecção por *P. vivax* também leva a modificações estruturais na membrana do eritrócito, porém, não na forma de protuberâncias, mas sim invaginações da membrana denominadas “cavéolas” (Bracho *et al*., 2006) que parecem estar envolvidas na captação ou exportação de antígenos entre parasita e hospedeiro. Ainda, foi mostrado que a infecção pelo *P. vivax* leva a uma maior deformabilidade da membrana do eritrócito, quando comparada a Pf-EI, o que poderia facilitar a passagem do eritrócito infectado pela barreira dos sinusóides esplênicos e o escape da depuração (Handayani *et al.*, 2009). Uma superfamília gênica variante também foi encontrada em *P. vivax*. Esta superfamília multigene, denominada *vir*, foi subdividida em subfamílias e alguns dos antígenos correspondentes (VIR) foram encontrados expressos na superfície de eritrócitos infectados por *P. vivax* (Pv-EI), mas de uma forma não clonal, ou seja, mais de um antígeno são expressos simultaneamente na membrana do eritrócito (Del Portillo *et al*., 2001; Fernandez-Becerra *et al*., 2005). Por este motivo, a função dos antígenos VIR provavelmente não está diretamente relacionada às variações antigênicas em sentido estrito (del Portillo *et al*. 2004). Recentemente foi proposto que os antígenos VIR desempenham papel na adesão de Pv-EI em células específicas do baço, que se localizam em regiões protegidas da depuração (Fernandez-Becerra *et al*. 2005). Porém, o fato de que nem todos os antígenos VIR são exportados para a superfície dos eritrócitos reforça a idéia de que estas proteínas possam ter diferentes funções (Merino *et al*., 2006).

Ainda em relação ao *P. vivax*, devido à ausência de *knobs*, de genes *var* e de proteínas homólogas à PfEMP-1, por muito tempo inferiu-se que este parasita não era capaz de citoaderir ao endotélio. Atualmente, com a crescente documentação de casos graves de infecções por *P. vivax*, inclusive na Amazônia Brasileira (Daniel-Ribeiro *et al.*, 2008) estudos pioneiros vêm sendo desencadeados nesta direção. Vale lembrar que

mesmo sem apresentar *knobs*, Pv-EI são capazes de formar rosetas (Udomsangpetch *et al*., 1995); ainda, alguns plasmódios de roedores, como *P. berghei* e *P.chabaudi,* que também não possuem *knobs*, são capazes de citoaderir ao endotélio (Coquelin *et al.* 1999; Mota *et al*. 2000; Neres *et al*. 2008) sugerindo que a citoadesão ao endotélio é uma característica antiga dentro deste gênero, não restrita ao *P. falciparum,* aos *knobs* ou à PfEMP-1.

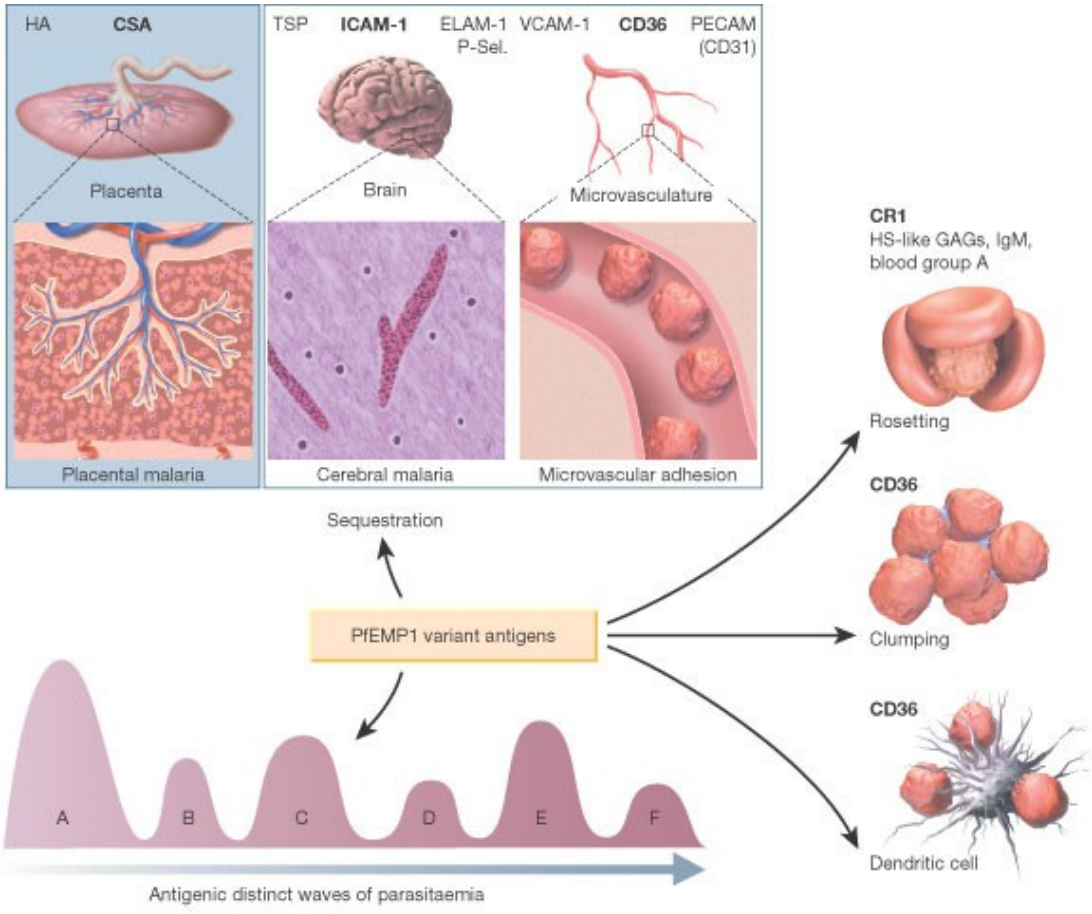

Figura 5. Citoaderência em *P. falciparum*. A PfEMP1 pode se ligar a receptores de diferentes células do hospedeiro, através de seus vários domínios de adesão. Miller *et al.*, Nature 2002.

A infecção por *P. vivax* leva a Complicações Clínicas Graves?

No que diz respeito aos estudos clínico-epidemiológicos referentes à malária grave, a grande maioria das análises tem focalizado indivíduos infectados por *P. falciparum,* sendo a malária vivax descrita como "malária benigna". Uma diferença importante entre as duas infecções é o fato do *P. falciparum* invadir eritrócitos em uma grande amplitude de fases da hematopoiese, o que possibilita uma alta carga parasitária, principalmente na falta de tratamento ou de resposta imune protetora. Entretanto, o *P. vivax* apenas infecta reticulócitos, eritrócitos jovens que surgem logo no início da hematopoiese. Esta peculiaridade limita sua capacidade multiplicativa, assim, a parasitemia na malária vivax raramente ultrapassa 2% dos eritrócitos circulantes, o que garante sintomas mais brandos e menor mortalidade. Outra diferença relevante entre *P. vivax* e *P. falciparum* é a capacidade de *P. vivax* apresentar estágios latentes, chamados "hipnozoítas", e que viabiliza recidivas da infecção. Acredita-se que estas recidivas possam gerar maior resposta imune protetora (revisto por Anstey *et al.*, 2007), corroborando com a existência de infecções assintomáticas.

Entretanto, nos últimos anos, tem-se observado que as infecções por *P. vivax* também podem evoluir para as formas graves da doença, quebrando-se o dogma de que a malária vivax é "benigna" (Baird, 2009). Dois importantes estudos realizados em Papua relataram taxas equivalentes de internações entre pacientes infectados por *P. falciparum* ou *P. vivax,* com taxas de mortalidade também similares: 2,2% para os pacientes internados com *P. falciparum* e 1,6% para pacientes com *P. vivax* (Tjitra *et al*., 2008; Genton *et al*., 2008). No entanto, não está claro o quanto estas mortes foram resultado direto da infecção por *P. vivax.* Ainda, ambos os estudos reportaram complicações pulmonares graves e complicações cerebrais decorrentes da malária vivax, o que era normalmente associado à infecção por *P. falciparum*. No Brasil, onde complicações em infecções por *P. vivax* também foram observadas, um estudo realizado na cidade de

Manaus mostrou o crescente aumento do número de internações hospitalares de pacientes infectados por *P. vivax* (Santos-Ciminera *et al*. 2007).

As complicações na malária vivax, assim como na malária falciparum, estão geralmente associadas à disfunção de determinados órgãos, sugerindo que semelhantes mecanismos de patogênese possam ser compartilhados por esses dois parasitas. Estudo realizado na Tailândia revelou uma correlação entre mulheres grávidas, principalmente na primeira gravidez, e o risco de anemia materna e de nascimento de neonatos de baixo peso (Nosten *et al*., 1999). Além disto, foi observada a deposição de pigmento malárico na placenta de mulheres infectadas por *P. vivax* (McGready *et al*., 2004). Estas são características observadas em mulheres grávidas infectadas pelo *P. falciparum,* cuja adesão na placenta está amplamente descrita (Duffy & Fried, 2005). Recentemente, além das complicações relatadas em mulheres grávidas, estudos de casos de indivíduos com malária vivax originários de diferentes países endêmicos fora da África Subsaariana diagnosticaram formas graves da infecção tais como: trombocitopenia severa, malária cerebral e síndrome do desconforto respiratório agudo (ARDS; Makkar *et al*., 2002; Ozen *et al*., 2006; Lomar *et al*., 2005). O caso reportado de malária cerebral se refere a uma criança da Turquia de quatro anos de idade apresentando convulsões e um eletro-encefalograma característico de um quadro epilético (Ozen *et al*., 2006); enquanto que o caso reportado de ARDS se refere a uma mulher de 43 anos de idade, originária da cidade de Manaus que apresentou sorologia e cultura microbiológica negativa para diferentes vírus e bactérias relacionadas a síndromes respiratórias (Lomar *et al*., 2005). Outros casos de complicações pulmonares graves em pacientes infectados por *P. vivax* já foram reportados (revisto por Lomar *et al*., 2005). No entanto, uma explicação plausível para estes casos de malária severa em infecções pelo *P. vivax* poderia estar associada a infecções mistas com *P. falciparum*. De fato, apesar de todos estes casos citados terem sido diagnosticados por meio de esfregaços sanguíneos e pelo *kit OptiMal® Rapid*

Malária, em nenhum deles foi realizado ensaio de detecção por amplificação de DNA pela reação em cadeia da polimerase (PCR), na presença de oligonucleotídeos específicos para cada espécie de parasita causador da malária em humanos. Porém, em estudos recentemente conduzidos na Índia, não foi detectado DNA específico de *P. falciparum*, ou outro plamódio além do *P. vivax*, após sucessivas análises de PCR a partir do DNA extraído do sangue periférico dos pacientes. No primeiro estudo, onze pacientes infectados por *P. vivax* apresentaram formas graves de malária; tais como malária cerebral, edema pulmonar, anemia profunda e insuficiência renal, todos decorrentes de infecção pelo *P. vivax* (Kochar *et al*., 2005). No segundo estudo, foram descritos 40 casos de complicações clínicas em pacientes infectados unicamente por *P. vivax* (Kochar *et al*., 2009).

Ainda é desconhecido o mecanismo responsável pelas complicações da malária vivax e se este parasita possui capacidades citoadesivas similares àquelas apresentadas pelo *P. falciparum,* que ao aderirem ao endotélio vascular, desaparecem da circulação periférica. Como todas as etapas do ciclo eritrocítico de *P. vivax* são visíveis no sangue periférico, não se acreditava que esta espécie também era capaz de aderir ao endotélio vascular. No entanto, a sequestração de *P. vivax* chegou a ser proposta há mais de 50 anos, ao se observar que apenas uma pequena proporção de estágios maduros do parasita (esquizontes) é encontrada na circulação periférica (Field & Shute, 1956). Segundo revisão feita por Anstey e colaboradores em 2009, apesar de que poucos estudos *post mortem* foram descritos para o *P. vivax,* especialmente nos tempos modernos, em estudos datados do início do século XX foi reportada uma maior concentração de *P. vivax* na vasculatura cerebral e no intestino (Billings & Post, 1915; Bruetsch, 1932). Porém, foi mostrado que eritrócitos infectados por *P. falciparum* não são encontrados aderidos na microvasculatura após três dias de tratamento com antimaláricos (Pongponratn, 2003), com isso a dificuldade de se abordar a questão do sequestro de *P.*

vivax através de estudos *post mortem* nos dias atuais, em que se preconiza o acesso ao tratamento, com ampla utilização de antimaláricos.

Por outro lado, um caso relatado em Goa, Índia, refere-se a uma mulher de 20 anos tratada com antibióticos após diagnóstico de uma infecção bacteriana do trato respiratório superior. Uma semana depois, a malária vivax foi diagnosticada, mas a paciente evoluiu rapidamente com insuficiência respiratória, perda de consciência e morreu em poucos minutos. O diagnóstico da malária vivax foi confirmado por PCR e exames *post-mortem* mostraram forte infiltração monocítica nos alvéolos e parasitas também foram detectados no tecido pulmonar (Valecha *et al*., 2009).

Recentemente, estudo comparativo entre as respostas inflamatórias de pacientes da Indonésia infectados com *P. falciparum* ou *P. vivax* demonstrou significativa redução do fluxo vascular nos capilares pulmonares, e apresentando níveis similares em ambas as infecções, sugerindo que os sinais clínicos possam ser causadom pelo sequestro de Pv-EI neste órgão, assim como nas infecções por *P. falciparum* (Anstey *et al*., 2007). De fato, *P. vivax* comumente afeta o pulmão, sendo a tosse um sintoma frequente na maioria dos pacientes com malária vivax (Anstey *et al*., 2007). Ainda, a maioria das complicações pulmonares parece estar associada ao início do tratamento com antimaláricos (Anstey *et al.*, 2007; Tan *et al.*, 2008). Estes achados são consistentes com uma exacerbação da resposta inflamatória local decorrente da liberação de toxinas durante a destruição do parasita.

Além disto, outro estudo identificou a presença de antígenos variáveis expressos na superfície de Pv-EI codificados a partir de uma família multigênica denominada *vir* (del Portillo *et al.*, 2001). Os autores responsáveis pela descoberta dos genes *vir* acreditam que os antígenos codificados a partir desta família multigênica possam mediar a adesão do parasita no baço (del Portillo *et al*., 2004). É importante ressaltar que a presença de antígenos variáveis na superfície de eritrócitos infectados, codificados a partir de genes

variáveis (*var*), foi descrito anteriormente como característica de *P. falciparum*, e estão diretamente relacionados com a virulência deste parasita (revisto por Craig & Scherf, 2001).

Tabela 1. Malária vivax Grave: Casos reportados de 1998 a 2007. Fonte: Baird *et al.*, TRENDS in Parasitology, 2007.

Location	Year	No. of cases	Presentation	Fatal
India	2003	11 adults	Renal failure = 4 Jaundice = 4 ARDS = 3 (1 fatal) Cerebral = 3 (1 fatal)	2
Pakistan	2000	1 adult	Cerebral	0
Venezuela	2005	1 adult	ARDS	0
India	2006	1 adult	ARDS	0
Afghanistan	2004	1 adult	ARDS	0
Singapore	2003	2 adults	ARDS (fatal)	1
Columbia	1998	1 adult	ARDS	0
Malaysia	2003	2 adults	ARDS = 1 DIC[a]/Renal Failure = 1 (fatal)	1
India	1999	2	Renal failure = 2	?
India	2002	16	Renal failure = 16	3
Turkey	2005	1 child	Convulsions	0
Indonesia	2000	21 children 17 adults	Cerebral = 3 (2 fatal) Siezures = 2 (1 fatal) Anemia = 24 Hyperparasitemia = 1 Renal failure = 4 Liver dysfunction = 10 (3 fatal) Acidosis = 3 (1 fatal) ARDS = 2 (1 fatal) Cardiac arrest = 1 (fatal)	9
Afghanistan	2003	1 adult	ARDS	0
India	2000	22	Liver dysfunction = 8 Cerebral = 1 (fatal) Anemia = 8 Thrombocytopenia = 4 Pancytopenia = 1	1
Brazil	2000	1 adult	Thrombocytopenia	0
New Guinea	2000	1 adult	ARDS	0
India	1998	1 adult	Thrombocytopenia	0
Kenya	2004	1 adult	Splenic rupture	0
Turkey	2003	2 adults	Splenic rupture	0
India	2002	1 adult	ARDS	0
India	2006	1 child	Renal failure	0
Total				17

[a]DIC, disseminated intravascular coagulation.

Malária vivax - Negligenciada

Poucos pesquisadores no mundo têm voltado atenção para entender os mecanismos pelos quais ocorre o agravamento da malária vivax e uma possível capacidade citoadesiva de *P. vivax* permanecia por ser demonstrada, diferentemente do que acontece com *P. falciparum*, cujas capacidades citoadesivas são exaustivamente exploradas nos grandes centros de pesquisa do mundo, com emprego de tecnologias cada vez mais sofisticadas.

A negligência em relação à malária vivax ocorre, em parte, devido aos menores índices de morbidade e mortalidade decorrentes das infecções por *P. vivax,* consideradas equivocadamente como uma “malária benigna”. Existe grande dificuldade em se estudar *P. vivax* fora das regiões endêmicas, já que uma técnica de cultivo *in vitro* ainda não foi estabelecida, diferentemente de *P. falciparum,* cujo cultivo *in vitro* está estabelecido há décadas.

Sendo o *P. vivax* a espécie mais prevalente no Brasil (Figura 7), temos aqui não apenas condições, mas também o dever e a necessidade de buscar compreender os mecanismos patológicos específicos da malária vivax. Ainda, diante da impossibilidade de controle da malária com as estratégias até hoje empregadas, o melhor entendimento da biologia parasitária como um todo, incluindo os mecanismos de virulência, transmissibilidade, variação antigênica e mecanismos de escape do sistema imunológico do hospedeiro, continuam sendo imprescindíveis para traçar novas estratégias mais eficazes de controle e tratamento.

Figura 6. Risco de infecção malárica no Brasil.

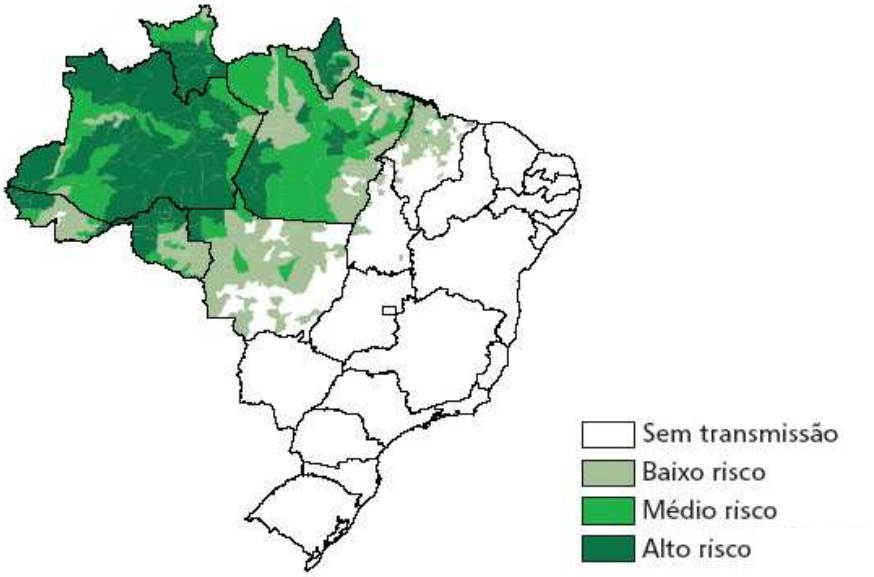

Fonte: Sivep-Malária/SVS/MS

Figura 7. Proporção de casos de malária, por espécie de plasmódio. Brasil, 2007.

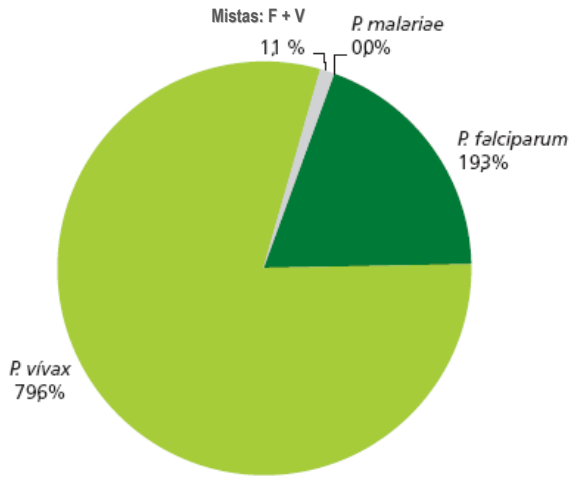

Fonte: Sivep-Malária/SVS/MS

OBJETIVOS

Buscando entender os mecanismos envolvidos no agravamento da malária vivax, e aproveitando-se dos conhecimentos teóricos e práticos adquiridos nos estudos de citoadesão de Pf-EI desenvolvidos no laboratório em Campinas (SP), experimentos pioneiros foram então realizados nas cidades de Porto Velho (RO) e Manaus (AM), com o intuito de:

i. avaliar a capacidade citoadesiva de Pv-EI em células endoteliais que expressam receptores como CSA, ICAM-1 e CD36;
ii. quantificar e qualificar a adesão em condições estáticas, ou em sistema que mimetiza o fluxo sanguíneo;
iii. quantificar e qualificar a adesão em um contexto infamatório, ou não.

Buscamos ainda, analisar a diversidade de fenótipos citoadesivos de isolados frescos de Pf-EI amazônicos e, por fim, relacionar a capacidade citoadesiva de *Plasmodium vivax e Plasmodium falciparum,* obtidos de pacientes da Amazônia Brasileira.

MÉTODOS

Cultura de células endoteliais

Nos ensaios de citoadesão foram utilizadas células endoteliais do pulmão humano (HLEC), células endoteliais do cérebro de macacos *Saimiri* (SBEC – Sc1D) e células de ovário de hamster chinês (CHO). As linhagens celulares foram cultivadas em meio DMEM/F12 suplementado com 30 µg/mL fator de crescimento de células endoteliais (ECGS) e 10% de soro fetal bovino. As células foram mantidas em incubadora com pressão constante de 5% de CO_2 e 37°C.

Meio de cultura: DMEM-F12 (Nutricell), enriquecido com ECGS (Sigma, E0760) 30µg/mL. Para o repique é utilizado Tripsina EDTA (Nutricell).

Meio de congelamento: DMEN-F12, 40% de SFB e 8% de DMSO (Sigma, R4540).

Cultura de formas sanguíneas de *P. falciparum*

Como parâmetro positivo nos ensaios de adesão de eritrócitos infectados por *P. vivax,* foram utilizados os isolados de *P. falciparum* FCR3, e 3D7. Os parasitas foram gentilmente cedidos pelo Prof. Dr. Jürg Gysin (*Université de La Méditerranée*) e pelo Prof. Dr. Gerhard Wunderlich (ICB-2, USP). Os eritrócitos infectados por *P. falciparum* são cultivados em sangue O^{+} em atmosfera hipóxica (5% $O_{2,}$ 5% CO_2 e 90% N_2) de acordo com protocolo descrito anteriormente (Ljungström *et al*, 2004).

Enriquecimento de estágios maduros da cultura de *P. falciparum*

O enriquecimento das formas maduras foi realizado utilizando-se 2.4 volumes de Voluven™ (Frenesius) em relação ao volume do pellet de hemácias, e 1.4 volumes de meio RPMI 10% plasma. O gradiente foi deixado em um tubo na posição vertical, a 37°C

durante 30 minutos. Após este período, a fase superior, contendo as formas maduras, foi removida e lavada com meio RPMI sem plasma.

Seleção de Pf-EI monofenotípicos para ligação a CSA e CD36 (Panning)

Esta técnica foi realizada de acordo com o protocolo de Scherf *et al*. (1998) e tem como objetivo a seleção monofenotípica do parasita. Células endoteliais SBEC-Sc1D, capazes de expressar os receptores CSA, CD36 e ICAM-1 (Gysin *et al*., 1999), foram crescidas até a confluência em garrafas de 75 cm^3. Eritrócitos infectados foram enriquecidos por passagem no Voluven™, ressuspendidos em meio RPMI pH 6,8 e transferidos para a garrafa contendo as células. Após incubação por 2 h a 37°C, o excesso de parasitas não aderidos foi removido por meio de lavagens em meio RPMI pH 6,8. Em seguida, foi adicionado meio RPMI pH 6,8 contendo CSA livre na concentração de 1 mg/mL para liberar apenas eritrócitos ligantes a CSA (Pf-EI^{CSA}). Após incubação de 30 min, os parasitas, não mais aderidos devido à competição pela CSA solúvel (dessequestração), foram retirados da garrafa e colocados imediatamente em cultura (Figura 8). Este processo foi repetido por 4 vezes para aumentar a eficiência da seleção de parasitas com o fenótipo desejado. Para a obtenção de parasitas ligantes a CD36 (Pf-EI^{CD36}), foi feito ensaio de adesão utilizando CHO transfectadas que expressam exclusivamente o receptor CD36. Após lavagem, os eritrócitos que permaneceram aderidos foram então removidos mecanicamente com auxílio de uma pipeta e meio RPMI pH 7,2, e colocados em cultura novamente. Este processo também foi repetido por 4 vezes.

Figura 8. Esquema da seleção de Pf-EI monofenotípicos (*Panning*).

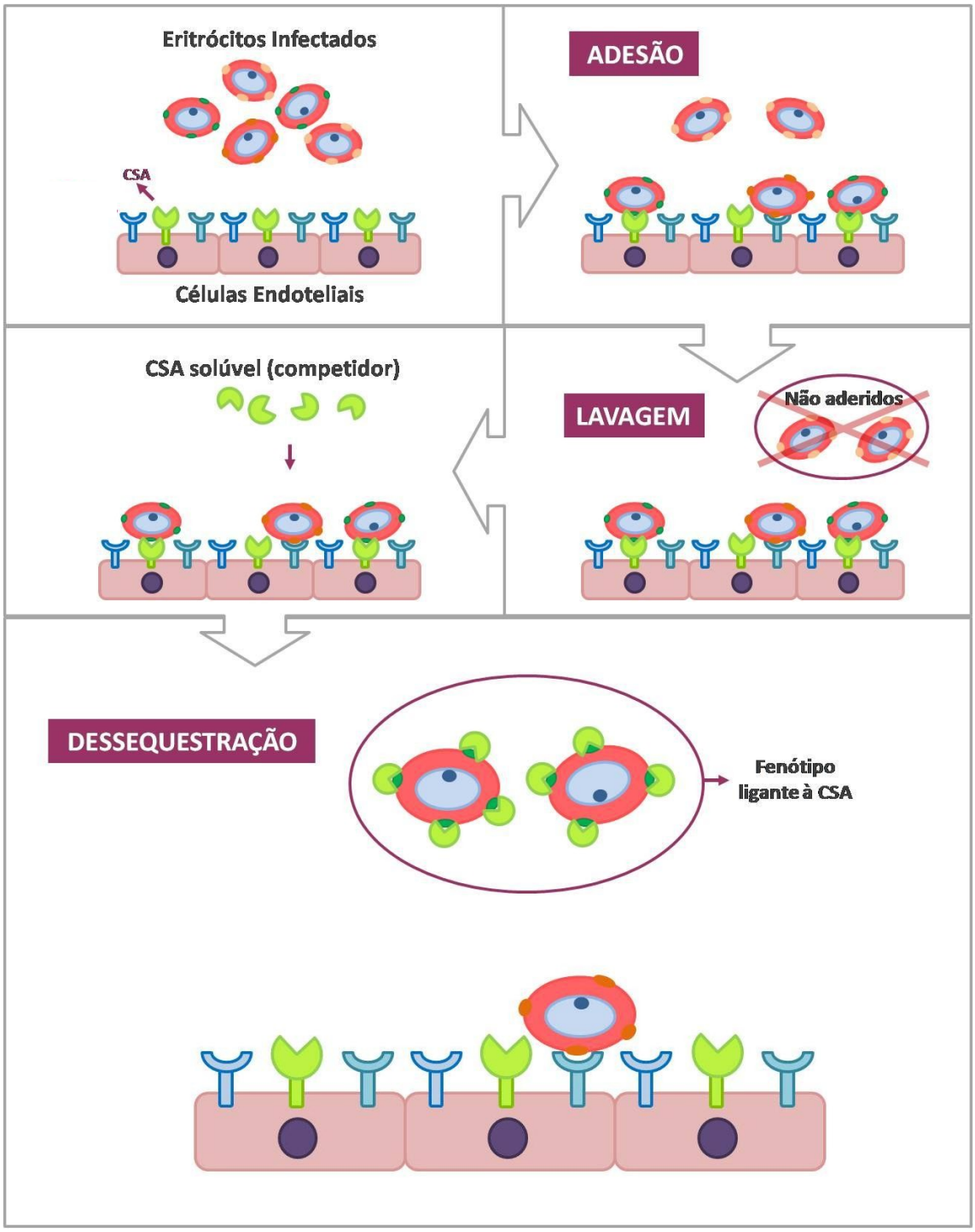

Preparo de lâminas de cortes histológicos de placenta humana

Pedaços de 1 cm^3 foram removidos da porção materna de placenta de mulheres sadias a termo. Em seguida, o pedaço do tecido foi mergulhado em nHexano (Merck) previamente esfriado em nitrogênio líquido. Após o congelamento, o tecido foi embebido em solução *Tissue-Teck*® e armazenado a -20°C. Os cortes histológicos de 5 µm foram feitos em criostato a -20°C e as lâminas foram estocadas a -80°C até o momento do uso. Para os ensaios de citoadesão, uma área circular foi delimitada com uma *Dako-Pen*®.

Obtenção de isolados parasitários de sangue periférico e enriquecimento de estágios maduros

Os isolados de *P. falciparum* e *P. vivax* utilizados neste trabalho foram coletados de pacientes apresentando malária não complicada, provenientes da Fundação de Medicina Tropical do Amazonas, na cidade de Manaus. Após confirmação de malária (gota espessa) e com o devido consentimento do paciente, foram coletados 5 – 10 mL de sangue por punção venosa utilizando tubos estéreis contento citrato de sódio como anticoagulante (Vacuette). Uma pequena quantidade de sangue foi separada para realização de análises moleculares por *Nested-PCR*. O sangue foi centrifugado a 1.500 x g por 10 min, o plasma recuperado e armazenado a -20°C para futuras análises imunológicas. Os eritrócitos foram lavados 3 vezes e ressuspendidos em meio RPMI acertando-se o hematócrito para 10%. Em seguida, 5 mL da suspensão foram transferidos para tubo plástico cônico de 15 mL. Com auxílio de uma pipeta *Pasteur* longa, 5 mL de uma solução de *Percoll*® 45% em RPMI foram depositados abaixo da suspensão de eritrócitos. O material foi centrifugado a 1.500 x g por 15min, em baixa aceleração e sem freio. Após centrifugação os eritrócitos sadios estão depositados no fundo do tubo, enquanto as formas maduras são encontradas na interface. Os eritrócitos infectados foram retirados na interface e passaram por 3 lavagens em meio RPMI para a

completa remoção da solução de *Percoll*®. Após a última lavagem os eritrócitos infectados foram ressuspendidos em meio RPMI, para serem utilizados em ensaios de adesão. A parasitemia após *Percoll*® foi determinada por meio de esfregaços corados com Giemsa.

Confirmação do diagnóstico por *Nested*-PCR

Com o intuito de excluir a possibilidade de infecções mistas, o material nuclear do sangue dos pacientes selecionados foi purificado de acordo com o *kit gDNA Blood* (Invitrogen), seguindo-se a instruções do fabricante. O DNA extraído foi utilizado como molde de reações de *Nested*-PCR, de acordo com protocolo descrito (Snounou & Singh, 2002), na presença de oligonucleotídeos específicos para *P. vivax, P. falciparum* e *P. malariae*.

Ensaios de Imunofluorescência

Os ensaios de imunofluorescência indireta (IFA) foram realizados em lâminas de IFA de 12 poços contendo estágios maduros de *P. vivax*, como descrito por Bargieri *et al.*, 2008. Brevemente, após enriquecimento em solução 45% de *Percoll*®, Pv-EI foram lavados em RPMI, ressuspendidos em igual volume de soro fetal bovino (Nutricell) e depositados na lâmina de IFA (50 µl/poço). O material foi fixado em acetona por 10 min e as lâminas foram estocadas a -20°C até o uso. Cada anticorpo monoclonal (MAb; 3F8 e K23) anti-vivax-MSP-1_{19} (do Inglês, *Merozoite surface protein-1*) foram incubados com os eritrócitos infectados, numa concentração de 10µg/mL, por 30 min e a 37°C. Soro de camundongo imunizado apenas com adjuvante foi utilizado como controle negativo. Depois de extensivas lavagens em PBS, as lâminas foram incubadas com 10µg/mL de conjugado FITC anti-IgG de camundongo (Sigma) e 100 µg/mL de DAPI (4',6-diamidino-2-

phenylindole, dihydrochloride; Molecular Probes) por 30 min a 37°C, seguido de novas lavagens. O reconhecimento positivo pelos MAb foi detectado com o auxílio de microscópio de imunofluorescência (Nikon). O reconhecimento de antígenos VIR expressos na superfície de Pv-EI foi determinado nas mesmas condições descritas acima, porém com soro coletado de camundongos imunizados com a proteína de fusão VIRA4 ou VIRE5 glutationa S-transferase (GST), correspondentes às subfamílias *vir* A e E. A expressão das proteínas de fusão e o regime de imunização dos camundongos foram descritos por Fernandez-Becerra *et al*., 2005 e Oliveira *et al*., 2006.

Amadurecimento *in vitro* de Pv-EI

Logo após enriquecimento em *Percoll®,* os eritrócitos foram ressuspendidos em 10 mL de RPMI contendo 10% de plasma humano AB+ e mantidos a 37°C por 5h. Em seguida a suspensão foi centrifugada e os eritrócitos lavados por 3 vezes em RPMI para que o plasma fosse retirado e a capacidade adesiva fosse então avaliada.

Ensaios de citoadesão estática de Pv-EI e Pf-EI

As células foram cultivadas em lâminas de oito poços com cerca de 1 cm^2 cada (*Culture Slides*, Becton & Dickinson), até atingirem confluência total. Nesta etapa utilizamos 5 x 10^4 Pf-EI e Pv-EI em 200 µL de meio RPMI (pH 6,8) para cada poço, seguido de incubação durante 1h. Após este período, os eritrócitos não aderidos foram removidos por meio de extensivas lavagens em meio RPMI em condições estáticas. Em seguida, as lâminas foram fixadas com formoldeído 3,7% em PBS e coradas com o *kit Panótico Rápido* (Laborclin). Os ensaios de adesão no trofoblasto placentário foram realizados de maneira similar aos das células endoteliais, porém utilizando criocortes histológicos de placenta sadia, com área demarcada com tinta hidrofóbica (*Dako Pen*).

Nos ensaios de inibição da adesão os eritrócitos foram colocados para aderir na presença de 5 µg/mL de IgG anti-CD36 (Santa Cruz); ou 100 µg/mL de CSA (Sigma) ou CSB solúveis (Sigma). Para o tratamento com Condroitinase- ABC, previamente à adesão, células já confluentes foram tratadas com 100µl de condroitinase 0.5U/mL seguido por 1h de incubação. Para analisar o envolvimento de antígenos protéicos, eritrócitos foram tratados com tripsina (1mg/mL) por 45min, previamente ao ensaio de adesão. O número de eritrócitos infectados, ou não, depositados sobre a monocamada endotelial ou sobre os cortes histológicos foi contado com auxílio de microscópio, e a adesão foi expressa como a média ± desvio padrão do número de eritrócitos por mm^2 observados em 4 poços. O envolvimento dos antígenos VIR na adesão de Pv-EI foi avaliado em ensaios de inibição da adesão com soro anti VIRA4 ou VIRE5 diluídos 1:5 ou 1:10. Soro de camundongos imunizados somente com adjuvante ou imunizados com GST foram utilizados como controle negativo e controle de especificidade, respectivamente. Para esses ensaios a inibição foi determinada como porcentagem em relação ao controle negativo e expressa como média ± desvio padrão de três a quatro poços.

Ensaios de citoadesão de Pv-EI e Pf-EI em Sistema de Fluxo

Para avaliar a resistência da citoadesão de Pv-EI então observada, realizamos ensaios de citoadesão em sistema de fluxo, adaptado de um método descrito anteriormente (Pouvelle *et al*., 2003, Costa et. al., 2003, Avril *et al*., 2004). Resumidamente, HLEC foram cultivadas em lâmina de cultura com um único poço (Becton & Dickinson); o ensaio de adesão foi realizado como na condição estática, porém, o volume determinado pelo poço único da lâmina permitia a incubação de 1,5 mL de meio com 5 x 10^5 Pv-EI, proporcionalmente à nova área de superfície. Após 1 hora de incubação a 37°C, as lâminas foram adaptadas em uma câmara (sistema Immunetics, E.U.A.) que permitia um fluxo de meio de adesão (RPMI pH 6,8) com pressão controlada,

correspondendo a um *shear stress* de 0,09 e 0,36 Pascal (Pa), por 10 e 5 min, respectivamente. É sabido que o *shear stress* nos microcapilares está em torno de 0.08 Pascal (Kroll *et al.*, 1996). Em seguida, os Pv-EI que restaram aderidos foram contados, filmados e fotografados em 20 campos aleatoriamente selecionados com a ajuda de uma câmera digital 5.0 megapixels (Motic, Moticam 2500). Em alguns ensaios, as lâminas foram coradas com Giemsa após a mesma condição de *shear stress.* Alternativamente, HLEC foram incubadas com LPS (endotoxina lipopolissacarídeo; SIGMA) 1,0 μg/mL a 37°C por 4h e então extensivamente lavadas, previamente à citoadesão.

Análises Estatísticas

A significância estatística da adesão aos diferentes tipos de células e em diferentes condições foi determinada através de testes *U* Mann-Whitney ou Kruskal-Wallis, utilizando-se os programas BioEstat™ versão 3.0 (CNPq, Brasil) e Prism™ versão 3.02 (Graphpad, USA). Os valores foram considerados significativos quando $P<0.05$.

Figura 9. Fluxograma representando a sequência dos experimentos.

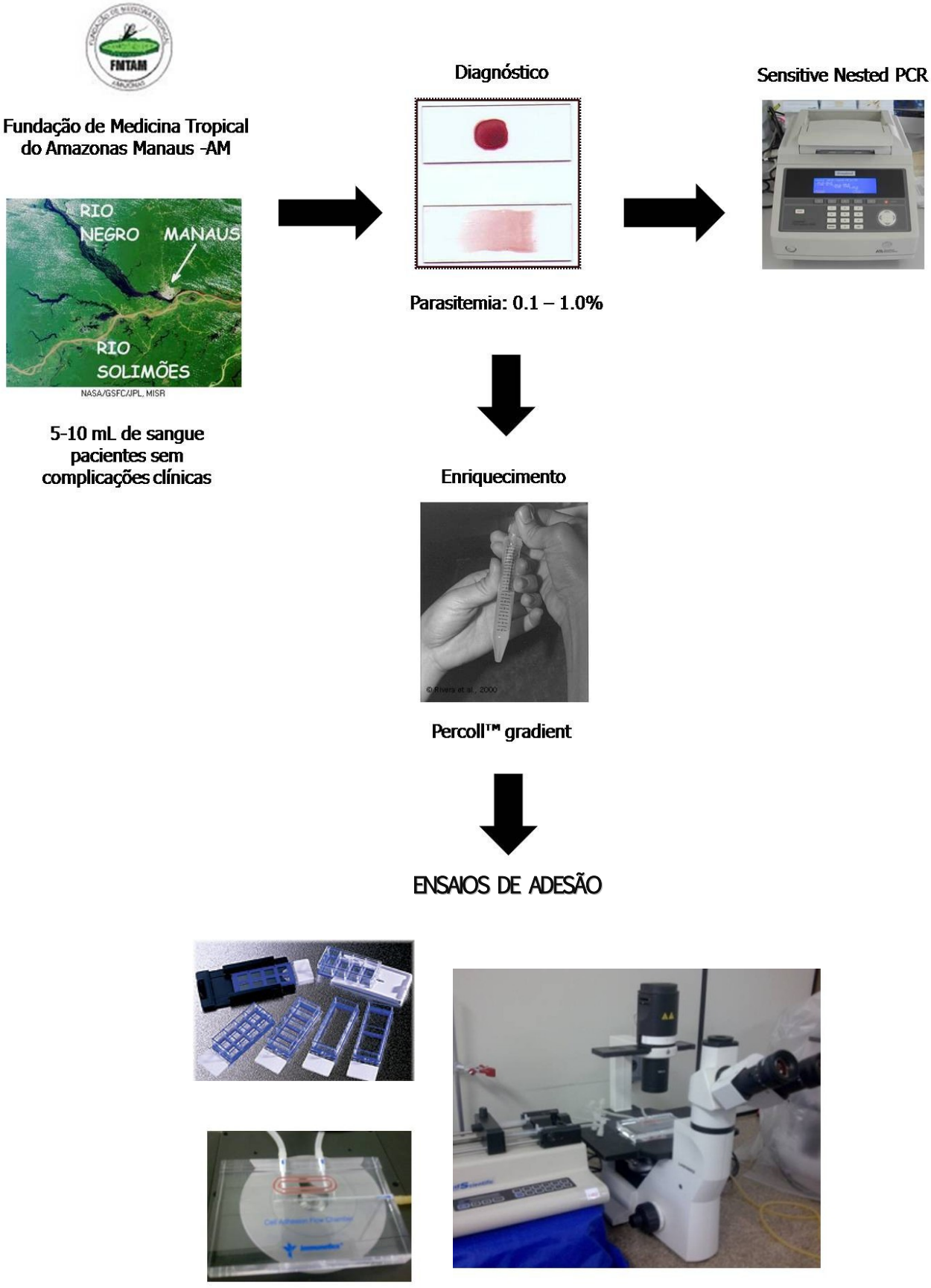

Resultados e Discussão

Como parâmetro positivo nos ensaios de adesão de eritrócitos infectados por *P. vivax,* foram utilizados isolados de *P. falciparum* mantidos em cultivo *in vitro*. Realizamos ensaio de citoadesão com formas maduras de isolados 3D7 ou FCR3. Conforme é mostrado na Figura 10A, formas maduras do isolado FCR3, monofenotípicos ou não, são capazes de aderir às células endoteliais HLEC ou SBEC, enquanto que apenas uma minoria de Pf-EI isolado 3D7 permanece aderida após as lavagens. Estes resultados corroboram com os achados da literatura, os quais demonstram que o isolado FCR3 possui uma elevada capacidade citoadesiva em comparação ao 3D7 (Costa *et al*., 2003; Salanti *et al.*, 2004). Ainda, o aumento da adesão de parasitas monofenotípicos ($FCR3^{CSA}$ ou $FCR3^{CD36}$) demonstra a similaridade estrutural das moléculas CSA das células SBEC, ou CD36 das células CHO (utilizadas na seleção por *Panning*) com as moléculas de superfície de HELC. Por último, com a finalidade de se determinar a quantidade de CSA solúvel ou anti-CD36 a ser utilizada nos ensaios de inibição da citoadesão, parasitas monofenotípicos foram deixados aderir na presença, ou ausência, de inibidores capazes de competir pelos ligantes parasitários. Conforme pode ser observado na Figura 10B, parasitas $FCR3^{CSA}$ e $FCR3^{CD36}$ têm sua capacidade adesiva significativamente reduzida (P<0,05) na presença de CSA solúvel ou anti-CD36, respectivamente. A especificidade de inibição também é observada, uma vez que não foi verificada alta taxa de inibição da adesão de $FCR3^{CSA}$ na presença de anti-CD36 e do $FCR3^{CD36}$ pela CSA solúvel. Além disto, foram realizados diferentes tipos de tratamento com tripsina para avaliar qual a concentração e tempo ideais para inibir a adesão sem comprometer a viabilidade do parasita. Para tanto, após o tratamento com tripsina e realizados os ensaios de adesão, os parasitas foram novamente colocados em cultura demonstrando que o tratamento não afetou a viabilidade dos mesmos. Como esperado, a capacidade adesiva foi quase completamente inibida pelo tratamento com tripsina, demonstrando que o tratamento foi eficiente para inibição da adesão de $FCR3^{CSA}$ ou $FCR3^{CD36}$.

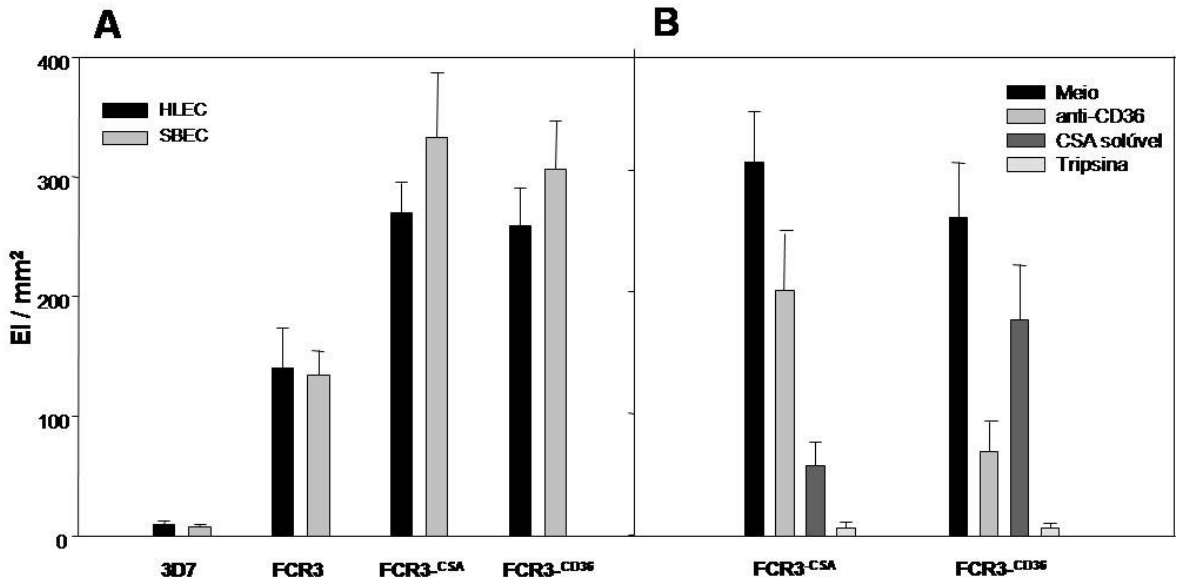

Figura 10. Citoadesão de isolados de Pf-EI cultivados *in vitro*. Pf-EI, 5 x 10^4 / poço (aproximadamente 1000 Pv-EI/ mm^2 da monocamada celular), foram deixados aderir a monocamada de células endoteliais durante 1 h na (**A**) ausência ou (**B**) presença de inibidores como a CSA solúvel a 100 μg / mL, 0,5μg de anti-CD36 ou tratamento prévio com tripsina a 1 mg/mL durante 45 min. Resultados são expressos como a média de eritrócidos aderidos por mm^2 (EI / mm^2) ± desvio padrão de 4 poços.

A fim de verificar a habilidade de Pv-EI de aderir em células endoteliais, coletamos sangue periférico de pacientes infectados por *P. vivax*, sendo o diagnóstico microscópico confirmado, num segundo momento, através de análises moleculares. A Figura 11 exemplifica como foi feita a confirmação do diagnóstico prévio dos pacientes, por Nested PCR sensível a partir do sangue coletado. Não houve divergências entre o diagnóstico molecular e o diagnóstico microscópico por gota espessa para nenhum dos pacientes incluídos neste trabalho.

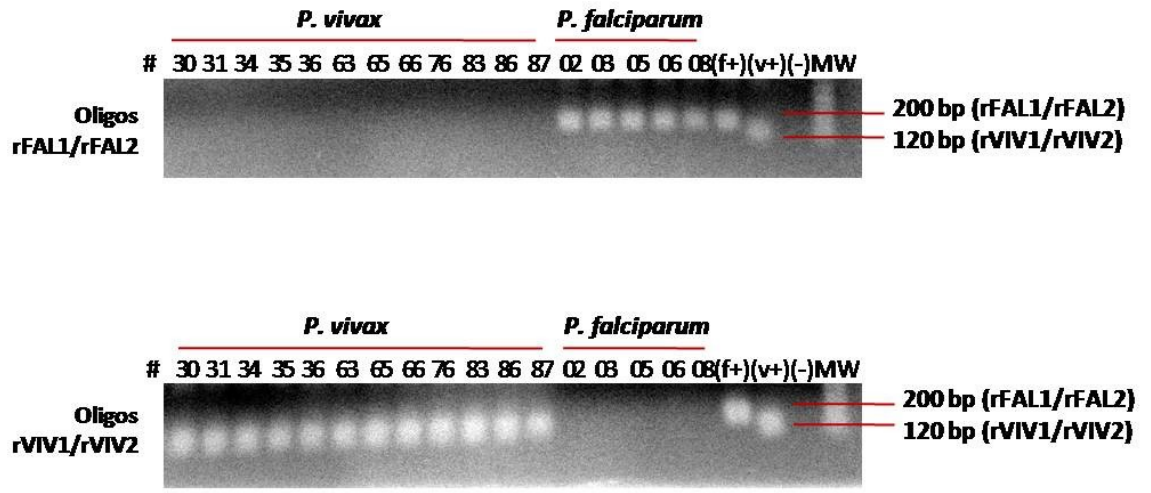

Figura 11. Confirmação do diagnóstico por Sensitive Nested-PCR. O material genético do sangue dos pacientes estudados foi isolado e utilizado como molde em reações de NESTED-PCR na presença de oligonucleotídeos específicos para *P. vivax* ou *P. falciparum,* resultando num produto amplificado de fragmentos 120 ou 200 pares de base (bp), respectivamente. MW: padrão de peso molecular; (v+) e (f+): controles positivos para cada espécie; (-): controle negativo. Não houve divergências entre o diagnóstico prévio por gota espessa e o realizado por Nested-PCR, em nenhuma das amostras testadas.

Após a coleta, a proporção de eritrócitos infectados era enriquecida através da separação em gradiente de *Percoll®.* A separação de formas maduras de *P. falciparum* está bem descrita, mas existem diferenças significativas entre as densidades dos eritrócitos infectados por cada uma das espécies, uma vez que *P. vivax* invade reticulócitos. Durante os meses iniciais desse trabalho buscamos adaptar protocolos para o enriquecimento de Pv-EI. Foi necessário coletar sangue infectado de cerca de 30 pacientes até chegarmos a condições mais favoráveis para a separação de estágios maduros de Pv-EI, que se baseia na utilização de uma concentração de 45% de *Percoll®* em meio RPMI (Figura 12). O estabelecimento deste protocolo possibilitou a realização dos ensaios de adesão e poderá ser de grande valia para o aprofundamento do conhecimento sobre *P. vivax*.

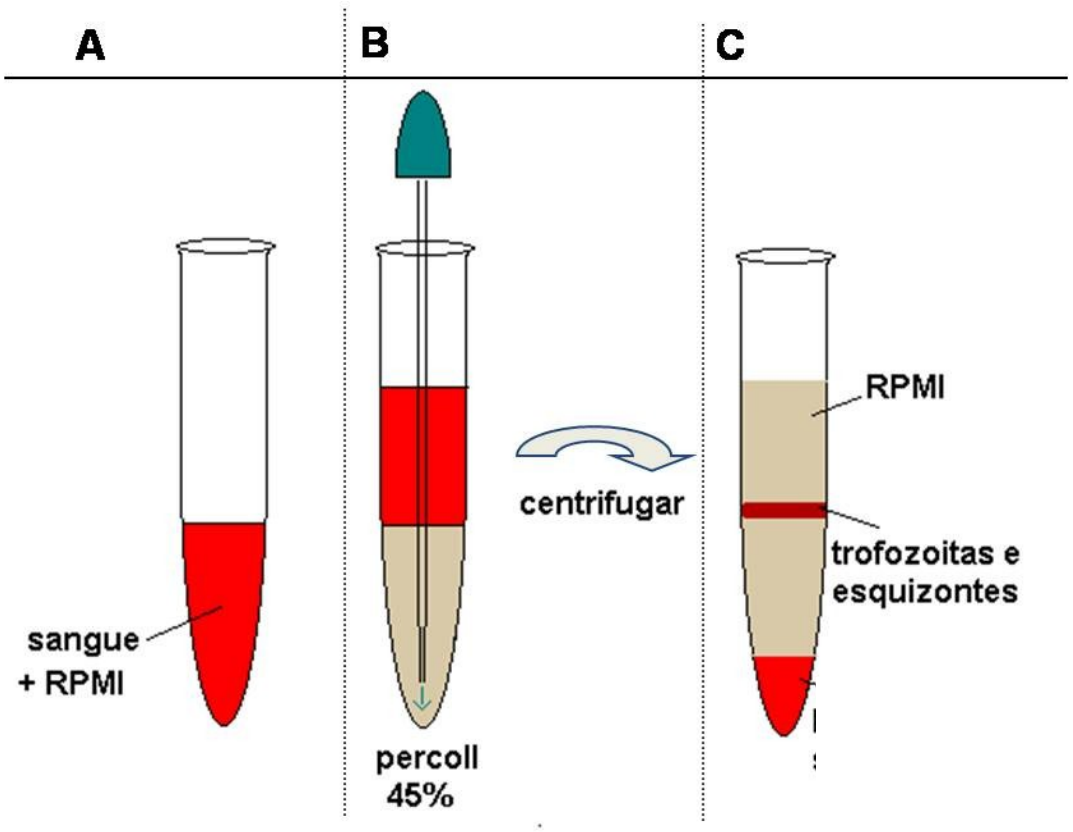

Figura 12. Protocolo de enriquecimento de formas maduras de *P.vivax*. O sangue coletado de pacientes infectados foi lavado e ressuspendido em meio RPMI, acertando-se o hematócrito para 10%. **(A)** Em seguida, 5 mL dessa suspensão foram transferidos para tubo falcon de 15 ml. **(B)** Com auxílio de uma pipeta *Pasteur* longa, 5 mL de uma solução de *Percoll*® 45% em RPMI foram depositados abaixo da suspensão de eritrócitos. O material foi centrifugado a 1.500 x g por 15min, em baixa aceleração e sem freio. **(C)** Após centrifugação os eritrócitos não infectados estão depositados no fundo do tubo, enquanto as formas maduras são encontradas na interface.

No entanto, antes do protocolo de enriquecimento de Pv-EI ser estabelecido, um protocolo de enriquecimento de formas maduras de *P. falciparum* era utilizado. Esta técnica se baseava na separação em 60% de *Percoll*® em RPMI. Com este protocolo obtivemos uma quantidade considerável de formas jovens (anéis) e também de eritrócitos não infectados. Os primeiros ensaios de adesão foram realizados nestas condições. De acordo com a Figura 13A, foi observada adesão de Pv-EI de dois pacientes analisados

em ambas as células endoteliais. Em contraste, nenhum eritrócito não infectado foi observado aderido à monocamada celular. Além disto, quando verificamos a porcentagem das diferentes formas parasitárias presentes após o enriquecimento (anel, trofozoíta e esquizonte), notamos que o paciente #11, com a maior proporção de formas maduras (trofozoítas e esquizontes), apresentou níveis significativamente mais elevados de citoadesão. Estes resultados sugerem que a adesão de Pv-EI, tal qual em Pf-EI, é mediada por formas maduras. É importante ressaltar que estes dois pacientes (#10 e #11) apresentavam parasitemias relativamente altas (1 a 2%) para infecções por *P. vivax*, que raramente chegam a apresentar tais níveis. Já a partir das parasitemias normalmente encontradas (<0,2%), foi obtido um baixo enriquecimento em *Percoll*® (média de 20% de enriquecimento), mas que ainda viabilizou alguns ensaios de adesão, conduzidos com $5x10^4$ Pv-EI por poço, porém, na presença de uma quantidade cerca de cinco vezes maior de eritrócitos não infectados, devido ao baixo enriquecimento. Como mostra a Figura 14, eritrócitos não infectados foram encontrados depositados à monocamada, mas em níveis muito mais baixos que Pv-EI, mostrando que, de alguma forma, a monocamada celular interage e seleciona eritrócitos infectados após a lavagem. Estes dados foram resultados preliminares obtidos em condições ainda de adaptação, mas é válido apresentá-los aqui, pois corroboram com o fato de que há uma interação entre estas células endoteliais e Pv-EI. Como o enriquecimento de muitos outros pacientes infectados por *P. vivax* não foi eficiente em tais condições, buscamos adaptar o protocolo de enriquecimento para viabilizar os testes de adesão de Pv-EI.

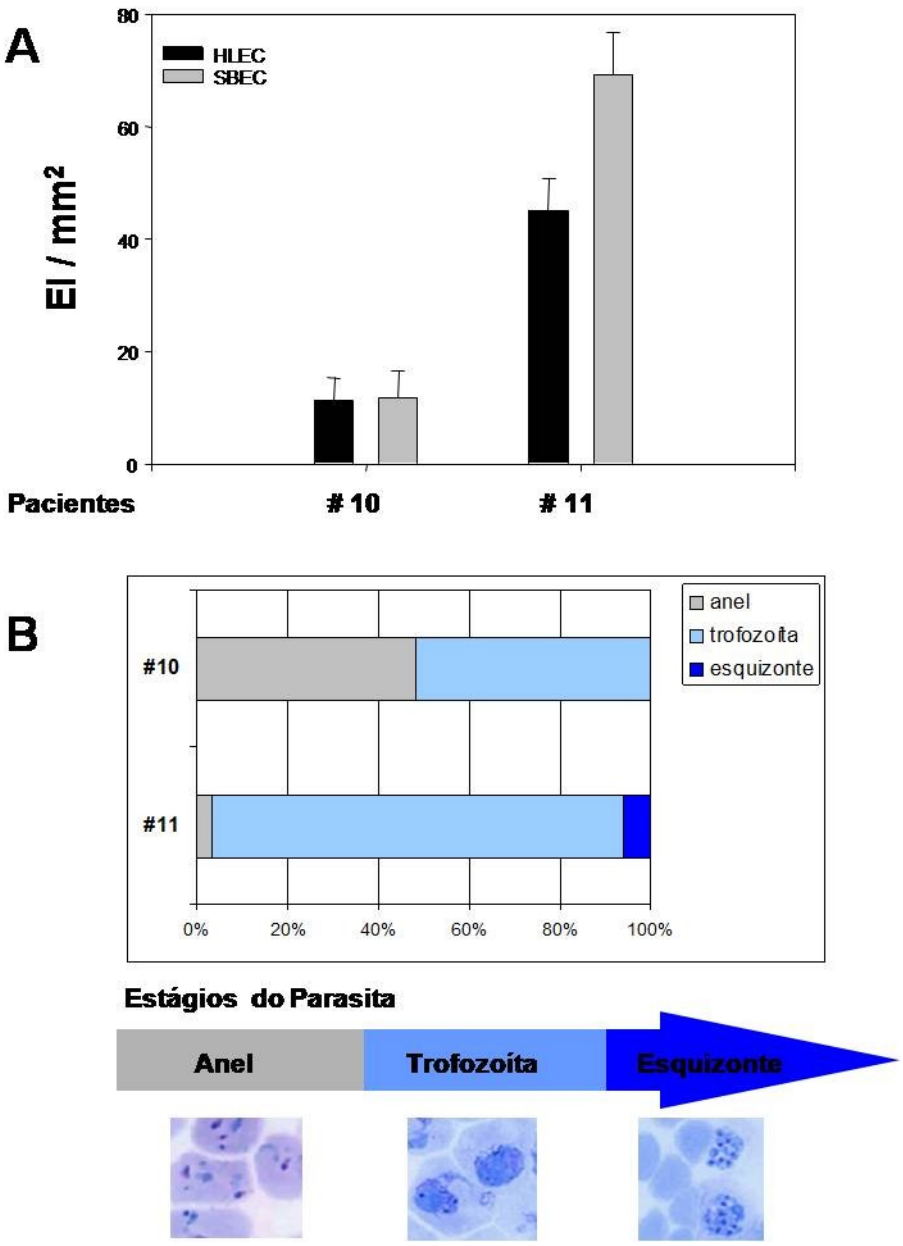

Figura 13. Citoadesão de Pv-EI em células endoteliais. (A) Pv-EI, 5 x 10^4 por poço (aproximadamente 1000 Pv-EI/ mm^2 da monocamada celular), foram deixados aderir a monocamada de células endoteliais durante 1 h a 37ºC. (**B**) porcentagem de formas jovens (anel) e maduras (trofozoíta e esquizonte) dos pacientes #10 e #11. Resultados são expressos como a média de eritrócidos aderidos por mm^2 (EI / mm^2) ± desvio padrão de 4 poços.

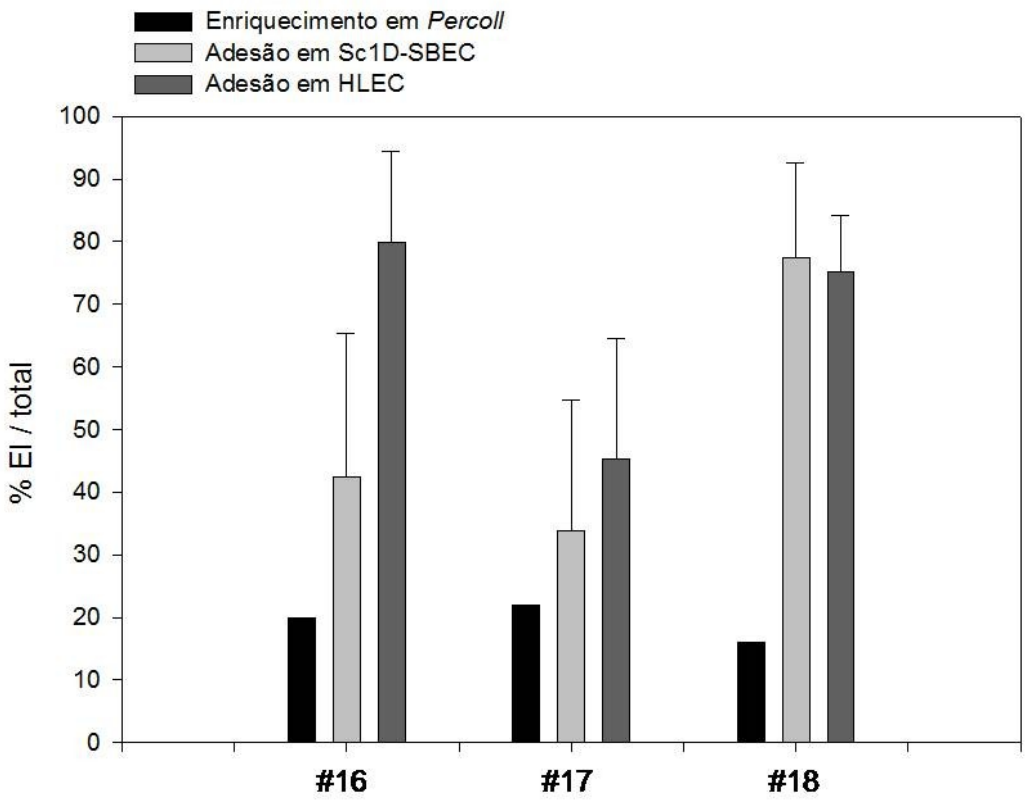

Figura 14. Comparação entre a proporção de EI enriquecidos em *Percoll*® e a proporção de EI encontrados aderidos em HLEC ou SBEC-1D em relação ao número de eritrócitos totais (infectados ou não). Pv-EI, 5 x 10^4 por poço (aproximadamente 1000 Pv-EI/ mm^2 da monocamada celular), foram deixados aderir a monocamada de células endoteliais (HLEC e SBEC-1D) durante 1 h a 37ºC. Resultados são expressos como a média de eritrócidos aderidos por mm^2 (EI / mm^2) ± desvio padrão de 4 poços.

Após inúmeros testes, chegamos à conclusão de que uma concentração de 45% de *Percoll*® em RPMI é a ideal para a separação de Pv-EI (Figura 12). Para assegurar que o enriquecimento de formas maduras ocorre e para excluir a hipótese de que os antígenos de superfície poderiam ser danificados pelo *Percoll*®, foram realizados ensaios de imunofluorescência a partir do material enriquecido. Os anticorpos monoclonais 3F8 e K23 reconhecem epítopos conformacionais da MSP-1_{19} de *P. vivax,* mas após a denaturação da proteína em DTT (Dithiothreitol), o reconhecimento não é observado (Bargieri *et al*., 2008). A Figura 15 mostra que tais anticorpos reconheceram cerca de 80-

90% das células marcadas também com DAPI. Estes dados demonstraram claramente que o enriquecimento preserva a estrutura conformacional dos epítopos de superfície e, sendo a MSP-1_{19} uma proteína expressa tardiamente em relação ao ciclo parasitário, formas maduras como trofozoítos e esquizontes são as fases principalmente encontradas.

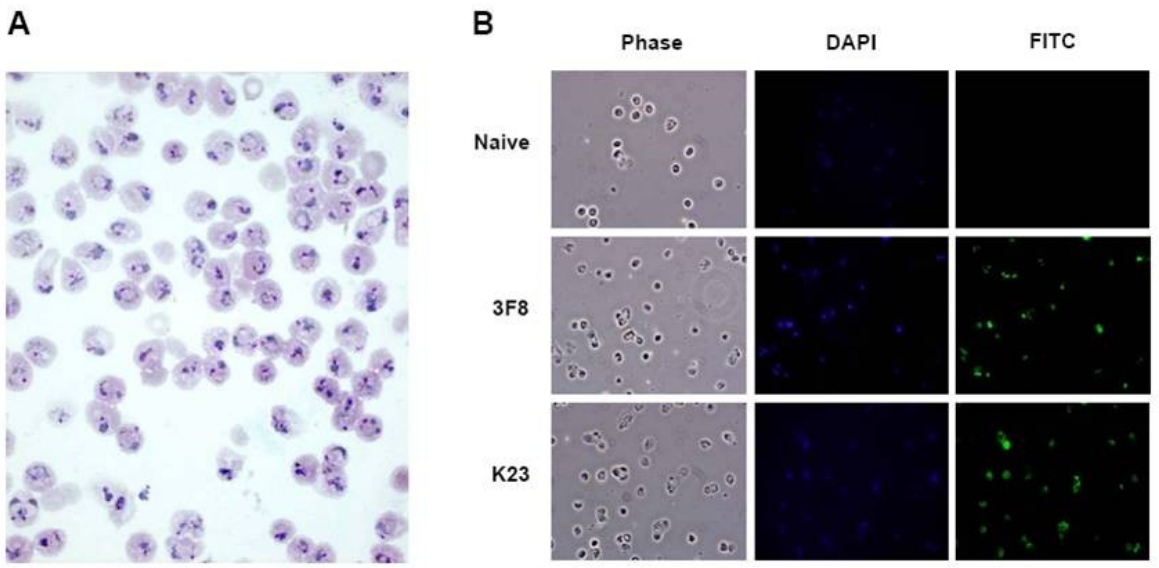

Figura 15. Gradiente de *Percoll*® a 45% leva a um alto enriquecimento de formas maduras de *P. vivax,* preservando a estrutura dos antígenos da superfície. **(A)** Coloração por Giemsa de Pv-EI após enriquecimento em *Percoll*® 45% evidenciando a alta porcentagem de enriquecimento (85-97%) de formas maduras; e **(B)** reconhecimento de formas maduras por IFA usando MABs anti-vivax-MSP-1_{19} (3F8 e K23) diluídos 1:50. Soro de camundongo imunizado apenas com adjuvante foi utilizado como controle negativo.

Com o intuito de determinar a natureza do ligante parasitário e dos receptores endoteliais possivelmente envolvidos na adesão de Pv-EI, diversos ensaios de citoadesão foram realizados a partir de Pv-EI coletados de diferentes pacientes, na presença ou não, de competidores ou inibidores para a adesão aos receptores CSA e CD36 (CSA solúvel e anti-CD36) e após tratamento, ou não, com tripsina. Conforme exposto na Tabela 2, Pv-EI enriquecidos coletados de todos os pacientes testados exibiram algum nível de adesão em HLEC ou SBEC-Sc1D.

Tabela 2. Adesão de Pv-EI e Pf-EI coletados de 24 pacientes.

		HLEC					SBEC				Placenta	
		Adesão [a]	% Inibição [b]				Adesão [a]	% Inibição [b]			Adesão [a]	% Inibição [b]
Parasita	Paciente		Tripsina	+sCSA	+αCD36	CaseABC		Tripsina	+sCSA	+αCD36		+sCSA
Pv-iE	008						**58.2±9.8**	19±10				
Pv-iE	015						**32.4±11.04**	52±11*				
Pv-iE	016	**52.4±8.5**	70±7*									
Pv-iE	019	**36.1±10.6**	59±10**	25±21								
Pv-iE	021						**30.6±3.7**	74±7**	63±10**	20±12		
Pv-iE	022	**28.3±4.5**	29±21**	52±8**	2±27							
Pv-iE	023	**57.8±5.5**	85±6**	81±7**	38±20							
Pv-iE	024	**33.9±3.7**	76±7**	65±8**	20±11							
Pv-iE	030	**16.6±3.4**	46±10***				**12.8±2.8**	42±18*				
Pv-iE	031	**26.1±4.5**	47±15***									
Pv-iE	034	**56.7±7.4**		18±10*			**49.5±7.9**		28±9*			
Pv-iE	035	**37.5±9.4**		41±13**			**23.9±8.0**		31±30			
Pv-iE	036										**22.3±5.4**	23±19
Pv-iE	063										**20.4±4.4**	30±12*
Pv-iE	065	**33.5±8.8**		51±13***								
Pv-iE	066										**9.9±3.2**	15±40
Pv-iE	076	**19.7±4.0**		34±18***		7±25						
Pv-iE	083	**38.6±7.3**		49±15**		4±21						
Pv-iE	086	**30.1±6.5**		40±16**		13±22						
Pv-iE	087	**41.3±5.2**		16±23		3±15						
Pf-iE	002	**130.1±23.7**										
Pf-iE	003	**636.7±119.2**										
Pf-iE	005										**773.5±179.5**	87±7*
Pf-iE	008	**454.4±45.4**										

[a] Média de EI aderidos / mm^2 (± desvio padrão) normalizados para um *input* de 10^3 EI / mm^2.

[b] Porcentagem de inibição da adesão (± desvio padrão) por CSA solúvel, anti-CD36 ou Condroitinase ABC (CaseABC)..

* 0,05>p>0,01 , ** 0,01>p>0,001 , *** p<0,001

A Tabela 2 resume a inibição da adesão como uma porcentagem de controle, das amostras testadas para ambas as células endoteliais em várias condições inibitórias. Quando Pv-EI foram incubados na presença de CSA solúvel, uma alta inibição de adesão (45,8 a 80,0%) foi verificada em amostras coletadas a partir de quase todos os pacientes, menos # 34 (18,0%, p <0,05). Em contraste, a adesão na presença de anti-CD36 não sofreu influência significativa, assim, o CD36 parece não ser o receptor majoritário na adesão de Pv-EI. Ainda, o tratamento com tripsina diminuiu a capacidade adesiva de Pv-EI em níveis significativos para quase todos os pacientes, exceto para o indivíduo # 08. Importante notar que em alguns casos a adesão de Pv-EI tratados com tripsina foi até 4 vezes inferior ao controle não tratado. O fato da adesão de Pv-EI ser inibida em diferentes níveis pela tripsina corrobora com a observação de que os antígenos VIR da superfície de Pv-EI, diferentemente dos *var* genes de *P. falciparum*, não são clonalmente expressos (Del Portillo *et al*., 2001; Fernandez-Becerra *et al*., 2005), isto é, mais de um antígeno está expresso em determinado período em uma mesma célula. Caso os antígenos VIR estejam envolvidos na adesão, este mecanismo de expressão não clonal poderia explicar as diferentes sensibilidades à tripsina observadas.

Conforme mostrado na Figura 16 e na Tabela 2, Pv-EI recolhidos a partir de 3 indivíduos testados (# 36, # 63 e # 66) foram capazes de aderir aos criocortes de placenta em níveis semelhantes aos ensaios com células endoteliais (Tabela 2). Porém, a presença de CSA solúvel inibiu significativamente a adesão (30%±12) apenas da amostra # 63.

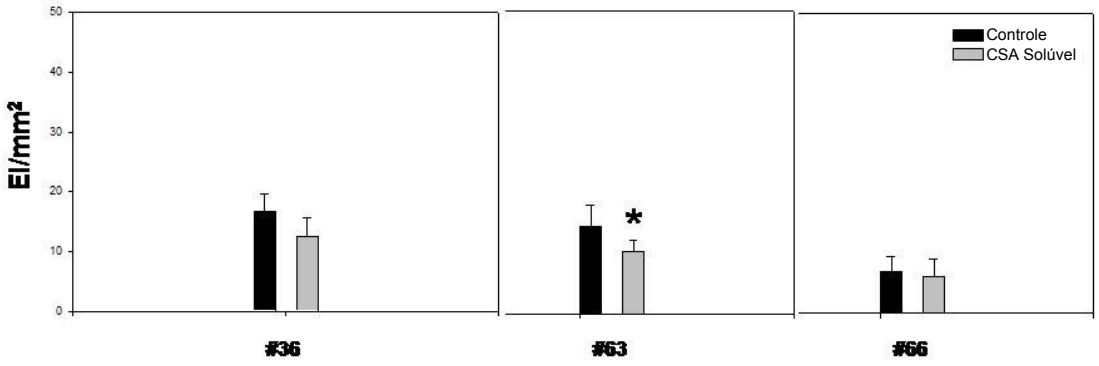

Figura 16. Adesão estática de Pv-EI em cortes histológicos de placenta humana. Pv-EI ($5x10^4$) foram incubados por 1h a 37°C com os criocortes de placenta, previamente demarcados por caneta hidrofóbica, e então lavados extensivamente. O número de eritrócitos aderidos foi expresso como uma média / mm^2 ± desvio padrão de três a quatro cortes. * $p < 0.05$.

Com o intuito de elucidar o papel da CSA como possível receptor na adesão de Pv-EI então observada, realizamos ensaios na presença de outro glicosaminoglicano solúvel, a CSB e, alternativamente, as células endoteliais foram tratadas com condroitinase ABC antes da adesão. Ensaios preliminares foram realizados com o isolado *P. falciparum* FCR3 paneado para a CSA ($FCR3^{CSA}$), mantido em cultura. Como mostra a Figura 17, o tratamento com Condroitinase ABC bloqueou completamente a adesão de $FCR3^{CSA}$. Em relação à CSB solúvel, altos níveis de inibição não eram esperados, no entanto, a CSB inibiu significativamente a adesão do $FCR3^{CSA}$ e de Pv-EI nos mesmos níveis da CSA solúvel (Figuras 17 e 18). Estes achados indicam uma possível adesão não específica para a CSA até mesmo no fenótipo parasitário monofenotípico ligante a este receptor. Outras explicações seriam possíveis, como a contaminação por CSA no extrato de CSB ou, o fato de ambas as moléculas apresentarem estruturas tão similares que a CSB se torna capaz de competir pelos mesmos domínios antigênicos envolvidos na adesão à CSA.

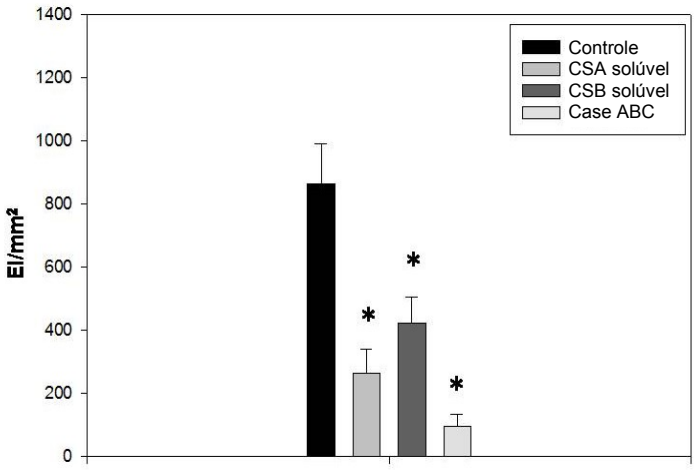

Figura 17. Adesão estática de FCR3^{CSA} em HLEC. Pf-EI (5x10^4 / poço) foram incubados por 1h a 37°C com HLEC, na presença de CSA ou CSB solúveis, ou ainda, em HLEC previamente tratadas com condroitinase ABC (Case ABC). O número de eritrócitos aderidos foi expresso como uma média / mm^2 ± desvio padrão de quatro poços. * $p < 0.05$.

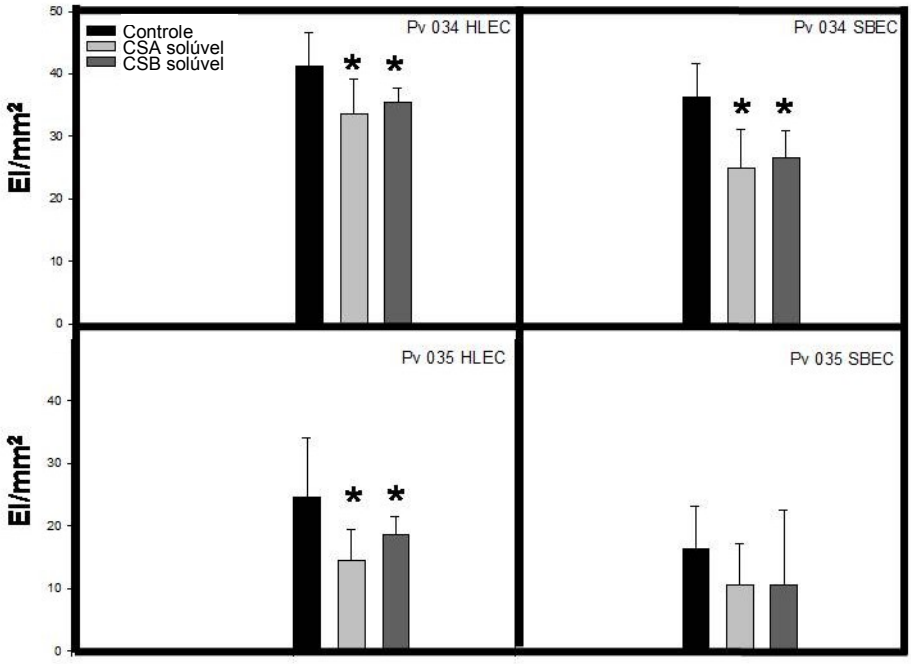

Figura 18. Adesão estática de Pv-EI em células endoteliais na presença dos inibidores CSA ou CSB solúveis. Em todos os casos 5x10^4 Pv-EI foram incubados por 1h a 37°C com HLEC ou SBEC-1D e, comparativamente, na presença de CSA ou CSB solúveis como descrito nos materiais e métodos. As lâminas foram lavadas extensivamente e o número de eritrócitos aderidos contados foi expresso como uma média / mm^2 ± desvio padrão de quatro poços. * $p < 0.05$.

Ainda tentando elucidar o envolvimento da CSA como receptor da adesão de Pv-EI, novos ensaios foram realizados utilizando células tratadas por Condroitinase ABC. Como mostra a Figura 19, Pv-EI de 4 pacientes foram utilizados em ensaios de inibição com CSA solúvel paralelamente ao tratamento com Condroitinase ABC. Como observado, ao passo que a CSA solúvel inibiu todas as amostras testadas (15 - 49%), o tratamento prévio com Condroitinase ABC inibiu a adesão no máximo em 13%, sugerindo assim que a CSA não está diretamente envolvida na aderência parasitária. De fato, como a CSA é altamente carregada negativamente devido à presença de sulfato, a inibição da adesão poderia ser sustentada apenas por interações não específicas. O fato de que a adesão de Pv-EI mostrar-se menos expressiva que a adesão de Pf-EI pode ser a explicação para tal interferência inespecífica ser constatada apenas em Pv-EI.

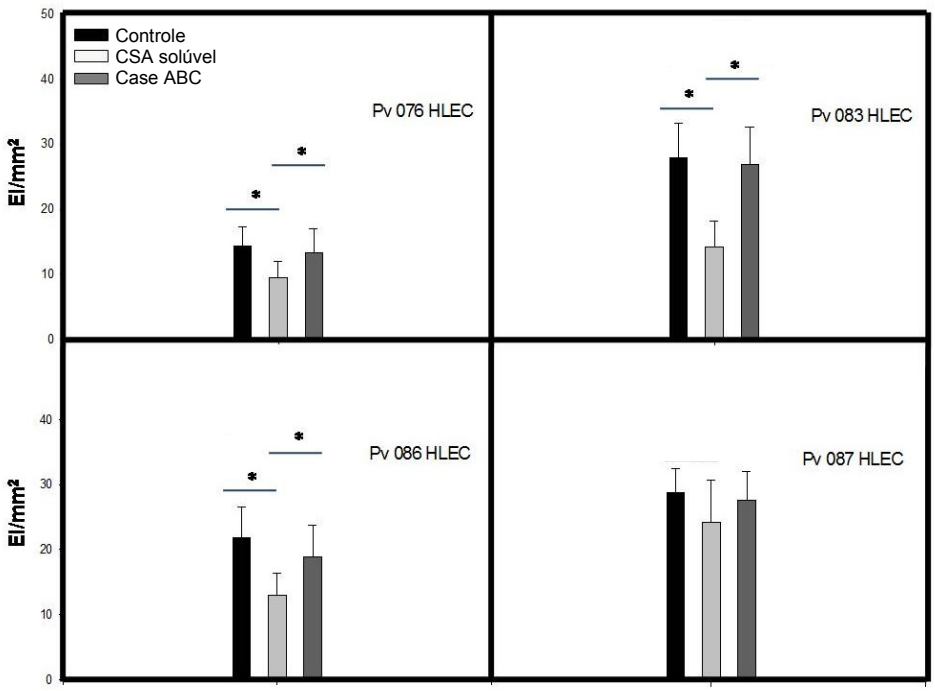

Figura 19. CSA parece não estar diretamente envolvida na adesão de Pv-EI. Eritrocitos infectados coletados dos pacientes #76, #83, #86 e #87 foram incubados com HLEC pré-tratadas com Condroitinase ABC (Case ABC) ou na presença de CSA solúvel como descrito nos materiais e métodos. Como controle positivo a incubção de Pv-EI foi relaizada em HLEC não tratada e na ausência de competidores solúveis. Os resultados foram expressos como média de Pv-EI aderidos / mm^2 ± desvio padrão de quatro poços. * $p < 0.05$.

Em seguida, utilizamos células CHO transfectadas com CD36 ou ICAM-1 nos ensaios de adesão estática de 3 pacientes infectados por *P. vivax* (#98, #100 e #101). Células CHO-745 não transfectadas foram utilizadas como controle negativo, por apresentarem apenas expressão basal de alguns receptores. Como mostra a Figura 20, as 3 amostras testadas não apresentaram capacidade de ligação ao CD36, já que os níveis da adesão observada para a célula CHO-CD36 equiparam-se aos da adesão em célula não transfectada (CHO-745). Em contrapartida, foi observado um aumento da adesão (2,7 e 2,1 vezes) em CHO-ICAM-1 para as amostras #100 e #101 em relação ao controle CHO-745 (Figura 20), indicando um possível envolvimento do receptor ICAM-1 na adesão de Pv-EI.

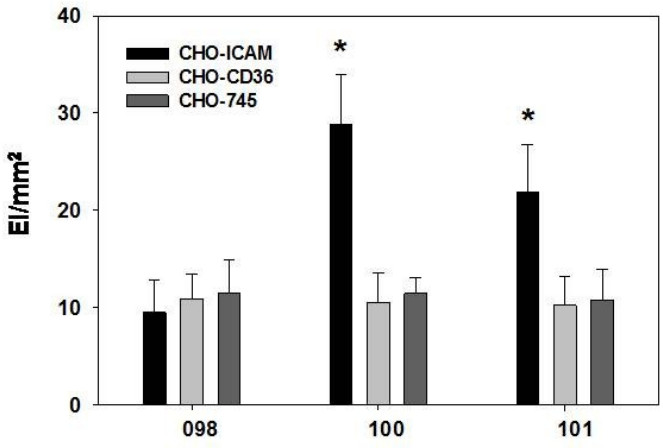

Figura 20. Ensaios de adesão de Pv-EI em CHO transfectadas. A adesão em CHO-CD36 apresenta os mesmos níveis basais da adesão em CHO-745 não transfectada. Foi observado aumento da adesão (2,7 e 2,1 vezes) em CHO-ICAM-1 para as amostras #100 e #101. Os resultados foram expressos como média de EI aderidos / mm^2 ± desvio padrão de quatro poços. *$p < 0.05$.

A adesão parasitária em todos os ensaios descritos foi visualizada com auxílio de microscópio e corando-se com Giemsa cada lâmina após o ensaio de adesão. Constatamos que Pv-EI eram obrigatoriamente encontrados em associação direta com as células endoteliais, como mostra a Figura 21.

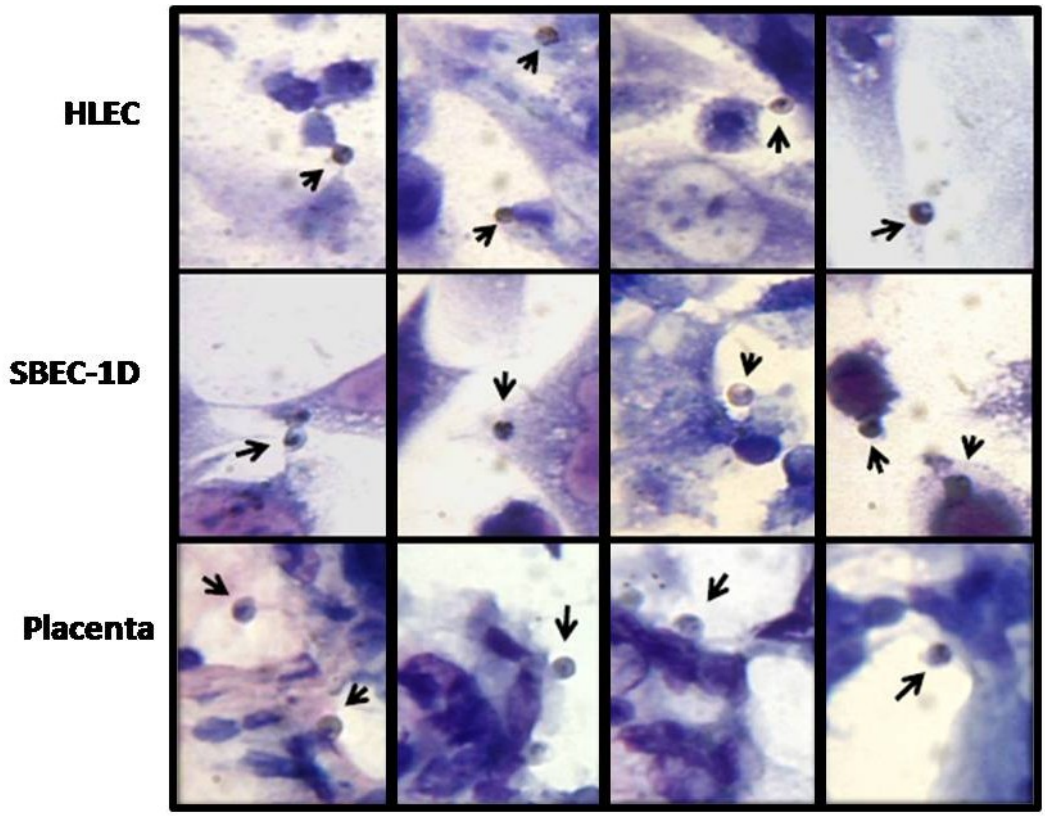

Figura 21. Fotomicrografias de Pv-EI aderidos em HLEC, SBEC-1D e cortes histológicos de placenta. As lâminas pós adesão foram coradas com Giemsa e visualizadas com o auxílio de microscópio Nikon, aumento de 100X.

Como a capacidade adesiva de formas maduras de *P. falciparum* está amplamente descrita, realizamos ensaios de adesão a partir de indivíduos infectados por *P. falciparum*, para efeito comparativo. Também buscamos caracterizar alguns fenótipos citoadesivos do *P. falciparum* da Amazônia Brasileira, e observar se apresentam os mesmos fenótipos adesivos descritos para populações Africanas ou Asiáticas do parasita. Foi mostrado que *var* genes de *P. falciparum* da Amazônia apresenta pouca diversidade quando comparados com *P. falciparum* provenientes de outras regiões do mundo (Albrecht *et al*, 2010). Algumas hipóteses levantadas sugerem que tal característica poderia levar a uma menor quantidade de fenótipos adesivos, e explicar a menor virulência aparente em relação aos parasitas encontrados na África e Ásia. Pf-EI provenientes de 4 indivíduos foram enriquecidos em gradiente de *Percoll*® 45%, como

nos ensaios com Pv-EI. Como esperado, os ensaios de adesão com Pf-EI em HLEC revelaram uma média de 300 EI / mm^2 para HLEC, correspondentes a 90, 480 e 328 EI / mm^2, respectivamente para os pacientes # 02, # 03 e # 08 (Figura 22A). Esta adesão é quase 10 vezes superior aos níveis observados para Pv-EI.

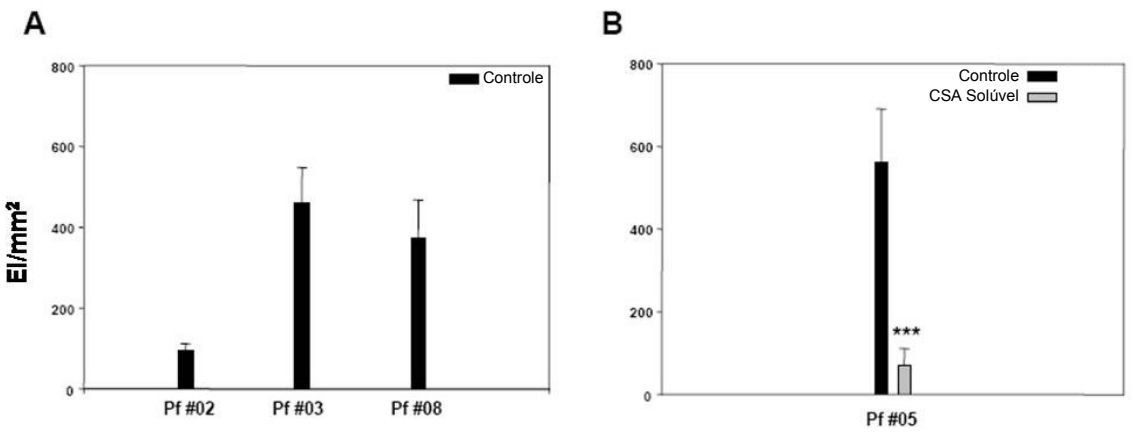

Figura 22. Ensaios de adesão com eritrócitos coletados de pacientes infectados por *P. falciparum*. Pf-EI (5 x 10^4/poço) coletados dos pacientes Pf#02, Pf#03 e Pf#8 **(A)** e Pf#05 **(B)** foram depositados em HLEC **(A)** ou cortes de placenta **(B)**, respectivamente e, para um dos pacientes (Pf#5), também na presença de CSA solúvel. Os resultados foram expressos como média de Pf-EI aderidos / mm^2 ± desvio padrão de quatro poços. *** $P < 0.001$.

Ainda, o ensaio em criocorte de placenta com Pf-EI recolhidos a partir do paciente # 05 revelou o maior número de EI / mm^2 (569); e a CSA solúvel inibiu significativamente e em altos níveis (87,3%; Figura 22B). Esta alta inibição pela CSA sugere que o *P. falciparum* amazônico é capaz de se ligar à CSA, porém apenas um paciente foi testado. Não conseguimos ter acesso a muitos casos de infecções por *P. falciparum*, o que impossibilitou os estudos dos fenótipos do parasita amazônico durante este estudo. Assim, o foco foi mantido nas análises da adesão de *P. vivax,* e os dados provenientes da adesão de isolados naturais de *P. falciparum* serviram apenas como comparação entre as duas espécies.

O fato da adesão de P. vivax mostrar-se cerca de 10 vezes menor que a apresentada por *P. falciparum*, sugere que apenas uma pequena parte da população de Pv-EI é capaz de interagir com o endotélio. A retenção de *P. vivax* na microvasculatura, sendo parcial, poderia explicar porque formas maduras de Pv-EI são encontradas no sangue periférico dos pacientes infectados. Ainda, esta menor adesão apresentada poderia ser explicada pela participação de uma menor proporção de estágios do desenvolvimento intra-eritrocítico, como por exemplo, esquizontes. De fato, o sequestro de esquizontes já havia sido sugerido por Field & Shute, em 1956. Para verificar o quanto formas extremamente maduras, como esquizontes, estariam associadas a uma maior capacidade adesiva, ensaios de citoadesão estática foram conduzidos em HLEC, utilizando-se Pv-EI enriquecidos e que passaram, ou não, por processo de amadurecimento *in vitro.* De fato, após 5h de incubação em meio de cultura (período de amadurecimento), um maior número de esquizontes foi observado e, como é mostrado na Figura 23, o amadurecimento aumentou a adesão em até 3,7 vezes (#153). Porém, Pv-EI provenientes de outros pacientes não se desenvolveram durante o precesso de amadurecimento *in vitro,* por isso decidimos permanecer a conduzir os ensaios a partir de isolados frescos.

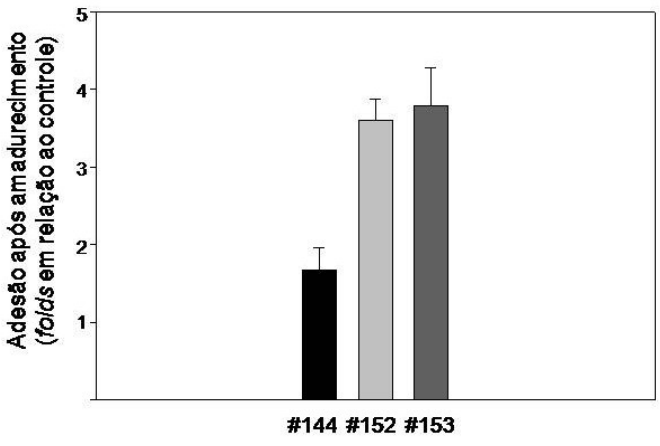

Figura 23. Ensaio de citoadesão após 5h de amadurecimento *in vitro.* Após enriquecimento em *Percoll*, os eritrócitos foram mantidos a 37ºC por 5h em RPMI contendo 20% de plasma AB^+. Os Pv-EI ($5x10^4$) foram então incubados com HLEC por 1h a 37°C. Como controle, parte dos Pv-EI enriquecidos foram utilizados em um ensaio de adesão previamente ao amadurecimento. Os resultados foram expressos como uma representação do aumento do número de Pv-EI aderidos após amadurecimento em relação à adesão conduzida no tempo zero (controle não amadurecido).

Observada a citoadesão de Pv-EI em ensaios estáticos, buscamos verificar se a mesma adesão poderia ser sustentada em sistema que mimetiza o fluxo sanguíneo, em diferentes condições de pressão. Realizamos ensaios de adesão com Pv-EI recolhidos a partir de 7 indivíduos (Tabela 3). Após incubação estática, a lavagem foi realizada com meio de cultura, porém, em sistema de fluxo. A Tabela 3 mostra que a adesão de Pv-EI suporta a pressão de forma equivalente a Pf-EI. Além disso, como tem sido relatado que as complicações da malária vivax ocorrem normalmente após tratamento com drogas antimaláricas e que *P. vivax* infectados apresentam altos níveis de TNF-α (Karunaweera *et al*., 1992; Wijesekera *et al*., 1996, Singh *et al*., 2000; Tan *et al*., 2008), levantou-se a questão de saber se a destruição parasitária, com aumento nos níveis de citocinas pró-inflamatórias, poderia levar a um aumento da expressão dos níveis de ICAM-1, permitindo então, uma maior adesão parasitária ao endotélio. Assim, HLEC foram tratadas com LPS previamente aos ensaios de citoadesão, para estimular um padrão inflamatório. Conforme mostrado na Figura 24, Pv-EI provenientes dos pacientes #104 e #106 foram capazes de sustentar a adesão em sistema que mimetiza o fluxo sanguíneo e o estímulo por LPS aumentou a força da adesão às células endoteliais (Figura 24 e Tabela 3), provavelmente pelo aumento dos níveis de ICAM-1. De fato, análises por citometria de fluxo mostraram que o LPS é capaz de aumentar a expressão de ICAM-1 (Figura 25).

Tabela 3. Adesão, em sistema de fluxo, de Pv-EI coletados de 7 pacientes; ou Pf-EI paneados para CSA (FCR3^{CSA}). A força de ligação da adesão de FCR3^{CSA} aqui exposta apresentou alta reprodutibilidade e é representativa da adesão descrita na literatura para diferentes isolados de Pf-EI em condições de fluxo.

Shear stress (Pa)			0.00	0.09		0.36		1.44	
			Adesão [a]	Adesão [a]	(%) [b]	Adesão [a]	(%) [b]	Adesão [a]	(%) [b]
Parasita	**Paciente**	**LPS**							
Pv-iE	090	-	67.4±14.4	34.2 ±8.6	50.8	30.4 ±9.6	45.2	ND	
Pv-iE	090	+	55.6 ±9.6	48.0 ±17.8	86.3	42.7 ±15.4	76.9	ND	
Pv-iE	091	+	53.0 ±6.1	39.0 ±7.7	73.6	38.5 ±10.1	72.6	ND	
Pv-iE	092	-	17.6 ±9.6	13.4 ±8.2	76.1	10.8 ±2.9	61.1	ND	
Pv-iE	093	-	47.9 ±12.0	29.9 ±8.2	62.4	ND		ND	
Pv-iE	094	-	60.4 ±13.8	51.3 ±9.1	84.9	ND		ND	
Pv-iE	104	-	30.4 ±9.1	26.3 ±5.3	86.5	16.1 ±5.3	52.9	9.2 ±7.7	30.3
Pv-iE	104	+	32.5 ±13.8	25.0 ±5.3	76.9	24.6 ±5.3	75.7	16.4 ±6.7	50.5
Pv-iE	106	-	28.6 ±8.6	20.5 ±14.9	71.7	19.8 ±6.1	69.2	6.8 ±5.8	23.8
Pv-iE	106	+	29.1 ±8.2	27.9 ±10.6	96.2	23.6 ±7.2	81.1	16.4 ±6.7	56.4
Pf-iE	FCR3^{CSA}	-	370.9±50.9	333.1±25.0	89.8	294.5±36.9	79.4	190.8±34.7	51.4

[a] Adesão expressa em EI / mm^2 (± desvio padrão) normalizados para um *input* de 10^3 EI por mm^2 de HLEC estimulada (+) ou não (-) por 1 µg/mL de LPS.

[b] Porcentagem de eritrócitos que permanaceram citoaderidos após diferentes *shear stress*.

ND Adesão não foi determinada.

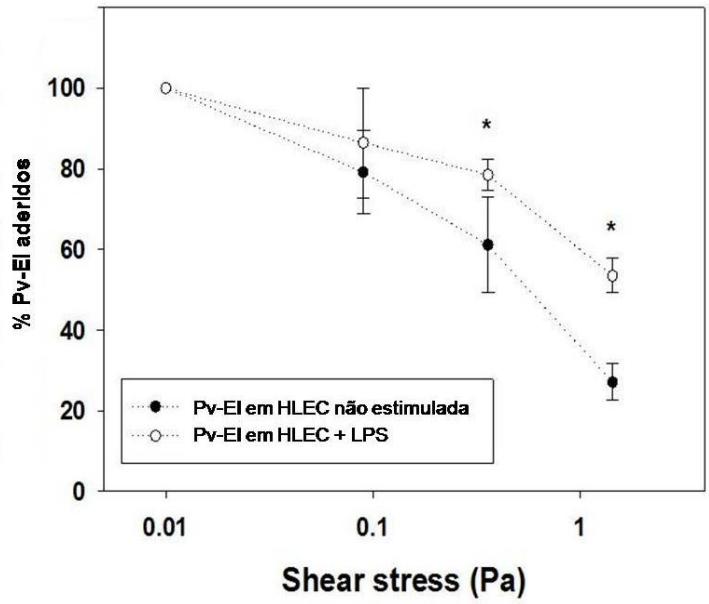

Figura 24. Ensaio de citoadesão em sistema de fluxo: Pv-El sustentam adesão em diferentes *shear stress.* Pv-El (5 x 10^5) foram incubados com HLEC (aproximadamente 1000 Pv-El / mm^2 da monocamada celular) por 1h a 37°C (*shear stress* 0.00). As lâminas foram então acopladas na câmara do sistema de fluxo por onde passa meio de citoadesão (RPMI pH6,8) com pressão controlada (*shear stress* de 0.09, 0.36 e 1.44 Pascal). Pv-El que restaram aderidos foram contados em 20 campos selecionados aleatoriamente e os resultados foram expressos como uma porcentagem em relação à adesão em pressão zero (*shear stress* 0.00), como média de 2 pacientes (#104 e #105) ± desvio padrão. * $p < 0.05$.

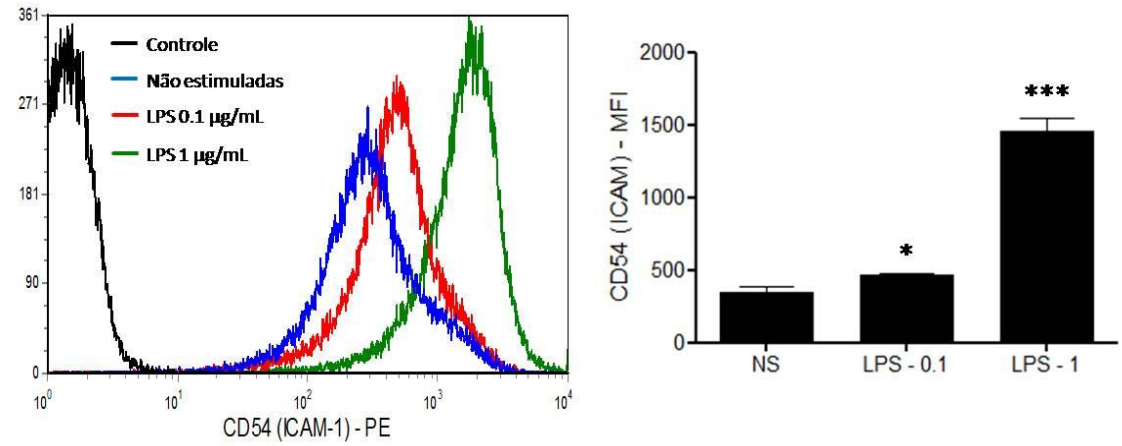

Figura 25 . Avaliação da expressão de ICAM-1 em células endoteliais após estímulo por LPS. 1 x 10^6 HLEC tratadas ou não com LPS (1.0 µg/mL), foram pré-incubadas com anti-CD54 (ICAM-1) por 30 min a 4°C, lavadas e então fixadas em formaldeído 2%. As análises de citometria de fluxo foram feitas em FACScanto (BD).

O padrão de expressão de alguns receptores como CD36, ICAM-1 e E-Selectina foi caracterizado, através de citometria de fluxo, para cada célula testada. Como mostra a Tabela 4, 99,8% das HLEC expressam ICAM-1 em condições normais, logo, o aumento da intensidade de fluorescência (MIF) observado na Figura 25 representa uma maior expressão de ICAM-1 por célula, o que pode, por sua vez, ter fortalecido a interação entre Pv-EI e células endoteliais.

	CD36		CD54		CD62E	
Cell	%	MFI	%	MFI	%	MFI
CHO-745	0.73	9.4	0.77	15.42	1.66	10.16
CHO-CD36	49.1	66.0	6.96	14.28	25.9	14.8
CHO-ICAM	5.44	12.8	77.6	35.7	33.3	20.8
HLEC	0.8	11.2	99.8	345.8	43.9	9.4
SBEC	1.8	19.6	99.6	414.5	27.7	11.2

Tabela 4. Caracterização da expressão de receptores endoteliais das células utilizadas. As células foram marcadas por anticorpos contra CD36, ou CD54 (ICAM-1), ou CD62E (E-Selectina) e analisadas em citômetro de fluxo. Os resultados foram expressos indicando a porcentagem (%) das células que expressavam cada um dos receptores, além da intensidade de fluorescência detectada (MIF).

De modo geral, nossos dados indicam claramente que Pv-EI podem sustentar adesão avaliada com base nos ensaios estáticos e de fluxo, embora Pf-EI coletados de pacientes infectados tenham exibido níveis de adesão 10 vezes maior em comparação aos níveis de adesão de Pv-EI (Tabelas 2 e 3). No entanto, a força de ligação induzida por Pv-EI parece não diferir de Pf-EI (Tabela 3). Além disso, a exposição das células ao LPS aumentou a força da adesão de Pv-EI (Figura 24). Estes dados podem explicar não só o número relativamente menor de casos de complicações nas infecções por *P. vivax*

quando comparados com *P. falciparum*, mas também trazer à luz a discussão de que o tratamento com drogas antimaláricas pode destruir o parasita e, por sua vez, ativar o sistema imunológico aumentando os níveis de citocinas que induzem a expressão de receptores endoteliais, como ICAM-1.

Os ensaios acima descritos se resumem em uma incubação estática dos eritrócitos com as lâminas contendo as células endoteliais, que foram então adaptadas ao sistema de fluxo para avaliar a capacidade de sustentação da adesão e a força de ligação dos eritrócitos às células. Porém, foram feitos outros ensaios de adesão de Pv-EI em HLEC, diretamente em sistema de fluxo a 0.09 ou a 0.36 Pascal. Estes ensaios foram filmados em tempo real (*movies* 1 e 2, respectivamente), e a adesão observada se mostrou semelhante à de formas maduras de *P. falciparum* (movie 3). Os filmes estão disponíveis nos web sites:

http://www.ib.unicamp.br/dep_parasitologia/parasit/Costa_FTM/Movie1.mpg;

http://www.ib.unicamp.br/dep_parasitologia/parasit/Costa_FTM/Movie2.mpg;

http://www.ib.unicamp.br/dep_parasitologia/parasit/Costa_FTM/Movie3.mpg.

Como já mencionado, em *P. falciparum*, a PfEMP-1, codificada por uma família gênica variante denominada *var*, está associada com a adesão parasitária em vários receptores endoteliais (Scherf *et al.,* 2001; Andrews *et al*., 2002). No entanto, uma superfamília gênica variante também foi encontrada em *P. vivax*. Esta superfamília multigene, denominada *vir*, foi subdividida em 12 subfamílias (A-L) e parte dos antígenos correspondentes VIR foram encontrados expressos na superfície de Pv-EI, mas de uma forma não clonal (Del Portillo *et al*., 2001; Fernandez-Becerra *et al*., 2005). Assim, buscamos verificar se os antígenos VIR estariam envolvidos na citoadesão de Pv-EI. Foram utilizados soros de camundongos imunizados com proteínas de fusão VIRA4 ou VIRE5 – GST (Oliveira *et al*., 2006). Como controle negativo, camundongos foram imunizados apenas com adjuvante, e como controle de especificidade, camundongos foram imunizados com a proteína GST. Como mostrado na Figura 26A, os soros anti VIRA4 e VIRE5 foram capazes de reconhecer Pv-EI recolhidos a partir dos 2 pacientes testados nesta etapa (# 95 e # 96). Conforme mostrado na Figura 26B, os soros anti VIRA4 e VIRE5 inibiram significativamente a adesão de Pv-EI em comparação com o soro anti-GST, demonstrando assim a especificidade e sugerindo o envolvimento dos antígenos VIR na citoadesão parasitária.

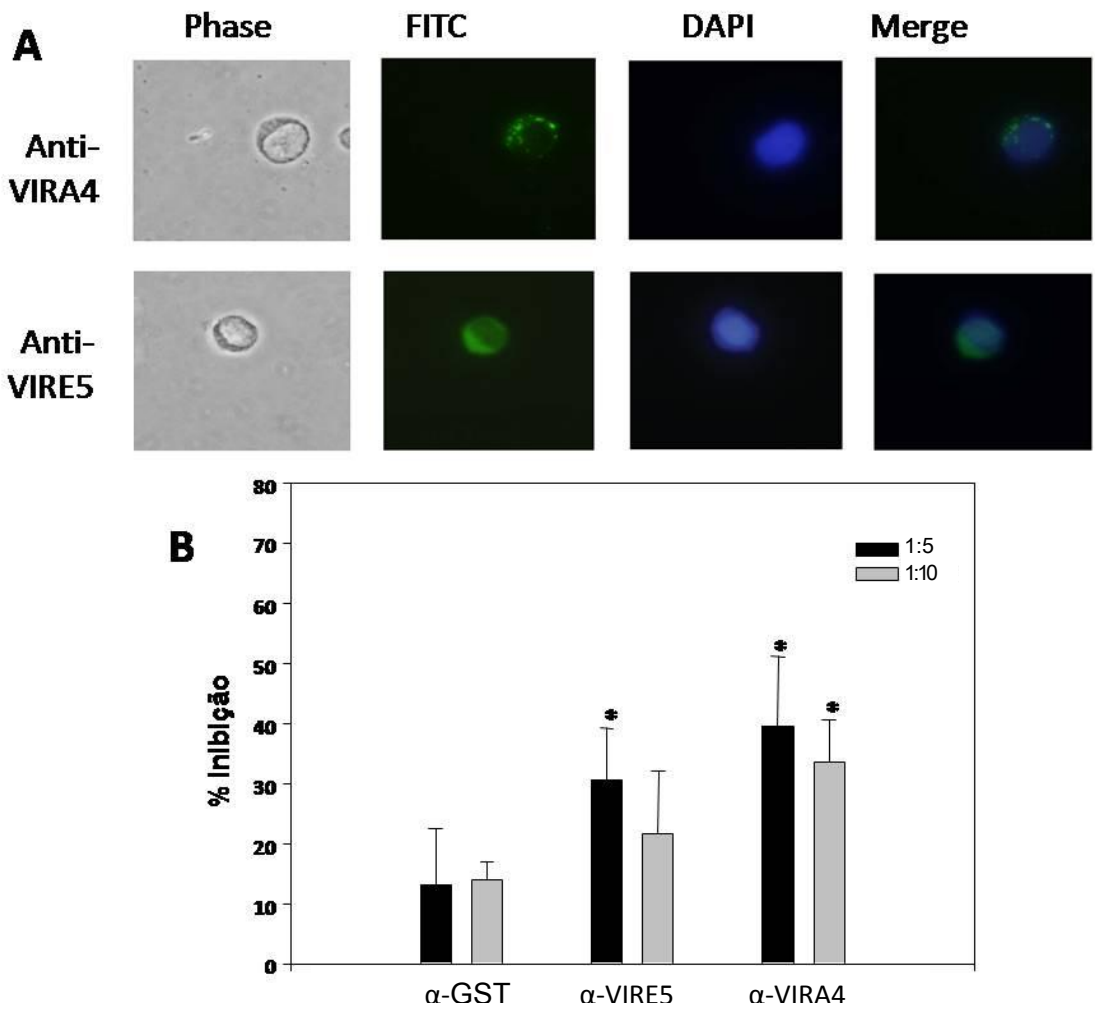

Figura 26. Antígenos VIR envolvidos na citoadesão de Pv-EI. (A) Reconhecimento em IFA de estágios maduros enriquecidos em *Percoll®.* Soro anti VIRA4 e anti VIRE5 (1:50) induzido após imunização de camundongos com as proteínas de fusão VIRA4-GST e VIRE5-GST. Soro de camundongos imunizados apenas com adjuvante foi utilizado como controle negativo. **(B)** Pv-EI (5 x 10^4/poço) foram incubados por 1h a 37°C na presença ou não dos soros anti VIRA4-GST e VIRE5-GST 1:5 (paciente #95), ou 1:10 (paciente #96). Soro de animais imunizados apenas com adjuvante ou com a proteína GST foram utilizados como controle negativo ou controle da especifidade, respectivamente. Para estes ensaios, a inibição foi determinada como porcentagem em relação ao controle negativo e foi expressa pela média ± desvio padrão de 4 poços. $p< 0.05$.

Importante ressaltar que, embora não se tenha identificado a função de tais antígenos, foi demonstrada homologia entre *vir* genes de *P. vivax* e genes variantes de outras espécies de plasmódios, sendo esta superfamília recentemente descrita como a maior superfamília multigênica presente no gênero *Plasmodium*, e então denominada *pir* genes (*Plasmodium* Interspersed Repeats; Janssen *et al*., 2004). Ainda, recentemente foi proposto que antígenos VIR estão envolvidos na adesão de Pv-EI no baço, protegendo o parasita contra o ataque de macrófagos (Fernandez-Becerra *et al*., 2009). No entanto, não há evidências diretas de que ocorra o sequestro na microvasculatura ou a adesão no baço, o que não são hipóteses mutuamente exclusivas. O fato de Pv-EI apresentar potencial de ligação a receptores endoteliais reforça ambas as hipóteses. É importante frisar que outros ligantes parasitários não podem ser excluídos.

Conclusões

Os resultados aqui apresentados sugerem fortemente que:

i. Eritrócitos infectados por *Plasmodium vivax* são capazes, em ensaios *ex vivo*, de citoaderir à superfície de células endoteliais e cortes criopreservados de palcenta humana.

ii. A adesão parece estar relacionada com formas extremamente maduras (esquizontes).

Além disso, nossos dados dos diferentes níveis de inibição pela tripsina corroboram com a idéia de mais de um ligante parasitário envolvido na adesão, ou talvez um grupo deles, como sugerido por del Portilho e colaboradores em 2004, em relação à adesão no baço e aos antígenos VIR, cuja expressão não é clonal (Fernandez-Becerra *et al.*, 2005). Soro de animais imunizados com antígenos VIR foi capaz de reconhecer Pv-EI e inibir significativamente a adesão, evidenciando que:

iii. Antígenos VIR parecem ter papel fundamental na adesão de Pv-EI.

No entanto, ainda não se sabe quais mecanismos o *P. vivax* utiliza para escapar do apuramento no baço e estabelecer uma infecção crônica, assim como não há evidências diretas de que ocorra o sequestro na microvasculatura ou a adesão no baço, o que não são hipóteses mutuamente exclusivas.

Corroborando com relatos clínicos, é bastante plausível que um microambiente inflamatório, originado por uma infecção de base ou mesmo pelo início do tratamento quimioterápico, possa modular o endotélio e favorecer a adesão de Pv-EI, o que, por sua vez, potencializaria ainda mais a resposta inflamatória local. Assim, com a prevalência de fenótipos resistentes e destruição parcial da população de parasitas durante o tratamento quimioterápico, poderia estar potencializando a virulência de *P. vivax* e evidenciando aspectos patológicos antes ignorados. Esta hipótese permanece por ser testada futuramente. No entanto, o estímulo prévio por LPS induziu uma maior expressão de ICAM-1 em HLEC o que parece estar associado com uma maior força de ligação de Pv-

EI. Células CHO transfectadas com ICAM-1 também apresentaram maior número de eritrócitos aderidos, sugerindo que:

iv. A molécula ICAM-1 é um provável receptor para a adesão de Pv-EI.

Importante, alguns plasmódios de roedores e também o *P. knowlesi,* que infecta primatas incluindo o homem, apesar de não possuírem ortólogos da PfEMP-1, são capazes de aderir ao endotélio (Coquelin *et al.* 1999; Mota *et al*. 2000; Neres *et al*. 2008; Cox-Singh *et al*., 2010). Estes achados, aliados a observações clínicas como as de Anstey e colaboradores em 2007, juntamente com o que foi mostrado no presente trabalho, são evidências fortíssimas de que a capacidade de aderir ao endotélio não está relacionada exclusivamente com a PfEMP-1. De fato, a citoadesão e seus diferentes desdobramentos fenotípicos são característicos do Gênero *Plasmodium.* Estudos filogenéticos e a descoberta de novos antígenos expressos na superfície dos eritrócitos infectados por diferentes espécies de plasmódios poderiam nos trazer maiores evidências, inclusive evolutivas.

Este trabalho abre caminho para um novo campo de estudo, até que consigamos melhor compreender as interações parasito-hospedeiro e a patologia associada, em infecções maláricas causadas pelo *P. vivax*.

Referências Bibliográficas

Aikawa M. Morphological changes in erythrocytes induced by malarial parasites. Biol Cell. 1988;64(2):173-81.

Albrecht L, Castiñeiras C, Carvalho BO, Ladeia-Andrade S, da Silva NS, Hoffmann EH, Dalla Martha RC, Costa FT, Wunderlich G. The South-American *Plasmodium falciparum* var gene repertoire is limited, highly shared and possibly lacks several antigenic types. Gene 2010. Mar 15;453(1-2):37-44.

Alger NE. Distribution of schizonts of *Plasmodium berghei* in tissues of rats, mice and hamsters. *J. Protozool.* 1963. 10, 6–10.

Allison AC. Protection Afforded by Sickle-cell Trait Against Subtertian Malarial Infection. *Br Med.* 1954. 1(4857):290-294.

Amino R, Thiberge S, Martin B, Celli S, Shorte S, Frischknecht F, Ménard R. Quantitative imaging of Plasmodium transmission from mosquito to mammal. Nat Med. 2006 Feb; 12 (2): 220-4

Anders RF & Brown GV. Vaccines against asexual blood stages of *Plasmodium falciparum*. In *New generation vaccines* 1990 (ed. G. C. Woodrow & M. M. Levine), pp. 491– 512.

Andrews KT, Lanzer M. Maternal malaria: *Plasmodium falciparum* sequestration in the placenta. Parasitol Res. 2002. 88: 715-23.

Angus BJ, Thanikkul K, Silamut K, White NJ, Udomsangpetch R. Rosette formation in *Plasmodium ovale* infection. *Am. J. Trop. Med. Hyg.* 1996. 55, 560–561.

Anstey NM, Handojo T, Pain MC, Kenangalem E, Tjitra E, Price RN, Maguire GP. Lung injury in vivax malaria: pathophysiological evidence for pulmonary vascular sequestration and posttreatment alveolar-capillary inflammation. J Infect Dis. 2007; 195:589-96.

Anstey NM, Russell B, Yeo TW, Price RN. The pathophysiology of vivax malaria. Trends Parasitol 2009; 25:220-7.

Avril M, Traore B, Costa FT, Lepolard C, Gysin J. Placenta cryosections for study of the adhesion of *Plasmodium falciparum*-infected erythrocytes to chondroitin sulfate A in flow conditions. Microbes Infect 2004; 6:249-55.

Baird JK. Neglect of *Plasmodium vivax* malaria. Trends Parasitol. 2007 Nov; 23 (11): 533-9.

Baird JK. Severe and fatal vivax malaria challenges 'benign tertian malaria' dogma. Ann Trop Paediatr. 2009 Dec;29(4):251-2.

Bargieri DY, Rosa DS, Braga CJ, Carvalho BO, Costa FT, Espíndola NM, Vaz AJ, Soares IS, Ferreira LC, Rodrigues MM. New malaria vaccine candidates based on the *Plasmodium vivax* Merozoite Surface Protein-1 and the TLR-5 agonist Salmonella Typhimurium FliC flagellin. Vaccine. 2008; 26:6132-42.

Barnwell JW, Howard RJ, Coon HG, Miller LH. Splenic requirement for antigenic variation and expression of the variant antigen on the erythrocyte membrane in cloned *Plasmodium knowlesi* malaria. *Infect. Immun.* 1983. 40, 985–994.

Berendt AR, Simmons DL, Tansey J, Newbold CI, Marsh K. Intercellular adhesion molecule-1 is an endothelial cell adhesion receptor for *Plasmodium falciparum*. Nature. 1989 Sep 7;341(6237):57-9.

Billings F and Post W. Fatal malária due to the tertian parasite. Trans. Chicago Path. Soc. 1915; 9, 209–215

Bir N, Yazdani SS, Avril M, Layez C, Gysin J, Chitnis CE. Immunogenicity of Duffy binding-like domains that bind chondroitin sulfate A and protection against pregnancy-associated malaria. Infect Immun. 2006 Oct;74(10):5955-63.

Brabin BJ. An analysis of malaria in pregnancy in Africa. Bull World Health Organ. 1983; 61(6):1005-16.

Bracho C, Dunia I, Romano M, Raposo G, De La Rosa M, Benedetti EL, Pérez HA. Caveolins and flotillin-2 are present in the blood stages of *Plasmodium vivax*. Parasitol Res. 2006 Jul;99(2):153-9. Epub 2006 Mar 7.

Bruetsch W. The histopathology of therapeutic (tertian) malaria. Am. J. Psychiatry. 1932; 12, 19–65

Chotivanich, K, Udomsangpetch R, Simpson JA, Newton P, Pukrittayakamee S, Looareesuwan S, White NJ. Parasite multiplication potential and the severity of falciparum malaria. J. Infect. Dis. 2000; 181, 1206–1209.

Coatney GR, Collins WE, Warren M, Contacos PG. The Primate Malarias. Bethesda: U.S. Department of Health, Education and Welfare; 1971.

Coquelin F, Boulard Y, Mora-Silvera E, Richard F, Chabaud AG, Landau I. Final stage of maturation of the erythrocytic schizonts of rodent Plasmodium in the lungs. C R Acad Sci III. 1999 Jan; 322(1):55-62.

Costa FT, Fusaï T, Parzy D, Sterkers Y, Torrentino M, Douki JB, Traoré B, Petres S, Scherf A, Gysin J Immunization with recombinant duffy binding-like-gamma3 induces pan-reactive and adhesion-blocking antibodies against placental chondroitin sulfate A-binding *Plasmodium falciparum* parasites. Infect Dis. 2003. 188:153-64.

Cox J, Semoff S & Hommel M. *Plasmodium chabaudi*: a rodent malaria model for *in vivo* and *in vitro* cytoadherence of malaria parasites in the absence of knobs. *Parasite Immunol.* 1987. 9, 543–561.

Cox-Singh J, Hiu J, Lucas SB, Divis PC, Zulkarnaen M, Chandran P, Wong KT, Adem P, Zaki SR, Singh B, Krishna S. Severe malaria - a case of fatal Plasmodium knowlesi infection with post-mortem findings: a case report. Malar J. 2010 Jan 11;9(1):10.

Craig A, Scherf A. Molecules on the surface of the *Plasmodium falciparum* infected erythrocyte and their role in malaria pathogenesis and immune evasion. Mol Biochem Parasitol. 2001 Jul;115(2):129-43.

Daily JP. Antimalarial drug therapy: the role of parasite biology and drug resistance. J Clin Pharmacol. 2006 Dec; 46(12):1487-97. Review.

Daniel-Ribeiro CT, Lacerda MV, Oliveira-Ferreira J. *Plasmodium vivax* malaria in the Brazilian Amazon: some aspects of its epidemiology, clinical spectrum and naturally induced immune responses. Bull Soc Pathol Exot. 2008 Jun;101(3):243-8.

David PH, Handunetti SM, Leech JH, Gamage P, Mendis KN. Rosetting: a new cytoadherence property of malaria-infected erythrocytes. *Am. J. Trop. Med. Hyg.* 1988. 38, 289–297.

David PH, Hommel M, Miller LH, Udeinya IJ, Oligino LD. Parasite sequestration in *Plasmodium falciparum* malaria: spleen and antibody modulation of cytoadherence of infected erythrocytes. *Proc. Natl Acad. Sci. USA* 1983. 80, 5075–5079.

del Portillo HA, Fernandez-Becerra C, Bowman S, Oliver K, Preuss M, Sanchez CP, Schneider NK, Villalobos JM, Rajandream MA, Harris D, Pereira da Silva LH, Barrell B, Lanzer M. A superfamily of variant genes encoded in the subtelomeric region of *Plasmodium vivax*. Nature. 2001. 410: 839-42.

del Portillo HA, Lanzer M, Rodriguez-Malaga S, Zavala F, Fernandez-Becerra C. Variant genes and the spleen in *Plasmodium vivax* malaria. Int J Parasitol. 2004 Dec;34(13-14):1547-54. Review.

Desowitz RS, Miller LH, Buchanan RD & Permpanicer B. The sites of deep vascular schizogony in *P. coatneyi* malaria. *Trans. R. Soc. Trop. Med. Hyg.* 1969. 63, 198–202.

Duffy PE, Fried M. Malaria in the pregnant woman. Curr Top Microbiol Immunol. 2005;295:169-200.

Ferguson HM, Mackinnon MJ, Chan BHK & Read AF. Mosquito mortality and the evolution of malaria virulence. Evolution 2003. 57, 2792–2804.

Fernandez-Becerra C, Pein O, de Oliveira TR, Yamamoto MM, Cassola AC, Rocha C, Soares IS, de Bragança Pereira CA, del Portillo HA. Variant proteins of *Plasmodium vivax* are not clonally expressed in natural infections. Mol Microbiol. 2005. 58:648-58.

Fernandez-Becerra C, Yamamoto MM, Vêncio RZ, Lacerda M, Rosanas-Urgell A, del Portillo HA. *Plasmodium vivax* and the importance of the subtelomeric multigene vir superfamily. Trends Parasitol. 2009. 25: 44-51.

Field JW, Shute PG. The microscopic diagnosis of human malaria. II. A morphological study of the erythrocytic parasites. Kuala Lumpur: Government Press 1956.

Fried M & Duffy PE. Adherence of *Plasmodium falciparum* to chondroitin sulfate A in the human placenta. Science. 1996; Jun 7;272(5267):1502-4.

Gay F, Robert C, Pouvelle B, Peyrol S, Scherf A, Gysin J. Isolation and characterization of brain microvascular endothelial cells from Saimiri monkeys. An in vitro model for sequestration of *Plasmodium falciparum*-infected erythrocytes. J Immunol Methods 1995; 184:15-28.

Genton B, D'Acremont V, Rare L, Baea K, Reeder JC, Alpers MP, Müller I. *Plasmodium vivax* and mixed infections are associated with severe malaria in children: a prospective cohort study from Papua New Guinea. PLoS Med. 2008; 5:e127.

Gilks CF, Walliker D, Newbold CI. Relationships between sequestration, antigenic variation and chronic parasitism in *Plasmodium chabaudi chabaudi*: a rodent malaria model. *Parasite Immunol.* 1990. 12, 45–64.

Greenwood B. Malaria vaccines: Evaluation and Implementation. Acta Trop. 2005 Sep; 95(3):298-304.

Gysin J, Pouvelle B, Fievet N, Scherf A, Lépolard C. Ex vivo desequestration of Plasmodium falciparum-infected erythrocytes from human placenta by chondroitin sulfate A. Infect Immun. 1999 Dec; 67(12): 6596-602.

Handayani S, Chiu DT, Tjitra E, Kuo JS, Lampah D, Kenangalem E, Renia L, Snounou G, Price RN, Anstey NM, Russell B. High deformability of *Plasmodium vivax*-infected red blood cells under microfluidic conditions. J Infect Dis. 2009 Feb 1; 199(3):445-50.

Handunetti SM, David PH, Perera KL, Mendis KN. Uninfected erythrocytes form 'rosettes' around *Plasmodium falciparum* infected erythrocytes. *Am. J. Trop. Med. Hyg.* 1989. 40, 115–118.

Handunetti SM, Mendis KN & David PH. Antigenic variation of cloned *Plasmodium fragile* in its natural host *Macaca sinica*. *J. Exp. Med.* 1987. 165, 1269–1283.

Havryliuk T & Ferreira MU. A closer look at multiple-clone *Plasmodium vivax* infections: detection methods, prevalence and consequences. Mem Inst Oswaldo Cruz, Rio de Janeiro, 2009. Vol. 104(1): 67-73

Ho M & White NJ. Molecular mechanisms of cytoadherence in malaria. *Am. J. Physiol.* 1999. 276, C1231–C1242.

Hommel M, David PH & Oligino LD. Surface alterations of erythrocytes in *Plasmodium falciparum* malaria: antigenic variation, antigenic diversity and the role of the spleen. *J. Exp. Med.* 1983. 157, 1137–1148.

Jambou R, Legrand E, Niang M, Khim N, Lim P, Volney B, Ekala MT, Bouchier C, Esterre P, Fandeur T, Mercereau-Puijalon O. Resistance of *Plasmodium falciparum* field isolates to in-vitro artemether and point mutations of the SERCA-type PfATPase6. Lancet 2005; 366: 1960-1963.

Janssen CS, Phillips RS, Turner CM, Barrett MP. Plasmodium interspersed repeats: the major multigene superfamily of malaria parasites. Nucleic Acids Res. 2004. (19):5712-20.

Kappe SH, Vaughan AM, Boddey JA, Cowman AF. That was then but this is now: malaria research in the time of an eradication agenda. Science. 2010 May 14;328(5980):862-6. Review.

Karunaweera ND, Carter R, Grau GE, Kwiatkowski D, Del Giudice G, Mendis KN. Tumour necrosis factor-dependent parasite-killing effects during paroxysms in non-immune *Plasmodium vivax* malaria patients. Clin Exp Immunol. 1992. 88: 499-505.

Kaul DK, Nagel RL, Llena JF, Shear HL. Cerebral malaria in mice: demonstration of cytoadherence of infected red blood cells and microrheologic correlates. Am J Trop Med Hyg. 1994 Apr;50(4):512-21.

Knisely MH, Stratman-Thomas WK & Eliot TS. *Anat. Rec.* 1941.

Kochar DK, Saxena V, Singh N, Kochar SK, Kumar SV, Das A. *Plasmodium vivax* malaria. Emerg Infect Dis 2005; 11:132-4.

Kochar DK, Das A, Kochar SK, Saxena V, Sirohi P, Garg S, Kochar A, Khatri MP, Gupta V. Severe Plasmodium vivax malaria: a report on serial cases from Bikaner in northwestern India. Am J Trop Med Hyg. 2009; 80:194-8.

Kun JFJ, Schmidt-Ott RJ, Lehman LG, Lell B, Luckner D, Greve B, Matousek P & Kremsner PG. Merozoite surface antigen 1 and 2 genotypes and resetting of *Plasmodium falciparum* in severe and mild malaria in Lambarene, Gabon. *Trans. R. Soc. Trop. Med. Hyg.* 1998. 92, 110–114.

Langreth G & Peterson E. Pathogenicity, stability and immunogenicity of a knobless clone of *Plasmodium falciparum* in Colombian owl monkeys. *Infect. Immun.* 1985. 47, 760–766.

Le Bras J & Durand R. The mechanisms of resistance to antimalarial drugs in *Plasmodium falciparum*. Fundam Clin Pharmacol. 2003 Apr;17(2):147-53. Review.

Lomar AV, Vidal JE, Lomar FP, Barbas CV, de Matos GJ, Boulos M. Acute respiratory distress syndrome due to vivax malaria: case report and literature review. Braz J Infect Dis. 2005 Oct;9(5):425-30. Epub 2006 Jan 6. Review.

Mackinnon MJ & Read AF. Genetic relationships between parasite virulence and transmission in the rodent malaria *Plasmodium chabaudi*. Evolution. 1999; 53, 689–703.

MacPherson GG, Warrell MJ, White NJ, Looareesuwan S & Warrell DA. Human cerebral malaria: a quantitative ultrastructural analysis of parasitized erythrocyte sequestration. *Am. J. Pathol.* 1985. 119, 385–401.

Makkar RP, Mukhopadhyay S, Monga A, Gupta AK. *Plasmodium vivax* malaria presenting with severe thrombocytopenia. Braz J Infect Dis. 2002 Oct;6(5):263-5.

Marsh K. Malaria disaster in Africa. Lancet. 1998 Sep 19;352(9132):924.

McGready R, Davison BB, Stepniewska K, Cho T, Shee H, Brockman A, Udomsangpetch R, Looareesuwan S, White NJ, Meshnick SR, Nosten F. The effects of *Plasmodium falciparum*

and *P. vivax* infections on placental histopathology in an area of low malaria transmission. Am J Trop Med Hyg. 2004 Apr;70(4):398-407.

McGregor IA, Wilson ME, Billewicz WZ. Malaria infection of the placenta in The Gambia, West Africa; its incidence and relationship to stillbirth, birthweight and placental weight. Trans R Soc Trop Med Hyg. 1983;77(2):232-44.

Menendez C. Malaria during pregnancy: a priority area of malaria research and control. Parasitol Today. 1995 May; 11 (5): 178-83.

Merino EF, Fernandez-Becerra C, Durham AM, Ferreira JE, Tumilasci VF, d'Arc-Neves J, da Silva-Nunes M, Ferreira MU, Wickramarachchi T, Udagama-Randeniya P, Handunnetti SM, Del Portillo HA. Multi-character population study of the vir subtelomeric multigene superfamily of *Plasmodium vivax*, a major human malaria parasite. Mol Biochem Parasitol. 2006 Sep;149(1):10-6. Epub 2006 May 11.

Miller LH. Distribution of mature trophozoites and schizonts of *Plasmodium falciparum* in the organs of *Aotus trivigatus*, the night monkey. *Am. J. Trop. Med.* 1969. *Hyg.* 18, 860–865.

Miller LH, Baruch DI, Marsh K, Doumbo OK. The pathogenic basis of malaria. Nature. 2002 Feb 7;415(6872):673-9. Review.

Mota MM, Jarra W, Hirst E, Patnaik PK, Holder AA. *Plasmodium chabaudi*-infected erythrocytes adhere to CD36 and bind to microvascular endothelial cells in an organ-specific way. *Infect. Immun.* 2000. 68, 4135–4144.

Muanza K, Gay F, Behr C, Scherf A. Primary culture of human lung microvessel endothelial cells: a useful in vitro model for studying *Plasmodium falciparum*-infected erythrocyte cytoadherence. Res Immunol. 1996 Mar-Apr;147(3):149-63.

Neres R, Marinho CR, Gonçalves LA, Catarino MB, Penha-Gonçalves C. Pregnancy outcome and placenta pathology in *Plasmodium berghei* ANKA infected mice reproduce the pathogenesis of severe malaria in pregnant women. PLoS One. 2008 Feb 13; 3 (2):1608.

Newbold, CI, Craig A, Kyes S, Rowe JA, Fernandez- Reyes D & Fagan T. Cytoadherence, pathogenesis and the infected red cell surface in *Plasmodium falciparum*. *Int. J. Parasitol.* 1999. 29, 927–937.

Nosten F, McGready R, Simpson JA, Thwai KL, Balkan S, Cho T, Hkirijaroen L, Looareesuwan S, White NJ. Effects of *Plasmodium vivax* malaria in pregnancy. Lancet 1999; 354:546-9.

Ockenhouse CF, Tandon NN, Magowan C, Jamieson GA, Chulay JD. Identification of a platelet membrane glycoprotein as a falciparum malaria sequestration receptor. Science. 1989 Mar 17;243(4897):1469-71.

Oliveira TR, Fernandez-Becerra C, Jimenez MC, Del Portillo HA, Soares IS. Evaluation of the acquired immune responses to *Plasmodium vivax* VIR variant antigens in individuals living in malaria-endemic areas of Brazil. Malar J 2006; 5:83.

Ozen M, Gungor S, Atambay M, Daldal N. Cerebral malaria owing to *Plasmodium vivax*: case report. Ann Trop Paediatr. 2006 Jun;26(2):141-4.

Pain A, Ferguson DJP, Kai O, Urban BC, Lowe BS, Marsh K & Roberts DJ. Platelet-mediated clumping of *Plasmodium falciparum*-infected erythrocytes is a common adhesive phonotype and is associated with severe malaria. *Proc. Natl Acad. Sci. USA* 2001. 98, 1805–1810.

Pasloske BL, Howard RJ. Malaria, the red cell, and the endothelium. Annu Rev Med. 1994; 45:283-95. Review.

Pongponratn E. An ultrastructural study of the brain in fatal *Plasmodium falciparum* malaria. Am. J. Trop.Med.Hyg. 2003; 69, 345–359

Pouvelle B, Traore B, Nogueira PA, Pradines B, LePolard C, Gysin J. Modeling of *Plasmodium falciparum*-infected erythrocyte cytoadhesion in microvascular conditions: chondroitin-4-sulfate binding, A competitive phenotype. J Infect Dis 2003; 187:292-302.

Ringwald P, Peyron F, Lepers JP, Rabarison P, Rakptpmalala C, Razanamparany M, Rabodonirina M, Roux J & Lebras J. Parasite virulence factors during *falciparum*-malaria: rosetting, cytoadherence, and modulation of cytoadherence by cytokines. *Infect. Immun.* 1993. 61, 5198–5204.

Robert C, Pouvelle B, Meyer P, Muanza K, Fujioka H, Aikawa M, Scherf A, Gysin J. Chondroitin-4-sulphate (proteoglycan), a receptor for *Plasmodium falciparum*-infected erythrocyte adherence on brain microvascular endothelial cells. Res Immunol. 1995 Jul-Aug; 146(6):383-93.

Roberts DJ, Craig AG, Berendt AR, Pinches R, Nash G, Marsh K & Newbold CI. Rapid switching to multiple antigenic and adhesive phenotypes in malaria. *Nature* 1992. 357, 689–692.

Roberts DJ, Pain A, Kai O, Kortok M & Marsh K. 2000 Autoagglutination of malaria-infected red blood cells and malaria severity. *Lancet,* 2000. 355, 1427–1428.

Rogerson SJ, Chaiyaroj SC, Ng K, Reeder JC, Brown GV. Chondroitin sulfate A is a cell surface receptor for *Plasmodium falciparum*-infected erythrocytes. J Exp Med. 1995 Jul 1;182(1):15-20.

Rowe JA, Obeiro J, Newbold CI & Marsh K. *Plasmodium falciparum* rosetting is associated with malaria severity in Kenya. *Infect. Immun.* 1995. 63, 2323–2326.

Russell B, Chalfein F, Prasetyorini B, Kenangalem E, Piera K, Suwanarusk R, Brockman A, Prayoga P, Sugiarto P, Cheng Q, Tjitra E, Anstey NM, Price RN. Determinants of in vitro drug susceptibility testing of *Plasmodium vivax*. Antimicrob. Agents Chemother. 2008; 52, 1040–1045).

Salanti A, Dahlbäck M, Turner L, Nielsen MA, Barfod L, Magistrado P, Jensen AT, Lavstsen T, Ofori MF, Marsh K, Hviid L, Theander TG. Evidence for the involvement of VAR2CSA in pregnancy-associated malaria. J Exp Med. 2004 Nov 1;200(9):1197-203.

Santos-Ciminera PD, Roberts DR, Alecrim MG, Costa MR, Quinnan GV Jr. Malaria diagnosis and hospitalization trends, Brazil. Emerg Infect Dis. 2007;13:1597-600.

Scherf A, Hernandez-Rivas R, Buffet P, Bottius E, Benatar C, Pouvelle B, Gysin J, Lanzer M Antigenic variation in malaria: in situ switching, relaxed and mutually exclusive transcription of var genes during intra-erythrocytic development in *Plasmodium falciparum*. EMBO J. 1998 Sep 15;17(18):5418-26

Scherf A, Pouvelle B, Buffet PA, Gysin J. Molecular mechanisms of *Plasmodium falciparum* placental adhesion. Cell Microbiol. 2001;3:125-31.

Schmidt JA, Udeinya IJ, Leech JH, Hay RJ, Aikawa M, Barnwell J, Green I, Miller LH. *Plasmodium falciparum* malaria. An amelanotic melanoma cell line bears receptors for the knob ligand on infected erythrocytes. J Clin Invest. 1982 Aug;70(2):379-86.

Schofield L, Grau GE. Immunological processes in malaria pathogenesis. Nat Rev Immunol 2005; 5:722–735. Review

Sharma YD. Knobs, knob proteins and cytoadherence in falciparum malaria. Int J Biochem. 1991; 23(9):775-89.

Singh B, Kim Sung L, Matusop A, Radhakrishnan A, Shamsul SS, Cox-Singh J, Thomas A, Conway DJ. A large focus of naturally acquired *Plasmodium knowlesi* infections in human beings. Lancet. 2004 Mar 27;363(9414):1017-24.

Singh S, Singh N, Handa R. Tumor necrosis factor-alpha in patients with malaria. Indian J Malariol. 2000. 37: 27-33.

Smalley ME, Abdalla S & Brown J. The distribution of *Plasmodium falciparum* in the peripheral blood and bone marrow of Gambian children. *Trans. R. Soc. Trop. Med. Hyg.* 1980. 75, 103–105.

Smith H, Nelson JA, Gahmberg CG, Crandall I, Sherman IW. *Plasmodium falciparum*: cytoadherence of malaria-infected erythrocytes to human brain capillary and umbilical vein endothelial cells--a comparative study of adhesive ligands. Exp Parasitol. 1992 Nov;75(3):269-80.

Smith JD, Subramanian G, Gamain B, Baruch DI, Miller LH. Classification of adhesive domains in the *Plasmodium falciparum* erythrocyte membrane protein 1 family. Mol Biochem Parasitol. 2000 Oct;110(2):293-310.

Snounou G, Singh B. Nested PCR analysis of Plasmodium parasites. Methods Mol Med 2002; 72:189-203.

Tan LK, Yacoub S, Scott S, Bhagani S, Jacobs M. Acute lung injury and other serious complications of *Plasmodium vivax* malaria. Lancet Infect Dis 2008; 8:449-54.

Thiberge S, Blazquez S, Baldacci P, Renaud O, Shorte S, Ménard R, Amino R. In vivo imaging of malaria parasites in the murine liver. Nat Protoc. 2007;2(7):1811-8.

Thomson JG & Robertson A. The structure and development of *Plasmodium falciparum* gametocytes in the internal organs and peripheral circulation. *Trans. R. Soc.Trop. Med. Hyg.* 1935. 29, 31–40.

Tjitra E, Anstey NM, Sugiarto P, Warikar N, Kenangalem E, Karyana M, Lampah DA, Price RN. Multidrug-resistant *Plasmodium vivax* associated with severe and fatal malaria: a prospective study in Papua, Indonesia. PLoS Med 2008; 5:e128.

Treutiger CJ, Hedlund I, Helmby H, Carlson J, Jepson A, Twumasi P, Kwiatkowski D, Greenwood BM & Wahlgren M. Rosette formation in *Plasmodium falciparum* isolates and anti-rosette activity of sera from Gambians with cerebral or uncomplicated malaria. *Am. J. Trop. Med. Hyg.* 1992. 46, 503–510.

Turner CM, Aslam N, Dye C. Replication, differentiation, growth and the virulence of Trypanosoma brucei infections. Parasitology. 1995 Sep; 111 (Pt 3):289-300.

Udeinya IJ, Magowan C, Chulay JD. Long-term cultured human vascular endothelial cells (EC-FP5) bind *Plasmodium falciparum* infected erythrocytes. Am J Trop Med Hyg. 1989 Oct;41(4):400-5.

Udeinya IJ, Schmidt JA, Aikawa M, Miller LH, Green I. Falciparum malaria-infected erythrocytes specifically bind to cultured human endothelial cells. Science. 1981 Jul 31;213(4507):555-7.

Udomsangpetch R, Brown AE, Smith CD & Webster HK. Rosette formation by *Plasmodium coatneyi*infected red blood cells. *Am. J. Trop.Med. Hyg.* 1991. 44, 399–401.

Udomsangpetch R, Thanikkul K, Pukrittayakamee S, White NJ. Rosette formation by *Plasmodium vivax*. *Trans. R. Soc. Trop. Med. Hyg.* 1995. 89, 635–637.

Valecha N, Pinto RG, Turner GD, Kumar A, Rodrigues S, Dubhashi NG, Rodrigues E, Banaulikar SS, Singh R, Dash AP, Baird JK. Histopathology of fatal respiratory distress caused by Plasmodium vivax malaria. Am J Trop Med Hyg. 2009 Nov;81(5):758-62.

Wahlgren M, Carlson J, Udomsangpetch R, Perlmann P. Why do *Plasmodium falciparum*-infected erythrocytes form spontaneous erythrocyte rosettes? *Parasitol. Today* 1989. 5, 183–185.

Wernsdorfer WH & Payne D. The dynamics of drug resistance in *Plasmodium falciparum*. Pharmacol Ther. 1991;50(1):95-121. Review.

Wijesekera SK, Carter R, Rathnayaka L, Mendis KN. A malaria parasite toxin associated with *Plasmodium vivax* paroxysms. Clin Exp Immunol. 1996. 104: 221-7.

Wyler DJ. Splenic functions in malaria. Lymphology. 1983, Jun;16(2):121-7.

Yoeli M & Hargreaves B. Brain capillary blockage produced by a virulent strain of rodent malaria. *Science* 1974. 184, 572–573.

ANEXOS

Dear Dr. Costa,

We are pleased to inform you that your revised manuscript has been accepted for publication in The Journal of Infectious Diseases. In additions, we are interested in considering one of your figures (1A) as possible cover art for the issue in which your article will appear. Let us know if you are interested, and we will tell you what we need. If selected, we will deduct $125 from your costs of publication.

You will receive an e-mail from our publisher, the University of Chicago Press (UCP), when your proofs are ready to be downloaded from the Internet. On return of your proofs to UCP, your paper will be scheduled for publication.

The page charges are $55 per printed page for up to six pages and $85 for each additional page. Charges for color use may also apply: a minimum of $500 for the first page of color and $400 for each additional page of color. Written assurance of payment for these charges is required. A request for payment of the appropriate charges will be sent with the proofs.

If you prefer, you can avoid color charges by having color figures published in black and white; to do so, please send electronic files of all new black and white figures to the JID office e-mail address below. Use Word to make tables. Make figures in TIFF or EPS files, not PowerPoint.

Note that IDSA now grants NIH-funded authors permission to deposit their accepted manuscripts with PubMed central and to publish it there twelve (12) months after publication in the Journal.

A publication agreement is attached below. Please review and return this document to this office as soon as possible. For your convenience, you may fax it to us at 617-367-2624 or e-mail it to jid@press.uchicago.edu

Sincerely,
Martin S. Hirsch, MD
Editor
Peter Weller, MD
Associate Editor

The Journal of Infectious Diseases
225 Friend St., 7th Floor
Boston, MA 02114
Phone: 617-367-1848
Fax: 617-367-2624
E-mail: jid@press.uchicago.edu

On cytoadhesion of *Plasmodium vivax*-infected erythrocytes

Running Title: ***Plasmodium vivax* cytoadhesion**

Bruna O. Carvalho [1,2,#], Stefanie C. P. Lopes [1,#], Paulo A. Nogueira [2], Patricia P. Orlandi [2], Daniel Y. Bargieri [3,4], Yara C. Blanco [1], Ronei Mamoni [1], Juliana A. Leite [1], Mauricio M. Rodrigues [3,4], Irene S. Soares [5], Tatiane R. Oliveira [5], Gerhard Wunderlich [6], Marcus V. G. Lacerda [7,8], Hernando A. del Portillo [9], Maria O. G. Araújo [10], Bruce Russell [11], Rossarin Suwanarusk [11], Georges Snounou [11,12,13,14], Laurent Rénia [11] and Fabio T. M. Costa [1,*]

[#] These two authors equally contributed to this work.

[1] Departamento de Genética, Evolução e Bioagentes; Instituto de Biologia, Universidade Estadual de Campinas (UNICAMP), Campinas - SP, Brazil.
[2] Instituto Leônidas & Maria Deane, Fiocruz, Manaus, AM, Brazil .
[3] Centro Interdisciplinar de Terapia Gênica (CINTERGEN), Universidade Federal de São Paulo (UNIFESP), São Paulo, SP, Brazil.
[4] Departamento de Microbiologia, Imunologia e Parasitologia, UNIFESP, São Paulo, SP, Brazil.
[5] Departamento de Análises Clínicas e Toxicológicas, Faculdade de Ciências Farmacêuticas, Universidade de São Paulo (USP), São Paulo, SP, Brazil.
[6] Departamento de Parasitologia – ICB. USP, São Paulo, SP, Brazil.
[7] Fundação de Medicina Tropical do Amazonas, Gerência de Malária, Manaus, AM, Brazil.
[8] Universidade do Estado da Amazônia, Manaus, Brazil.
[9] Barcelona Centre for International Health Research (CRESIB) and Institució Catalana de Recerca I Estudis Avançats (ICREA), Barcelona, Spain.
[10] Universidade de Brasília (UnB). Brasília, DF. Brazil.
[11] Singapore Immunology Network, Agency for Science, Technology and Research (A*STAR), Biopolis. Singapore.
[12] INSERM UMR S 945, Paris, France.
[13] Université Pierre & Marie Curie, Faculté de Médecine Pitié-Salpêtrière, Paris, France.
[14] Department of Microbiology, National University of Singapore, Singapore.

***Corresponding author:** Dr. Fabio T. M. Costa
Departamento de Genética, Evolução e Bioagentes;
Instituto de Biologia, Universidade Estadual de Campinas (UNICAMP),
P.O. Box 6109. 13083-970. Campinas - SP, Brazil.
Tel.: +55 19 3521-6594; Fax: +55 19 3521-6276
E-mail: costaftm@unicamp.br or fabiotmc72@gmail.com

Word Count: Abstract 200; Main Body 3,466.

FOOTNOTE PAGE

Conflicts of Interest. The authors declared no conflict of interest exists.

Grants and financial supports: This work received financial support from the Fundação de Amparo à Pesquisa do Estado de São Paulo (FAPESP) and the Conselho Nacional de Desenvolvimento Científico e Tecnológico (CNPq). BOC and JAL were sponsored by FAPESP fellowships. SCPL and RM were supported by CNPq and YCB received a Coordenação de Aperfeiçoamento de Pessoal de Nível Superior (CAPES) fellowship. MMR, ISS, GW and FTMC are CNPq fellows. LR was supported by the Agency for Science, Technology and Research (A*STAR), Singapore, and GS by INSERM, France. The funders had no role in study design, data collection and analysis, decision to publish, or preparation of the manuscript.

Requests for reprints: Dr. Fabio T. M. Costa, Departamento de Genética, Evolução e Bioagentes; Instituto de Biologia, Universidade Estadual de Campinas (UNICAMP). P.O. Box 6109. 13083-970. Campinas - SP, Brazil. Tel.: +55 19 3521-6594; Fax: +55 19 3521-6276.

E-mail: costaftm@unicamp.br or fabiotmc72@gmail.com

ABSTRACT

Background.

Plasmodium falciparum and *P. vivax* are responsible for most of the global malaria burden. While accentuated pathogenicity of *P. falciparum* occurs due to sequestration of the mature erythrocytic forms in microvasculature, this phenomenon was not yet noted in *P. vivax*. The rising number of severe manifestations in *P. vivax* infections, similar to those observed for severe falciparum malaria, suggests that key pathogenic mechanisms (e.g. cytoadherence) might be shared by the two parasites.

Methods.

Mature *P. vivax*-infected erythrocytes (Pv-iE) were isolated from blood samples collected from 34 infected patients. Pv-iE enriched on Percoll gradients were used in cytoadhesion assays to human lung endothelial cells (HLEC), to *Saimiri* brain endothelial cells (SBEC), and to placental cryosections.

Results.

Pv-iE were able to cytoadhere under static and flow conditions to cells expressing endothelial receptors known to mediate cytoadhesion of *P. falciparum*. Although Pv-iE cytoadhesion levels were 10-fold lower than those observed for Pf-iE, the strength of the interaction was similar. Cytoadhesion of Pv-iE was in part mediated by VIR proteins, since specific antisera inhibited the iE-endothelial cell interaction.

Conclusions.

These observations prompt a modification of the current paradigms of malaria pathogenesis, and open the way to investigate the pathophysiology of *P. vivax* infections.

Keywords: Malaria; *Plasmodium vivax*; *Plasmodium falciparum;* Cytoadhesion; Endothelial cells; Placental cryosections; VIR proteins.

Abbreviations: Pv-iE, mature *P. vivax*-infected erythrocytes; Pf-iE, mature *P. falciparum*-infected erythrocytes; HLEC, human lung endothelial cells; SBEC, *Saimiri* brain endothelial cells-1D, CHO, chinese hamster ovary cells; ICAM-1, intercellular adhesion molecule-1; CSA, chondroitin sulfate A; CaseABC, chondroitinase ABC; DAPI, 4',6-diamidino-2-phenylindole, dihydrochloride; GST, glutathione S-transferase; MAbs, monoclonal antibodies; FCS, fetal calf serum; CFA, complete Freund's adjuvant; IFA, incomplete Freund's adjuvant.

INTRODUCTION

It was long recognized that the directly attributable morbidity and mortality differed for the two most prevalent parasite species, *P. falciparum* and *P. vivax*. The higher multiplicative potential of *P. falciparum*-infected erythrocytes (Pf-iE) no doubt contributes to their increased virulence. However, it is the withdrawal of mature Pf-iE (parasites older than 24 h) from the peripheral circulation to that of the internal organs, a phenomenon known as sequestration (1), which is considered as the key pathogenic event. *P. falciparum* is characterized by almost total sequestration, such that few if any Pf-iE mature forms are observed in peripheral blood samples during infections. Given that mature *P. vivax*-infected red blood cells (Pv-iE) are frequently observed in peripheral blood samples, it was concluded that sequestration did not occur with this parasite. In consequence, the paradigm was formulated that sequestration of Pf-iE in specific organs is the principal initial cause of pathology and when it occurs in the brain or the placenta, the likelihood of cerebral malaria and pregnancy-associated malaria increases. Indeed, most forms of severe malaria and nearly all mortality were almost exclusively recorded for falciparum cases.

P. vivax, the most prevalent malaria species outside sub-Saharan Africa, imposes a substantial global public health burden (2), with recent estimates of 130 - 435 million infected persons per year among the 2.6 billion people at risk. Of equal importance was the observation that many types of severe malaria – for long considered specific to *P. falciparum* - also commonly occur in *P. vivax*-infected persons. For instance, infection by *P. vivax* during pregnancy was associated with substantial reduction in birth weight (3). Furthermore, in some endemic areas progression of vivax malaria to clinically severe forms, including cerebral malaria and acute respiratory distress syndrome, was found to occur as frequently as for falciparum infections, with similar levels of fatality (4-7). This

raises the possibility that pathological processes linked to cytoadhesion might also operate in *P. vivax*.

In *P. falciparum*, cytoadhesion of Pf-iE to endothelial cells is mediated by interactions between members of the *P. falciparum* erythrocyte membrane protein-1 (PfEMP-1); polymorphic proteins encoded by the *var* multigene family (8-9), and defined host receptors on endothelial cells. Of the ten or so receptors identified to date (10-11), three have been extensively investigated: CD36, ICAM-1 and CSA. The latter has been specifically associated with Pf-iE binding to the placenta (12).

We wished to establish whether *P. vivax* parasites were able to cytoadhere under static or flow conditions to endothelial cells and placental cryosections, and if the receptors for Pf-iE were also implicated. Furthermore, we assessed the involvement of VIR proteins as a potential Pv-iE ligand.

MATERIALS AND METHODS

Ethical approval

Informed consent was sought and granted from all patients attending the Tropical Medicine Foundation of Amazonas (FMT-AM), Amazonas state, in Northern Brazil. The procedures were approved by the Ethics Committee Board of the FMT-AM (process 2758/2008-FMT-AM; approval number 1943).

Parasite isolation and enrichment

Once microscopic diagnosis of uncomplicated *vivax* or *falciparum* malaria was made and prior to initiating treatment, 5 to 10 ml of blood were collected into citrate-coated vacutainer tubes. Parasitaemias rarely exceeded 5,000 parasites per microlitre of blood. The blood was immediately processed to obtain enriched Pv-iE. In the average, a total of about 1 x 10^6 Pv-iE could be obtained, allowing only a limited number of cytoadhesion assays to be conducted. Patients who were under previous antimalarial treatment 3-4 weeks before the test were excluded. Immediately after collection, the red blood cells containing trophozoites and schizonts were separated from the younger forms on a 45% Percoll® (Amersham) gradient as previously described (13) with minor modifications. Briefly, following plasma separation by centrifugation, blood pellets were washed 3 times and then resuspended in RPMI 1640 medium (Sigma) to a final haematocrit of 10%. 5 ml of this suspension was overlaid on a 5 ml 45% Percoll® solution (2.25 ml of Percoll®, 0.5 ml of RPMI 10x and 2.25 ml of distilled water) in a 15 ml tube. After centrifugation, floating mature iE were collected and resuspended in RPMI 1640 medium. *Ex-vivo* Pf-iE were enriched in Percoll® gradient at 60% as described elsewhere (14). Giemsa-stained thick smears (prior to enrichment) and thin smears (post-

enrichment) were examined to determine the *Plasmodium* species and the percentage of mature stages, respectively. A sensitive nested PCR assay was applied to the samples to confirm the diagnosis (15).

P. vivax slide preparation and immunofluorescence assays (IFA)

IFA were carried out in 8-well slides containing mature stages of *P. vivax*. Immediately after enrichment on Percoll®, Pv-iE were washed and resuspended in 10% of FCS (Nutricell), and then deposited on IFA slides (50 μl/well), fixed in acetone for 10 min, air dried and stored at -20 °C prior to use. Ten μg/ml of each MAb 3F8 or K23 against PvMSP1 (16) were diluted in PBS, were applied to slides for 30 min at 37°C. After washing in PBS, slides were incubated with 10 μg/ml of FITC-conjugated sheep anti-mouse IgG (Sigma) and 100 μg/ml of DAPI (Molecular Probes) for 30 min at 37°C, and then washed several times. Positive MAb recognition was detected with the aid of an immunofluorescence microscope (Nikon). For IFA conducted using VIR antisera Pv-iE were left in suspension (liquid phase). Briefly, parasites were fixed in 2% paraformaldehyde, washed and diluted in FCS, and then VIR-A4 and VIR-E5 mouse and antisera were added in a final dilution of 1:20 and incubated for 60 min. After two washes with FCS cells were incubated with 100 μg/ml of Alexa-Fluor 488 conjugated goat anti-mouse IgG (Molecular Probes) and 500 μg/ml of DAPI for 30 min at 37°C, and then washed twice with FCS. In both assays positive recognition by MAb, VIR-A4, VIR-E5 or MSP-1_{19} antisera was detected with the aid of an immunofluorescence microscope.

Polyclonal VIR antisera were generated by injecting mice with VIR-A4 or VIR-E5 GST fusion proteins, belonging to the A or the E *vir* subfamilies, respectively (17-18), and raised after two immunizations (21-day-interval) with 5 μg/animal/dose of each

recombinant protein emulsified in complete or incomplete Freund's adjuvant. No Pv-iE positive labeling was visualized by anti-GST sera.

Selection of mono-phenotypic cultured *P. falciparum* parasites and cells

The *P. falciparum* lines FCR3 (19) and S20 (20) were cultured in candle jars. Briefly, Pf-iE were cultivated in fresh type O^+ human erythrocytes (Blood Center - UNICAMP) suspended at a final haematocrit of 4% in complete medium (RPMI 1640, pH 7.2) (Sigma) and supplemented with 10% homologous human plasma.

The following cells lines were used in this study: SBEC and HLEC (21-22) adapted from cultured primary explants; and CHO-ICAM, CHO-CD36 and CHO-K1 cells (23). Selection of FCR3 parasites to CSA ($FCR3^{CSA}$) was performed by panning (5 rounds) of mature-stage iE on endothelial cells (21, 24) in the presence of soluble CSA (100 μg/ml) (Sigma).

S20 mature trophozoites were selected on CHO-ICAM cells (5 rounds), and then by a further two rounds on plastic plates coated with recombinant ICAM-1 (25). The selected $S20^{ICAM}$ parasite line binds strongly to CHO-ICAM cells, but poorly to non-transfected CHO-K1 cells (data not shown).

Static cytoadhesion assays.

We assessed the ability of Pv-iE or Pf-iE collected from infected patients to adhere to placenta cryosections, HLEC and SBEC by performing static cytoadhesion assays as described (19, 21, 26) with minor modifications. Briefly, HLEC or SBEC were grown to confluence on 8-well culture slides (0.69 cm^2 each well) (BD), and 5 x 10^4 Percoll®-enriched iE were then added per well in total volume of 200 μl of cytoadhesion medium (RPMI-1640, pH 6.8), alone or in the presence of 100 μl of soluble CSA (100

μg/ml) or anti-CD36 (5 μg/ml). Culture slides were incubated for 1 hour at 37°C, and then extensively washed in cytoadhesion medium. For confirmation that the ligands on the surface of Pv-iE were proteins, Pv-iE were treated with trypsin (1 mg/ml) for 45 min at 37°C, prior to incubation over endothelial cells. For confirmation of CSA as a receptor, HLEC were previously incubated with chondroitinase-ABC (0.5 U/ml) (Sigma) during 2 hours at 37°C. Involvement of VIR antigens in Pv-iE cytoadhesion to HLEC was evaluated in an assay where inhibition of parasite binding was tested with antisera (diluted at 1:5 or 1:10) to VIR-A4 or VIR-E5 GST-fused proteins. Sera from mice immunized solely with GST in CFA/IFA were used as specificity controls. For these assays, inhibition was determined as a percentage of the negative control and was expressed as the mean ± SD of three wells.

Adhesion assays to placental trophoblast were performed as described elsewhere (19, 26-27) with minor modifications. Placental biopsies from 3 malaria and HIV negative Brazilian women were collected immediately after delivery and snap-frozen in liquid nitrogen/n-Hexane (Merck), then stored frozen in Tissue-Teck® prior to use. Serial placenta cryosections (5-7 μm) were cut with a cryostome and mounted on individual glass slides. Cryosections were washed, air-dried and an area of approximately 1 cm^2 was delimited with a Dako-Pen®. Pv-iE adhesion assays to placental cryosections were performed as for endothelial cells. Three to four placenta cryosections were used for each adhesion assay. After 1-hour incubation at 37°C, and following Giemsa staining, the number of iE that adhered to the endothelial cell monolayer or to placenta cryosections was counted under the microscope.

Involvement of CD36 or ICAM-1 host receptors was verified by allowing Pv-iE to adhere under static conditions to CHO-CD36, CHO-ICAM or to CHO-745 a cell line that does not express any of these receptors (23). In these experiments, we performed

adhesion assays without using human sera in the medium since it has been shown that human immunoglobulins present in normal sera can mediate binding of Pf-iE to CHO-745 (28).

Flow-based cytoadhesion assays

To assess the resistance of Pv-iE to shear stress we performed flow-based cytoadhesion assays according to a modified version of a previously described method (19, 26-27). Briefly, HLEC were cultured to confluence in single-well culture microslides (8.6 cm^2, corresponding to 12.5 x the area of each well in a 8-well culture slide) to which 1.5 ml of 5 x 10^5 Pv-iE enriched on 45% Percoll® gradient were added. After 1-hour incubation at 37 °C, microslides were mounted in a flow-chamber-system (Immunetics) and cytoadhesion medium (RPMI pH 6.8) was flowed through at a wall shear stress of 0.09, 0.36 or 1.44 Pascal (Pa) for 10, 5 and 2.5 min, respectively. Following this, the remaining bound Pv-iE were counted in 20 randomly selected fields through a digital camera attached to a microscope (Motic, Moticam 2500®). Results were expressed as the number of iE/mm^2 ± SD. In some experiments, microslides were stained with Giemsa after a determined shear stress condition, to visualize bound Pv-iE. Alternatively, HLEC were incubated with LPS (1.0 μg/ml) (Sigma) during 4 hours at 37°C, and then washed prior to parasite cytoadhesion. Cultured *P. falciparum* panned-isolates $FCR3^{CSA}$ and $S20^{ICAM}$ were used as controls. To ascertain whether *P. vivax* adhesion to HLEC occurred under flow conditions, 1 x 10^6 enriched Pv-iE diluted in cytoadhesion medium were flowed at wall shear stress of 0.09 or 0.36 Pa during 1 hour, then filmed. For both, static or flow-based assays, parasite adhesion was normalized to 10^3 iE/mm^2, taken into account the area and the number of iE used in each assay, 5 x 10^4 iE in 0.69 cm^2 or 5 x 10^5 iE in 8.6 cm^2.

Flow cytometry

ICAM-1 expression levels on HLEC were assessed by flow cytometry. Briefly, 1 x 10^6 cells treated, or not, with LPS (1.0 μg/ml), were harvested and then incubated with anti-human anti-CD54 (ICAM-1) (PE; BD-Bioscience) for 30 min at 4°C, then washed and fixed in 2% formaldehyde. Analysis was performed using a FACScanto (BD) and the mean fluorescence intensity (MFI) and the percentage of positive cells were analyzed with the aid of FCS Express v.3.00.0320 – De Novo™ software. For each sample a minimum of 100,000 events were acquired.

Statistical analysis

Statistical significance of adhesion to different cells types at various conditions was determined using the Mann-Whitney *U* test, or Kruskal-Wallis test. Calculations were performed using BioEstat™ version 3.0 (CNPq, Brazil) and Prism™ version 3.02 (Graphpad, USA) softwares. Values were considered significant when $P<0.05$.

RESULTS

Pf-iE cytoadherence were substantially facilitated by the availability of *in vitro*-cultured *P. falciparum*, an avenue not open for *P. vivax*. Therefore, we conducted our studies with Pv-iE directly obtained from patients presenting with uncomplicated *P. vivax* malaria in Manaus, Brazil. The limitations imposed by reliance on clinical samples with parasites of diverse genotypes and of varying suitability for cytoadherence assays were compensated by collection of a relatively large number of samples (n=34). As controls for the cytoadhesion assays, *P. falciparum*-infected blood was also obtained from four patients attending the same hospital. In all cases, a sensitive PCR assay was used to exclude the presence of mixed species infections. In a first instance, cytoadherence was assessed using HLEC, SBEC and human placental cryosections. These cell lines and placental cryosections have been previously characterized and validated for assays of *P. falciparum* cytoadhesion (19, 21-22, 26-27). In *P. falciparum*, mature forms of the parasite cytoadhere more strongly in comparison to freshly invaded forms. We hypothesized that this could be also the case for *P. vivax*. Given the different densities of mature stage and early stage parasites, we subjected *P. vivax* parasites collected from the patients directly and without prior short-term culturing to a Percoll® gradient which enables the recovery of almost pure trophozoite and schizont stage Pv-iE (Figure 1). Of note, after enrichment the percentage of MSP-1_{19} expressing forms observed in IFA varied between 85 to 97%.

The Pv-iE were first tested for their ability to cytoadhere to HLEC, SBEC and placental cryosections under static conditions. For some patients, aliquots of the same Pv-iE suspension were tested after digestion with trypsin, or in the presence of soluble CSA, anti-CD36 MAb in the cytoadhesion medium or in HLEC pre-treated with CaseABC (Figure 2 and Table 1). All the Pv-iE tested displayed some level of cytoadherence to HLEC or SBEC, or both, or to placental cryosections. Pv-iE binding to areas not containing endothelial cells was not observed. Pre-treatment of Pv-iE with trypsin

generally decreased adhesion to HLEC or SBEC by 19% to 85% (mean 54%) depending on the parasite isolate. Significant inhibition of cytoadherence was also observed in the presence of soluble CSA (16% to 81%, mean 42%). By contrast, when the assays were conducted in the presence of anti-CD36 the extent of inhibition of cytoadherence was not statistically significant (Table 1), though only few isolates could be tested. Moreover, unlike the higher inhibition noticed by soluble CSA, HLEC pre-treated with CaseABC did not significantly abolish adhesion of same Pv-iE (Table 1). Cytoadhesion assays were also conducted in parallel with similarly enriched matured Pf-iE derived from four patients. The levels of cytoadherence observed were about 10-fold higher than those recorded for Pv-iE (Table 1).

Having demonstrated that Pv-iE could cytoadhere to endothelial cells under static conditions, it was important to evaluate if the observed cytoadherence was biologically relevant and that it could be maintained under flow conditions to which parasites would be subjected in the blood stream. Shear stress in post-capillary venules is close to 0.08 Pascal (Pa) (29). Thus, we enriched Pv-iE from seven individuals and conducted flow-based cytoadhesion assays on the HLEC at shear stress conditions varying 0.09 to 1.44 Pa. The parasites remaining attached after being subjected to increasing flow rates for defined period were enumerated by microscopic examination after Giemsa staining (Figure 3 and Table 2). Given that HLEC express CSA and ICAM-1 on their surface, we performed parallel assays using *P. falciparum* FCR3 and the S20 iE pre-selected on CSA ($FCR3^{CSA}$) and ICAM-1 ($S20^{ICAM}$). As for Pf-iE ($FCR3^{CSA}$), even at relatively high shear stress (1.44 Pa) a substantial proportion (30%) of the cytoadherent Pv-iE could not be detached (Table 2). Furthermore, stimulation of the HLEC cells with LPS increased significantly strengthened cytoadherence, because 56% of the cytoadherent Pv-iE could not be detached at 1.44 Pa (Figure 3). Of note, LPS treatment augmented by 3-fold ICAM-1 expression levels (data not shown). The strength of Pv-iE adhesion was similar

to that observed for *P. falciparum* FCR3^{CSA} to the unstimulated HLEC (Table 2). The behavior of the cytoadherent Pv-iE to HLEC under flow conditions (0.09 and 0.36 Pa) was recorded in real-time (Supplementary Movies 1 and 2), and showed that cytoadherent Pv-iE displayed the rolling characteristics of cytoadherent *P. falciparum* parasites (30).

We then tested whether CD36 or ICAM-1, both present on HLEC surface (21-22), were implicated in the observed Pv-iE cytoadherence. For this, CHO lines transfected with CD36 or ICAM-1 were used. None of the Pv-iE from the three samples tested showed binding to CD36 (Figure 4), as the levels of cytoadherent Pv-iE were not significantly different from background (Pv-iE binding to untransfected CHO-745 cells). By contrast, a 2.1 to 2.7-fold increase in cytoadhesion to ICAM-1 as compared to background was observed for Pv-iE from two of the three samples tested (Figure 4). Low cytoadhesion of Pv-iE isolated from patient 098 may indicate variations in the binding phenotypes of different isolates.

Finally, we investigated potential parasite ligands involved in Pv-iE cytoadhesion. A multigene family orthologous to the *P. falciparum var* genes does not occur in the genome of *P. vivax* (31). However, a superfamily of surface-expressed variant antigens genes (*vir*) is present in *P. vivax* with around 350 members which can be subdivided into 10 subfamilies and unclustered members (17, 31-32). Hence, we tested two polyclonal specific antisera, VIR-A4 and VIR-E5 from the A and E subfamilies, respectively (18). Pv-iE were specifically recognized by both antisera in IFA (Figure 5A), but not by the control anti-GST serum. Significant inhibition of Pv-iE cytoadherence on HLEC was observed when either anti-VIR sera were included in the assay medium, but not in the presence of the anti-GST serum (Figure 5B).

DISCUSSION

Our observations provide the first evidence that mature Pv-iE are capable to cytoadhere to endothelial cells and placental cryosections. Two receptors used by *P. falciparum* for binding to endothelial cells, ICAM-1 and CSA, were also implicated in the cytoadhesion of *P. vivax* parasites, at least to some extent. However, CaseABC treatment suggested that cytoadhesion to CSA, a highly negative charged molecule, might be due to charge interaction. Indeed, it has been shown that binding to CSA is highly dependent on ionic strength (33).The fraction of Pv-iE that cytoadhered was up to 10-fold lower than for Pf-iE. Importantly, once established cytoadhesion of Pv-iE is as strong as that of CSA-selected Pf-iE, as demonstrated by the flow assays (Table 2). Since the parasites we assayed were directly obtained from patients, our data suggest that only a minor population of *P. vivax* would have the capacity to cytoadhere *in vivo*. Partial retention of *P. vivax* from the peripheral circulation would explain why the mature forms of this parasite are generally found in peripheral blood. This is consistent with the observation of partial and differential accumulation of Pv-iE in organs of *P. vivax*-infected squirrel monkeys (34), and also with observations of partial depletion of mature *P. vivax* in the peripheral blood of humans (35-36). Our observation of Pv-iE cytoadhesion to placental tissue from sections of the placenta made after delivery (data not shown), suggests that the phenomenon can occur *in vivo*. However, histopathological studies of post-mortem tissues that would be required to indicate if this phenomenon extends to other organs in infected individuals are limited.

In all isolates where trypsin treatment was tested, the only partially abrogated Pv-iE cytoadhesion suggests that trypsin-resistant ligands commonly occur on the Pv-iE surface. It would be important to establish whether other receptors are implicated in Pv-iE cytoadhesion and explore the precise role of ICAM-1 and CSA. Finally, detailed investigations of the role of *vir* genes as cytoadhesive ligands, for which we present

indirect evidence, are complicated since a) multiple members of the VIR protein family are expressed at the infected red blood cell surface (17) unlike the clonally expressed *var* genes of *P. falciparum* (37), and b) the high number of *vir* genes present in the genome (346 *vir* for Sal line of *P. vivax* (31), as opposed to 59 *var* for the 3D7 line of *P. falciparum*) (38). Nevertheless, our data call for further investigations on the role of *VIR* proteins in Pv-iE cytoadhesion.

Despite infections with *P. vivax* are less life threatening than those caused by *P. falciparum*, morbidity in *P. vivax* is associated with anemia and a pronounced cytokine-mediated inflammatory response (4). Differential accumulation of a proportion of parasites to some organs, such as the lung or the placenta, might be targeted by the inflammatory response to this organ, then leading to a more severe clinical presentation (4, 39-40).

In conclusion, our observations add a new aspect to the pathophysiology of a major, yet mostly neglected human pathogen, which could lead to novel therapeutic approaches to alleviate the increasingly recognized health burden imposed globally by this distinctly not-so-benign parasite.

ACKNOWLEDGEMENTS

Special thanks to Dr. Jürg Gysin (Institut Pasteur, Guadeloupe, France) and Dr. Artur Scherf (Institut Pasteur, Paris, France) for providing endothelial cells, *P. falciparum* FCR3 parasites and CHO-CD36 cells, respectively. We thank Dr. Cristina Vicente and Dr. Claudio C. Werneck for providing the megapixel digital camera and for discussion. We are grateful to Anne Charlotte Grüner for her critical comments. LR and GS are currently part of an official collaboration between SIgN-/A*-STAR and INSERM (Laboratoire International Associé, INSERM). FTMC dedicates this study to Zeci T. M. Costa (*in memoriam*).

AUTHOR CONTRIBUTIONS

All authors discussed the results and commented on the manuscript. FTMC, LR and GS conceived and designed the experiments. BOC, JAL, PAN, SCPL, DYB, RM, PPO, BR, RS and YCB performed the experiments. BOC, SCPL, PAN, RM, MVGL, GW, LR, GS, BR, RS, HDP and FTMC analyzed the data. MMR, ISS, TRO, MOGA HDP and MVGL contributed reagents/ materials/analysis tools. GW, MVGL, GS, LR, HDP and FTMC wrote the paper.

REFERENCES

1. Miller LH, Baruch DI, Marsh K, Doumbo OK. The pathogenic basis of malaria. Nature **2002**; 415:673-9.
2. Mendis K, Sina BJ, Marchesini P, Carter R. The neglected burden of Plasmodium vivax malaria. Am J Trop Med Hyg **2001**; 64:97-106.
3. Nosten F, McGready R, Simpson JA, et al. Effects of Plasmodium vivax malaria in pregnancy. Lancet **1999**; 354:546-9.
4. Anstey NM, Russell B, Yeo TW, Price RN. The pathophysiology of vivax malaria. Trends Parasitol **2009**; 25:220-7.
5. Genton B, D'Acremont V, Rare L, Baea K, Reeder JC, Alpers MP, Muller I. Plasmodium vivax and mixed infections are associated with severe malaria in children: a prospective cohort study from Papua New Guinea. PLoS Med **2008**; 5:e127.
6. Kochar DK, Saxena V, Singh N, Kochar SK, Kumar SV, Das A. Plasmodium vivax malaria. Emerg Infect Dis **2005**; 11:132-4.
7. Tjitra E, Anstey NM, Sugiarto P, et al. Multidrug-resistant Plasmodium vivax associated with severe and fatal malaria: a prospective study in Papua, Indonesia. PLoS Med **2008**; 5:e128.
8. Kyes S, Horrocks P, Newbold C. Antigenic variation at the infected red cell surface in malaria. Annu Rev Microbiol **2001**; 55:673-707.
9. Scherf A, Lopez-Rubio JJ, Riviere L. Antigenic variation in Plasmodium falciparum. Annu Rev Microbiol **2008**; 62:445-70.
10. Cserti CM, Dzik WH. The ABO blood group system and Plasmodium falciparum malaria. Blood **2007**; 110:2250-8.

11. Fairhurst RM, Wellems TE. Modulation of malaria virulence by determinants of Plasmodium falciparum erythrocyte membrane protein-1 display. Curr Opin Hematol **2006**; 13:124-30.

12. Duffy PE. Plasmodium in the placenta: parasites, parity, protection, prevention and possibly preeclampsia. Parasitology **2007**; 134:1877-81.

13. Ihalamulla RL, Mendis KN. Plasmodium vivax: isolation of mature asexual stages and gametocytes from infected human blood by colloidal silica (Percoll) gradient centrifugation. Trans R Soc Trop Med Hyg **1987**; 81:25-8.

14. Fernandez V, In: Ljungström I, Perlmann H, Schlichtherle M, Scherf A, Wahlgren M. Methods in Malaria Research. 4th ed. MR4 / ATCC: Manassas, Virginia, **2004**:26-7.

15. Snounou G, Singh B. Nested PCR analysis of Plasmodium parasites. Methods Mol Med **2002**; 72:189-203.

16. Bargieri DY, Rosa DS, Braga CJ, et al. New malaria vaccine candidates based on the Plasmodium vivax Merozoite Surface Protein-1 and the TLR-5 agonist Salmonella Typhimurium FliC flagellin. Vaccine **2008**; 26:6132-42.

17. Fernandez-Becerra C, Pein O, de Oliveira TR, et al. Variant proteins of Plasmodium vivax are not clonally expressed in natural infections. Mol Microbiol **2005**; 58:648-58.

18. Oliveira TR, Fernandez-Becerra C, Jimenez MC, Del Portillo HA, Soares IS. Evaluation of the acquired immune responses to Plasmodium vivax VIR variant antigens in individuals living in malaria-endemic areas of Brazil. Malar J **2006**; 5:83.

19. Costa FT, Fusai T, Parzy D, et al. Immunization with recombinant duffy binding-like-gamma3 induces pan-reactive and adhesion-blocking antibodies against placental chondroitin sulfate A-binding Plasmodium falciparum parasites. J Infect Dis **2003**; 188:153-64.

20. di Santi SM, Boulos M, Vasconcelos MA, Oliveira S, Couto A, Rosario VE. [Characterization of Plasmodium falciparum strains of the State of Rondonia, Brazil, using microtests of sensitivity to antimalarials, enzyme typing and monoclonal antibodies]. Rev Inst Med Trop Sao Paulo **1987**; 29:142-7.

21. Gay F, Robert C, Pouvelle B, Peyrol S, Scherf A, Gysin J. Isolation and characterization of brain microvascular endothelial cells from Saimiri monkeys. An in vitro model for sequestration of Plasmodium falciparum-infected erythrocytes. J Immunol Methods **1995**; 184:15-28.

22. Muanza K, Gay F, Behr C, Scherf A. Primary culture of human lung microvessel endothelial cells: a useful in vitro model for studying Plasmodium falciparum-infected erythrocyte cytoadherence. Res Immunol **1996**; 147:149-63.

23. Hasler T, Albrecht GR, Van Schravendijk MR, et al. An improved microassay for Plasmodium falciparum cytoadherence using stable transformants of Chinese hamster ovary cells expressing CD36 or intercellular adhesion molecule-1. Am J Trop Med Hyg **1993**; 48:332-47.

24. Pouvelle B, Fusai T, Lepolard C, Gysin J. Biological and biochemical characteristics of cytoadhesion of Plasmodium falciparum-infected erythrocytes to chondroitin-4-sulfate. Infect Immun **1998**; 66:4950-6.

25. Noviyanti R, Brown GV, Wickham ME, Duffy MF, Cowman AF, Reeder JC. Multiple var gene transcripts are expressed in Plasmodium falciparum infected erythrocytes selected for adhesion. Mol Biochem Parasitol **2001**; 114:227-37.

26. Pouvelle B, Traore B, Nogueira PA, Pradines B, LePolard C, Gysin J. Modeling of Plasmodium falciparum-infected erythrocyte cytoadhesion in microvascular conditions: chondroitin-4-sulfate binding, A competitive phenotype. J Infect Dis **2003**; 187:292-302.

27. Avril M, Traore B, Costa FT, Lepolard C, Gysin J. Placenta cryosections for study of the adhesion of Plasmodium falciparum-infected erythrocytes to chondroitin sulfate A in flow conditions. Microbes Infect **2004**; 6:249-55.

28. Andrews KT, Adams Y, Viebig NK, Lanzer M, Schwartz-Albiez R. Adherence of Plasmodium falciparum infected erythrocytes to CHO-745 cells and inhibition of binding by protein A in the presence of human serum. Int J Parasitol **2005**; 35:1127-34.

29. Kroll MH, Hellums JD, McIntire LV, Schafer AI, Moake JL. Platelets and shear stress. Blood **1996**; 88:1525-41.

30. Cooke BM, Berendt AR, Craig AG, MacGregor J, Newbold CI, Nash GB. Rolling and stationary cytoadhesion of red blood cells parasitized by Plasmodium falciparum: separate roles for ICAM-1, CD36 and thrombospondin. Br J Haematol **1994**; 87:162-70.

31. Carlton JM, Adams JH, Silva JC, et al. Comparative genomics of the neglected human malaria parasite Plasmodium vivax. Nature **2008**; 455:757-63.

32. del Portillo HA, Fernandez-Becerra C, Bowman S, et al. A superfamily of variant genes encoded in the subtelomeric region of Plasmodium vivax. Nature **2001**; 410:839-42.

33. Resende M, Ditlev SB, Nielsen MA, et al. Chondroitin sulphate A (CSA)-binding of single recombinant Duffy-binding-like domains is not restricted to Plasmodium falciparum Erythrocyte Membrane Protein 1 expressed by CSA-binding parasites. Int J Parasitol **2009**; 39:1195-204.

34. Fremount HN, Rossan RN. The sites of sequestration of the Uganda-Palo Alto strain of plasmodium falciparum-infected red blood cells in the squirrel monkey, Samimiri sciureus. J Parasitol **1974**; 60:534-6.

35. Rudolf GD, Ramsay JC. Enumeration of parasites in therapeutic malaria. Journal of Tropical Medicine and Hygiene **1927**; 30:1-8.

36. Field JW, Shute PG. The microscopic diagnosis of human malaria. II. A morphological study of the erythrocytic parasites. Kuala Lumpur: Government Press, **1956**.

37. Chen Q, Fernandez V, Sundstrom A, Schlichtherle M, Datta S, Hagblom P, Wahlgren M. Developmental selection of var gene expression in Plasmodium falciparum. Nature **1998**; 394:392-5.

38. Gardner MJ, Hall N, Fung E, et al. Genome sequence of the human malaria parasite Plasmodium falciparum. Nature **2002**; 419:498-511.

39. Anstey NM, Handojo T, Pain MC, Kenangalem E, Tjitra E, Price RN, Maguire GP. Lung injury in vivax malaria: pathophysiological evidence for pulmonary vascular sequestration and posttreatment alveolar-capillary inflammation. J Infect Dis **2007**; 195:589-96.

40. Tan LK, Yacoub S, Scott S, Bhagani S, Jacobs M. Acute lung injury and other serious complications of Plasmodium vivax malaria. Lancet Infect Dis **2008**; 8:449-54

FIGURE LEGENDS

Figure 1. Percoll gradient enrichment of *P. vivax* maturing forms. (**A**) Giemsa staining of the mature trophozoites and young schizonts obtained after Percoll® gradient enrichment, yielding cell suspensions with 85% - 97% Pv-iE. (**B**) Parasite species and maturity was confirmed by IFA using anti-PvMSP-1_{19} conformational MAbs (3F8 and K23) diluted at 1:50. Normal mouse sera were used in the negative controls.

Figure 2. Adhesion of Pv-iE to lung, brain endothelial cells, or placental cryosections. Representative photomicrographs (left panel) and cytoadhesion assays (right panel) of Pv-iE to HLEC **(A)**, SBEC **(B)** and placental cryosections **(C)** stained with Giemsa and visualized with the aid of a Nikon microscope at 100 X magnification. Arrows indicate Pv-iE bound to host cells. Representative results from Pv-iE collected from different patients that were used for cytoadhesion assays conducted on untreated cells, using Pv-iE pre-treated with trypsin, or in the presence of soluble CSA or anti-CD36 antibody. In all cases parasites (5×10^4) were left for 1 hour at 37°C in 8-well culture slides (0.69 cm^2 per well), then extensively washed and adhered Pv-iE were counted. Results are expressed as the mean number (± SD) of iE bound per mm^2, normalized to an input of 10^3 iE/mm^2. Significance was calculated using a Kruskal-Wallis test: * $0.05 > P > 0.01$; ** $0.01 > P > 0.001$.

Figure 3. Resistance of Pv-iE cytoadhesion to flow conditions. Enriched Pv-iE (5×10^5) were allowed to adhere to HLEC for 1-hour incubation at 37° C in single-well microslides (8.6 cm^2) to a flow chamber system and cytoadhesion medium (RPMI pH 6.8) was flowed through at a wall shear stress of 0.09, 0.36 and 1.44 Pascal (Pa) (numbers do

not correspond with the figures and in the text), for 10, 5 and 2.5 min, respectively, with control chambers without flow. The Pv-iE still bound at the end of the flow period were counted in 20 randomly selected fields and the percentages of binding compared to that in the control chamber were calculated. Results are expressed as mean binding percentages of 2 patient isolates (104 and 106) ± SD on HLEC previously treated with LPS (1.0 μg/ml) or left untreated. Significance was calculated using the Mann-Whitney *U* test: * *P*< 0.05 adhesion on non-stimulated vs. LPS-stimulated HLEC.

Figure 4. Adhesion of Pv-iE to specific receptors. Pv-iE (5 x 10^4/well) were allowed to adhere to CHO–ICAM, CHO-CD36 or control CHO-745. Results are expressed as the mean of iE/mm^2 ± SD normalized for an input of 10^3 iE/mm^2**.** Significance was calculated using the Kruskal-Wallis test: * *P*< 0.001 adhesion on CHO-ICAM vs. CHO-CD36 or CHO-745.

Figure 5. Recognition and blocking of Pv-iE cytoadhesion to HLEC by specific anti-VIR sera. (A) Immunofluorescence of a Pv-iE labeled with antiserum against VIR-A4 (1:20) or VIR-E5 (1:20). Upper panel from left to right: Phase contrast; DAPI staining; mouse α-VIR-E5 and Alexa-Fluor 488-conjugated goat anti-mouse IgG. Note that α-VIR-A4 was used in the bottom panel. **(B)** Pv-iE (5 x 10^4/well) were incubated for 1 hour at 37°C alone or in the presence of VIR-A4 or VIR-E5 antisera diluted at 1:5 (isolate 095) or 1:10 (isolate 096). In both assays, sera from mice immunized solely with GST in Freund's adjuvant were used as a negative control. For these assays, inhibition was determined as the percentage of negative control counts expressed as mean ± SD of triplicate wells. Significance was calculated using the Kruskal-Wallis test: * *P*< 0.05 vs. inhibition by α-GST antisera.

MOVIE LEGENDS

Supplementary Movie Legend 1

This 00:26 min movie shows the rolling and binding of a Pv-iE to HLEC. Parasites were diluted in medium and flowed at a wall shear stress of 0.09 Pa.

Supplementary Movie Legend 2

This 00:48 min movie shows two Pv-iE bound to HLEC under a flow condition of 0.36 Pa.

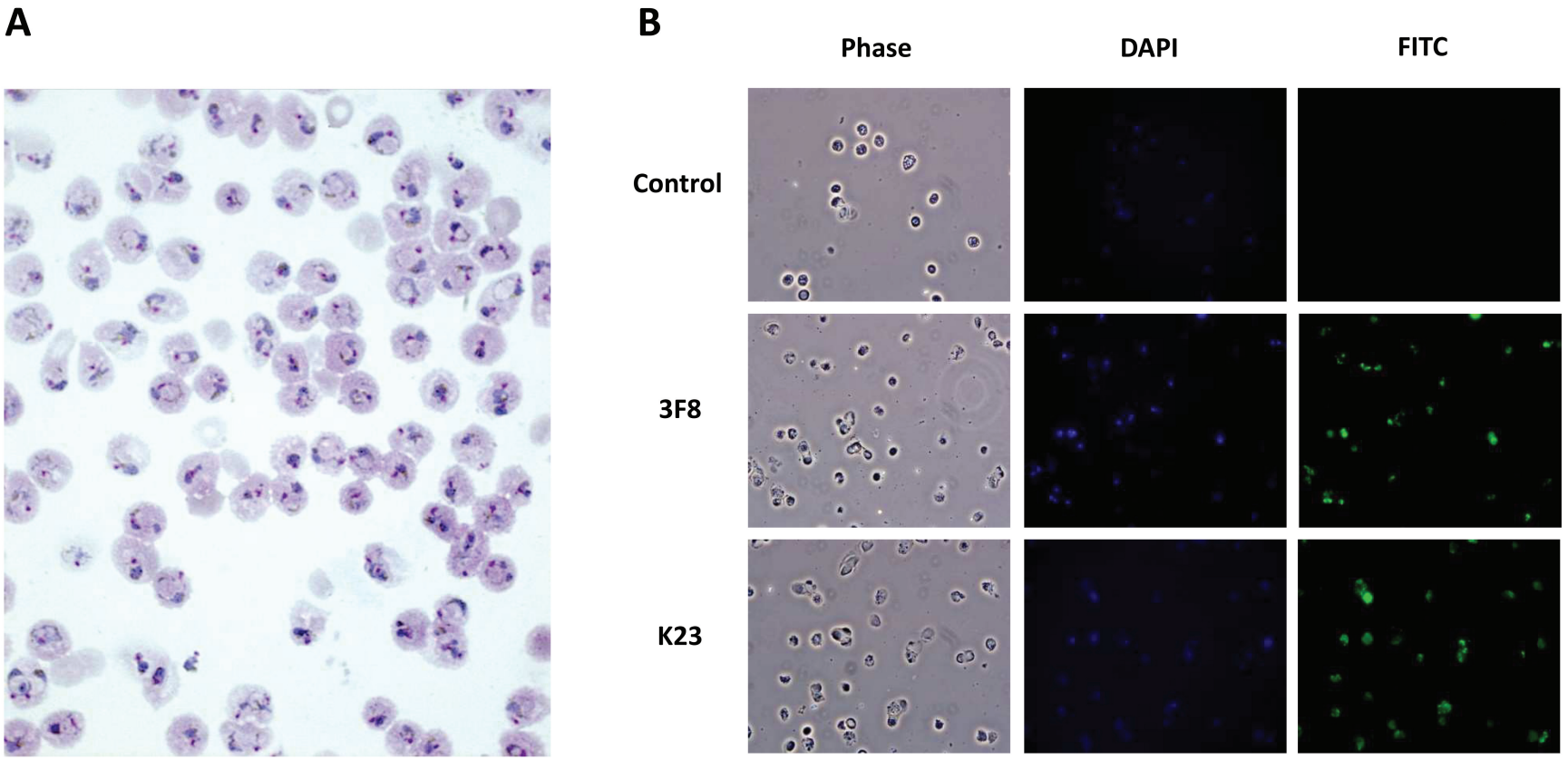

Carvalho *et al*. Figure 1

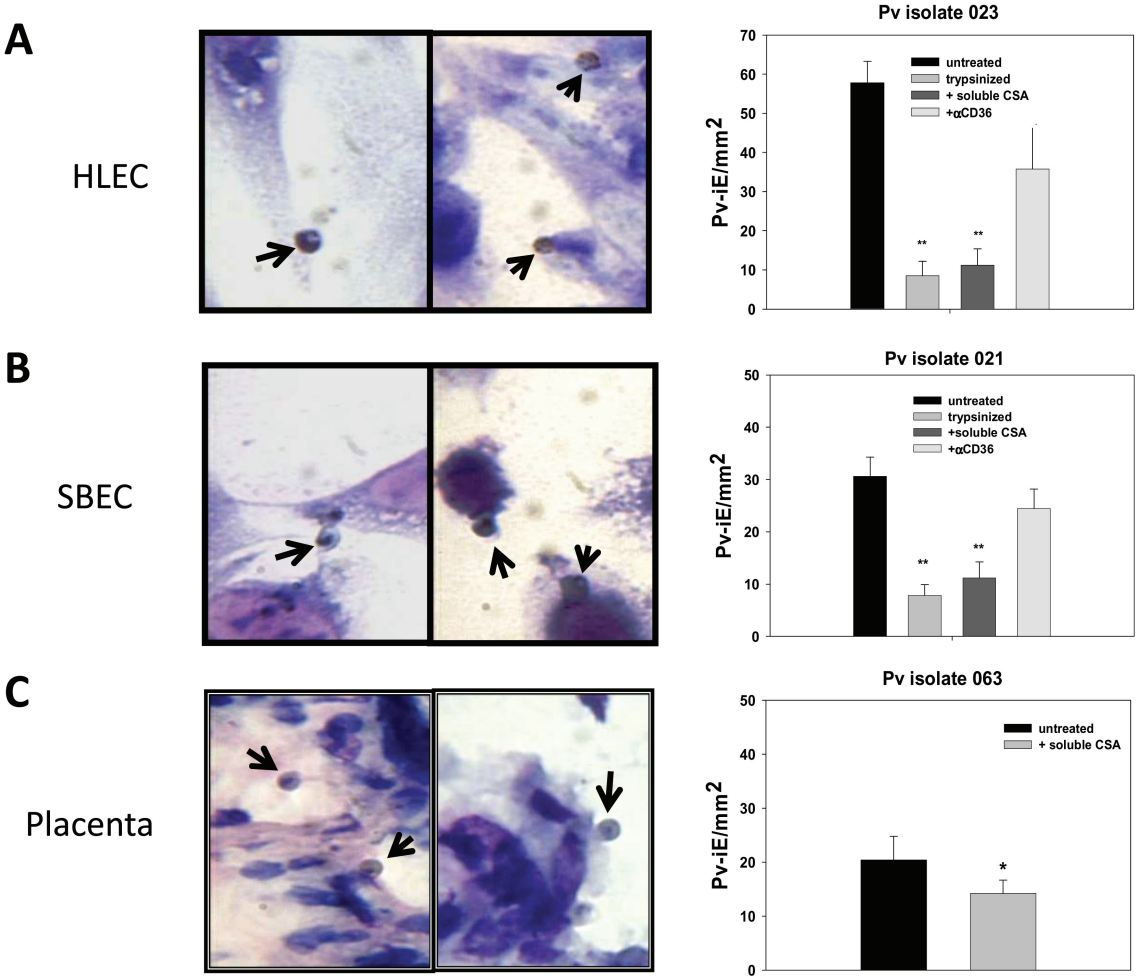

Carvalho *et al*. Figure 2

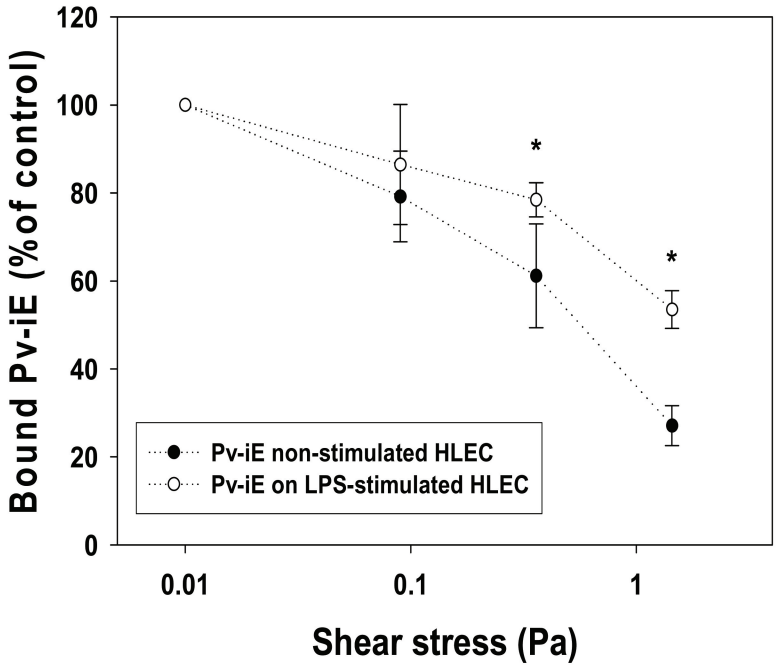

Carvalho *et al*. Figure 3

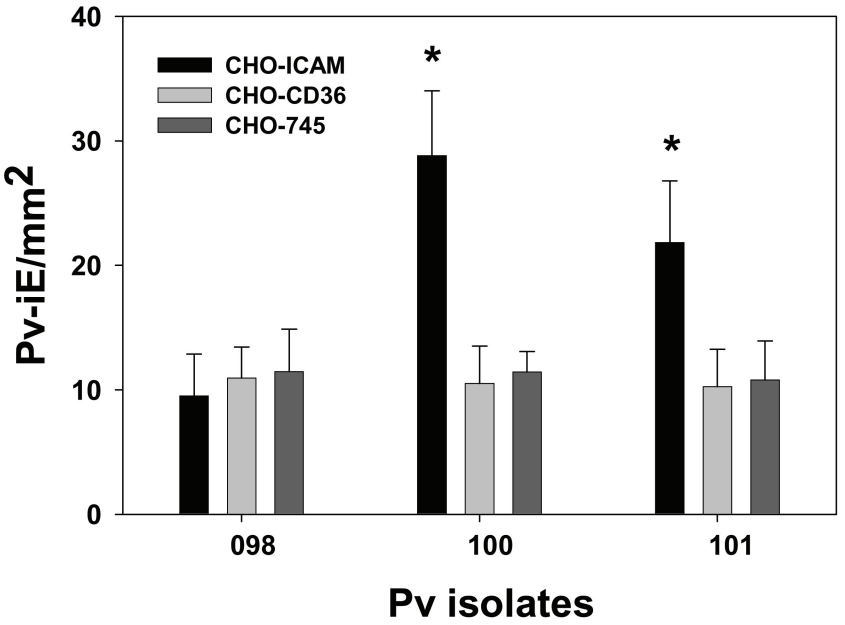

Carvalho *et al*. Figure 4

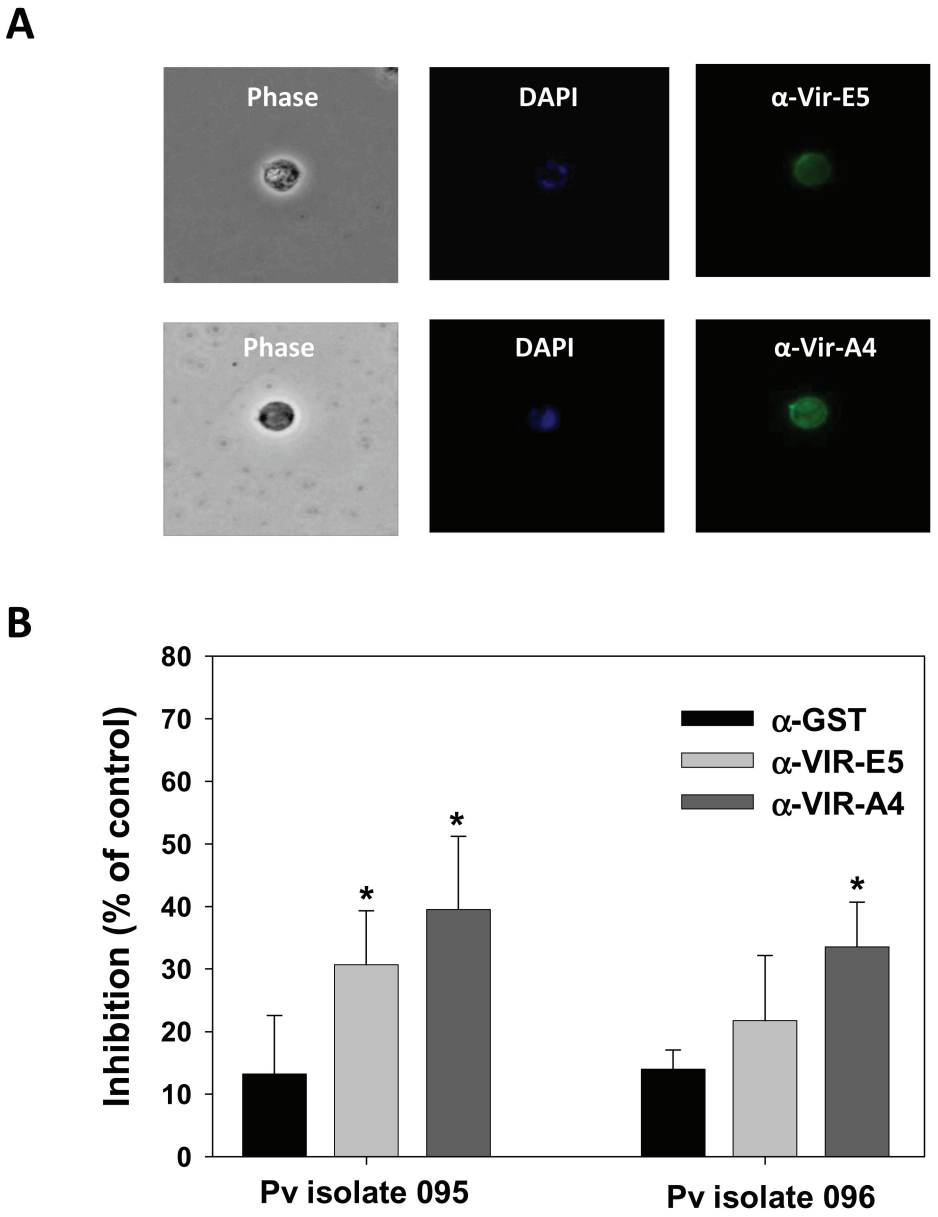

Carvalho *et al*. Figure 5

Table 1. Cytoadhesion assays of Pv-iE and Pf-iE collected from 24 patients.

		HLEC				SBEC				Placental cryosections	
		Adhesion[a]	% Inhibition[b]			Adhesion[a]	% Inhibition[b]			Adhesion[a]	% Inhibition[b]
Parasite	Patient		Trypsinized	+sCSA	+αCD36	CaseABC		Trypsinized	+sCSA	+αCD36		+sCSA
Pv-iE	008						**58.2±9.8**	19±10				
Pv-iE	015						**32.4±11.04**	52±11*				
Pv-iE	016	**52.4±8.5**	70±7*									
Pv-iE	019	**36.1±10.6**	59±10 **	25±21								
Pv-iE	021						**30.6±3.7**	74±7**	63±10**	20±12		
Pv-iE	022	**28.3±4.5**	29±21**	52±8**	2±27							
Pv-iE	023	**57.8±5.5**	85±6**	81±7**	38±20							
Pv-iE	024	**33.9±3.7**	76±7**	65±8**	20±11							
Pv-iE	030	**16.6±3.4**	46±10***				**12.8±2.8**	42±18*				
Pv-iE	031	**26.1±4.5**	47±15***									
Pv-iE	034	**56.7±7.4**		18±10*			**49.5±7.9**		28±9*			
Pv-iE	035	**37.5±9.4**		41±13**			**23.9±8.0**		31±30			
Pv-iE	036										**22.3±5.4**	23±19
Pv-iE	063										**20.4±4.4**	30±12*
Pv-iE	065	**33.5±8.8**		51±13***								
Pv-iE	066										**9.9±3.2**	15±40
Pv-iE	076	**19.7±4.0**		34±18***		7±25						
Pv-iE	083	**38.6±7.3**		49±15**		4±21						
Pv-iE	086	**30.1±6.5**		40±16**		13±22						
Pv-iE	087	**41.3±5.2**		16±23		3±15						
Pf-iE	002	**130.1±23.7**										
Pf-iE	003	**636.7±119.2**										
Pf-iE	005										**773.5±179.5**	87±7*
Pf-iE	008	**454.4±45.4**										

[a] Mean number (± SD) of iE bound per mm^2, normalized to an input of 10^3 iE/mm^2.
[b] Percentage inhibition (± SD) of adhesion was calculated after enumeration of adherent iE either following trypsinization of iE or prior to the assay, or when the assay was conducted in the presence of soluble CSA (sCSA), anti-CD36 monoclonal antibody (αCD36) or in endothelial cells pre-treated with chondroitinase ABC (CaseABC).
[c] Significance with respect to adhesion value: * 0.05 > *P* > 0.01; ** 0.01 > *P* > 0.001; *** *P* < 0.001. Data from *P. falciparum* isolates (presented in dark red) confirmed that the host cells and placental cryosections employed were able to sustain parasite cytoadhesion.

Table 2. Cytoadhesion assays of Pv-iE, collected from 7 patients, or cultured Pf-iE to HLEC[a] under flow conditions

Shear stress (Pa)			0.00	0.09		0.36		1.44	
			Adhesion[b]	Adhesion	% Binding[c]	Adhesion	%Binding	Adhesion	% Binding
Parasite	Patient	LPS							
Pv-iE	090	-	67.4±14.4	34.2 ±8.6	50.8	30.4 ±9.6	45.2	ND[d]	
Pv-iE	090	+	55.6 ±9.6	48.0 ±17.8	86.3	42.7 ±15.4	76.9	ND	
Pv-iE	091	+	53.0 ±6.1	39.0 ±7.7	73.6	38.5 ±10.1	72.6	ND	
Pv-iE	092	-	17.6 ±9.6	13.4 ±8.2	76.1	10.8 ±2.9	61.1	ND	
Pv-iE	093	-	47.9 ±12.0	29.9 ±8.2	62.4	ND[d]		ND	
Pv-iE	094	-	60.4 ±13.8	51.3 ±9.1	84.9	ND[d]		ND	
Pv-iE	104	-	30.4 ±9.1	26.3 ±5.3	86.5	16.1 ±5.3	52.9	9.2 ±7.7	30.3
Pv-iE	104	+	32.5 ±13.8	25.0 ±5.3	76.9	24.6 ±5.3	75.7	16.4 ±6.7	50.5
Pv-iE	106	-	28.6 ±8.6	20.5 ±14.9	71.7	19.8 ±6.1	69.2	6.8 ±5.8	23.8
Pv-iE	106	+	29.1 ±8.2	27.9 ±10.6	96.2	23.6 ±7.2	81.1	16.4 ±6.7	56.4
Pf-iE	$S20^{ICAM}$	-	39.8±15.8	19.2±13.0	47.9	12.0±5.8	30.0	9.6±8.2	24.3
Pf-iE	$FCR3^{CSA}$	-	370.9±50.9	333.1±25.0	89.8	294.5±36.9	79.4	190.8±34.7	51.4

[a] *Plasmodium vivax* or cultured *P. falciparum*, selected on ICAM-1 ($S20^{ICAM}$) or CSA ($FCR3^{CSA}$), were allowed to adhere to HLEC, previously incubated (+) or not (-) with 1.0 µg/mL of LPS, then cytoadhesion medium were flowed through at a shear stress of 0.09, 0.36 and 1.44 (Pa) for 10, 5 and 2.5 min, respectively.
[b] Number of remaining adherent parasites after a determined flow condition. Results are expressed as iE/mm^2± SD, normalized to an input of 10^3 iE/mm^2.
[c] Percentage of parasites that remained cytoadherent after being subjected to a wall shear stress.
[d] Not determined.

OUTROS ARTIGOS PUBLICADOS RELACIONADOS COM A TEMÁTICA

Gene 453 (2010) 37–44

Contents lists available at ScienceDirect

Gene

journal homepage: www.elsevier.com/locate/gene

The South American *Plasmodium falciparum var* gene repertoire is limited, highly shared and possibly lacks several antigenic types

Letusa Albrecht [a], Catarina Castiñeiras [a], Bruna O. Carvalho [b], Simone Ladeia-Andrade [a,1], Natal Santos da Silva [a], Erika H.E. Hoffmann [c], Rosimeire C. dalla Martha [d], Fabio T.M. Costa [b], Gerhard Wunderlich [a,*]

[a] Department of Parasitology, Institute for Biomedical Sciences, University of São Paulo, Av. Prof. Lineu Prestes, 1374, 05508-900 São Paulo-SP, Brazil
[b] Department of Genetics, Evolution and Bioagents, Institute of Biology, State University of Campinas (UNICAMP), Campinas-SP, Brazil
[c] Institute for Tropical Medicine, University of São Paulo, Brazil
[d] Center for Research in Tropical Medicine (CEPEM), Porto Velho, Brazil

ARTICLE INFO

Article history:
Received 26 May 2009
Received in revised form 5 January 2010
Accepted 6 January 2010
Available online 15 January 2010

Received by S. Goldenberg

Keywords:
Antigenic variation
var
PfEMP1

ABSTRACT

The *Plasmodium falciparum var* gene family encodes large variant antigens, which are important virulence factors, and also targets of the humoral host response. The frequently observed mild outcomes of falciparum malaria in many places of the Amazon area prompted us to ask whether a globally restricted variant (*var*) gene repertoire is present in currently circulating and older isolates of this area. By exhaustive analysis of *var* gene tags from 89 isolates and clones taken during many years from all over the Brazilian Amazon, we estimate that there are probably no more than 350–430 distinct sequence types, less than for any similar sized area studied so far. Detailed analysis of the *var* tags from genetically distinct clones obtained from single isolates revealed restricted and redundant repertoires suggesting either a low incidence of infective bites or restricted variant gene diversity in inoculated parasites. Additionally, we found a structuring of *var* gene repertoires observed as a higher pairwise typing sharing in isolates from the same microregion compared to isolates from different regions. Fine analysis of translated *var* tags revealed that certain Distinct Sequence Identifiers (DSIDs) were differently represented in Brazilian/South American isolates when compared to datasets from other continents. By global alignment of worldwide *var* DBLα sequences and sorting in groups with more than 76% identity, 125 clusters were formed and more than half of all genes were found in nine clusters with 50 or more sequences. While Brazilian/South American sequences were represented only in 64 groups, African sequences were found in the majority of clusters. DSID type 1 related sequences accumulated almost completely in one single cluster, indicating that limited recombination occurs in these specific *var* gene types. These data demonstrate the so far highest pairwise type sharing values for the *var* gene family in isolates from all over an entire subcontinent. The apparent lack of specific sequences types suggests that the *P. falciparum* transmission dynamics in the whole Amazon are probably different from any other endemic region studied and possibly interfere with the parasite's ability to efficiently diversify its variant gene repertoires.

1. Introduction

The severe forms of malaria are caused by the apicomplexan blood parasite *Plasmodium falciparum.* A very important virulence factor of this parasite is a family of variant proteins – *P. falciparum* erythrocyte membrane protein 1, PfEMP1, (Leech et al., 1984) – which are localized at the surface of the host's infected red blood cell (IRBC). Variants of the PfEMP1 family are able to interact with a number of endothelial receptor molecules leading to the sequestration of the IRBC and the failure to eliminate IRBC by spleen passage (reviewed by Craig and Scherf, 2001). It is believed that in many but not all cases sequestration ultimately leads to the frequently observed severe manifestations in non-immune subjects, who eventually succumb to disease if not treated in time (reviewed in Miller et al., 2002). PfEMP1 proteins are encoded by the *var* gene family with around 60 members per haploid parasite genome (Baruch et al., 1995). The particular transcription mode of the *var* genes (Scherf et al., 1998; reviewed in Scherf, 2006) permits the parasite to establish long-lasting infections by constant immune evasion. In addition, the parasite is able to redistribute variant genes during meiosis and rarely during mitosis by a process termed ectopic

Abbreviations: DBL, Duffy-binding like; DSID, Distinct sequence identifier; PCR, Polymerase chain reaction; PfEMP1, *Plasmodium falciparum* erythrocyte membrane protein 1; PNG, Papua New Guinea; PTS, pairwise type sharing.

* Corresponding author. Tel.: +55 11 30917265; fax: +55 11 30917417.
E-mail address: gwunder@usp.br (G. Wunderlich).
[1] Present address: Oswaldo Cruz Institute (FIOCRUZ), Rio de Janeiro, Brazil.

0378-1119/$ – see front matter © 2010 Elsevier B.V. All rights reserved.
doi:10.1016/j.gene.2010.01.001

recombination in which non-homologous telomere ends and the variant gene copies located therein are recombined by gene conversion events (Freitas-Junior et al., 2000; Duffy et al., 2009). As a consequence, *var* genes are hypervariable and differ significantly from strain to strain, unlike most other parts of the genome. Accordingly, previous reports showed that the *var* repertoire is virtually unlimited in Southeast Asian or Kenyan isolates (Barry et al., 2007). In contrast, we (Albrecht et al., 2006) and others (Barry et al., 2007) have shown that in distinct geographic areas and/or times of sample collection the *var* repertoire may be limited to a certain extent. In order to expand the previous finding of a limited *var* gene repertoire in Brazilian isolates independently from the year of collection or geographic origin, we analyzed exhaustively the genomic *var* gene repertoires in isolates from all over Brazil and included the public sequence data from the HB3 strain from Honduras, the Brazilian strain 7G8, collected in the early 1980s, three Venezuelan strains and compared the data against *var* DBLα sequences available in GenBank.

2. Material and methods

2.1. Parasite origin

Parasite isolates analyzed herein were from *P. falciparum* infected individuals with differing degrees of symptoms, ranging from moderate acute malaria (non-severe) to non-symptomatic infections. The parasites were collected between 1985 and 2008. Eight isolates were cloned before genomic DNA preparation and genotyped using a number of microsatellite loci (described in Hoffmann et al., 2006). The projects generating the parasite samples was previously approved by the local Committee for Research involving humans and all donors gave their informed consent before participating in the study. The geographic origin of all Brazilian isolates analyzed during this study is given in Figure S1.

2.2. Nucleic acid extraction, PCR and sequencing

Genomic DNA from isolates was obtained from 200 μl of frozen blood by the method described in Moll et al., 2008). For the amplification of the 360–420 bp *var* DBLα tags the previously published degenerated *var* oligonucleotides (Taylor et al., 2000a; Peters et al., 2002) were used. These oligonucleotides were previously tested on genomic *P. falciparum* DNA from Brazilian isolates and did not result in significantly biased amplification of determined *var* tags (Albrecht et al., 2006). Amplified products were separated in TAE agarose gels, excised and purified by the modified glassmilk method (Boyle and Lew, 1995) and ligated in pTZ57-T (Fermentas). Individual plasmid clones were then sequenced in an Applied Biosystems 3100 DNA sequencer using BigDye3.1 chemistry. Sequence results were quality-analyzed by the E-gene platform (Durham et al., 2005) using a PHRED quality cutoff value of 20 and a sliding "good sequence" window of 300 base pairs. Short sequences or low quality reads were individually re-sequenced. For each isolate, differing numbers of clones with good sequence quality were obtained and the sequencing effort per parasite isolate or clone was up to 150 plasmid clones (see Supplemental Table 1 for details).

2.3. Origin of published sequences

We analyzed more than 2000 public sequences from DBLα tags from isolates of different regions of the world. Following their geographic origin, these sequences were divided in three groups: Asia (from continental Asia and islands), Africa (from the African continent) and America (from Latin America Countries). The sequences extracted from GenBank from Africa were 22 sequences from Sudan (four isolates) (Ward et al., 1999), 55 sequences from Kenya (10 isolates) and 8 sequences from Cape Verde (one isolate) (Taylor et al., 2000b), 632 different sequences from Kenya (Bull et al., 2005), 241 sequences from Uganda (Normark et al., 2007), 141 sequences from Mali (Kyriacou et al., 2006), 23 sequences from isolate NF36 (Fowler et al., 2002), 212 sequences from different African regions (Barry et al., 2007) and 55 DBLα tags from the clone 3D7. The Asian group consisted of 1140 *var* DBLα tags (including isolates from islands of this continent). Among these sequences, 799 sequences were from the study of Barry et al. (2007), 199 sequences from Fowler and colleagues (Fowler et al., 2002), and 142 *var* α tag sequences from Kaestli and colleagues (Kaestli et al., 2006).

From the Americas, 82 sequences were from Brazil (Kirchgatter and del Portillo, 2002; Barry et al., 2007), 61 sequences from Venezuela (Tami et al., 2003) and 18 sequences from the clone HB3, from Honduras, Central America (Kraemer et al., 2007). The remaining sequences were either published by us (Albrecht et al., 2006) or sequenced herein (Supplemental Table S1). The complete list of GenBank entries can be found in Supplemental Table 2 and the dataset of different tags sequenced in this work and the previous work of Albrecht et al. (2006) is in Supplemental File 1.

2.4. Sequence analysis

In a first step, the oligonucleotide primers were deleted from all sequences. All sequences from each isolate or clone were separately aligned using ClustalX 2 software (Larkin et al., 2007) and pairwise identity matrix tables were created. From each alignment, sequences with less than 98% identity were extracted, which contain the different sequence tags of the respective parasite clone or isolate. These resulting sequence groups representing DBLα sequence tags of specific parasite clones or isolates are further termed isolate or clone *var* repertoire. The *var* repertoires from individual clones or isolates were then joined in multifasta files and realigned in order to identify shared *var* repertoires. Shared sequences between parasite isolates/clones were identified from pairwise identity matrices after the alignment. Sequences shared between individual repertoires were considered identical if they showed 98% or more identical sequence positions. In order to quantify the redundancy of sequence types in repertoires found in different isolates or clones, we applied the formula suggested by Barry et al. (2007), where the pairwise type sharing (PTS) is defined as follows:

$2*Seqs_{shared}$ / $(Seqs_{isolA}+Seqs_{isolB})$, where $Seqs_{shared}$ is the number of sequence types shared between isolate A and B, and $Seqs_{isolA/B}$ is the number of different sequence types detected in each isolate A and B.

Var sequences from other datasets (see above) were also aligned together with the Brazilian repertoires to obtain globally shared sequences. Different (98%) sequences were translated and analyzed for their DSID (distinct sequence identifier) distribution using Perl scripts provided by Bull et al. (2007). In order to analyze peptide sequences with imperfect anchoring sequences, polypeptides with an intact [I/V]RGD-POLV1 and POLV4-DYV flanked downstream by PQ residues were arbitrarily completed with the full anchoring peptide sequence (DIGDI or PQLYR, respectively) and analyzed. A number of sequences in all datasets could be included by this modification. For the analysis of DSIDs distribution, DSID repertoires from all Asian, African, separately from Amele and from Kilifi isolates (Bull et al., 2007) were compared. The differences of DSID group distribution between the Brazilian/South American (Br/SA) data set and data sets from Asia, Africa, Amele and Kilifi were evaluated using C-square statistics. The distributions were considered different when $p<0.05$. The statistical significance of the peptide length distribution of different DBLα tags was evaluated using Mann–Whitney's non-parametrical test with Gaussian *p*-value approximation considered different when $p<0.05$. This analysis was done in PRISM 4.0 software.

For the analysis of DSID distribution after alignment of world-wide sequences, different sequences (<98% sequence identity) which formed the longest continuous peptide were first extracted from the global sequence dataset and realigned using ClustalX 2. The resulting percent identity matrix was then used to group sequences in clades with >76% sequence identity. In parallel, the sequences (98% identity) were translated, trimmed as above to contain a perfect anchoring motif and their DSIDs were evaluated using the Perl script published by Bull et al. (2007). Distribution discrepancies of Br/SA sequences per group were statistically accessed using C-square statistics, comparing the number of Br/SA sequences with the number observed in the entire dataset.

The sequence diversity of isolates from the Amazon and Kilifi/Kenya was estimated using EstimateS 8.0 software (Colwell, 2006) and estimated diversities were calculated using Jacknife1 or mean bootstrap values applying Chao's classical method and 100 reiterations. For this, repertoires from single isolates were considered "samples" and each sequence was considered a "species". The repertoires from the 30 Ariquemes clones were entered as eight isolates by eliminating shared sequences between clones of each original isolate and maintaining only different sequences ("virtual" isolates, e.g., sequences with less than 98% identity from clones 121_1, 121_3, 121_4 and 121_17). This method permits the estimation of the species richness in a given sample — in this case, the total *var* tag repertoire size in the sample was estimated.

3. Results

3.1. Parasite clones from individual isolates contain limited var repertoires

First we looked at individual *var* repertoires from parasite clones which were previously generated by limiting dilution from individual isolates obtained during a Malaria outbreak in Ariquemes/Rondônia in 1985. The cloning was initially performed in order to monitor the parasite's mechanisms of diversification by analyzing repeat regions of merozoite surface antigens and their linkage to microsatellite markers (Hoffmann et al., 2006). After analysis of a differing number of sequences per clone and isolate, we observed that the cumulative number of different sequences from the initial isolates 113, 121, 122, 123, 127, 128, 153 and 154 was always below or close to 60 different sequences (Supplemental Table 4). This indicates that genetically distinct parasite clones circulating in single individuals in this particular situation contained highly overlapping *var* repertoires. Accordingly, the observed "intra-isolate" PTS values pointed to approximately 53% of shared sequences in clones from each isolate (Ariquemes1, Fig. 1). A previously performed microsatellite analysis (Hoffmann et al., 2006) revealed that in most cases clones from these isolates were similar and in a few cases identical. Nevertheless, in clones 121_1 and 121_17 nine different microsatellite loci were identified and even these clearly different parasite lines shared a significant number of *var* tags (Supplemental Table 4).

In the following, we analyzed the PTS of sequences between "virtual" isolates. For this, the repertoires of different sequences from clones originating from the same infected blood sample were aligned and the pairwise shared sequences between the virtual isolates were determined. The averaged PTS showed that 38% of *var* sequence types were shared between the isolates (Ariquemes2, Fig. 1). The co-analyzed isolate S20, collected in 1985 in Porto Velho, also showed a high number of shared sequences. This result suggests the presence of a distinct, limited *var* repertoire in the circulating isolates. In contrast, the isolates collected in Kilifi showed almost no overlap and the number of clones per isolate frequently exceeded the average repertoire size of 50–60 *var* genes (Supplemental Table 4). This indicates the presence of *P. falciparum* clones with significantly different *var* repertoires in the original blood samples from Kilifi.

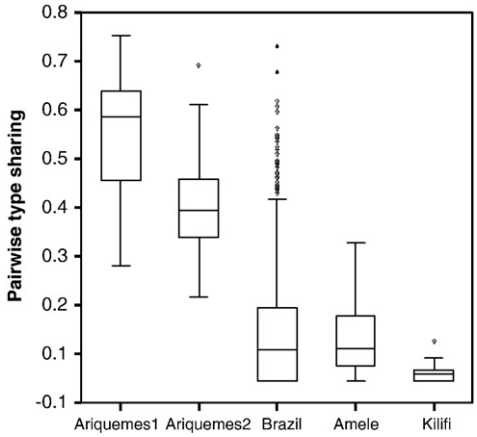

Fig. 1. Pairwise type sharing (PTS) of *var* DBLα encoding tags in different data sets. Shown are interquartile ranges (boxes), median (horizontal line) and approximate 95% sampling interval (whiskers). Ariquemes 1 shows the PTS in 30 parasite clones prepared from eight isolates from Ariquemes/Rondonia, Ariquemes 2 shows PTS for joined repertoires of Ariquemes clones (combining the <98% different sequences of all clones of respective isolates). Brazil documents the PTS of all isolates from Brazil/Amazonia including HB3 and 7G8 strains. For comparison, the datasets from Kilifi (653 sequences in 12 isolates) and from Amele (30 isolates, (Barry et al., 2007) were included. See Supplemental Table 4 for raw data.

3.2. Brazilian var DBLα sequences are conserved over time

Due to the ectopic recombination, *P. falciparum* parasites are able to interchange their variant gene repertoires (Freitas-Junior et al., 2000), as a consequence, it may be expected that *var* repertoires change over time. To address the question if there is a conservation of *var* tags over time, we separated the 2667 *var* sequence reads from 89 different isolates and clones from Brazil in two groups according of the year of collection of these isolates (Supplemental Table 1). The first group contained the 30 clones from Ariquemes and the S20 isolate from Porto Velho (1557 sequence reads) collected in 1985. The second group contained 43 isolates collected 2001–2006 in Porto Velho, and two from Jaú, Amazonas State, collected in 2002 and nine from the eastern region of Acre and from Manaus, Amazonia, collected between 1999 and 2008 (total of 1110 sequences). The number of sequence reads was different for the isolates (Supplemental Tables 1 and 4).

When we analyzed separately both groups we found that 152 different sequences were detected in clones/isolates from 1985 and 169 different sequences in isolates from year 1999 or later. When both groups were analyzed together, we found only 221 different sequences (cutoff 98% identity), of which 100 or 45.2% were shared between the two groups, while 52 (23.5%) were found exclusively in the isolates from 1985/1987 and 69 (31.2%) in the year 1999 or later collected isolates indicating a high number of conserved sequences among these groups (Fig. 2) which persist over decades in the

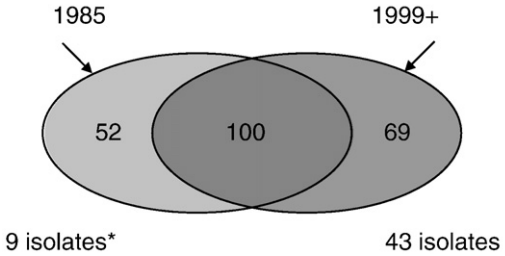

Fig. 2. The global *var* gene repertoire in Brazilian isolates is stable over time. In the parasites from 1985, 52 *var* tags were unique while 100 sequences were shared with 1999+ parasites, which itself showed 69 unique sequences. The number of analyzed isolates per timepoint is indicated. * indicates data from 30 parasite clones generated from eight Ariquemes isolates plus the S20 isolate.

circulating parasites. Importantly, each sequence was read with more than 10fold coverage. Shared sequences were found in isolates from very distant locations (e.g., Jaú National Park and Acrelândia-AC) and different time points of retrieval (S20 and isolate MA5, see Supplemental Table 4, overlap of all Brazilian isolates).

3.3. The Brazilian/South American var repertoire is limited and smaller than from other regions

We then asked if the relatively small and limited *var* repertoire identified until now was also found in other isolates from Latin America. For this, we co-aligned the 221 different Brazilian sequences with additional 160 sequences from Mato Grosso, Brazil (Kirchgatter and del Portillo, 2002; Barry et al., 2007), Venezuela (Tami et al., 2003), from Manaus (7G8 strain), and HB3 from Honduras, Central America (Kraemer et al., 2007). Analyzing these sequences together, the total number of sequences increased to 293 different sequences (Genbank entries in Supplemental Table S3). Again, a number of sequences from the strain HB3 (Honduras) and 7G8 could also be found in older or more recent isolates from Rondônia or Manaus, confirming conservation of several *var* tags (Supplemental Table 4). When the PTS were calculated, we found that still 6.7% of the sequences were shared (Fig. 1). The magnitude of PTS variation in a sample may be interpreted as genetic structuring of isolates, and we asked if this structuring was dependent on geographic origin or time point of collection of the isolates. We observed a high number of outliers in the plot indicating high PTS variation in the dataset (Fig. 1, sample Brazil). In fact, an increase of PTS was observed for specific regions: for example, the PTS for isolates from Manaus and Ariquemes were higher than the average (26% and 38%, respectively; Supplemental Table 4), indicating the circulation of isolates with limited *var* repertoires which still share numerous *var* tags between geographic regions and time points. In the following we compared the datasets from Barry et al. (2007) and Bull et al. (2005) with our data. While the PTS values calculated from isolates from Amele/PNG showed a PTS of 7% and no significant numbers of outliers indicating homogenous values of PTS, samples from Kilifi shared very few sequences and the PTS value for twelve Kilifi isolates is near 1% (Fig. 1).

We then tried to estimate the global number of different *var* sequences in Amazonian *P. falciparum* using the software EstimateS (Colwell, 2006) which was originally designed for the estimation of species richness in biotopes. There seems to be a limit of around 349–429 different sequences in the analyzed isolates, depending on the estimation algorithm applied (Jackknife 1 or Bootstrap, Fig. 3, Supplemental Table 6). In comparison, the graph for the analysis of sequences from the Kilifi dataset suggests that there is no limit in *var* sequence diversity. Out of more than 1700 sequence reads, 653 different sequences are obtained from twelve isolates (Bull et al., 2005), resulting in an estimated repertoire size of 877–1233 sequences in this sample (Supplemental Table 6). On the other hand, the diversity of *var* tags from Amele is limited to around 400 sequences in their dataset (data not shown, see Barry et al., 2007). Importantly, Barry et al. (2007) found limited *var* repertoires exclusively in isolates taken during a few months in a single location, while our dataset comprises of sequences from isolates taken at different geographic locations and during two decades.

When we compared aligned Brazilian sequences with DBLα sequence tags from *P. falciparum* strains A4 and ItG2 we observed only five shared sequences (AJ319696, AJ319700, AJ319686, AJ319680 and AJ319685, Supplemental File 2) within different Brazilian isolates and these specific sequence types could also be identified in other regions of the world. This underlines the presumption that a cross-contamination occurred in the IT isolate (parental to ItG2 and A4, Roberts et al., 1992). Therefore, ItG2- and A4-derived sequences were not considered South American sequences.

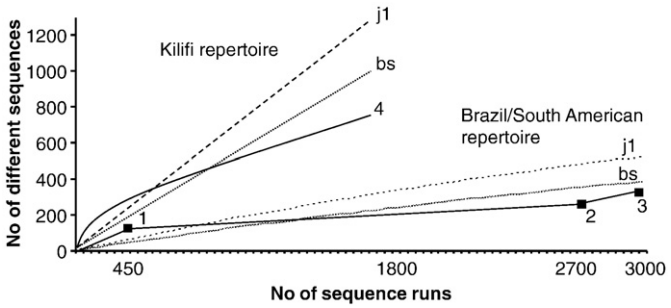

Fig. 3. Analysis of cumulative *var* DBLα diversity in Brazilian isolates versus the Kilifi dataset. Shown are outputs from Estimates 8.0 software which calculates the species diversity considering 293 different sequences in 67 isolates (30 clones of Ariquemes isolates counted as eight isolates) including literature sequences by either the jacknife1 (j1) or the mean bootstrap algorithm (bs) (dotted lines). The observed number of sequences are indicated at three intervals, considering the analysis of 450 clones (1; 106 different sequences at 98% identity cutoff, data from the study by Albrecht et al. 2006), 2667 clones (2; resulting in 221 different sequences) and after the addition of literature sequences from Mato Grosso, Venezuela, 7G8 and HB3 (3). A total repertoire of 429 (j1) or 349 (bs) different *var* tags were estimated for isolates from the Amazonian area. The Kilifi dataset with 653 different sequences from 12 isolates was estimated to contain 1233 (j1) or 877 (bs) different sequences in the total parasite population circulating in Kilifi at the occasion when these isolates were obtained. See also Supplemental Table 6 for raw data.

3.4. Fine analysis of DBLα peptides reveals an altered DSID distribution in Brazilian isolates

In the following, we addressed the question whether there were specific peptide motifs that were differently distributed in sequences from Brazilian isolates. In 2007, Bull and colleagues applied and tested a novel approach to classify *var* tags based on small semi-conserved sequence tags, the number of cysteines in the DBLα region and its size (DSID; Bull et al., 2007). We first analyzed if certain tags were over- or underrepresented in Brazilian isolates as compared to isolates from other locations. For this, we analyzed the DSIDs from all different peptide sequences in five different datasets (Br/SA, Asia, Africa, Amele, Kilifi, see Supplemental Table 5 for raw data) and deleted duplicate DSIDs also considering the peptide length. We observed that DSIDs of group 3 were less frequently identified in the Br/SA isolates than in any other data set (Fig. 4), although statistically significant only in comparison to the Asia sample (χ^2 test, $p<0.01$). On the other hand, the Amele sample showed a strong over-representation of group 4 DSIDs compared to Br/SA sequences ($p<0.005$). Also, group 5 and group 6 sequences were over-represented in the Brazilian dataset.

We then classified the five different datasets for the DBLα peptide size in the DSIDs groups 1–6 (Fig. 4, raw data, see Supplemental Table 5). Brazilian/Amazonian sequences showed a differential length distribution in DSID groups 1 and 3 (compared to Asian sequences) and 6 (compared to African and Asian sequences, Table in Fig. 4G). On the other hand, the Asian dataset presented also a different length distribution when compared to African/Kilifi datasets in DSID groups 3. The observed differences were significant ($p<0.05$) to highly significant ($p<0.0001$, Mann–Whitney test, two-tailed, Gaussian approximation).

3.5. Many var gene variants may be absent in Brazilian isolates

var genes and their corresponding PfEMP1 proteins are subjected to selection whenever the parasite is in its malaria-causing blood stage. Therefore, it is reasonable to assume that the immune selection shapes *var* gene repertoires so that encoded PfEMP1s do not cause – or to a small extent – the production of antibodies which recognize more than one or a few PfEMP1 variants. When the pairwise identities of DBLα tags (DNA) from isolates are plotted against their frequency, the most abundant sequence identities are found around 65–67% and

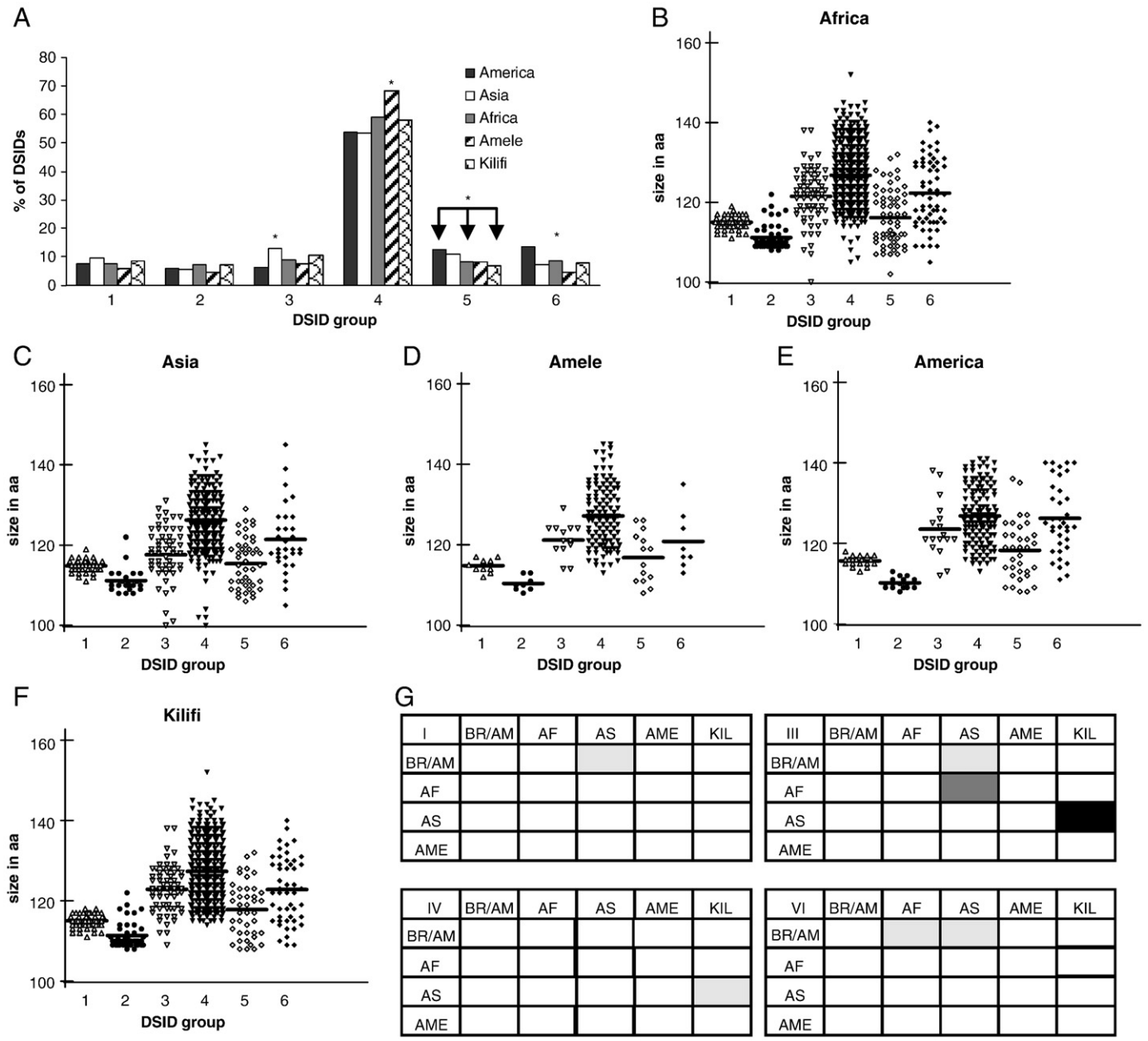

Fig. 4. Analysis of Distinct Sequence Identifiers (DSID). DSIDs were calculated as described by Bull and colleagues (Bull et al., 2007). (A) The frequency distributions of different DSIDs without considering their peptide sizes were plotted for five datasets (raw data in Supplemental Tables 5). Significant differences in DSID distribution are marked by an asterisk. Significance ($p<0.05$) was calculated by the χ^2 test. (B–F) Size distribution of DSID groups in different datasets. The peptide sizes of all DSIDs were plotted per DSID group and differences between size values between groups and datasets were evaluated by Mann–Whitney's *U* test. (G) Only in DSID groups 1, 3 and 6 could be observed significant differences in the peptide sizes of South American DBLα sequences and sequences from other origins (light grey boxes, $p<0.05$, dark grey box, $p<0.025$, black box $p<0.0001$).

there are few sequences with identities higher than 80%. We hypothesize that sequences showing more than 70–75% identity may encode DBLα domains which are possibly recognized by cross-reactive antibodies and sequences with identities of less than 70% may result in PfEMP1 which are not cross-reactive. We therefore performed an alignment of all DBLα coding sequences in our and published datasets. By this procedure, the "worldwide" DBLα sequences can be divided in 2255 different sequence tags (cutoff 98% identity, Supplemental File 2). After extraction and realignment of these 2255 sequences and clustering in groups with <76% identity, 125 subsets of sequences were formed. In this global alignment, 294 different sequences from Br/SA and 188 from the village of Amele could be identified. The slight difference in the number of different sequences than described for the Brazilian/South American dataset is due to the higher number of input sequences in the ClustalX analysis.

In the following, we asked in how many clusters sequences from different datasets were distributed. Br/SA sequences were found in 64 groups, six of which contained exclusively Brazilian sequences. Sequences from Amele were present in 51 groups, in contrast, sequences of African origin could be identified in 119 groups. Interestingly, the distribution in 76% cutoff groups is highly biased and nine groups contained 50 or more sequences while 88 groups contained less than 10 sequences (Fig. 5). In order to evaluate if Br/SA sequences were equally distributed, we tested if these were over- or under-represented in groups with more than 49 sequences and significantly less Br/SA sequences were found only in group 89 when compared to the entire dataset (χ^2 test, $p<0.05$).

We then asked if the Clustal analysis was related to the DSID classification of sequences, focusing on the DSID-defined sequence type distribution in the nine clusters with more than 49 sequences

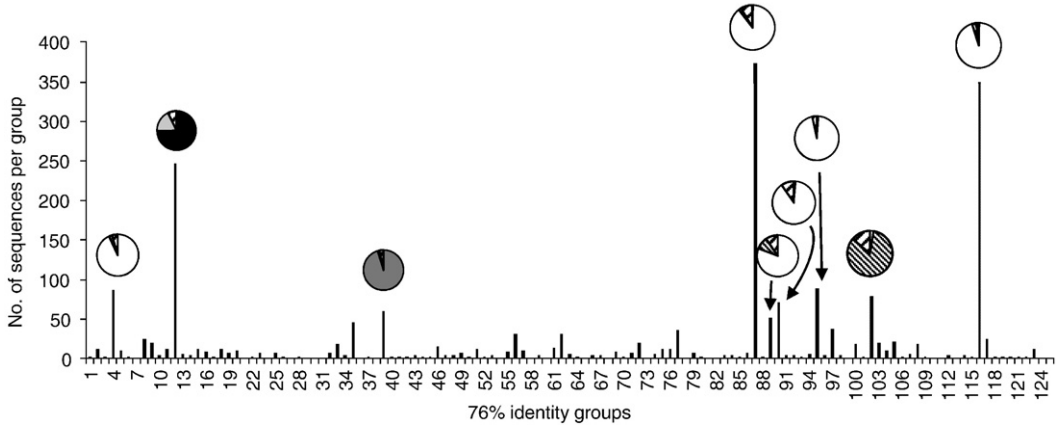

Fig. 5. Frequency distribution of 2255 var DBLα coding sequences after clustering in 76% identity groups. The number of sequences in each 76% identity group was plotted. The DSID distribution in groups with 50 or more sequences is depicted in pie graphs, where numbers refer to the group for which the DSID distribution is shown. The DSID groups are as follows: Black area: DSID type 1, dark grey, DSID type 2, light grey, DSID type 3, white, DSID type 4, fine stripes, DSID type 5 and gross stripes, DSID type 6. Only in cluster 89, the observed distribution of Brazilian/South American sequences in the >49 sequence containing groups is different from the expected distribution (χ^2 test, $p<0.05$). See Supplemental File 2 for raw data.

(Fig. 5 and Supplemental Figure 2). This was done because Bull and colleagues showed that DSID group 1–3 genes were strongly associated with upsA-type telomeric *var* genes (Bull et al., 2007) which are believed to show restricted recombination and less diversity than upsB *var* genes, due to their chromosomal orientation. In our analysis, all but two DSID group 1 *var* genes were almost exclusively detected in one cluster (group 12). DSID type 2 sequences clustered separately from the DSID type 1 sequences and also showed higher dispersion. Nevertheless, more than 50% of DSID type 2 associated *var* genes accumulated in two clusters (groups 34 and 39). Another accumulation was found for the cluster 102 which contained mainly DSID type 5 associated sequences. Many DSID group 4 associated genes, which may represent upsB and upsC flanked *var* genes were dominantly found in the remaining large clusters (Fig. 5). When we compared the distribution of DSID groups in the remaining clades with less than 50 members, DSID type 1 sequences were strongly under-represented while the remaining groups 2, 4, 5 and 6 were distributed in a statistically similar fashion, compared to the total DSID distribution (Supplemental Figure 2), reinforcing the observation that limited diversity is found in DSID type 1 *var* sequences. The inverse effect was found for DSID type 3 associated *var* gene sequences: These sequences were predominantly encountered in smaller groups indicating the presence of more polymorphisms in sequences with DSID type 3, although they presumably represent upsA *var* genes. Sequences with DSID type 3 were found in 39 of 125 groups. The distribution pattern in larger or smaller groups was also found for the restricted *var* repertoires of Br/SA and Amele and differed not significantly from the distribution pattern found in the whole dataset (Supplemental File 2). We finally analyzed if there were sequences (98% identity cutoff) that were present in isolates from all geographic locations (Brazil/South America, South East Asia and Africa). Seven sequences, including the conserved *var1csa* were found in isolates from the three global regions Africa, Asia and Latin America. These sequences belonged to DSID groups 2 (DQ265561, AAL11664.1), 3 (DQ135454.1, CAD60873.2), 4 (AAL11142.1, DQ135353.1) and 6 (AAL11285.1).

4. Discussion

In Brazil, field studies have shown two principal types of malaria outcomes: The so-called "frontier malaria," which affects mainly non-immune migrants which settle in gold mining or logging camps, exposing themselves to malaria infection (Sawyer, 1986; Camargo et al., 1994) and mild, often non-symptomatic infection (Alves et al., 2002; da Silva-Nunes and Ferreira, 2007; Ladeia-Andrade et al., 2007), mainly found in stable riverine and rural populations. Although quantitative long-term studies designed as described for example by Roussilhon et al. (2007) are not available, not at least because of the relatively low and seasonal incidence of falciparum malaria, it seems that the dynamics of malarial infection and severity differ greatly from typical African settings such as found in Ghana or lowland Kenya. This happens most probably due to (i) the rapid diagnosis and the facilitated access to most effective therapies, and ii) to the different transmission intensity with *Anopheles darlingi* as principal vector. We speculated that parasite derived factors, such as the herein described smaller repertoire of antigenic variants, might also be of importance. Importantly, *P. falciparum* was almost eradicated from the Amazon in the 1960s, probably resulting in a significant depletion of antigenic variants. The number of antigenically different PfEMP1 variants certainly is a factor in the development of an efficient immune response against these antigens (Marsh and Kinyanjui, 2006).

In this report, we sequenced exhaustively and characterized *var* DBLα tags from many Brazilian isolates obtained in a time frame of twenty years and compared them to published DBLα tags from around the globe. By the analysis of *var* repertoires from clones/isolates taken from infected individuals during a malaria epidemic in 1985 we could show that the infecting isolates contained quite redundant variant antigen repertoires, very differently from highly endemic regions such as lowland Kenya. Applying a similar sequencing effort, the identification of only 152 sequences from 9 isolates is largely different from the 653 different sequences identified in 12 isolates from Kilifi. The herein described PTS values for the isolates from the town of Ariquemes are the highest described so far, much higher than the values documented for the other dataset from the area of Amele/PNG, where also less diversity in *var* sequences was reported (Barry et al., 2007). Elevated PTS values were also found for isolates from other areas such as the metropolitan area of Manaus or in isolates from Porto Velho. In addition to increased PTS in isolates from microregions, huge sequence type sharing was also found in isolates from distant locations and different time points, such as the S20 isolate (from Porto Velho, 1985) which seems to share 25% of its *var* repertoire with the MA7 isolate, obtained in Manaus in 2006 (Supplemental Table 4). Despite of the huge sampling effort, we believe that the calculated median PTS of 6.7% for Brazilian/Amazonian isolates (including Honduras strain HB3) is only an approximated value given that we sampled only few sequences from multiple isolates, resulting in decreased chances of finding shared sequences. This may

have also contributed to a non-homogenous distribution of PTS and to the creation of many outliers in the PTS plot for the Brazilian/Amazonian sample. On the other hand, it is possible that we have missed a number of sequences due to experimental limitations such as PCR primer bias on individual target DNAs or failure in the cloning of certain sequence tags, which then may have led to an erroneous estimation of the overall number of variant sequences, although we consider this a remote possibility. The herein used primer pairs were thoroughly tested by us (Albrecht et al., 2006) and others (Peters et al., 2002). The clone count after amplification led in the majority of cases to the expected number of different sequences per sequencing effort (primer performance) and only sporadically to the over-representation of single sequences (primer bias, Albrecht et al., 2006). In examples where few sequences were amplified, such as in the case of DNA samples from the Jaú National Park, a biased amplification of a determined *var* tag may have resulted in the overestimation of PTS since even in few clones the given sequence would be represented. Interestingly, when genomic DNAs from different origins where amplified, determined sequences showed slightly biased amplification in one sample while in another sample the same sequences were not preferentially amplified (Albrecht et al., 2006) suggesting that biased amplification is not only dependent on the specific target but also on its genomic context.

We then tested the saturation of sequence diversity using the Estimates software applying two different algorithms and already applied by Barry et al. (2007). In our analysis, we applied the test for 89 clones or alternatively 67 isolates and a limit of ~430 different sequences was observed for the dataset. Given that we included sequence tags from many different locations of Brazil and also included the clones HB3 and 7G8, it appears that the repertoire of different *var* tags in *P. falciparum* from Brazil/the Amazon is indeed very limited. In contrast, no saturation of different sequences can be identified by the analysis of few isolates taken during short time periods in Kilifi (Bull et al., 2005), underlining the limited total repertoire of *var* genes in the Amazonian *P. falciparum* isolates.

A number of reasons may account for this decreased repertoire diversity in the isolates. Firstly, the presence of *Anopheles darlingi* which is considered a less antropophilic vector than *A. gambiae* is certainly a reason for decreased numbers of infected bites. A smaller number of infected mosquitoes would explain why in limited epidemic situations such as in Ariquemes 1985 so little *var* diversity was discovered. Specifically, a single infective bite with an almost clonal (in terms of *var* diversity) parasite isolate would then lead to an infection with a number of detectable *var* variants close to one complete repertoire, which was indeed observed. Further, the combination of less infective bites and fewer genetically different *P. falciparum* genotypes in circulation may decrease the chances for a profound exchange of variant genes by ectopic recombination during meiosis in the anopheline vector. It must also be remembered that even in conditions of intense transmission, mosquitoes infected with different genotypes are rarely found (Razakandrainibe et al., 2005) and we believe that the chances of mosquitoes being infected with two or more genetically different parasites is still lower in Amazonian settings. Experimental data are necessary to confirm or refute this hypothesis. Secondly, the finding that identical *var* sequences were found in isolates obtained in remote regions of the rain forest (for example the Jaú National Park) and also in isolates from Porto Velho evidences the existence of only a very few, genetically entirely different *P. falciparum* in circulation, possibly due to the almost complete eradication of the parasite in the 1960s and the possible absence of introduction of new genotypes. Coincidently, there is strong genetic structuring in Brazilian isolates (Machado et al., 2004). We estimate that a similar result of very limited *var* diversity should also be obtained analyzing *var* repertoires during island breakouts such as during the epidemic reported in Cape Verde in 1998 (Arez et al., 1999).

Bull and colleagues described and tested a system for the classification of *var* tags based on the occurrence of determined small sequence tags within the DBLα peptide sequence. They suggested that DSID types 1-3 are mostly found in *var* genes controlled by type A and B/C upstream regions, at least in the laboratory strains 3D7, HB3 and IT4 (Bull et al., 2007). Upon analysis of the Distinct Sequences Identifiers (DSIDs), we observed a significantly decreased occurrence of type 3 DSIDs in Brazilian/Amazonian isolates only when compared to Asian sequences, while the other upsA related groups 1 and 2 were similarly frequent. Type A *var* gene transcription was associated to severe malaria during childhood (Jensen et al., 2004) or cerebral Malaria and type B/C types with hyperparasitemia (Kyriacou et al., 2006), outcomes that are very rarely observed in endemic areas in Brazil (da Silva-Nunes and Ferreira, 2007) and we hypothesized that there might be less upsA type sequences or less diverse upsA type sequences which is not the case when compared to other datasets.

When we analyzed the size distribution per DSID group we observed significant differences in the groups 1, 3 and 6 between datasets, and length discrepancies were dominantly between the Br/SA and the Asian datasets, while the African dataset was only different in DSID group 6 sizes. Interestingly, the datasets from Amele and Kilifi did not show significant differences to the Brazilian/South American data in this test, despite a very low number of shared sequences between the regions. From the perspective of shared DSID between global regions, the probable African origin of South American *var* sequences could not be confirmed: While 55 DSID were shared between Africa (total of 732 unique DSIDs) and South America, 30 were shared with the Asian sample (total of 420 unique DSIDs) and the resulting proportion of shared DSIDs is not significantly different between the populations (χ^2 Test). This outcome is perfectly probable, due to the highly recombinogenic nature of *var* genes.

The global alignment of *var* tags and the grouping of DNA sequences in clusters with 76% or less identity may be considered as an indirect indicator of the absence or presence of important antigenic groups. By computational analysis, we evaluated that the majority of *var* tags per genome (analyzing the *var* DBLα encoding tags of 3D7, HB3 and 7G8) share less than 80% identical positions. We assume that host immune pressure maintains the *var* repertoires in parasites as diverse and as functional as possible.

Based on this hypothesis, we identified a limited number of sequence clusters in isolates from all over the world, and, as expected from their very high diversity, African isolates were present in the majority of groups. On the other hand, limited repertoires such as from Amele or Brazil/ SA showed a restricted diversity and Amele or Brazil/SA sequences were absent in many groups. We believe that the lack of members in 76% sequence groups may contribute to a decreased potential antigenic diversity of parasites from these areas.

Through the clustering in 76% identity groups, we also observed that a few groups contained more than half of all different sequences. We suggest that these groups contain sequences with limited variability, perhaps associated with specific functions. Again, empiric studies with defined antigens need to be performed in order to establish a connection between sequence identity and antigenic cross-reactivity or even association to determined cytoadherent or other functions.

Nevertheless, we observed that the 76% clustering led to an accumulation of all but two DSID group 1 sequences into one cluster (group 12, Fig. 5 and Supplemental File 2). Group 12 also contains 3D7 *var* PF11_0008, DSID type 3, of which domains were dominantly recognized by immune sera in a field study in Tanzania when expressed as a recombinant peptide (Cham et al., 2009). Additionally, 15 of 47 sequences previously associated to cerebral malaria (Kyriacou et al., 2006) were also contained in group 12, while 6 of 47 were associated to group 35 and 39. In the latter groups accumulated type 2 DSID sequences: 95 of 147 sequences (64.6%)

were represented in these groups, although single DSID type 2 sequences were found throughout 19 groups. It is tempting to suggest that groups 12, 35 and 39 may concentrate sequences which – upon transcription – associate to specific outcomes of malaria. We propose that the approach of the clustering in groups with 76% identity may enhance the DSID classification system in the identification of *var* genes associated to specific forms of disease, although more sequence data with well documented anamnestic data are obviously necessary.

Besides *var1csa*, we also detected six *var* sequences which were encountered in isolates from all regions of the world. Possibly, these sequence tags are remnants of ancestral *var* genes. Another possibility is that they are well adapted sequences and that there is an evolutionary pressure to maintain these sequences in an otherwise highly recombinogenic background.

In conclusion, our study reveals for the first time that (i) there is an unprecedented pairwise *var* type sharing in Amazonian isolates and that there are probably less circulating *var* genes, at least DBLα coding domains, which seem to be stable over time (ii) that a major group of *var* genes found in other regions of the world are absent in the Amazon, although the perhaps most common, globally found antigenic variants – deduced from the 76% clustering of sequences – are present. Further quantitative field studies are necessary to evaluate if the possible lack of antigenic variants can be associated to a faster buildup of immunity in exposed Amazonian populations.

Acknowledgements

The authors thank Wolfgang Fischer and Márcio Yamamoto for help with sequencing. LA and BC received a FAPESP postgraduate fellowship, CC received a CNPq fellowship. This work was supported by a FAPESP grant to GW. FTMC and GW are CNPq fellows.

Appendix A. Supplementary data

Supplementary data associated with this article can be found, in the online version, at doi:10.1016/j.gene.2010.01.001.

References

Albrecht, L., et al., 2006. Extense variant gene family repertoire overlap in Western Amazon *Plasmodium falciparum* isolates. Mol. Biochem. Parasitol. 150, 157–165.

Alves, F.P., Durlacher, R.R., Menezes, M.J., Krieger, H., Silva, L.H., Camargo, E.P., 2002. High prevalence of asymptomatic *Plasmodium vivax* and *Plasmodium falciparum* infections in native Amazonian populations. Am. J. Trop. Med. Hyg. 66, 641–648.

Arez, A.P., et al., 1999. A clonal *Plasmodium falciparum* population in an isolated outbreak of malaria in the Republic of Cabo Verde. Parasitology 118 (Pt. 4), 347–355.

Barry, A.E., et al., 2007. Population genomics of the immune evasion (var) genes of *Plasmodium falciparum*. PLoS Pathog. 3, e34.

Baruch, D.I., et al., 1995. Cloning the *P. falciparum* gene encoding PfEMP1, a malarial variant antigen and adherence receptor on the surface of parasitized human erythrocytes. Cell 82, 77–87.

Boyle, J.S., Lew, A.M., 1995. An inexpensive alternative to glassmilk for DNA purification. Trends Genet. 11, 8.

Bull, P.C., et al., 2005. *Plasmodium falciparum* variant surface antigen expression patterns during malaria. PLoS Pathog. 1, e26.

Bull, P.C., et al., 2007. An approach to classifying sequence tags sampled from *Plasmodium falciparum* var genes. Mol. Biochem. Parasitol. 154, 98–102.

Camargo, L.M., Ferreira, M.U., Krieger, H., De Camargo, E.P., Da Silva, L.P., 1994. Unstable hypoendemic malaria in Rondonia (western Amazon region, Brazil): epidemic outbreaks and work-associated incidence in an agro-industrial rural settlement. Am. J. Trop. Med. Hyg. 51, 16–25.

Cham, G.K., et al., 2009. Sequential, ordered acquisition of antibodies to *Plasmodium falciparum* erythrocyte membrane protein 1 domains. J. Immunol. 183, 3356–3363.

Colwell, R. Estimates: sStatistical estimation of species richness and shared species from samples. Version 8, 2006. (downloaded from http://viceroy.eeb.uconn.edu/estimates).

Craig, A., Scherf, A., 2001. Molecules on the surface of the *Plasmodium falciparum* infected erythrocyte and their role in malaria pathogenesis and immune evasion. Mol. Biochem. Parasitol. 115, 129–143.

da Silva-Nunes, M., Ferreira, M.U., 2007. Clinical spectrum of uncomplicated malaria in semi-immune Amazonians: beyond the " symptomatic " vs " asymptomatic " dichotomy. Mem. Inst. Oswaldo Cruz 102, 341–347.

Duffy, M.F., Byrne, T.J., Carret, C., Ivens, A., Brown, G.V., 2009. Ectopic recombination of a malaria var gene during mitosis associated with an altered var switch rate. J. Mol. Biol. 389, 453–469.

Durham, A.M., et al., 2005. EGene: a configurable pipeline generation system for automated sequence analysis. Bioinformatics 21, 2812–2813.

Fowler, E.V., Peters, J.M., Gatton, M.L., Chen, N., Cheng, Q., 2002. Genetic diversity of the DBLalpha region in *Plasmodium falciparum* var genes among Asia-Pacific isolates. Mol. Biochem. Parasitol. 120, 117–126.

Freitas-Junior, L.H., et al., 2000. Frequent ectopic recombination of virulence factor genes in telomeric chromosome clusters of *P. falciparum*. Nature 407, 1018–1022.

Hoffmann, E.H., et al., 2006. Origins of sequence diversity in the malaria vaccine candidate merozoite surface protein-2 (MSP-2) in Amazonian isolates of *Plasmodium falciparum*. Gene 376, 224–230.

Jensen, A.T., et al., 2004. *Plasmodium falciparum* associated with severe childhood malaria preferentially expresses PfEMP1 encoded by group A var genes. J. Exp. Med. 199, 1179–1190.

Kaestli, M., Cockburn, I.A., Cortes, A., Baea, K., Rowe, J.A., Beck, H.P., 2006. Virulence of malaria is associated with differential expression of *Plasmodium falciparum* var gene subgroups in a case-control study. J. Infect. Dis. 193, 1567–1574.

Kirchgatter, K., Portillo Hdel, A., 2002. Association of severe noncerebral *Plasmodium falciparum* malaria in Brazil with expressed PfEMP1 DBL1 alpha sequences lacking cysteine residues. Mol. Med. 8, 16–23.

Kraemer, S.M., et al., 2007. Patterns of gene recombination shape var gene repertoires in *Plasmodium falciparum*: comparisons of geographically diverse isolates. BMC Genomics 8, 45.

Kyriacou, H.M., et al., 2006. Differential var gene transcription in *Plasmodium falciparum* isolates from patients with cerebral malaria compared to hyperparasitaemia. Mol. Biochem. Parasitol. 150, 211–218.

Ladeia-Andrade, S., et al., 2007. Naturally acquired antibodies to merozoite surface protein (MSP)-1(19) and cumulative exposure to *Plasmodium falciparum* and *Plasmodium vivax* in remote populations of the Amazon Basin of Brazil. Mem. Inst. Oswaldo Cruz 102, 943–951.

Larkin, M.A., et al., 2007. Clustal W and Clustal X version 2.0. Bioinformatics 23, 2947–2948.

Leech, J.H., Barnwell, J.W., Miller, L.H., Howard, R.J., 1984. Identification of a strain-specific malarial antigen exposed on the surface of *Plasmodium falciparum*-infected erythrocytes. J. Exp. Med. 159, 1567–1575.

Machado, R.L., et al., 2004. Genetic structure of *Plasmodium falciparum* populations in the Brazilian Amazon region. J. Infect. Dis. 190, 1547–1555.

Marsh, K., Kinyanjui, S., 2006. Immune effector mechanisms in malaria. Parasite Immunol. 28, 51–60.

Miller, L.H., Baruch, D.I., Marsh, K., Doumbo, O.K., 2002. The pathogenic basis of malaria. Nature 415, 673–679.

Moll, K., Ljungström, I., Perlmann, H., Scherf, A., Wahlgren, M. Methods in Malaria Research, 5 ed. MR4/ATCC, Manassas, 2008. http://www.mr4.org/Portals/3/Methods_In_Malaria_Research-5theditionv5-2.pdf.

Normark, J., et al., 2007. PfEMP1-DBL1alpha amino acid motifs in severe disease states of *Plasmodium falciparum* malaria. Proc. Natl. Acad. Sci. U. S. A. 104, 15835–15840.

Peters, J., Fowler, E., Gatton, M., Chen, N., Saul, A., Cheng, Q., 2002. High diversity and rapid changeover of expressed var genes during the acute phase of *Plasmodium falciparum* infections in human volunteers. Proc. Natl. Acad. Sci. U. S. A. 99, 10689–10694.

Razakandrainibe, F.G., et al., 2005. "Clonal" population structure of the malaria agent *Plasmodium falciparum* in high-infection regions. Proc. Natl. Acad. Sci. U. S. A. 102, 17388–17393.

Roberts, D.J., et al., 1992. Rapid switching to multiple antigenic and adhesive phenotypes in malaria. Nature 357, 689–692.

Roussilhon, C., et al., 2007. Long-term clinical protection from falciparum malaria is strongly associated with IgG3 antibodies to merozoite surface protein 3. PLoS Med. 4, e320.

Sawyer, D.R., 1986. Malaria on the Amazon frontier: economic and social aspects of transmission and control. Southeast Asian J. Trop. Med. Public Health 17, 342–345.

Scherf, A., 2006. A greedy promoter controls malarial var-iations. Cell 124, 251–253.

Scherf, A., et al., 1998. Antigenic variation in malaria: in situ switching, relaxed and mutually exclusive transcription of var genes during intra-erythrocytic development in *Plasmodium falciparum*. EMBO J. 17, 5418–5426.

Tami, A., Ord, R., Targett, G.A., Sutherland, C.J., 2003. Sympatric *Plasmodium falciparum* isolates from Venezuela have structured var gene repertoires. Malar. J. 2, 7.

Taylor, H.M., Kyes, S.A., Harris, D., Kriek, N., Newbold, C.I., 2000a. A study of var gene transcription in vitro using universal var gene primers. Mol. Biochem. Parasitol. 105, 13–23.

Taylor, H.M., Kyes, S.A., Newbold, C.I., 2000b. Var gene diversity in *Plasmodium falciparum* is generated by frequent recombination events. Mol. Biochem. Parasitol. 110, 391–397.

Ward, C.P., Clottey, G.T., Dorris, M., Ji, D.D., Arnot, D.E., 1999. Analysis of *Plasmodium falciparum* PfEMP-1/var genes suggests that recombination rearranges constrained sequences. Mol. Biochem. Parasitol. 102, 167–177.

Vaccine 26 (2008) 6132–6142

Contents lists available at ScienceDirect

Vaccine

journal homepage: www.elsevier.com/locate/vaccine

New malaria vaccine candidates based on the *Plasmodium vivax* Merozoite Surface Protein-1 and the TLR-5 agonist *Salmonella* Typhimurium FliC flagellin

Daniel Y. Bargieri[a,b], Daniela S. Rosa[a], Catarina J.M. Braga[c], Bruna O. Carvalho[d], Fabio T.M. Costa[d], Noeli Maria Espíndola[e], Adelaide José Vaz[e], Irene S. Soares[e], Luis C.S. Ferreira[c], Mauricio M. Rodrigues[a,b,*]

[a] *Centro Interdisciplinar de Terapia Gênica (CINTERGEN), Universidade Federal de São Paulo, Escola Paulista de Medicina, Rua Mirassol, 207, São Paulo 04044-010, SP, Brazil*
[b] *Departamento de Microbiologia, Imunologia e Parasitologia, Universidade Federal de São Paulo, Escola Paulista de Medicina, Rua Mirassol, 207, São Paulo 04044-010, SP, Brazil*
[c] *Departamento de Microbiologia do Instituto de Ciências Biomédicas da Universidade de São Paulo, Av. Prof. Lineu Prestes, 1374, São Paulo 05508-900, SP, Brazil*
[d] *Departamento de Parasitologia, Instituto de Biologia, Universidade Estadual de Campinas, Rua Monteiro Lobato, 255, Campinas 13083-970, SP, Brazil*
[e] *Departamento de Análises Clínicas e Toxicológicas, Faculdade de Ciências Farmacêuticas da Universidade de São Paulo, Av. Prof. Lineu Prestes 580, São Paulo 05508-900, SP, Brazil*

ARTICLE INFO

Article history:
Received 29 April 2008
Received in revised form 31 July 2008
Accepted 31 August 2008
Available online 18 September 2008

Keywords:
P. vivax
Vaccine
Flagellin
FliC
TLR5
CpG ODN
TLR9

ABSTRACT

The present study evaluated the immunogenicity of new malaria vaccine formulations based on the 19 kDa C-terminal fragment of *Plasmodium vivax* Merozoite Surface Protein-1 ($MSP1_{19}$) and the *Salmonella enterica* serovar Typhimurium flagellin (FliC), a Toll-like receptor 5 (TLR5) agonist. FliC was used as an adjuvant either admixed or genetically linked to the *P. vivax* $MSP1_{19}$ and administered to C57BL/6 mice via parenteral (s.c.) or mucosal (i.n.) routes. The recombinant fusion protein preserved $MSP1_{19}$ epitopes recognized by sera collected from *P. vivax* infected humans and TLR5 agonist activity. Mice parenterally immunized with recombinant *P. vivax* $MSP1_{19}$ in the presence of FliC, either admixed or genetically linked, elicited strong and long-lasting $MSP1_{19}$-specific systemic antibody responses with a prevailing IgG1 subclass response. Incorporation of another TLR agonist, CpG ODN 1826, resulted in a more balanced response, as evaluated by the IgG1/IgG2c ratio, and higher cell-mediated immune response measured by interferon-γ secretion. Finally, we show that $MSP1_{19}$-specific antibodies recognized the native protein expressed on the surface of *P. vivax* parasites harvested from infected humans. The present report proposes a new class of malaria vaccine formulation based on the use of malarial antigens and the innate immunity agonist FliC. It contains intrinsic adjuvant properties and enhanced ability to induce specific humoral and cellular immune responses when administered alone or in combination with other adjuvants.

1. Introduction

Plasmodium vivax causes more than 130 million malaria cases every year [1]. Chemotherapy has remained almost unchanged in the past 50 years and drug resistance is developing in many parts of the world, reducing the efficacy of conventional treatment [2,3]. To make matters worse, the number of severe cases has recently increased [2,3]. Therefore, prophylactic alternatives such as effective vaccines are urgently needed. Because large-scale cultures of this parasite are not feasible, an effective vaccine must rely on recombinant DNA technology or synthetic polypeptides. Several target recombinant proteins have been tested as *P. vivax* vaccine candidates including pre-erythrocytic and blood stages antigens, such as the circumsporozoite protein, Merozoite Surface Proteins (MSP), Duffy-binding protein-1, apical membrane antigen-1 and reticulocyte-binding protein, among others [4–24].

Among blood stage malarial antigens, the MSP1 has been intensively investigated as a malaria vaccine candidate. The protein is synthesized in a precursor form with a high molecular weight during schizogony and, during the invasion process, a proteolytic cleavage releases most of the molecule from the merozoite membrane leaving a membrane-anchored 19 kDa fragment ($MSP1_{19}$) on the parasite surface [25]. Genetic modification studies with malaria parasites demonstrated that the essential role of $MSP1_{19}$ for parasite survival is the same among distantly related *Plasmodium* species [26]. Pre-clinical vaccination trials carried out with rhesus monkeys showed that animals immunized with a recombinant protein based on the *P. vivax* MSP1 C-terminal region ($MSP1_{42}$ kDa) and encompassing the $MSP1_{19}$ fragment developed partial protection

* Corresponding author at: CINTERGEN, UNIFESP, Escola Paulista de Medicina, Rua Mirassol 207, São Paulo 04044-010, SP, Brazil. Tel.: +55 11 5571 1095; fax: +55 11 5571 1095.
E-mail address: mrodrigues@unifesp.br (M.M. Rodrigues).

0264-410X/$ – see front matter © 2008 Elsevier Ltd. All rights reserved.
doi:10.1016/j.vaccine.2008.08.070

to infection with *P. cynolmogi*, a species closely related to *P. vivax* [17].

In earlier studies, we characterized the immunogenic properties of several recombinant malaria vaccine candidates, including genetically modified derivatives of the *P. vivax* $MSP1_{19}$ protein [27,28]. One of the tested $MSP1_{19}$ derivatives revealed a particularly strong immunological behavior after genetic linkage to the Pan allelic HLA DR-binding epitope (PADRE) [29]. The protein, named His_6MSP1_{19}-PADRE, was immunogenic when subcutaneously (s.c.) administered to mice in the presence of different adjuvants eliciting a strong and long-lasting specific antibody response [29]. More recent studies confirmed and extended these observations by showing potent antibody responses following mucosal administration of this recombinant protein to mice in the presence of the adjuvants cholera toxin or *Escherichia coli* heat labile enterotoxin [30].

Based on these successful experimental studies using the mouse model, pre-clinical immunization trials were carried out with non-human primates. Animals vaccinated with the *P. vivax* $MSP1_{19}$ genetically linked to two helper epitopes failed to develop strong specific antibody responses in the presence of different formulations except when Incomplete Freund Adjuvant was used [31]. This result showed that although the recombinant $MSP1_{19}$ protein can be highly immunogenic in non-human primates, the adjuvant properties of the vaccine formulation have to be improved. This assumption led us to pursue a novel type of vaccine that could incorporate intrinsic adjuvant properties, new T helper cell epitopes and recombinant $MSP1_{19}$ derivatives.

Recent advances in the field of innate immunity have disclosed the cellular and molecular mechanisms behind the adjuvant effects of pathogen-associated molecular patterns (PAMPs). The recognition of PAMPs in mammalian cells is mediated by innate immune receptors such as TLR5 (specific for bacterial flagellins) and TLR9 (specific for unmethylated CpG DNA), expressed by antigen presenting cells (APC). Following the binding of the specific agonists, the TLR receptor intracellular domain activates molecular signaling cascades and the recruitment of adaptor proteins, for example, the myeloid differentiation factor 88 (MyD88), and the activation of transcription factors such as NF-κB and mitogen activated kinases. These signaling events result in the activation of inflammatory responses and APC maturation, which mediate the activation of T and B cell-dependent adaptive immune responses [32,33].

Flagellins, the structural subunit of flagellar filaments, contribute both to the virulence of bacterial pathogens and to the activation of inflammatory responses in mammalian hosts [32,33]. Bacterial flagellins have been shown to bind extracellular TLR5 as well as intracellular receptors leading to strong inflammatory responses [34–36]. Very recently, flagellins such as those expressed by *Salmonella* species, have shown strong adjuvant effects when delivered via parenteral or mucosal routes either admixed or genetically linked to target antigens [37–43]. *Salmonella enterica* serovar Typhimurium strains may express two alternate flagellar antigens, FliC and FljB flagellins. The adjuvant properties of *S.* Typhimurium FljB have been experimentally demonstrated either by induction of specific antibody responses or activation of cell-dependent immune responses [38,40–43], but few groups have shown the potential adjuvant effects of *S.* Typhimurium FliC in vaccine formulations [44].

Here, we investigated the adjuvant properties of *S.* Typhimurium FliC in malaria vaccine formulations based on recombinant derivatives of the *P. vivax* $MSP1_{19}$ protein. The adjuvant properties of FliC were evaluated in mice immunized via parenteral (s.c.) or mucosal (i.n.) routes with purified His_6MSP1_{19} and His_6MSP1_{19}-PADRE admixed or genetically linked to FliC. Additionally, we investigated the role of a TLR9 agonist, CpG ODN 1826, on the modulation of the immune responses elicited in mice immunized with the $MSP1_{19}$/FliC vaccine formulations. The reported results demonstrated that the incorporation of TLR agonists to $MSP1_{19}$-based formulations represents a promising alternative for the development of simple and inexpensive malaria vaccine candidates.

2. Methods

2.1. Generation of recombinant $MSP1_{19}$-derived proteins

The recombinant His_6MSP1_{19} and His_6MSP1_{19}-PADRE proteins were obtained exactly as described previously [27]. Purified proteins were analyzed by SDS-PAGE and stained with Coomassie Blue. The nucleotide sequence encoding the *S.* Typhimurium FliC and $MSP1_{19}$-PADRE were obtained by PCR amplification using Platinum *Taq* High Fidelity DNA polymerase (Invitrogen). Specific oligonucleotides for amplification of FliC-encoding gene, containing EcoRI and HindIII restriction sites (GGGGAATTCATGGCACAAGTCATTAATACA and GGCAAGCTTGACGCAGTAAAGAGAGGAC) and the $MSP1_{19}$-PADRE nucleotide sequence, containing HindIII and XhoI restriction sites (GGCAAGCTTGCATGACTATGAGCTCCGAG and GGGCTCGAGTTTAAGCGGCAGCCTTCAGGGT) were purchased from Integrated DNA Technologies, Inc. Amplified fragments were cloned in frame in pET28a vector (Novagen). The recombinant protein was expressed and purified as described previously [27]. Briefly, recombinant *E. coli* was cultivated at 37 °C under aeration in flasks containing Luria broth (LB) and kanamycin (30 μg/ml). Protein expression was induced at an OD_{600} of 0.6 with 0.1 mM IPTG (Invitrogen) for 4 h. After centrifugation, bacteria were lysed on ice with the aid of an ultrasonic processor (Sonics and Materials INC Vibra Cell VCX 750) in a phosphate buffer with lysosyme (Sigma) and PMSF (Sigma). Bacterial lysate was centrifuged and the supernatant was applied to a column with Ni^{2+}–NTA–Agarose resin (Quiagen). After several washes, bound proteins were eluted with 0.5 M imidazole (Sigma). The eluted protein was dialyzed against 20 mM Tris–HCl, pH 8.0 and the recombinant proteins were purified by ion-exchange chromatography using a Mono Q column (GE Healthcare) coupled to an FPLC system (GE Healthcare). Fractions containing the recombinant proteins with a high degree of purity were pooled and extensively dialyzed against PBS. Protein concentration was determined with the Bradford assay and by SDS-PAGE analyses.

Recombinant proteins His_6-$MSP1_{19}$ or His_6FliC-$MSP1_{19}$-PADRE (0.25 mg) were reduced following incubation at 37 °C for 1 h in a solution containing 0.5 M Tris–HCl (pH 8.0), 2 mM EDTA, and 60 mM dithiothreitol (DTT; Sigma). After that period, urea was added to a final concentration of 4 M and the solution was incubated for 15 min at 95 °C. Iodoacetamide (Sigma) was added in a 2.5-fold molar excess over DTT. The samples were kept in the dark for 30 min. The reduced proteins were used to coat ELISA plates in carbonate buffer pH 9.6 containing 0.2 mM EDTA, 6 mM DTT and 0.4 M urea.

2.2. FliC purification

Native *S.* Typhimurium FliC*i* was purified of the attenuated *S.* Typhimurium SL3201 strain expressing FliC*i* but not FljB [45]. Briefly, bacteria were grown in LB supplemented with kanamycin (30 μg/ml) overnight at 37 °C under aeration (80 rpm). Cells were washed once with phosphate-buffered saline (PBS) and submitted to mechanical shearing with four 2 min cycles in a bench vortex mixer. The cell suspensions were centrifuged to remove the cells and the flagellar filaments collected from the supernatant following acetone precipitation. The protein content of FliC was determined with the Bradford assay and by SDS-PAGE analyses.

Recombinant FliC (rFliC) was expressed in pET28a vector and purified as described above for the other recombinant proteins.

2.3. Generation of monoclonal antibodies (MAb) to the recombinant His_6MSP1_{19}

BALB/c mice were immunized three times two weeks apart in the footpads with 20 μg of recombinant His_6MSP1_{19} emulsified in Complete Freund Adjuvant (first dose), Incomplete Freund Adjuvant (second dose) and in saline (third dose). Immunized mice had their spleen or popliteal lymph nodes removed 3 days after the third immunization and fused with myeloma cells (SP2/O) using polyethylene glycol 4000 (Merck, Darmstadt, Germany). Hybridomas were grown for 2 weeks in RPMI-1640 Medium (Invitrogen) with 10% Fetal Calf Serum, 1.5% HEPES buffer, 1% non-essential amino-acid solution, 2% sodium pyruvate, 1% L-glutamine, 0.1% streptomycin, and 3% hypoxanthine, aminopterin and thymidine (HAT) medium, at 37 °C in 5% CO_2 in air. Samples of medium from these cultures were screened by ELISA and immunoblotting for antibodies reacting with His_6MSP1_{19}. The positive hybridomas were cloned and recloned by limiting dilution. MAb k23 purified by Protein A agarose (Sigma) was used for the immunological assays. In addition, we used the MAb 3F8, kindly provided by Dr. J.W. Barnwell, CDC, Atlanta, and generated as described in reference [46].

2.4. Immunization regimens

Six to eight-week-old female C57BL/6 (H-2^b) and C57BL/10SCN (TLR4 deficient) mice were purchased from Federal University of São Paulo, Brazil. Experiments were performed in accordance with the guidelines of the Ethics Committee for Animal Handling of the Federal University of São Paulo. Mice were immunized three times, three weeks apart, via the s.c. route in the two hind footpads, using a final volume of 50 μl in each footpad (first dose) and at the base of the tail (second and third dose) with a final volume of 100 μl. The doses are indicated in each experiment. The intranasal (i.n.) immunizations were carried out in mouse under anesthesia (Ketamine-Xylazine at 40 and 16 mg/kg weight, respectively) with a micropipette and using a final volume of 8 μl in each nostril. CpG ODN 1826 (TCCATGACGTTCCTGACGTT) was synthesized with a nuclease-resistant phosphorothioate backbone (Coley Pharmaceutical Group). We used 10 μg per dose per mouse admixed with the antigen just before injection.

2.5. Immunological assays

Serum anti-$MSP1_{19}$ antibodies were detected by ELISA essentially as described previously [27]. The recombinant His_6MSP1_{19} (200 ng/well) antigen was employed as solid phase bound antigen. The peroxidase-conjugated goat anti-mouse IgG (KPL) was applied at a final dilution of 1:4000 while the tested mice sera were tested at serial dilutions starting from 1:100. Specific anti-$MSP1_{19}$ titers were determined as the highest dilution yielding an OD_{492} higher than 0.1. Detection of IgG subclass responses was performed as described above, except that the secondary antibody was specific for mouse IgG1, IgG2b, and IgG2c (purchased from Southern Technologies) diluted 1:2000. The results are presented as means ± S.D.

The detection of human anti-$MSP1_{19}$ IgG antibodies was performed by ELISA, as previously described [27,28,47–49]. The ELISA plates were coated with recombinant His_6MSP1_{19} (200 ng/well) or His_6FliC-$MSP1_{19}$-PADRE (50 ng/well). This amount of protein was adjusted to provide the same OD_{492} when we used a MAb to $MSP1_{19}$. A volume of 50 μl of each solution was added to each well of 96-well plates (high binding, Costar). After overnight incubation at room temperature, the plates were washed with PBS-Tween (0.05%, v/v) and blocked with PBS-milk (5%, w/v) for 2 h at 37 °C. Serum samples were diluted in PBS-milk (5%, w/v) with 1.5 μg/ml of FliC and 50 μl of each sample was added to each well in duplicate. After incubation for 1 h at room temperature and washes with PBS-Tween, we added to each well 50 μl of a solution containing peroxidase-conjugated goat anti-human IgG (Fc specific) diluted 1:10,000 (Sigma). The enzymatic reaction was developed by the addition of 1 mg/ml of *O*-phenylenediamine (Sigma) diluted in phosphate-citrate buffer, pH 5.0, containing 0.03% (v/v) hydrogen peroxide. The enzymatic reaction was stopped by the addition of 50 μl of a solution containing 4 N H_2SO_4. Plates were read at 492 nm (OD_{492}) with an ELISA reader (Labsystems Multiskan MS). To avoid recognition of FliC by human antibodies, we added a final concentration of 1.5 μg/ml of this protein in the buffer solution used to dilute each serum sample. This concentration was sufficient to completely inhibit the binding of immune antibodies to FliC (data not shown). Anti-Histidine tag (GE Amershan Bioscience) was used for ELISA and immunoblot.

Secreted IFN-γ in cell culture supernatants were determined with 10^6 spleen cells, collected from different immunization groups, cultivated in flat-bottom 96-well plates in a final volume of 200 μl. The His_6MSP1_{19} protein or the PADRE peptide was added to the culture at a final concentration of 10 μg/ml. After 120 h, the supernatants were collected for cytokine determination. Cytokine concentration was estimated by capture ELISA using antibodies and recombinant cytokines purchased from Pharmingen (San Diego, CA), as previously described [50]. Cytokine concentration in each sample was determined with standard curves with known concentrations of recombinant mouse IFN-γ. The detection limit of the assay was 0.2 ng/ml.

Determination of TLR5 bioactivity with native or recombinant flagellins, as well as with the His_6FliC-$MSP1_{19}$-PADRE protein, was carried out with the HEK293 cell line expressing mouse TLR5 (Invivogen). The cells were maintained in DMEM media 10% FBS and 10 μg/ml of blasticidin. Non-transfected or TLR5-transfected HEK293 cells (5×10^4 cells/well) were grown overnight in 96-well plates and stimulated with the recombinant proteins for 5 h. The culture supernatants were collected and concentration of secreted human IL-8 measured using a Human IL-8 ELISA Kit purchased from BD biosciences, as recommended by the manufacturer.

2.6. P. vivax slide preparation and indirect immunofluorescence assay (IFA)

Assays were carried out with 10-well IFA slides containing late stage forms of *P. vivax* enriched in Percoll® (Amershan) gradient, as described elsewhere [51]. Blood samples (5–10 ml) were collected into heparin-coated tubes from *P. vivax*-positive patients living in Manaus, AM, Brazil. All patients had given informed consent and the procedure was approved by the Oswaldo Cruz Foundation (FIOCRUZ) Research Committee. In brief, after plasma separation, red blood cell pellets were washed three times and ressuspended in RPMI 1640 medium (Sigma) to 10% hematocrit. The cell suspensions were distributed in 15 ml tubes (5 ml each) containing 5 ml of 45% Percoll. After centrifugation, floating mature forms of infected erythrocytes enriched up to 40–70% were collected, washed and ressuspended in 10% of Fetal Calf Serum. The infected erythrocytes were spread on IFA slides (50 μl/well), fixed in acetone for 10 min and air-dried. Pooled sera from different immunization groups were diluted 1:100 in PBS, applied to the slides and kept 30 min in a humid chamber at 37 °C. The slides were extensively washed with PBS and, then, incubated with 10 μg/ml of FITC-conjugated sheep anti-mouse IgG (Sigma) and 100 μg/ml of DAPI (4′,6-diamidino-2-phenylindole, dihydrochloride) (Molecular Probes) for 30 min in a humid chamber at 37 °C. After several washes with PBS, the slides

were sealed with coverslips and viewed in an immunofluorescence microscope.

2.7. Statistical analyses

The one-way ANOVA, Students' *t*-test and the Tukey HSD test were used to compare the differences between the mean values of the tested immunization groups. Correlations of serum affinity between two different recombinant proteins were analyzed by the Spearman test.

3. Results

3.1. Production, purification, antigenicity and TLR5 bioactivity of recombinant MSP1$_{19}$-derived peptides

In the present study, we used two previously described recombinant proteins derived from the *P. vivax* MSP1$_{19}$ peptide [29]: one with an N-terminal His-tag fusion (His$_6$MSP1$_{19}$) and another carrying the T cell PADRE epitope at the C-terminal end of the protein, as well as the N-terminal His-tag (His$_6$MSP1$_{19}$-PADRE). The native FliC protein, purified from the monophasic *S.* Typhimurium SL3201 strain, was employed as an adjuvant admixed with the recombinant MSP1$_{19}$-derived peptides. We also generated a recombinant fusion protein consisting of the MSP1$_{19}$-PADRE peptide linked to the C-terminal end of FliC (His$_6$FliC-MSP1$_{19}$-PADRE). The schematic representation of each of the recombinant proteins as well as the purified proteins sorted in SDS-PAGE are presented on Fig. 1A and B, respectively.

The recombinant His$_6$FliC-MSP1$_{19}$-PADRE protein was recognized by antibodies present in 44 serum samples from *P. vivax*-infected subjects. As shown on Fig. 1C, when tested side by side with His$_6$MSP1$_{19}$, the purified His$_6$FliC-MSP1$_{19}$-PADRE reacted similarly with the serum samples of malaria patients with a high correlation index ($r^2 = 0.7276$; $p < 0.0001$, Spearman test). Additionally, immunoblot analyses revealed that the His$_6$FliC-MSP1$_{19}$-PADRE was recognized by anti-FliC and anti-MSP1$_{19}$ antibodies (data not shown). These results indicate that the recombinant His$_6$FliC-MSP1$_{19}$-PADRE protein preserved the antigenicity of both flagellin and MSP1$_{19}$. TLR5-transfected HEK293 cells secreted HuIL-8 following exposure to the native *S.* Typhimurium FliC, a recombinant FliC and His$_6$FliC-MSP1$_{19}$-PADRE (Fig. 1D). On a molar basis, both *E. coli* recombinant proteins (regardless of

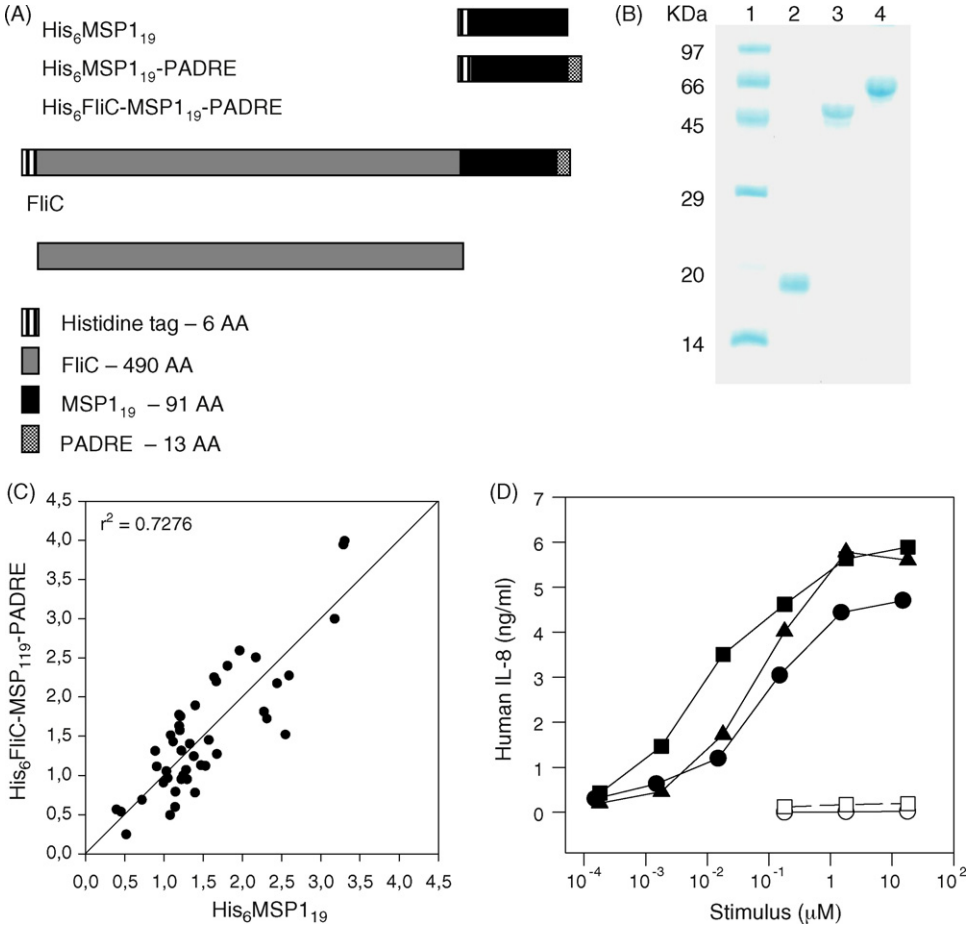

Fig. 1. Generation and characterization of the recombinant *P. vivax* MSP1$_{19}$-derived peptides. (A) Schematic representation of the recombinant proteins used in the present study. (B) SDS-PAGE analysis of the recombinant proteins. Lanes: 1, molecular weight markers; 2, purified His$_6$-MSP1$_{19}$-PADRE protein; 3, purified *S.* Typhimurium FliC flagellin; 4, purified His$_6$FliC-MSP1$_{19}$-PADRE protein. Each lane was loaded with approximately 1 μg of protein, sorted in a 12% polyacrylamide gel and stained with Coomassie Blue. (C) Reactivity of 44 sera from individuals with *P. vivax* malaria with the recombinant His$_6$MSP1$_{19}$ and His$_6$FliC-MSP1$_{19}$-PADRE proteins in ELISA. The serum samples were tested at a final dilution of 1:1600 or at a dilution corresponding to a final OD$_{492}$ value between 1.0 and 4.0. Symbols represent the average OD$_{492}$ of each serum sample tested in duplicate. The correlation coefficient (r^2) between values obtained with the two proteins is indicated on the left corner of the panel. Data are representative of two experiments performed with similar results. (D) HuIL-8 secretion by TLR5-transfected HEK 293 cells. Non-transfected HEK293 cells (white symbols) or TLR5-transfected HEK293 cells (black symbols) were stimulated with different concentrations of native FliC (squares), recombinant FliC (triangles) or His$_6$FliC-MSP1$_{19}$-PADRE (circles) during 5 h. The secreted HuIL-8 was determined in culture supernatant by capture ELISA. Data are representative of two experiments performed with similar results.

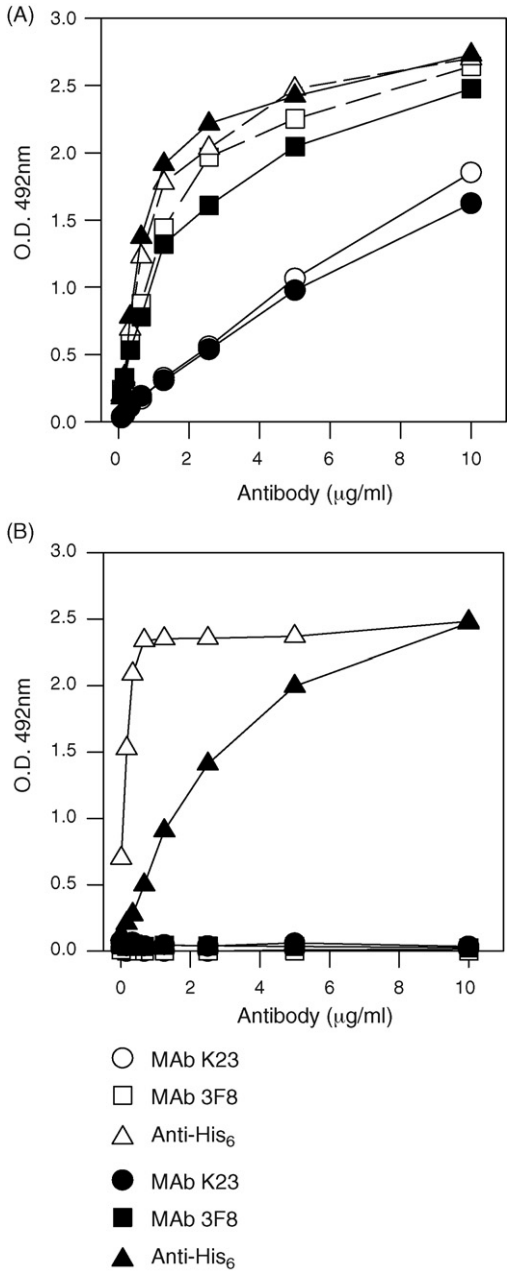

Fig. 2. Presence of conformational epitopes on the His_6FliC-$MSP1_{19}$-PADRE as recognized by two specific MAbs. ELISA was performed using recombinant proteins His_6-$MSP1_{19}$ (open symbols) or His_6FliC-$MSP1_{19}$-PADRE (closed symbols) as substrates. MAbs K23 and 3F8 specific for His_6-$MSP1_{19}$ or polyclonal antibodies specific for the Histidine tag (Anti-His_6) were used at the indicated concentrations. (A) Non-manipulated recombinant proteins; (B) recombinant proteins were reduced with DTT as described in Section 2. Data are average of duplicate samples representative of two experiments performed with identical results.

whether they contained the $MSP1_{19}$-PADRE at the C-terminus) showed a reduced induction of HuIL-8 when compared to the native FliC. Nonetheless, the results clearly demonstrate that the $MSP1_{19}$-PADRE C-terminal fusion did not impair the TLR5-specific bioactivity of the *E. coli* recombinant protein.

To study whether the recombinant protein His_6FliC-$MSP1_{19}$-PADRE still retained conformational epitopes present on His_6-$MSP1_{19}$, we reacted both proteins with two specific MAbs (K23 and 3F8). Both recombinant proteins were well recognized by these MAbs (Fig. 2A). After reduction with DTT, they were no longer recognized by them (Fig. 2B). As positive control, we used polyclonal antibodies to the Histidine tag which still recognized well both recombinant proteins after reduction (Fig. 2A and B). We conclude that these MAbs reacted to conformational epitopes present in both recombinant proteins.

3.2. Induction of $MSP1_{19}$-specific antibody responses in mice immunized with $MSP1_{19}$-derived peptides admixed or genetically fused to FliC

The serum IgG responses to the *P. vivax* $MSP1_{19}$ were determined in C57BL/6 mice immunized with the purified His_6MSP1_{19} or His_6MSP1_{19}-PADRE proteins (5 μg/dose of each antigen) admixed with FliC (2.5 μg/dose) via parenteral (s.c) or mucosal (i.n.) routes. Mice parenterally immunized with recombinant proteins in the presence of FliC developed significantly higher $MSP1_{19}$-specific IgG titers than mice immunized with the His_6MSP1_{19}-PADRE protein alone ($p < 0.01$). Maximal IgG antibody titers were achieved after the second dose in all mice receiving the $MSP1_{19}$ recombinant proteins admixed with flagellin and no significant adjuvant effect was attributed to the PADRE epitope on the induced $MSP1_{19}$-specific antibody responses (Fig. 3A). Similar results were obtained in mice immunized with different amounts (6, 25 and 100 μg/dose) of the recombinant protein genetically fused to flagellin (His_6FliC-$MSP1_{19}$-PADRE). No statistically significant differences were detected in the antibody titers of mouse groups immunized with different amounts of the recombinant protein, an indication that maximal anti-$MSP1_{19}$ responses were achieved after only two doses of the lowest tested protein concentration (Fig. 3A). Additionally, C57BL/10SCN (TLR4 deficient) LPS non-responsive mice s.c. immunized with His_6MSP1_{19}-PADRE in the presence of FliC developed $MSP1_{19}$-specific IgG responses similar to wild type mice, thus discarding any adjuvant effect attributed to contaminating LPS (data not shown). Mice submitted to an immunization regimen administered via the i.n. route mounted lower specific anti-$MSP1_{19}$ antibody titers when compared to animals immunized via s.c. route but the recorded IgG titers after the second or third doses were significantly higher than those detected in mice immunized with three doses of the His_6MSP1_{19}-PADRE protein alone ($p < 0.01$, Fig. 3B). Together, these results indicate that FliC can act as a potent adjuvant either admixed or genetically fused to the malarial $MSP1_{19}$ antigen.

In order to determine the quality of the humoral immune responses, we measured the IgG subclasses of the $MSP1_{19}$-specific antibody responses elicited in mice parenterally immunized with the recombinant proteins. All mice immunized with the malarial recombinant proteins in the presence of FliC, either admixed or genetically fused, developed higher IgG1 levels with IgG1/IgG2c ratios ranging from 200 (His_6MSP1_{19} + FliC) to 794 (His_6FliC-$MSP1_{19}$-PADRE). Similar results were observed in mice immunized via the mucosal route (Fig. 4A). We also tracked the longevity of the induced antibody responses in mice immunized with the recombinant proteins. Although the total anti-$MSP1_{19}$ IgG titers differed among the tested immunization groups, there was no relative difference in the kinetics of the responses decay among animals submitted to the distinct immunization regimens (Fig. 4B).

3.3. Incorporation of CpG ODN 1826 and FliC generated a more balanced Th1/Th2 immune response in mice immunized with $MSP1_{19}$-erived peptides

Because all immunization protocols that we tested generated strong Th2 biased immune responses against $PvMSP1_{19}$, we wondered whether the presence of a TLR9 agonist adjuvant would modulate the humoral immune response, balancing the IgG1/IgG2c

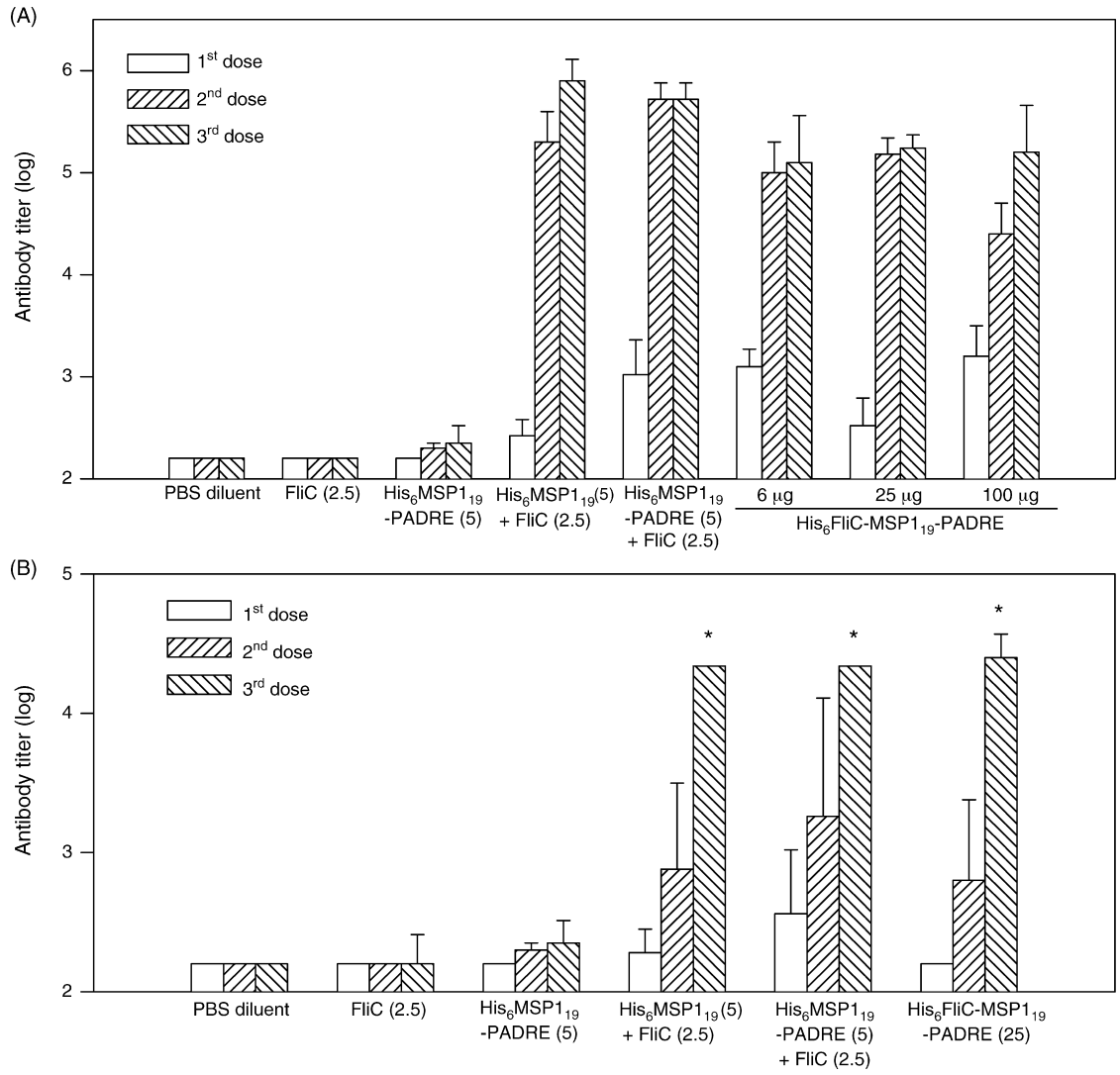

Fig. 3. Induction of anti-MSP1$_{19}$ IgG responses in mice immunized with the malarial recombinant proteins in the presence of FliC. Female C57BL/6 mice were immunized three times either with recombinant proteins alone (His$_6$MSP1$_{19}$-PADRE), admixed with flagellin (His$_6$MSP1$_{19}$ + FliC, His$_6$MSP1$_{19}$-PADRE + FliC), or genetically fused to flagellin (His$_6$FliC-MSP1$_{19}$-PADRE). Numbers in parenthesis indicate the amount (μg/dose) of each protein used in the immunizations. (A) Mice immunized via the s.c. route. (B) Mice immunized via the i.n. route. All mice immunized with a malarial recombinant protein in the presence of FliC had higher IgG titers than control groups, $p < 0.01$. Asterisks denote statistically significant lower antibody levels ($p < 0.01$) with regard to mice immunized by the s.c. route. Results are expressed as means ± S.D. ($n = 6$). Data are representative of multiple experiments performed with similar results.

ratio in the sera of the immunized mice. Although the addition of the TLR9 agonist CpG ODN 1826 to both His$_6$MSP1$_{19}$-PADRE plus FliC and His$_6$FliC-MSP1$_{19}$-PADRE did not enhance the total anti-MSP1$_{19}$ serum IgG response elicited in parenterally immunized mice (Fig. 5A), there was a clear modulation of the IgG subclass response pattern to a more balanced Th1/Th2 response (Fig. 5B). The IgG1/IgG2c ratios detected in mice immunized with His$_6$MSP1$_{19}$-PADRE plus FliC changed from 794 to 125 in the presence of CpG ODN 1826. Similarly, the IgG1/IgG2c ratios detected in mice immunized with His$_6$FliC-MSP1$_{19}$-PADRE dropped from 794 to 50 when the TLR9 agonist was admixed to the recombinant protein (Fig. 5B). A further demonstration of the CpG ODN 1826-dependent immune modulation effect was obtained after determining the IFN-γ secreted by spleen cells of mice immunized with the different vaccine formulations. As shown in Fig. 5C, spleen cells from mice immunized with His$_6$MSP1$_{19}$-PADRE admixed to FliC responded modestly to the PADRE epitope and did not respond at all to His$_6$MSP1$_{19}$. Nevertheless, spleen cells from mice immunized with His$_6$FliC-MSP1$_{19}$-PADRE secreted IFN-γ in response to PADRE or to His$_6$MSP1$_{19}$. The addition of CpG ODN 1826 drastically enhanced the amount of IFN-γ secreted by spleen cells harvested from mice immunized either with His$_6$MSP1$_{19}$-PADRE admixed to FliC or with His$_6$FliC-MSP1$_{19}$-PADRE, following *in vitro* stimulation with the PADRE peptide or the purified His$_6$MSP1$_{19}$. Together, these results indicate that the addition of the TLR9 agonist CpG ODN 1826 balanced the immune response pattern and improved activation of specific cell-dependent immune responses, as evaluated by IFN-γ secretion by spleen cells, induced by MSP1$_{19}$/FliC-based malaria vaccines.

3.4. Antibodies raised in mice immunized with MSP1$_{19}$/FliC-based vaccine formulations recognized P. vivax parasites from human blood cells

The MSP1$_{19}$-specific antibodies raised in mice immunized with the vaccine formulations had a similar affinity to the puri-

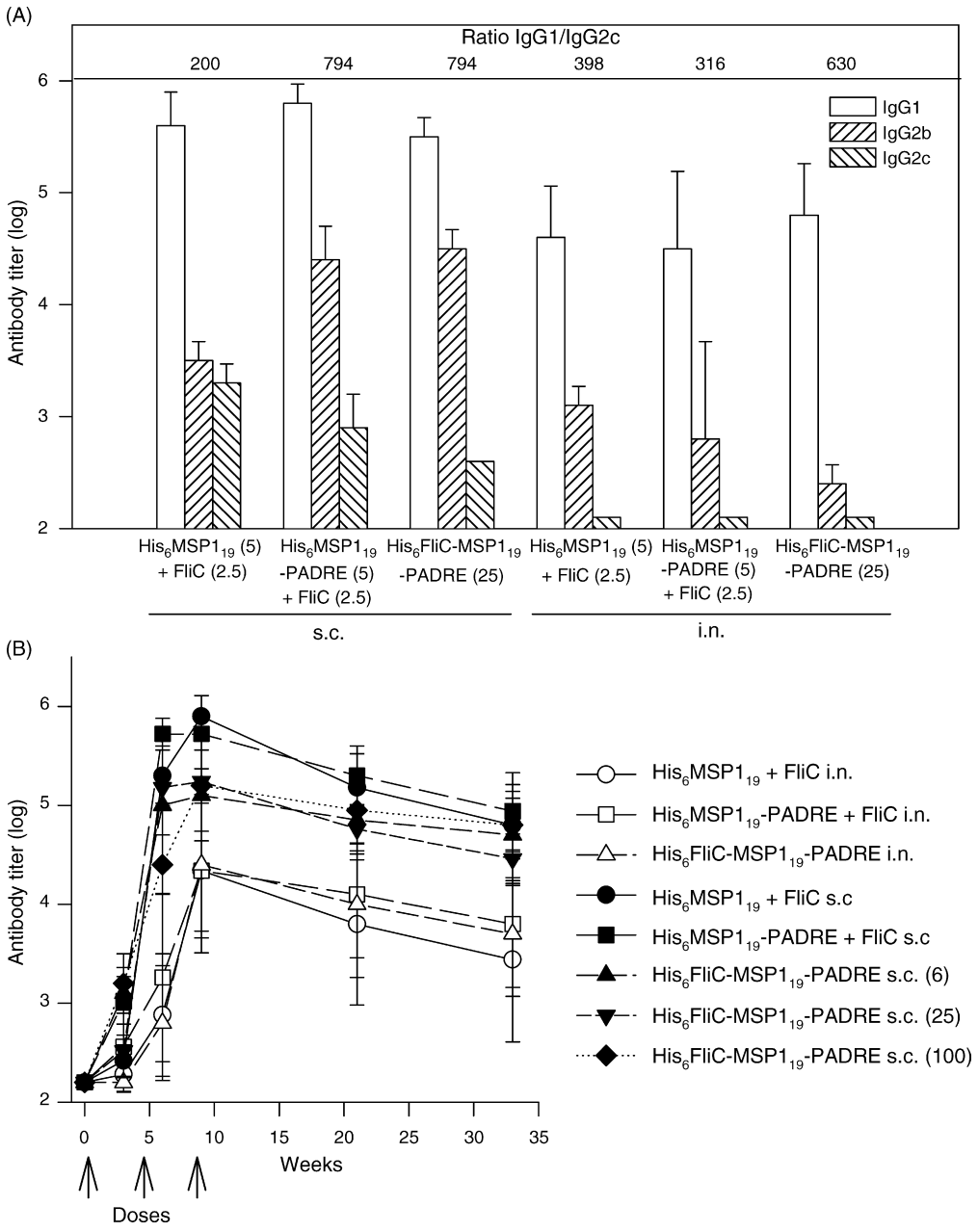

Fig. 4. Characterization of the specific serum IgG responses elicited in mice immunized with recombinant $MSP1_{19}$-derived proteins and FliC flagellin. (A) IgG subclasses responses and IgG1/IgG2c ratios in mice submitted to different immunization regimens. Immunization groups were as described in the legend of Fig. 3. Results are expressed as means ± S.D. ($n = 3$). (B) Longevity of the induced anti-$MSP1_{19}$ IgG responses in mice immunized with the different malarial vaccine formulations. Results are expressed as means ± S.D. ($n = 6$). Data are representative of two experiments performed with similar results.

fied His_6MSP1_{19} protein, as determined in ELISA carried out in the presence of different concentrations of a chaotropic reagent ammonium thiocyanate (data not shown). Moreover, the $MSP1_{19}$-specific antibodies that were induced in mice immunized with the different formulations by the s.c. route, bound to epitopes exposed on the surface of *P. vivax* parasites isolated from infected donors (Fig. 6). The antibodies induced in mice immunized by the i.n. route with His_6MSP1_{19}-PADRE mixed to FliC or His_6FliC-$MSP1_{19}$-PADRE were also capable of recognizing the parasites isolated from infected donors (Fig. 6). Nevertheless, antibodies from mice i.n. immunized with His_6MSP1_{19} mixed to FliC did not bind to the parasites, indicating that, in immunizations by this route, the PADRE epitope may influence the quality of the response.

4. Discussion

The present study provides evidence that a proteic TLR agonist (*Salmonella* FliC) can act as an adjuvant and molecular carrier to a malaria recombinant antigen (*P. vivax* $MSP1_{19}$) promoting a strong and long-lasting adaptive immune response in vaccinated mice. In addition, the immunogenicity of this malaria vaccine formulation can be further improved with the use of additional TLR agonists such as CpG ODN 1826. Recent studies have also examined the adjuvant/carrier property of *Salmonella* flagellin co-administered with distinct antigens. In some cases, admixing flagellin and antigen was sufficient to elicit antigen-specific antibody responses [37–39]. In other cases, the flagellin and the antigen had to be genetically linked in order to efficiently induce immune responses

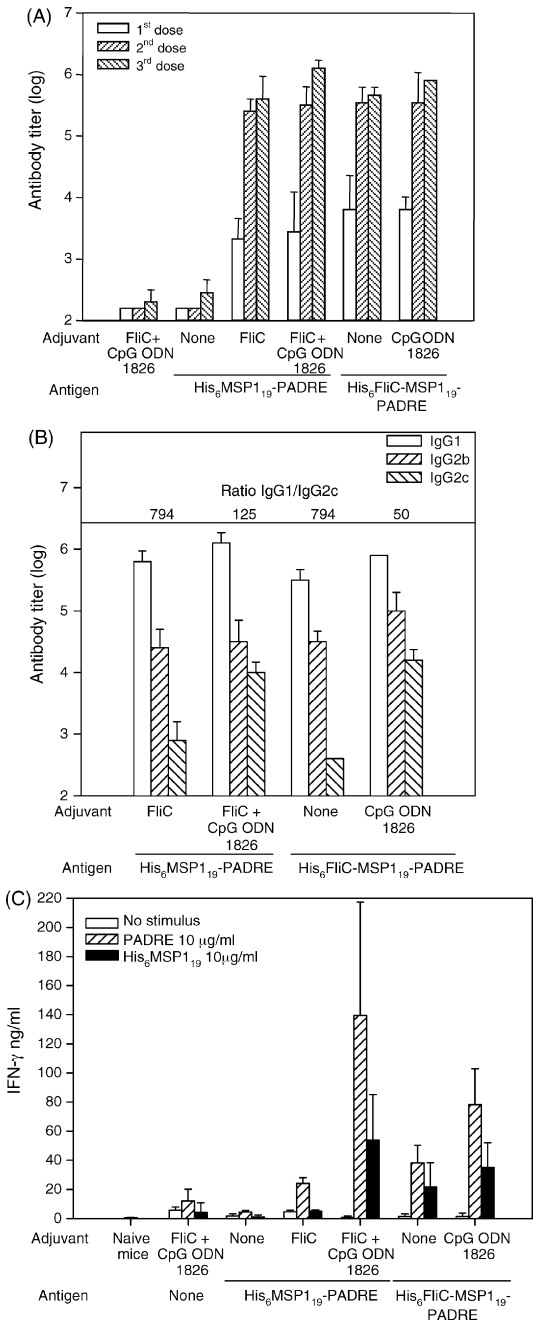

Fig. 5. $MSP1_{19}$-specific antibody and cell-dependent responses in mice immunized with vaccine formulations admixed with CpG ODN 1826. (A) $MSP1_{19}$-specific serum IgG responses in mice s.c. immunized (three doses) with His_6MSP1_{19}-PADRE (5 μg/dose) or His_6FliC-$MSP1_{19}$-PADRE (25 μg/dose) in the presence of FliC (2.5 μg/dose) and/or CpG ODN 1826 (10 μg/dose). All mouse groups immunized with the recombinant fusion proteins in the presence of FliC or CpG ODN 1826 had significantly higher IgG titers than control group immunized with His_6MSP1_{19}-PADRE alone ($p < 0.01$). Results are expressed as means ± S.D. ($n = 6$). (B) IgG subclasses responses in mice immunized with different vaccine formulations. The $MSP1_{19}$-specific IgG1, IgG2b, and IgG2c titers are indicated. The IgG1/IgG2c ratio of each immunization group is indicated at the top of the figure. Results are expressed as means ± S.D. ($n = 3$). (C) IFN-γ secretion by *in vitro* cultured spleen cells harvested from vaccinated mice. Splenocytes collected from different mouse groups were cultured in medium alone or in the presence of PADRE epitope or the His_6MSP1_{19} protein (10 μg/ml) during 120 h. The IFN-γ concentration in culture supernatants was monitored by ELISA. Results are expressed as means ± S.D. ($n = 3$). Data are representative of two experiments performed with similar results.

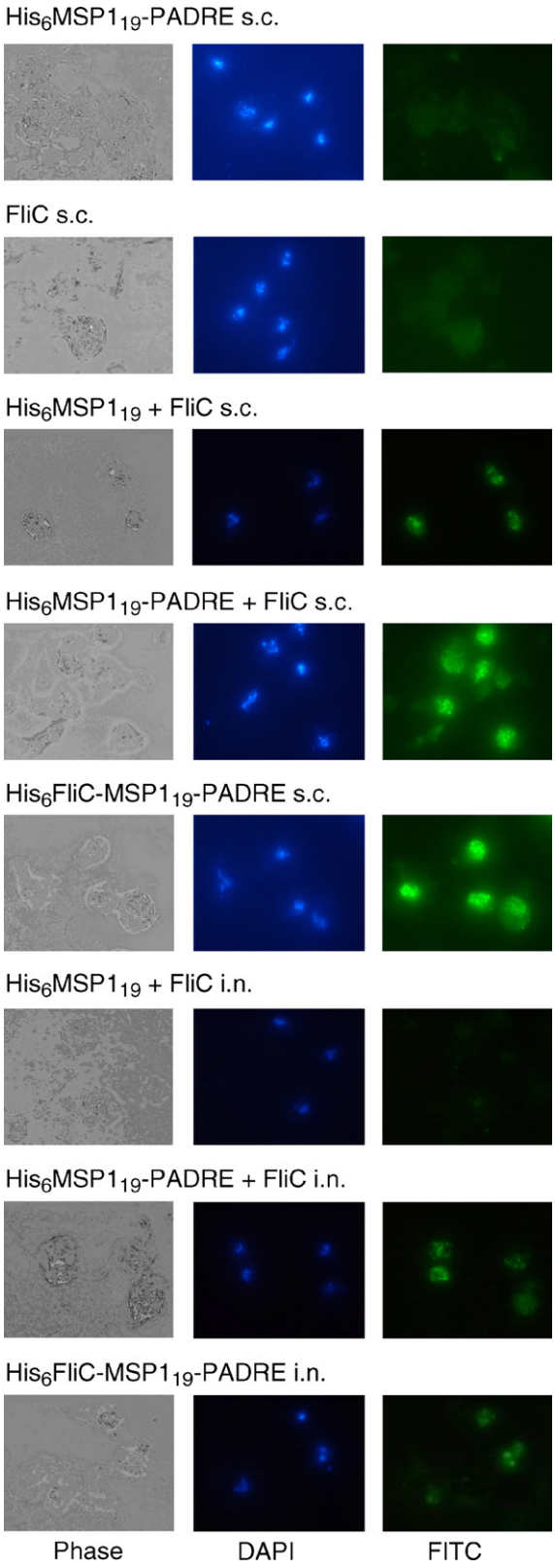

Fig. 6. $MSP1_{19}$-specific antibodies generated in vaccinated mice recognize the native protein expressed by *P. vivax* parasites. Fixed IFA slides were incubated with pooled sera diluted 1:100 in PBS from mice immunized as indicated. Bound IgG were stained with FITC and the parasite nuclei were stained with DAPI. Data are representative of two experiments performed with similar results.

[40–43]. The reasons for such discrepant results are not clear but may be dependent on the nature of the non-flagellin antigen.

Another ambiguous point is the importance of the route of administration on the induced immune responses in mice immunized with vaccine formulations containing *Salmonella* flagellins. A single comparison between the different routes of immunization showed that the amount of antigen required to elicit specific antibody responses by the s.c. route was approximately 10 times lower than the amount required to achieve similar antibody levels in mice immunized via the i.n. route [43]. This result concurs with our present findings, in which significantly lower antibody titers to the malarial antigen were observed in mice immunized by the i.n. route.

The protective nature of the antibodies to the C-terminal domain of *Plasmodium* MSP1 proteins has been thoroughly documented in a number of *in vitro* and *in vivo* studies. In mice infected with the rodent malaria parasite *P. yoelii*, the passive transfer of $MSP1_{19}$-specific monoclonal antibodies to naïve mice conferred complete protection [52,53]. In subsequent studies, active immunization of recombinant proteins with Complete Freund Adjuvant also provided a high degree of protective immunity with a prevailing serum IgG1 subclass response [54–58]. The $MSP1_{19}$-specific serum antibody immune responses observed in mice vaccinated with flagellin and malarial recombinant proteins revealed a predominant IgG1 response, as showed in other models [37,39]. These finding are compatible with previous observations that flagellin promotes the secretion of IL-4 and IL-13 by antigen-specific $CD4^+$ T cells, promoting a Th2 biased immune response [59,60]. The Th2 biased responses elicited in mice immunized with bacterial flagellins is apparently due to the activation of TLR5, which relies solely on the MyD88 adaptor activation [59].

We observed that the genetic linkage of the flagellin with the malarial antigen did not dramatically influence the conformation of the *P. vivax* $MSP1_{19}$ epitopes. Antibodies from humans exposed to malaria parasites (native protein) clearly recognized the fusion protein and this recognition was not significantly different when compared to His_6-$MSP1_{19}$. These observations were complemented using two MAbs which recognized conformational epitopes in both recombinant proteins (Fig. 2). In addition, antibodies from immunized mice recognized by IFA parasites obtained from a infected human individual (Fig. 6). Previous studies using influenza or West Nile virus epitopes fused to flagellin presented similar conclusions [42,43]. The fact that all recombinant fusion proteins generated so far retained their bioactivity for TLR5 activation [40,42,43] suggests that the genetic linkage of antigens to *Salmonella* flagellins might be a general approach for the development of vaccines using distinct microbial antigens.

It is very likely that the mechanism that mediates the adjuvant properties of flagellin involves the activation of TLR5 in antigen presenting cells. This activation leads to an increase in the surface expression of B7-2, which seems to be required – at least in part – for the adjuvant properties of flagellin. B7-2 and B7-1/2 knockout mice had significantly lower antibody responses when immunized with the saliva-binding region of the adhesin AgI/II of *Streptococcus mutans* [38]. Alternatively, flagellin may act through an Ipaf (ICE protease-activating factor)-dependent mechanism that detects cytosolic flagellin and may activate antigen presenting cells [34,36,61,62]. We are currently exploring this second hypothesis using Ipaf deficient mice. Most recently, flagellin has been shown to activate APC through the reduction of IL-10 secretion, an immunosuppressive cytokine [63]. This may further improve the adjuvant properties of flagellin, allowing for a stronger adaptive immune response.

In addition to the strong systemic antibody responses, we observed that mice immunized with flagellin and $MSP1_{19}$-containing vaccine formulations acted also as an adjuvant for CMI, as demonstrated by the secretion of IFN-γ by immune spleen cells. However, in contrast to the induced $MSP1_{19}$-specific antibody responses, the genetic linkage between the malarial antigen and flagellin resulted in higher PADRE and $MSP1_{19}$-specific IFN-γ secretion by immune spleen cells of vaccinated mice (Fig. 5C). Therefore, even though the antibody responses that we observed were similar, the linkage of the antigen to flagellin may be an important strategy to improve the adjuvant activity in CMI. The presence of B-cell and helper epitopes in the flagellin, linked to the antigen, may enhance both the antigen presentation of $MSP1_{19}$ CD4-specific epitopes and the expansion of CD4 T cells specific for $MSP1_{19}$. These possibilities should be evaluated further in future studies.

The immunization of non-human primates with recombinant *P. falciparum* and *P. cynolmogi* MSP1 C-terminal regions provided a certain degree of protective immunity to the vaccinated animals when parenterally administered with Complete or Incomplete Freund Adjuvant [64–66]. Based on these promising results, phase I clinical trials with *P. falciparum* recombinant proteins have already been initiated [67,68]. However, it is important to mention that similar pre-clinical or clinical studies have yet to be initiated using recombinant proteins based on the C-terminal region of the *P. vivax* MSP1 protein. Indeed, the *P.vivax* and *P. falciparum* proteins share an overall structural homology. No cross-reaction is observed, however, at the level of antibody recognition or immune-protection.

We have also evaluated whether a second TLR agonist, CpG-containing oligonucleotides, could modify the immune response elicited in the presence of the TLR5 agonist flagellin. The TLR9 agonist CpG ODN 1826 is well-known for the ability to stimulate IL-12 and IFN-γ production when injected *in vivo* [69]. The addition of CpG ODN 1826 did not improve the magnitude of the antibody responses, though its presence changed the IgG1/IgG2c ratio to a more balanced Th1/Th2 pattern. Co-administration of the CpG ODN 1826 has also evoked a clear increase in the PADRE and $MSP1_{19}$-specific IFN-γ secretion by immune spleen cells (Fig. 5C). This result further emphasizes that the incorporation of both TLR agonists may confer broader immune responses elicited in animals immunized with $MSP1_{19}$ and provides new perspectives for the rational development of new malarial vaccine candidates.

Acknowledgments

This work was supported by grants from Fundação de Amparo à Pesquisa do Estado de São Paulo, Fundação de Amparo à Pesquisa do Estado do Rio de Janeiro, and The Millennium Institute for Vaccine Development and Technology (CNPq – 420067/2005-1). DYB, DSR, CJMB, BOC, NME were supported by fellowships from FAPESP. FTMC, AJV, LCSF, ISS, MMR were supported by fellowships from CNPq.

References

[1] Price RN, Tjitra E, Guerra CA, Yeung S, White NJ, Anstey NM. Vivax malaria: neglected and not benign. Am J Trop Med Hyg 2007;77(December (6 Suppl.)):79–87.
[2] Baird JK. Chloroquine resistance in *Plasmodium vivax*. Antimicrob Agents Chemother 2004;48(November (11)):4075–83.
[3] Baird JK. Neglect of *Plasmodium vivax* malaria. Trends Parasitol 2007; 23(November (11)):533–9.
[4] Rogers WO, Gowda K, Hoffman SL. Construction and immunogenicity of DNA vaccine plasmids encoding four *Plasmodium vivax* candidate vaccine antigens. Vaccine 1999;17(August 6 (3–24)):3136–44.
[5] Castellanos A, Arevalo-Herrera M, Restrepo N, Gulloso L, Corradin G, Herrera S. *Plasmodium vivax* thrombospondin related adhesion protein: immunogenicity and protective efficacy in rodents and Aotus monkeys. Memorias do Instituto Oswaldo Cruz 2007;102(June (3)):411–6.
[6] Herrera S, Bonelo A, Perlaza BL, Fernandez OL, Victoria L, Lenis AM, et al. Safety and elicitation of humoral and cellular responses in colombian malaria-naive volunteers by a *Plasmodium vivax* circumsporozoite protein-derived synthetic vaccine. Am J Trop Med Hyg 2005;73(November (5 Suppl.)):3–9.

[7] Arevalo-Herrera M, Solarte Y, Yasnot MF, Castellanos A, Rincon A, Saul A, et al. Induction of transmission-blocking immunity in *Aotus* monkeys by vaccination with a *Plasmodium vivax* clinical grade PVS25 recombinant protein. Am J Trop Med Hyg 2005;73(November (5 Suppl.)):32–7.
[8] Malkin EM, Durbin AP, Diemert DJ, Sattabongkot J, Wu Y, Miura K, et al. Phase 1 vaccine trial of Pvs25H: a transmission blocking vaccine for *Plasmodium vivax* malaria. Vaccine 2005;23(May 2 (24)):3131–8.
[9] Collins WE, Barnwell JW, Sullivan JS, Nace D, Williams T, Bounngaseng A, et al. Assessment of transmission-blocking activity of candidate Pvs25 vaccine using gametocytes from chimpanzees. Am J Trop Med Hyg 2006;74(February (2)):215–21.
[10] Ramjanee S, Robertson JS, Franke-Fayard B, Sinha R, Waters AP, Janse CJ, et al. The use of transgenic *Plasmodium berghei* expressing the Plasmodium vivax antigen P25 to determine the transmission-blocking activity of sera from malaria vaccine trials. Vaccine 2007;25(January 15 (5)):886–94.
[11] Miura K, Keister DB, Muratova OV, Sattabongkot J, Long CA, Saul A. Transmission-blocking activity induced by malaria vaccine candidates Pfs25/Pvs25 is a direct and predictable function of antibody titer. Malar J 2007;6:107.
[12] Saul A, Hensmann M, Sattabongkot J, Collins WE, Barnwell JW, Langermans JA, et al. Immunogenicity in rhesus of the *Plasmodium vivax* mosquito stage antigen Pvs25H with Alhydrogel and Montanide ISA 720. Parasite immunol 2007;29(October (10)):525–33.
[13] Herrera S, Corradin G, Arevalo-Herrera M. An update on the search for a *Plasmodium vivax* vaccine. Trends Parasitol 2007;23(March (3)):122–8.
[14] Valderrama-Aguirre A, Quintero G, Gomez A, Castellanos A, Perez Y, Mendez F, et al. Antigenicity, immunogenicity, and protective efficacy of *Plasmodium vivax* MSP1 PV200l: a potential malaria vaccine subunit. Am J Trop Med Hyg 2005;73(November (5 Suppl.)):16–24.
[15] Dutta S, Ware LA, Barbosa A, Ockenhouse CF, Lanar DE. Purification, characterization, and immunogenicity of a disulfide cross-linked *Plasmodium vivax* vaccine candidate antigen, Merozoite Surface Protein 1, expressed in *Escherichia coli*. Infect Immun 2001;69(September (9)):5464–70.
[16] Sachdeva S, Ahmad G, Malhotra P, Mukherjee P, Chauhan VS. Comparison of immunogenicities of recombinant *Plasmodium vivax* Merozoite Surface Protein 1 19- and 42-kiloDalton fragments expressed in *Escherichia coli*. Infect Immun 2004;72(October (10)):5775–82.
[17] Dutta S, Kaushal DC, Ware LA, Puri SK, Kaushal NA, Narula A, et al. Merozoite Surface Protein 1 of *Plasmodium vivax* induces a protective response against *Plasmodium cynomolgi* challenge in rhesus monkeys. Infect Immun 2005;73(September (9)):5936–44.
[18] Devi YS, Mukherjee P, Yazdani SS, Shakri AR, Mazumdar S, Pandey S, et al. Immunogenicity of *Plasmodium vivax* combination subunit vaccine formulated with human compatible adjuvants in mice. Vaccine 2007;25(July 9 (28)):5166–74.
[19] Kocken CH, Dubbeld MA, Van Der Wel A, Pronk JT, Waters AP, Langermans JA, et al. High-level expression of *Plasmodium vivax* apical membrane antigen 1 (AMA-1) in *Pichia pastoris*: strong immunogenicity in *Macaca mulatta* immunized with *P. vivax* AMA-1 and adjuvant SBAS2. Infecti Immun 1999;67(January (1)):43–9.
[20] Arevalo-Herrera M, Castellanos A, Yazdani SS, Shakri AR, Chitnis CE, Dominik R, et al. Immunogenicity and protective efficacy of recombinant vaccine based on the receptor-binding domain of the *Plasmodium vivax* Duffy binding protein in *Aotus* monkeys. Am J Trop Med Hyg 2005;73(November (5 Suppl.)):25–31.
[21] Grimberg BT, Udomsangpetch R, Xainli J, McHenry A, Panichakul T, Sattabongkot J, et al. *Plasmodium vivax* invasion of human erythrocytes inhibited by antibodies directed against the Duffy binding protein. PLoS Med 2007;4(December (12)):e337.
[22] Chitnis CE, Sharma A. Targeting the *Plasmodium vivax* Duffy-binding protein. Trends Parasitol 2008;24(January (1)):29–34.
[23] Oliveira-Ferreira J, Vargas-Serrato E, Barnwell JW, Moreno A, Galinski MR. Immunogenicity of *Plasmodium vivax* Merozoite Surface Protein-9 recombinant proteins expressed in *E. coli*. Vaccine 2004;22(May 7 (15–16)):2023–30.
[24] Rojas Caraballo J, Delgado G, Rodriguez R, Patarroyo MA. The antigenicity of a *Plasmodium vivax* reticulocyte binding protein-1 (PvRBP1) recombinant fragment in humans and its immunogenicity and protection studies in Aotus monkeys. Vaccine 2007;25(May 4 (18)):3713–21.
[25] Blackman MJ, Heidrich HG, Donachie S, McBride JS, Holder AA. A single fragment of a malaria Merozoite Surface Protein remains on the parasite during red cell invasion and is the target of invasion-inhibiting antibodies. J Exp Med 1990;172(July 1 (1)):379–82.
[26] O'Donnell RA, Saul A, Cowman AF, Crabb BS. Functional conservation of the malaria vaccine antigen MSP-119across distantly related *Plasmodium* species. Nat Med 2000;6(January 1):91–5.
[27] Cunha MG, Rodrigues MM, Soares IS. Comparison of the immunogenic properties of recombinant proteins representing the *Plasmodium vivax* vaccine candidate MSP1(19) expressed in distinct bacterial vectors. Vaccine 2001;20(November 12 (3–4)):385–96.
[28] Rodrigues MH, Cunha MG, Machado RL, Ferreira Jr OC, Rodrigues MM, Soares IS. Serological detection of *Plasmodium vivax* malaria using recombinant proteins corresponding to the 19-kDa C-terminal region of the Merozoite Surface Protein-1. Malar J 2003;2(November 14 (1)):39.
[29] Rosa DS, Tzelepis F, Cunha MG, Soares IS, Rodrigues MM. The pan HLA DR-binding epitope improves adjuvant-assisted immunization with a recombinant protein containing a malaria vaccine candidate. Immunol Lett 2004;92(April 15 (3)):259–68.
[30] Bargieri DY, Rosa DS, Lasaro MA, Ferreira LC, Soares IS, Rodrigues MM. Adjuvant requirement for successful immunization with recombinant derivatives of *Plasmodium vivax* Merozoite Surface Protein-1 delivered via the intranasal route. Memorias do Instituto Oswaldo Cruz 2007;102(June (3)):313–7.
[31] Rosa DS, Iwai LK, Tzelepis F, Bargieri DY, Medeiros MA, Soares IS, et al. Immunogenicity of a recombinant protein containing the *Plasmodium vivax* vaccine candidate MSP1(19) and two human CD4+ T-cell epitopes administered to non-human primates (*Callithrix jacchus jacchus*). Microbes Infect/Institut Pasteur 2006;8(July (8)):2130–7.
[32] Janeway Jr CA, Medzhitov R. Innate immune recognition. Annu Rev Immunol 2002;20:197–216.
[33] Akira S, Uematsu S, Takeuchi O. Pathogen recognition and innate immunity. Cell 2006;124(February 24 (4)):783–801.
[34] Miao EA, Alpuche-Aranda CM, Dors M, Clark AE, Bader MW, Miller SI, et al. Cytoplasmic flagellin activates caspase-1 and secretion of interleukin 1beta via Ipaf. Nat Immunol 2006;7(June (6)):569–75.
[35] Smith KD, Andersen-Nissen E, Hayashi F, Strobe K, Bergman MA, Barrett SL, et al. Toll-like receptor 5 recognizes a conserved site on flagellin required for protofilament formation and bacterial motility. Nat Immunol 2003;4(December (12)):1247–53.
[36] Franchi L, Amer A, Body-Malapel M, Kanneganti TD, Ozoren N, Jagirdar R, et al. Cytosolic flagellin requires Ipaf for activation of caspase-1 and interleukin 1beta in salmonella-infected macrophages. Nat Immunol 2006;7(June (6)):576–82.
[37] Lee SE, Kim SY, Jeong BC, Kim YR, Bae SJ, Ahn OS, et al. A bacterial flagellin, *Vibrio vulnificus* FlaB, has a strong mucosal adjuvant activity to induce protective immunity. Infect Immun 2006;74(January (1)):694–702.
[38] Pino O, Martin M, Michalek SM. Cellular mechanisms of the adjuvant activity of the flagellin component FljB of *Salmonella enterica* Serovar Typhimurium to potentiate mucosal and systemic responses. Infect Immun 2005;73(October (10)):6763–70.
[39] Honko AN, Sriranganathan N, Lees CJ, Mizel SB. Flagellin is an effective adjuvant for immunization against lethal respiratory challenge with *Yersinia pestis*. Infect Immun 2006;74(February (2)):1113–20.
[40] Cuadros C, Lopez-Hernandez FJ, Dominguez AL, McClelland M, Lustgarten J. Flagellin fusion proteins as adjuvants or vaccines induce specific immune responses. Infect Immun 2004;72(May (5)):2810–6.
[41] Huleatt JW, Jacobs AR, Tang J, Desai P, Kopp EB, Huang Y, et al. Vaccination with recombinant fusion proteins incorporating Toll-like receptor ligands induces rapid cellular and humoral immunity. Vaccine 2007;25(January 8 (4)):763–75.
[42] McDonald WF, Huleatt JW, Foellmer HG, Hewitt D, Tang J, Desai P, et al. A West Nile virus recombinant protein vaccine that coactivates innate and adaptive immunity. J Infect Dis 2007;195(June 1 (11)):1607–17.
[43] Huleatt JW, Nakaar V, Desai P, Huang Y, Hewitt D, Jacobs A, et al. Potent immunogenicity and efficacy of a universal influenza vaccine candidate comprising a recombinant fusion protein linking influenza M2e to the TLR5 ligand flagellin. Vaccine 2008;26(January 10 (2)):201–14.
[44] Applequist SE, Rollman E, Wareing MD, Liden M, Rozell B, Hinkula J, et al. Activation of innate immunity, inflammation, and potentiation of DNA vaccination through mammalian expression of the TLR5 agonist flagellin. J Immunol 2005;175(September 15 (6)):3882–91.
[45] Schmitt CK, Darnell SC, O'Brien AD. The attenuated phenotype of a *Salmonella* typhimurium flgM mutant is related to expression of FliC flagellin. J Bacteriol 1996;178(May (10)):2911–5.
[46] Barnwell JW, Galinski MR, DeSimone SG, Perler F, Ingravallo P. *Plasmodium vivax, P. cynomolgi*, and *P. knowlesi*: identification of homologue proteins associated with the surface of merozoites. Exp Parasitol 1999;91(March (3)):238–49.
[47] Soares IS, Levitus G, Souza JM, Del Portillo HA, Rodrigues MM. Acquired immune responses to the N- and C-terminal regions of *Plasmodium vivax* Merozoite Surface Protein 1 in individuals exposed to malaria. Infect Immun 1997;65(May (5)):1606–14.
[48] Soares IS, da Cunha MG, Silva MN, Souza JM, Del Portillo HA, Rodrigues MM. Longevity of naturally acquired antibody responses to the N- and C-terminal regions of *Plasmodium vivax* Merozoite Surface Protein 1. Am J Trop Med Hyg 1999;60(March (3)):357–63.
[49] Soares IS, Barnwell JW, Ferreira MU, Gomes Da Cunha M, Laurino JP, Castilho BA, et al. A *Plasmodium vivax* vaccine candidate displays limited allele polymorphism, which does not restrict recognition by antibodies. Mol Med 1999;5(July (7)):459–70.
[50] Rodrigues MM, Ribeirao M, Pereira-Chioccola V, Renia L, Costa F. Predominance of CD4 Th1 and CD8 Tc1 cells revealed by characterization of the cellular immune response generated by immunization with a DNA vaccine containing a *Trypanosoma cruzi* gene. Infect Immun 1999;67(August (8)):3855–63.
[51] Ljungström I, Perlmann H, Schlichtherle M, Scherf A, Wahlgren M. Methods in malaria research. 4th ed. Manassas, Virginia, USA: MR4/ATCC; 2004.
[52] Majarian WR, Daly TM, Weidanz WP, Long CA. Passive immunization against murine malaria with an IgG3 monoclonal antibody. J Immunol 1984;132(June (6)):3131–7.
[53] Spencer Valero LM, Ogun SA, Fleck SL, Ling IT, Scott-Finnigan TJ, Blackman MJ, et al. Passive immunization with antibodies against three distinct epitopes on *Plasmodium yoelii* Merozoite Surface Protein 1 suppresses parasitemia. Infect Immun 1998;66(August (8)):3925–30.

[54] Daly TM, Long CA. A recombinant 15-kilodalton carboxyl-terminal fragment of *Plasmodium yoelii yoelii* 17XL Merozoite Surface Protein 1 induces a protective immune response in mice. Infect Immun 1993;61(June (6)):2462–7.
[55] Ling IT, Ogun SA, Holder AA. Immunization against malaria with a recombinant protein. Parasite Immunol 1994;16(February (2)):63–7.
[56] Hirunpetcharat C, Tian JH, Kaslow DC, van Rooijen N, Kumar S, Berzofsky JA, et al. Complete protective immunity induced in mice by immunization with the 19-kilodalton carboxyl-terminal fragment of the Merozoite Surface Protein-1 (MSP1[19]) of *Plasmodium yoelii* expressed in *Saccharomyces cerevisiae*: correlation of protection with antigen-specific antibody titer, but not with effector CD4+T cells. J Immunol 1997;159(October 1 (7)):3400–11.
[57] Rotman HL, Daly TM, Clynes R, Long CA. Fc receptors are not required for antibody-mediated protection against lethal malaria challenge in a mouse model. J Immunol 1998;161(August 15 (4)):1908–12.
[58] Bates MD, Newbold CI, Jarra W, Brown KN. Protective immunity to malaria: studies with cloned lines of *Plasmodium chabaudi chabaudi* in CBA/Ca mice. III. Protective and suppressive responses induced by immunization with purified antigens. Parasite Immunol 1988;10(January (1)):1–15.
[59] Didierlaurent A, Ferrero I, Otten LA, Dubois B, Reinhardt M, Carlsen H, et al. Flagellin promotes myeloid differentiation factor 88-dependent development of Th2-type response. J Immunol 2004;172(June 1 (11)):6922–30.
[60] Cunningham AF, Khan M, Ball J, Toellner KM, Serre K, Mohr E, et al. Responses to the soluble flagellar protein FliC are Th2, while those to FliC on Salmonella are Th1. Eur J Immunol 2004;34(November (11)):2986–95.
[61] Molofsky AB, Byrne BG, Whitfield NN, Madigan CA, Fuse ET, Tateda K, et al. Cytosolic recognition of flagellin by mouse macrophages restricts *Legionella pneumophila* infection. J Exp Med 2006;203(April 17 (40)):1093–104.
[62] Ren T, Zamboni DS, Roy CR, Dietrich WF, Vance RE. Flagellin-deficient Legionella mutants evade caspase-1- and Naip5-mediated macrophage immunity. PLoS Pathog 2006;2(March (3)):e18.
[63] Vicente-Suarez I, Takahashi Y, Cheng F, Horna P, Wang HW, Wang HG, et al. Identification of a novel negative role of flagellin in regulating IL-10 production. Eur J Immunol 2007;37(November (11)):3164–75.
[64] Perera KL, Handunnetti SM, Holm I, Longacre S, Mendis K. Baculovirus Merozoite Surface Protein 1 C-terminal recombinant antigens are highly protective in a natural primate model for human *Plasmodium vivax* malaria. Infect Immun 1998;66(April (4)):1500–6.
[65] Darko CA, Angov E, Collins WE, Bergmann-Leitner ES, Girouard AS, Hitt SL, et al. The clinical-grade 42-kilodalton fragment of Merozoite Surface Protein 1 of *Plasmodium falciparum* strain FVO expressed in *Escherichia coli* protects *Aotus nancymai* against challenge with homologous erythrocytic-stage parasites. Infect Immun 2005;73(January (1)):287–97.
[66] Singh S, Miura K, Zhou H, Muratova O, Keegan B, Miles A, et al. Immunity to recombinant plasmodium falciparum Merozoite Surface Protein 1 (MSP1): protection in Aotus nancymai monkeys strongly correlates with anti-MSP1 antibody titer and in vitro parasite-inhibitory activity. Infect Immun 2006;74(August (8)):4573–80.
[67] Malkin E, Long CA, Stowers AW, Zou L, Singh S, MacDonald NJ, et al. Phase 1 study of two Merozoite Surface Protein 1 (MSP1(42)) vaccines for *Plasmodium falciparum* malaria. PLoS Clin Trials 2007;2(4):e12.
[68] Huaman MC, Martin LB, Malkin E, Narum DL, Miller LH, Mahanty S, et al. Ex vivo cytokine and memory T cell responses to the 42-kDa fragment of *Plasmodium falciparum* Merozoite Surface Protein-1 in vaccinated volunteers. J Immunol 2008;180(February 1 (3)):1451–61.
[69] Klinman DM. Immunotherapeutic uses of CpG oligodeoxynucleotides. Nature Rev 2004;4(April (40)):249–58.

OPEN ACCESS Freely available online

PLoS one

Hyperbaric Oxygen Prevents Early Death Caused by Experimental Cerebral Malaria

Yara C. Blanco[1,2], Alessandro S. Farias[1], Uta Goelnitz[3], Stefanie C. P. Lopes[1,2], Wagner W. Arrais-Silva[2], Bruna O. Carvalho[1,2], Rogério Amino[4], Gerhard Wunderlich[3], Leonilda M. B. Santos[1], Selma Giorgio[2], Fabio T. M. Costa[1,2]*

1 Department of Microbiology & Immunology, State University of Campinas – UNICAMP, Campinas, São Paulo, Brazil, **2** Department of Parasitology, UNICAMP, State University of Campinas, Campinas, São Paulo, Brazil, **3** Department of Parasitology – ICB, University of São Paulo – USP, São Paulo, São Paulo, Brazil, **4** Department of Biochemistry, Federal University of São Paulo – UNIFESP, São Paulo, São Paulo, Brazil

Abstract

Background: Cerebral malaria (CM) is a syndrome characterized by neurological signs, seizures and coma. Despite the fact that CM presents similarities with cerebral stroke, few studies have focused on new supportive therapies for the disease. Hyperbaric oxygen (HBO) therapy has been successfully used in patients with numerous brain disorders such as stroke, migraine and atherosclerosis.

Methodology/Principal Findings: C57BL/6 mice infected with *Plasmodium berghei* ANKA (PbA) were exposed to daily doses of HBO (100% O_2, 3.0 ATA, 1–2 h per day) in conditions well-tolerated by humans and animals, before or after parasite establishment. Cumulative survival analyses demonstrated that HBO therapy protected 50% of PbA-infected mice and delayed CM-specific neurological signs when administrated after patent parasitemia. Pressurized oxygen therapy reduced peripheral parasitemia, expression of TNF-α, IFN-γ and IL-10 mRNA levels and percentage of $\gamma\delta$ and $\alpha\beta$ $CD4^+$ and $CD8^+$ T lymphocytes sequestered in mice brains, thus resulting in a reduction of blood-brain barrier (BBB) dysfunction and hypothermia.

Conclusions/Significance: The data presented here is the first indication that HBO treatment could be used as supportive therapy, perhaps in association with neuroprotective drugs, to prevent CM clinical outcomes, including death.

Citation: Blanco YC, Farias AS, Goelnitz U, Lopes SCP, Arrais-Silva WW, et al. (2008) Hyperbaric Oxygen Prevents Early Death Caused by Experimental Cerebral Malaria. PLoS ONE 3(9): e3126. doi:10.1371/journal.pone.0003126

Editor: Mauricio Martins Rodrigues, Federal University of São Paulo, Brazil

Received March 22, 2007; **Accepted** August 14, 2008; **Published** September 4, 2008

Funding: This work was supported by Fundação de Amparo à Pesquisa do Estado de São Paulo (FAPESP), grant n° 2004/00638-6, and from Conselho Nacional de Desenvolvimento Científico e Tecnológico (CNPq). YCB, WWA, ASF and SCPL were supported by Coordenação de Aperfeiçoamento de Pessoal de Nível Superior (CAPES), and UG was sponsored by a FAPESP fellowship. GW, SG and FTMC are CNPq fellows.

Competing Interests: The authors have declared that no competing interests exist.

* E-mail: costaftm@unicamp.br

Introduction

Cerebral malaria (CM) causes 1–2 million deaths annually; mainly in sub-Saharan African children aged 2–6. It is estimated that 250,000 children that do not succumb to CM will develop neurocognitive impairments per year [1] and most CM patients die before the beneficial effects of drug treatment are observed [2]; thus indicating the need to explore new supportive therapies.

CM is a multi-factorial syndrome characterized by neurological signs, seizures and coma, which can, in turn, lead to death. This syndrome can be associated with a loss of cerebrospinal fluid spaces and ischemia [3], alterations in cerebral blood flow velocity [4], a decrease in cerebral oxygen consumption in CM comatose patients [5] and an increase in the lactate levels of the cerebrospinal fluid [6] which decreases after patients recover consciousness [7]. Recent imaging and postmortem analyses have revealed the presence of Durck granulomas, blood-brain barrier (BBB) dysfunction and diffuse cerebral edema with multiple petechial hemorrhages and ischemic changes in the brain of adults with CM [8,9].

Although the CM pathogenic process is controversial and still not fully understood, evidence suggests that the host's immune system plays a major role in expressing certain cytokines, e.g. TNF-α and IFN-γ, and activating immunocompetent cells [10–15]. In fact, recent immunological analyses have shown that, unlike individuals with mild and severe non-cerebral malaria, CM patients present elevated levels of a specific cluster of cytokines, which include TGF-β, TNF-α, IL-1β and IL-10 [16].

Hyperbaric oxygen therapy (HBO; $pO_2 = 760$ mmHg) has been successfully used against bacterial and fungal infections and as an adjunct therapy in surgeries [17–19]. In addition, reports have recently shown that HBO therapy transiently suppresses the inflammatory process of ischemic wounding and trauma [20,21]. Indeed, immunological analyses have revealed that HBO therapy significantly decreases the levels of TNF-α and IL-1β secreted by monocytes and macrophage collected from rats or from human peripheral blood after stimulation with LPS [22,23]. In an experimental model for ischemia, HBO reduces immunocompetent cell sequestration and the synthesis of TNF-α [24]; probably by decreasing ICAM-1 expression levels [25]. Moreover, HBO

reduces the expression of the cyclooxygenase-2 (COX-2) mRNA, an enzyme involved in inflammation, and the hypoxia-inducible factor-1α (HIF-1α), a transcriptional factor associated with low oxygen concentrations [26,27]. HBO therapy has been used in patients with numerous brain disorders such as stroke, migraine and atherosclerosis, due to its capacity to decrease cerebral edema and brain infarction while maintaining BBB integrity, reducing neuronal death and improving blood flow in damaged areas of the brain [28]. Nevertheless, depending on the protocol used for treatment, HBO therapy has potential side effects associated to ear and sinus barotraumas, myopia and convulsion [29].

In an early study, HBO was observed to alter the parasitemia levels of mice infected with a non-cerebral line of *Plasmodium berghei* [30]. However, the HBO effect on the entire curve of parasitemia, on the clinical symptoms and on the mechanisms of the illness were not further investigated. Moreover, although the pathological process involved in CM displays some features in common with brain stroke, the effect of HBO on CM, to our knowledge, has never been assessed. Here we show that in conditions also suitable for human use, HBO therapy prevents CM clinical symptoms in C57BL/6 mice infected with *P. berghei* ANKA, a model widely used for experimental cerebral malaria (ECM) [31].

Methods

Mice and parasites

C57BL/6 mice (7–10 weeks old) were purchased from the University of São Paulo (São Paulo, SP, Brazil) and maintained in our specific pathogen-free animal facility. All experiments and procedures were approved by the UNICAMP Committee for Ethics in Animal Research (Protocol No. 857-1).

Two different strains of *P. berghei* were used: the cloned line of *P. berghei* ANKA (PbA) and *P. berghei* NK-65 (PbNK-65), respectively an ECM- and non-ECM-causing strain; kindly provided by Dr. Laurent Rénia (Singapore Immunology Network, Agency for Science, Technology and Research, Biopolis, Singapore) and Dr. Nobuko Yoshida (Federal University of São Paulo, São Paulo, SP, Brazil), respectively. The blood stage forms of both parasites were stored in liquid nitrogen after *in vivo* passages in C57BL/6 mice according to the protocol described elsewhere [31]. Mice were infected intraperitoneally (i.p.) with 10^6 infected red blood cells (iRBC) and parasitemia and the neurological signs for CM were monitored daily.

Hyperbaric oxygen treatment

Groups of 8–10 PbA-infected mice were exposed daily to 100% oxygen at a pressure of 3.0 atmospheres (ATA) for 1 h per day in a hyperbaric animal research chamber (Research Chamber, model HB 1300B, Sechrist, USA) from day 0 to 10 post-infection (11-day exposure), or for 2 h from day 4–7 post-infection (4-day exposure). The chamber was pressurized and decompressed at a rate of 0.5 ATA/min as described elsewhere [32]. For the 11-day exposure protocol, mice were previously exposed to HBO for 1 h before PbA infection, whereas for the 4-day exposure protocol, PbA-infected mice were randomly selected and placed in the hyperbaric chamber. To determine the effect of 100% oxygen (hyperoxia), regardless of pressurization, PbA-infected mice were submitted to the 11-day exposure protocol, but at 1.0 ATA (normobaric) instead of 3.0 ATA. Infected mice in the control group (non-exposed) were left in an airy room. The temperature inside the hyperbaric chamber was 21°C, the same as in the room, and was measured with the aid of a high-pressure resistant thermometer (model TB-0261, Instrucamp, Brazil). For the direct HBO effect assays, normal red blood cells (nRBC) or iRBC were collected from a naïve mouse or a PbA-infected animal on day 6 post-infection (12% parasitemia), and then diluted in an RPMI 1640 medium (Sigma, USA) supplemented with 10% of fetal bovine serum (Hyclone, USA). One mL of nRBC or iRBC (10^7/mL) were plated in five replicates on a 24 well-plate and exposed to HBO (100% O_2, 3.0 ATA) in a hyperbaric chamber for up to 6 hours.

Parasitemia, temperature and red blood cell density assessment

The percentage of parasitemia was determined by counting the number of iRBC in at least 1,000 erythrocytes in Giemsa-stained blood smears. The mice's corporal temperature and the density of red blood cells (DRBC/mL$\times 10^9$) were evaluated daily, starting on day −1 post-infection (p.i.), by rectal introduction of a precision digital thermometer (model TE-300, Instrucamp, Brazil), and with the aid of a Neubauer chamber, respectively. In the *in vitro* assays, DRBC were counted from 0 hour. The percentage of RBC density relative to day −1 p.i. or to 0 hour was calculated with the following formula: [(DRBC per mL$\times 10^9$ of a determined day p.i. or hour/DRBC per mL$\times 10^9$ on day −1 p.i. or at 0 h)$\times$100].

Measuring cytokine gene expression in the brain

The expression of several cytokine genes was evaluated by real-time quantitative reserve transcription-PCR (RT-qPCR) in the brain of PbA-infected animals removed on day 7 p.i.. Mice brains were frozen with crushed liquid nitrogen placed in the Trizol™ reagent (Invitrogen, USA) according to the protocol described by the manufacturer. Shortly, after the addition of 1 mL of Trizol™ (Invitrogen, USA) in 40 mg of the brain powder, 0.2 mL of chloroform was added and the lysate was vigorously mixed. The sample was centrifuged at 12,000× g for 15 min and the aqueous phase was transferred to a new tube. The RNA was precipitated by adding 0.5 mL of isopropanol followed by a centrifugation at 12,000× g, then washed with 1 mL of 75% ethanol and resuspended in RNAse free water. RNA was then treated with Deoxyribonuclease I (Fermentas, Canada) in order to degrade contaminating genomic DNA. The cDNA was synthesized using approximately 2 µg of the total RNA with the aid of the High Capacity cDNA Reverse Transcription Kit (Applied Biosystems, USA) according to the protocol provided by the manufacturer. The polymerase chain reaction was performed with an ABI Prism 7500 (Applied Biosystems, USA) and the reactions were carried out in 25 µL volume and in the presence of the TaqMan PCR Master Mix™ (Applied Biosystems, USA) and different sets of oligonucleotides and probes for the amplification of the β-actin, IFN-γ, TNF-α, IL-1β, IL-6 and IL-10 genes. These corresponded (respectively) to the following reference numbers (Applied Biosystems, USA): Rn00667869_m1, Mm00443258_m1, Mm00443285_m1, Mm00434228_m1, Mm00446190_m1 and Mm00439616_m1. Expression levels of cytokine genes in PbA-infected animals were represented as a relative copy numbers by using the delta threshold cycle method ($2^{-\Delta Ct}$) [33].

Purification of brain-sequestered T cells (BST)

Adherent leukocytes were isolated from mice brains as described elsewhere [14]. Briefly, on day 7 p.i., PbA-infected mice were perfused intracardially with PBS to remove both circulating and non-adherent RBC and leukocytes. Brains were collected and crushed in an RPMI-1640 medium (Sigma, USA) supplemented with 10% fetal bovine serum (Hyclone, USA) and gentamycin. The cellular suspension was collected and centrifuged at 15,000× g for 5 min. The pellet was resuspended with 10 mL of an HEPES buffer (Sigma, USA) and supplemented with collagenase (Roche,

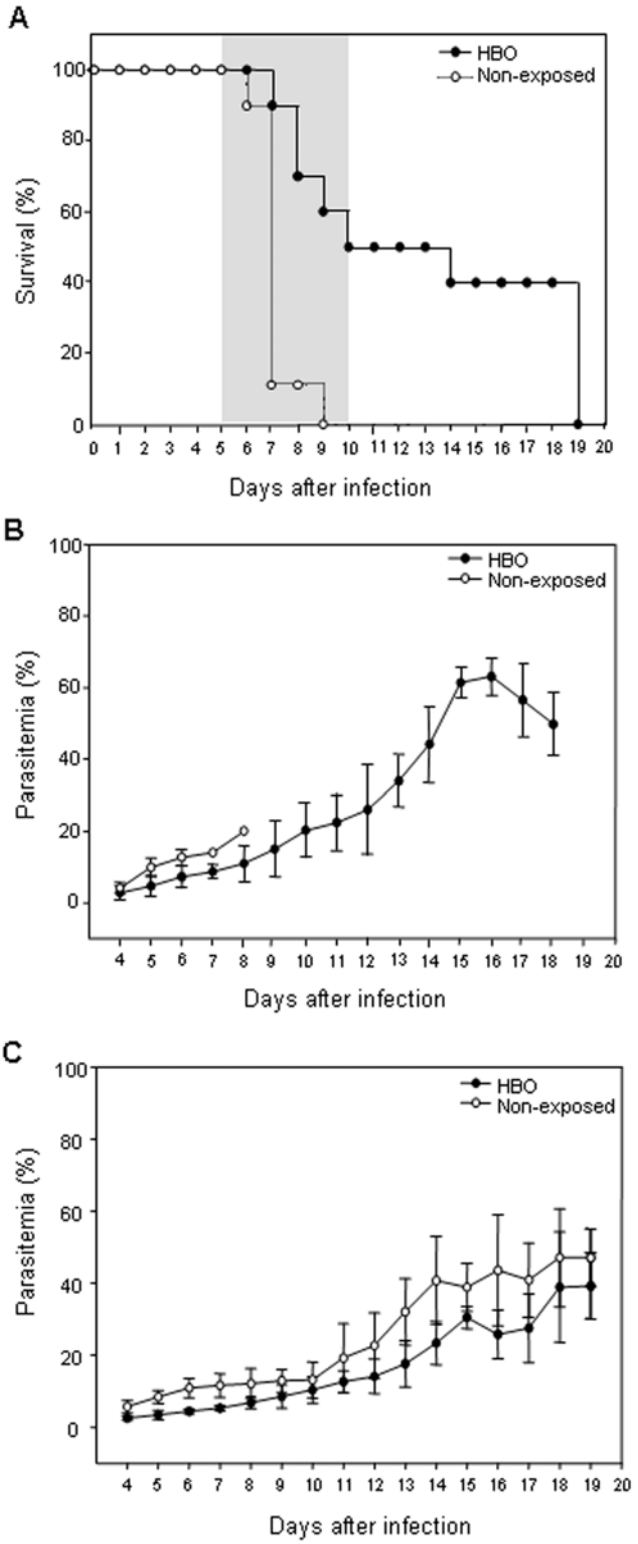

Figure 1. HBO's effect on the survival and the parasite development in *P. berghei*-infected mice. (**A**) Groups of 10 mice infected i.p. with 10^6 iRBC were exposed or not to HBO (100% O_2, 3.0 ATA) for 1 h from day 0 to 10. Pressurized oxygen significantly protected mice against CM neurological symptoms ($P<0.0005$). Neurological signs of CM appeared on days 5–10 with death occurring approximately 24 h after onset (shaded area). Parasitemia levels were assessed daily in mice infected with (**B**) *P. berghei* ANKA (PbA; cerebral line) or (**C**) *P. berghei* NK-65 (PbNK-65; non-cerebral line) regardless of exposure to HBO. HBO significantly ($P<0.05$) reduced the parasite burden on days 4–6 and 4–13 p.i., respectively in PbA- and PbNK-65-infected mice when compared to non-exposed animals.
doi:10.1371/journal.pone.0003126.g001

USA) and DNase I (Roche, Germany). The mixture was stirred at room temperature for 30 min. The tissue extract was passed through sterile gauze and centrifuged at 5,000× g for 30 s to remove debris. The supernatant was deposited on a 30% Percoll™ (GE Healthcare, Sweden) gradient and centrifuged at 3,000× g for 10 min. The pellet was collected and residual RBC were removed by an ACK lysis buffer. BST were resuspended in PBS containing 5% FBS and counted.

Immunolabeling and flow cytometry analysis of BST

Cells were stained with appropriate dilutions of the following fluorochrome-labeled monoclonal antibodies (mAbs): FITC/anti-CD4 (clone H129-19), FITC/anti-CD8 (clone 53-6.7), PE/anti-TCR γδ (clone GL3) and APC/anti TCR αβ (clone H57-597) and then washed with PBS, fixed and analyzed by flow cytometry in a FACSCanto™ device (Becton Dickinson, USA). All these reagents were purchased from Pharmingen/Becton-Dickinson (USA). Analyses were performed after recording 10,000 events for each sample using Diva™ software. BST were identified by their size (forward light scatter) and granulosity (side light scatter) as previously described [34].

Evaluating Blood-brain barrier dysfunction

Blood-brain barrier (BBB) integrity was assessed in PbA-infected mice on day 7 p.i. by i.v. injection of Evans Blue (1% in saline) in the retro-orbital plexus as previously described [35]. One hour after injection, mice brains were extracted and photographed using a digital camera (Nikon, USA). Brain staining was quantified by measuring the brightness intensity using the red channel in a delimited circular area of 12,294 pixels^2 with the aid of the ImageJ™ software (http://rsb.info.nih.gov/ij). The brightness intensity of mice brain was inversely proportional to the levels of Evans Blue staining.

Statistical analysis

The statistical significance between control and experimental groups were determined with the Log-Rank test for the cumulative survival experiments. The Mann-Whitney *U* test was used to compare parasitemia levels, the drop in relative temperature, the relative RBC density, BBB integrity and parasite and cytokine gene expression among brains collected from both naïve animals and infected mice. Calculations were performed using BioEstat™ version 3.0 (CNPq, Brazil) and Prism™ version 3.02 (Graphpad, USA) software. Values were considered significant when $P<0.05$.

Results

HBO effects on ECM associated mortality and on parasite development

To evaluate the neuroprotective effect of pressurized oxygen, two groups of 10 mice each were infected with PbA. One of these groups was submitted daily to HBO conditions (100% O_2, 3.0 ATA, 1 hour) during 11 consecutive days. As shown on Figure 1A, 100% of PbA-infected mice not exposed to HBO exhibited CM-specific neurological signs within 5 to 8 days after infection and died of fatal cerebral malaria in the following 24 hours; most (80%) died on day 7 p.i.. All animals from this group were dead by day 9 p.i.. In contrast to the non-exposed animals, 50% of the

mice from the HBO group did not develop CM symptoms and survived. In the HBO group, CM neurological signs began to appear later and the mortality rate increased slowly throughout days 7–10, representing 10, 20, 10 and 10%, respectively, on days 7–10. Of note, 1 animal (10%) died on day 14 and 4 (40%) on day 19 post-infection. Cumulative survival statistical analyses clearly demonstrated that HBO therapy had a significant ($P<0.0005$) neuroprotective effect against ECM. As expected, in the mice that did not develop CM, parasite burden progressed and mice died as a result of hyperparasitemia (Figure 1B).

As previously reported, HBO therapy inhibits the development of *Leishmania amazonensis* and of a non-cerebral line of *P. berghei* [30,32,36]. To further explore the effects of HBO, we monitored the parasitemia levels of infected mice exposed daily, or not, to HBO (11-day exposure protocol) for up to 19 days. We observed that HBO significantly ($P<0.05$) reduced the parasite burden of PbA-infected mice on days 4, 5 and 6 p.i., when compared to non-exposed animals (Figure 1B). However, since 100% of non-exposed PbA-infected mice died, we decided to evaluate whether the reduction on parasitemia levels in HBO exposed animals could be sustained over longer periods. Mice infected with *P. berghei* NK-65, a non-cerebral strain that displays similar parasitemia levels, were submitted to pressurized oxygen sessions as in the 11-day exposure protocol (Figure 1C). As observed in PbA-infected animals submitted to pressurized oxygen, a significant ($P<0.05$) decrease in PbNK-65 development was observed on day 4–13 p.i.. Nevertheless, no correlation was found between mice that presented a reduction of parasitemia levels with protection or attenuation of the neurological symptoms (Table S1).

Because we observed that HBO had a significant effect on the parasite burden in the infections of PbA and PbNK-65, we addressed the question as to whether pressurized oxygen therapy could damage normal red blood cells (nRBC) or inhibit parasite development directly. For this purpose, normal RBC (nRBC) collected from a naïve mouse were exposed to pressurized oxygen (100% O_2, 3 ATA) during 4 or 6 hours. The relative percentage of nRBC density was not significantly altered ($P>0.05$) after direct exposure to HBO for up to 6 hours (data not shown), demonstrating that HBO therapy was not toxic to healthy erythrocytes in these conditions. Next, to evaluate HBO's effect directly on parasite development, infected RBC (iRBC) from a PbA-infected mouse were collected and exposed to HBO (100% O_2, 3 ATA). Figure 2A shows a significant reduction ($P<0.05$) on parasite development after 4 and 6 hours in comparison to 0 hour, regardless of exposure to pressurized oxygen. However, when we compared the reduction on parasitemia levels of iRBC left in room air or exposed to HBO, we noticed a significant ($P=0.01$) and more pronounced reduction of the non-exposed iRBC than of the infected cells directly exposed to HBO up to 6 hours. Inhibition of parasite development was also observed after 4 hours of exposure; however, no statistical difference was found ($P>0.05$). Then, to assess whether these iRBC were still able to induce CM neurological signs, we collected 10^6 iRBC exposed directly to HBO or left outside the hyperbaric chamber for 6 hours and injected them in susceptible mice. As shown on Figure 2B, mice infected with iRBC directly exposed to HBO or with the cells left outside the chamber did not present significant differences ($P>0.05$) when the survival curves were compared. Taken together, these data suggest that 6 hours of HBO exposure do not directly affect PbA-infected erythrocytes nor alter their ability to induce CM clinical symptoms.

Next, to investigate whether pressurized oxygen could have an effect when parasitemia was already patent (4%), we randomly selected half of the PbA-infected mice on day 4 p.i. and exposed them to daily HBO sessions (100% O_2, 3.0 ATA, 2 hours per day) until day 7 (Figure 3A). As expected, non-treated mice started to display CM clinical features early on day 5 and 6 and began dying within 20–24 hours on days 5 (10%) and 6 (10%), though the majority (80%) died on day 7 p.i.. All mice were dead by day 7. Notably, hyperbaric oxygen significantly delayed ($P<0.01$) CM specific mortality by up to two days, when compared to non-exposed animals, and reduced the rate of mortality on day 7 from 80% to 40% (Figure 3A). Moreover, two HBO-exposed mice (20%) only exhibited CM neurological signs on days 8 and 9, dying within 24 hours on days 9 and 10. This shows that HBO is capable of interfering significantly with the manifestation of the CM clinical symptoms, including death, even when administrated after parasite establishment. As observed in the 11-day exposure protocol, the administration of pressurized oxygen starting on day 4 p.i. (4-day-exposure) in PbA-infected mice reduced the parasitemia levels ($P<0.01$) significantly on days 4–6 (data not shown).

To confirm that only pressurized oxygen had neuroprotective effects, PbA-infected mice were submitted to the 11-day exposure protocol, but using 1.0 ATA as the atmospheric air pressure (Figure 3B). In this assay, no significant difference ($P>0.05$) was observed after cumulative survival analyses between infected animals exposed to HBO-1.0 ATA and the control mice. Of note, most of the non-exposed mice began to present CM symptoms and died earlier than the HBO-1.0 ATA treated animals. Although a minimal beneficial effect was observed after the administration of 100% oxygen (hyperoxia) under normobaric conditions, this was not enough to protect or even delay CM neurological symptoms, thus demonstrating that HBO's neuroprotective effect does not rely solely on the administration of 100% oxygen.

The effect of HBO on cytokine expression levels and adherent T cells in the brain

Based on the anti-inflammatory features of the HBO treatment reported in ischemic models [21,26] and since the up-regulation of pro-inflammatory cytokines (IFN-γ, TNF-α and IL-1β) [10–12] and the participation of $CD4^+$ and $CD8^+$ T lymphocytes [14,37] is essential for CM pathology to occur, we examined the mRNA levels of different cytokines in the brain of PbA-infected mice scarified on day 7 p.i.. According to Figure 4, after RT-qPCR analysis the mRNA levels of IFN-γ ($P<0.05$), TNF-α ($P<0.01$) and IL-10 ($P<0.05$) significantly decreased in the brain of mice submitted to the 11-day exposure HBO protocol in comparison to non-exposed animals. No significant difference ($P>0.05$) was noted in the mRNA levels of IL-1β and IL-6. RT-negative controls did not generate a detectable amplification product. All cDNA samples resulted in a product when the β-actin set of oligonucleotides and specific probe were present. Regardless of exposure to HBO, animals that presented an increase in the expression of IFN-γ mRNA also presented elevated levels of TNF-α and IL-10.

Next, we asked whether the neuroprotective effect of the pressurized oxygen therapy could be associated to the percentage of $\gamma\delta$ and $\alpha\beta$ T lymphocytes sequestered in mice brains collected on day 7 p.i. (Figure 5). As compared with brains of non-exposed animals, HBO treatment reduced about 1.6 fold the percentage of both $\gamma\delta$ (1.9 vs. 1.2%) and $\alpha\beta$ (7.0 vs. 4.2%) $CD4^+$ T cells between the pools of mice of these two groups (Figure 5A–B). However, a more pronounced decline, about 2.5 fold, was observed on the percentage of both $\gamma\delta$ (7.1 vs. 2.8%) and $\alpha\beta$ (43.1 vs. 17.7%) $CD8^+$ T lymphocytes in the mice exposed to HBO in contrast to the non-exposed animals (Figure 5C–D). Taken together, our data demonstrate that HBO's neuroprotective effect is related to the reduction of the T cells sequestered in mice brains; and

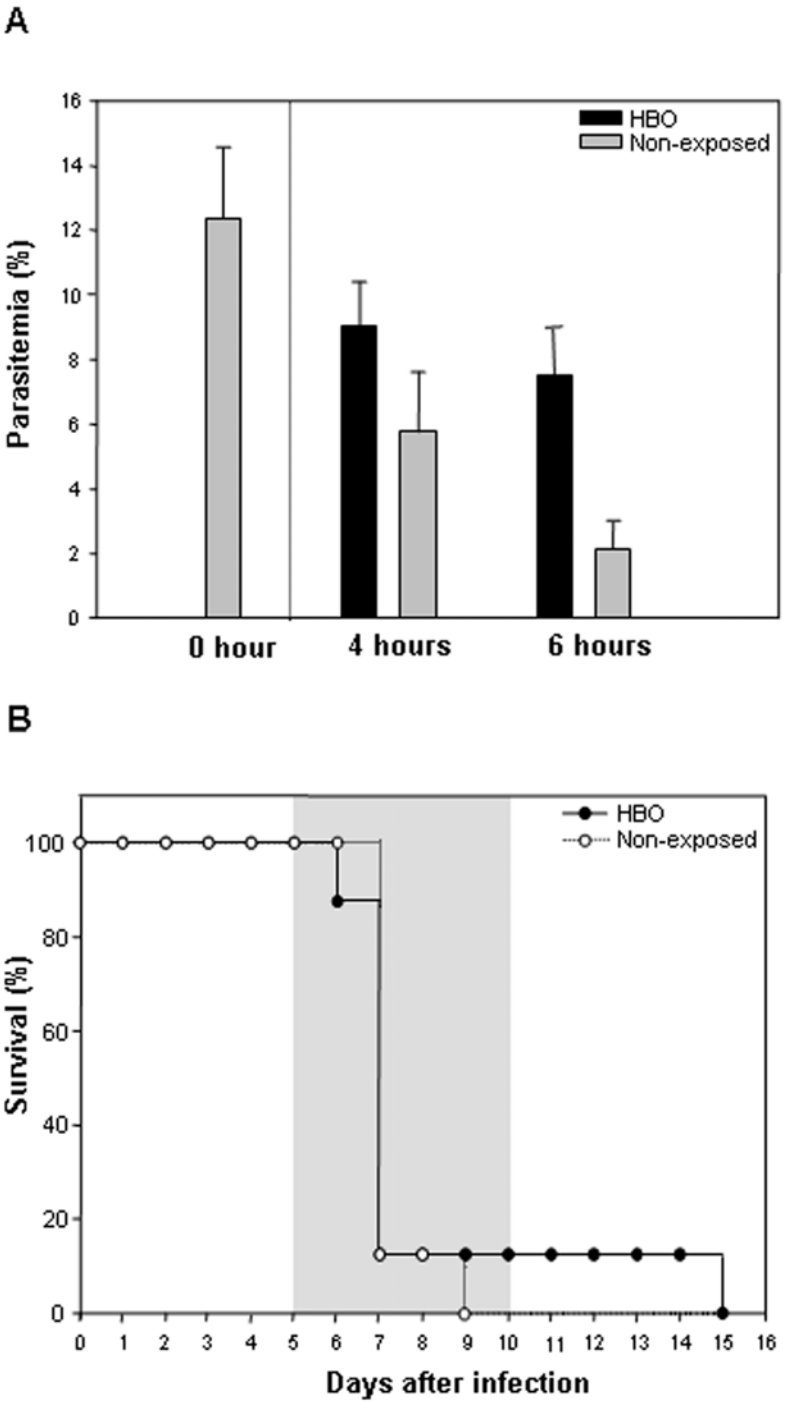

Figure 2. The direct effect of HBO therapy on RBC infected, or not, by PbA. 10^6 iRBC/mL of PbA in a 24-well-plate were directly exposed or not to HBO (100% O_2, 3 ATA). (**A**) Parasitemia levels were evaluated four or six hours after direct iRBC exposure to pressurized oxygen conditions. The parasite burden decreased significantly ($P<0.05$) after 4 or 6 hours in comparison to 0 hour. The reduction of parasitemia levels were more pronounced in infected cells left in normal room air than iRBC submitted directly to HBO after 4 ($P>0.05$) or 6 hour-exposure ($P=0.01$). Results are expressed as the mean of quadruplicates ± standard deviation. (**B**) Mice (n = 8 each group) were infected with 10^6 iRBC of PbA collected after either six hours of direct exposure or no exposure to HBO. No statistical difference was noted when survival curves were compared ($P>0.05$).
doi:10.1371/journal.pone.0003126.g002

corroborate with existing literature, in which T lymphocytes, mainly αβ $CD8^+$ T cells, are implicated in CM pathology [14,37] No immunolabeling was detected on T lymphocytes in the absence of mAbs (data not shown).

HBO effects on severe ECM symptoms

Severe hypothermia and dysfunction of the BBB are common features in ECM [35]. To investigate whether HBO therapy could improve poor ECM outcomes, we measured the corporal

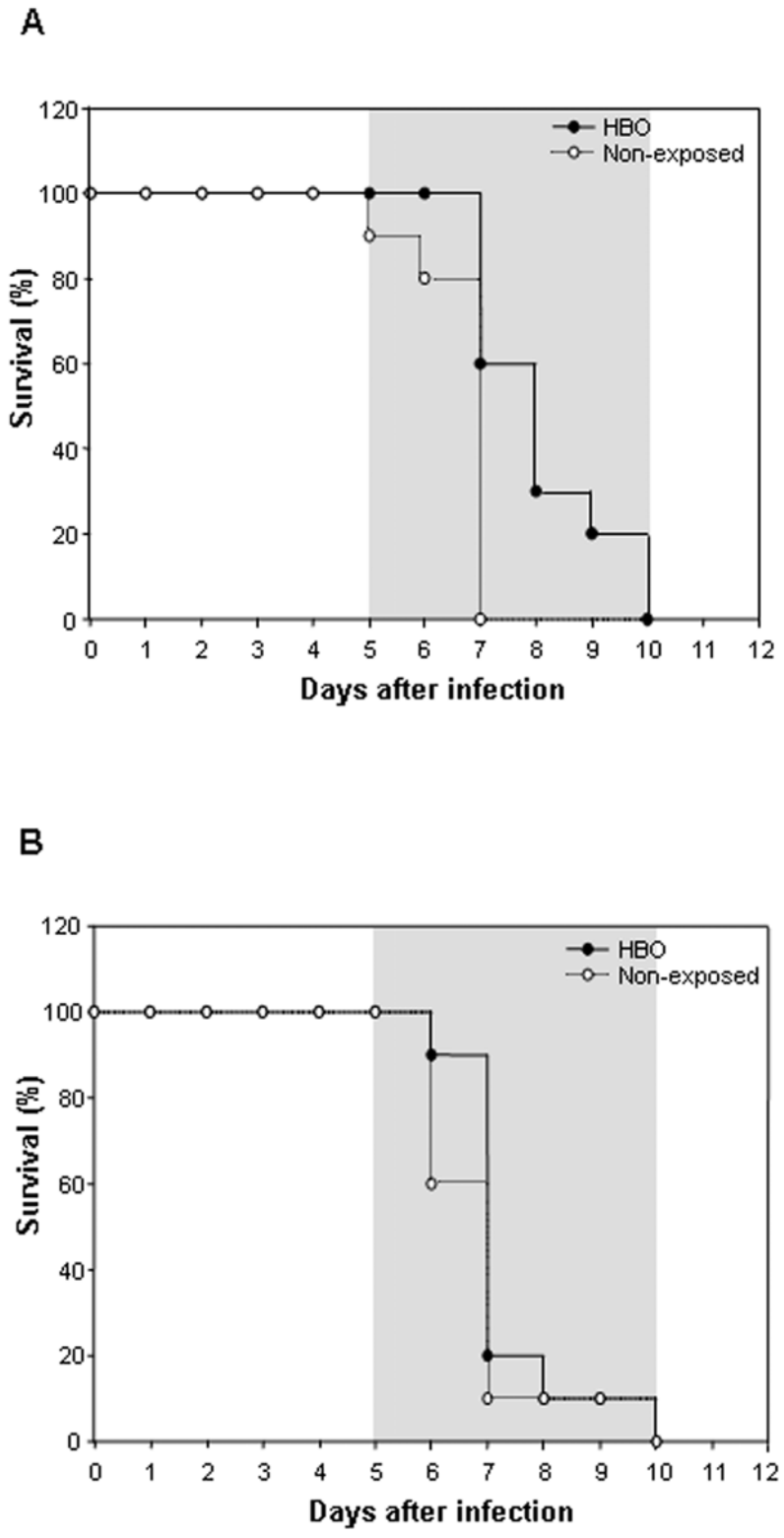

Figure 3. Evaluation of HBO's neuroprotective effect after parasite establishment and the role of pressure in mice survival. (**A**) Twenty mice were injected i.p. with 10^6 iRBC; on day 4 p.i. (parasitemia of 4%) 10 animals, randomly selected, were daily exposed to HBO therapy (100% O_2, 3.0 ATA) for 2 hours from days 4–7 after parasite inoculation. The survival curves of both groups demonstrated that HBO significantly delayed mice mortality ($P<0.01$). (**B**) Groups of 10 PbA-infected mice were exposed daily or not exposed to HBO (100% O_2, 1 hour per day) at 1.0 ATA until all the animals died. Survival curves of the one hundred percent normobaric oxygen exposed mice and animals exposed to normal air did not differ significantly ($P>0.05$).
doi:10.1371/journal.pone.0003126.g003

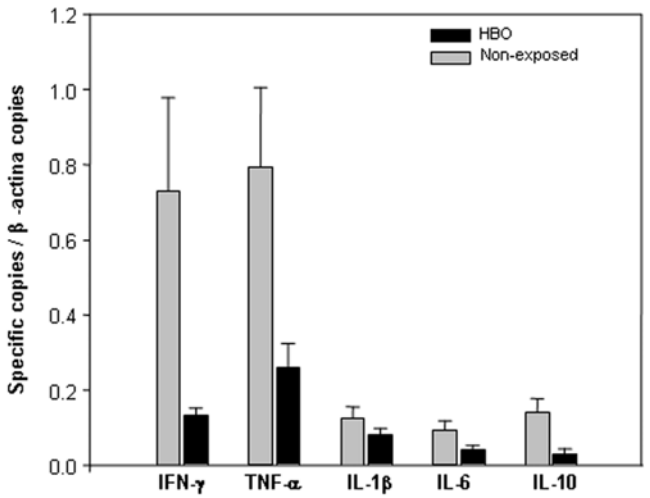

Figure 4. Cytokine gene expression is altered in the brains of PbA-infected mice exposed to HBO. Groups of 6–7 PbA-infected mice were either submitted or not to pressurized oxygen therapy (100% O_2, 3.0 ATA, 1 hour per day) and on day 7 p.i. brains were collected for real-time quantitative reserve transcription-PCR analysis. HBO significantly reduced IFN-γ ($P<0.05$), TNF-α ($P<0.01$) and IL-10 ($P<0.05$), but did not alter IL-1β and IL-6 mRNA expression levels in contrast to non-exposed mice. Values are expressed as the mean of specific cytokine genes copies relative to β–actin copies of six-seven mice±standard deviation.
doi:10.1371/journal.pone.0003126.g004

temperature of PbA-infected mice daily regardless of exposure to pressurized oxygen in the same conditions as the 11-day exposure protocol. Unlike in the case of non-exposed mice, HBO therapy significantly prevented ($P<0.001$) hypothermia in mice from day 6 p.i., when severe neurological signs were evident in most of the animals (data not shown). Then, by injecting Evans Blue solution, we analyzed and quantified the BBB integrity in HBO exposed and non-exposed animals and in naïve animals early on day 7 p.i.. One hour after Evans Blue injection, mice brains were collected and photographed. As seen in Figure 6A, brains collected from non-exposed mice were darker than those of HBO treated animals due to a high incorporation of Evans Blue in the brain tissue as a consequence of BBB destruction [26]. As expected, we did not observe any staining in naïve mice brains. To quantify the Evans Blue staining and, in turn the BBB integrity, we measured the light intensity in naïve animals and infected mice brains submitted or not to pressurized oxygen. According to Figure 6B, HBO therapy significantly reduced ($P<0.005$) the brain staining in treated mice. Moreover, when we compared the Evans Blue staining in naïve and PbA-infected animals that received HBO treatment, no significant difference was observed ($P>0.05$). As expected, a statistical difference in light intensity levels was observed between naïve mice and non-exposed infected animals ($P<0.005$). Collectively, these data clearly demonstrate that HBO prevents temperature drops and BBB dysfunction.

Discussion

In the present study, we show that HBO therapy (100% O_2, 3.0 ATA) is capable of partially protecting PbA-infected mice against CM and delaying CM-specific neurological signs (Figures 1 and 3). These observations demonstrate for the first time that pressurized oxygen therapy under hyperbaric conditions well-tolerated in humans and animals can prevent CM clinical outcomes, including death.

In an experimental rat model of brain trauma, recent studies have shown that HBO has a neuroprotective effect against focal cerebral ischemia, especially when initiated within the first 6 hours [38]. HBO was thus found to reduce BBB damage, prevent

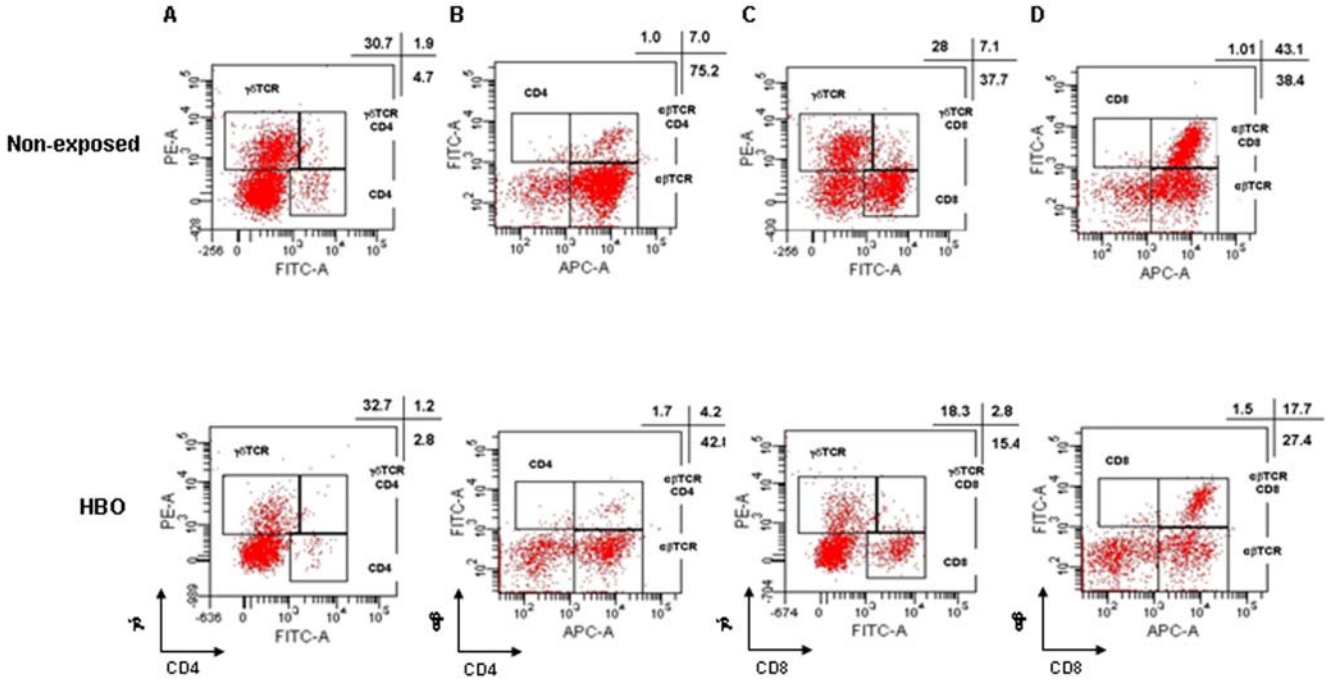

Figure 5. Reduced brain-sequestered T lymphocytes in PbA-infected mice exposed to HBO treatment. Flow cytometric analyses were done on γδ and αβ $CD4^+$ and $CD8^+$ T cells sequestered in mice brains (a pool of 4–5 mice per group) collected on day 7 after PbA infection between the groups regardless of exposure to HBO conditions. Pressurized oxygen therapy reduced the percentage of all cellular subsets, but mainly αβ $CD8^+$ T cells. Representative dot blots of (**A**) γδ and CD4, (**B**) αβ and CD4, (**C**) γδ and CD8, (**D**) αβ and CD8 double staining.
doi:10.1371/journal.pone.0003126.g005

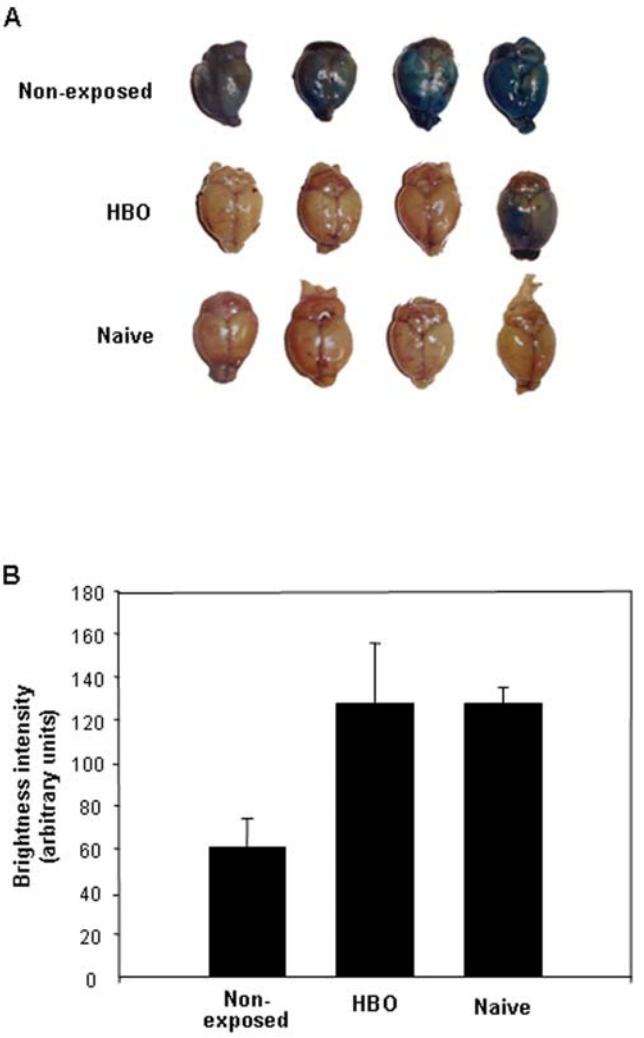

Figure 6. HBO preserves integrity of the blood-brain barrier in PbA-infected mice. Four PbA-infected mice, representative of each group (n = 8) exposed or not to HBO treatment (100% O_2, 3.0 ATA, 1 hour per day), received i.v. injections of 1% Evans Blue solution early on day 7 p.i.. **(A)** One hour after Evans Blue injection, brains of naïve animals, PbA-infected mice and HBO-treated PbA-infected mice were collected and photographed (n = 4 of each group). **(B)** The BBB dysfunction of naïve mice or PbA-infected animals, regardless of submission to hyperbaric conditions, was determined by brain staining quantification with the aid of the ImageJ™ software (n = 4 of each group). HBO significantly reduced ($P<0.005$) the staining in the brains of infected-mice in comparison to non-treated animals. No statistical difference ($P>0.05$) was noticed between naïve and HBO-treated infected mice and brains collected from non-treated infected mice were significantly ($P<0.005$) darker than naïve animals. Results are expressed as the mean of brightness intensity of each delimited brain area of six mice±standard deviation.
doi:10.1371/journal.pone.0003126.g006

apoptosis and maintain lipid oxidation levels stable [39–42]. HBO's neuroprotection was also observed in neonatal rats after the induction of the ischemic process [43]. Rabbits exposed to pressurized oxygen for 90 min during 3 consecutive days presented a significant reduction in the edema area of the brain and cerebral necrosis [44]. In addition, the preservation of BBB, the reduction in HIF-1α levels, and decreased apoptosis and neuronal damage were observed in a rat model for subarachnoid hemorrhage after exposure to HBO [45]. In humans, exposure of thirty-seven brain-injured patients to sixty minutes of HBO treatment every 24 hours increased the cerebral metabolic oxygen rate and reduced cerebrospinal lactate levels [46]. In another study, 10 out of 22 patients with cerebral infarction presented an amelioration of their motor function, while 7 of these patients experienced improved revascularization after pressurized oxygen sessions [47].

When comparing exposed animals with non-exposed animals, we noticed a significant reduction on the parasitemia levels of PbA-infected mice exposed to HBO (11-day exposure protocol) during infection (4–6 p.i.; Figure 1B). PbNK-65-infected mice exposed to HBO in the same conditions also presented a significant reduction of their parasite burden on day 4–13 p.i. (Figure 1C). These findings are in line with a recent study in which daily sessions of 100% pressurized oxygen at 2.5 ATA significantly reduced the size of *Leishmania amazonensis* induced lesions and the parasite development in infected mice [36]. Nevertheless, as in ECM parasites in the brain are necessary, but not sufficient, to neurological symptoms appearing [15], the lack of correlation between survival and the reduction of parasitemia levels, measured daily until the death of PbA-infected animals exposed to HBO, might be related to the fact that parasitemia levels probably do not determine the parasite load in the brain. Indeed, methods aimed at inducing protection against ECM often do not reduce parasitemia levels [48].

Also, direct exposure to HBO for up to 6 hours observed in our *in vitro* analyses was not harmful to normal or PbA-infected erythrocytes (data not shown and Figure 2), differing from previous studies where direct exposure of *L. amazonensis* promastigotes to HBO for up to 6 hours significantly decreased parasite viability [32]. However, as it is assumed that HBO increases the levels of reactive oxygen intermediates (ROI) [49], we believe that the disparity of these two protozoan parasites in terms of HBO susceptibility might be linked to differential killing mediated by reactive oxygen intermediates (ROI). In fact, it has been shown that *Leishmania* parasite killing is sensitive to ROI, whereas PbA-infected erythrocytes are resistant to killing by ROI, even at supraphysiological doses, and ROI are not essential for controlling *Plasmodium* sp. parasitemia [50–52].

We have also shown that the neuroprotective effects of daily hyperbaric sessions rely on the combination of hyperoxia and pressure at 3.0 ATA (Figure 1A), as ECM-specific mortality of PbA-infected mice submitted to 100% oxygen pressurized at 1.0 ATA did not differ significantly from the non-exposed animals (Figure 3B). In an experimental model for cerebral ischemia, HBO neuroprotection was not achieved in animals submitted to pure oxygen at only 1.0 ATA [39,40], and human stimulated monocyte-macrophages cultured in hyperoxia did not present changes in their cytokine expression levels [23]. More importantly, in a study of 12 CM comatose patients who breathed 95% oxygen, no improvement in the consciousness levels were observed in any of the individuals [7].

Brain macrophages from adults and children who died of CM had higher levels of immunological markers that are normally not upregulated [9], such as IFN-γ, IL-1β, IL-10 and TNF-α [10,11,16] neuroprotection in ECM is often associated with the reduction of IFN-γ, and TNF-α levels [53–55]. IL-10 is higher in severe malaria patients from different regions despite the fact that CM individuals presented lower levels of IL-10 in comparison to the non-cerebral malaria group [16,56] Furthermore, $CD8^+$ αβ T cells migrating to the brain have been implicated in cytotoxicity and BBB disruption, thus contributing to ECM mortality [14,15]. Here, we showed that HBO therapy reduced IFN-γ, TNF-α and IL-10 mRNA expression levels in the brain and the percentage of

brain-sequestered $CD4^+$ and $CD8^+$ γδ and αβ T lymphocytes (Figures 4–5). Moreover, the reduction in the IL-10 levels in PbA-infected mice exposed to HBO might be associated with the decrease in expression of IFN-γ and TNF-α. These data are in line with the fact that pressurized oxygen is able to inhibit synthesis of cytokines, such as TNF-α and IFN-γ, T lymphocyte proliferation, decrease the migration of immunocompetent cells and improve tissue transplantation by down-regulating lymphoid system functions [19,22,23,28,57,58].

Finally, when we assessed the HBO effects on cerebral outcomes, we noticed a significant reduction in hypothermia (data not shown) and in the BBB breakdown (Figure 6) in mice exposed to pressurized oxygen. This corroborates previous findings where HBO (100% O_2, 2.8–3.0 ATA) prevented BBB permeability and functionality in animals submitted to a brain injury [31,36]. Based on these observations, it is plausible to assume that HBO prevents BBB breakdown and then avoids vascular leakage by down-regulating the inflammatory immune response in ECM, but mainly, by reducing the percentage of brain-sequestered $CD8^+$ T lymphocytes [10]. Therefore, we cannot rule out that other mechanisms are also involved in HBO neuroprotective effects in ECM, as HBO also inhibits ICAM-1 expression and neuronal apoptosis and upregulates the expression of vascular endothelial growth factor (VEGF), which is involved in angiogenesis in human endothelial cells [22,23,25,28,59]. Also, HBO led to an increase in the brain levels of nitric oxide (NO) [60], a molecule that contributes to protection against ECM [61].

In summary, we have presented evidence of the beneficial effects induced by HBO therapy against ECM. We also demonstrated that the administration of pressurized oxygen down-regulates IFN-γ, TNF-α and IL-10 cytokine expression and the migration to the brain of T lymphocytes, preventing BBB breakdown and severe mice hypothermia without directly affecting iRBC viability and infectivity. Since complementary therapies such as steroids, sodium bicarbonate and heparin are deleterious in CM, and treatment with an anti-TNF-α monoclonal can worsen neurological symptoms [62]. The data presented here create promising perspectives for further investigation of additional HBO's neuroprotective mechanisms and to consider it as a new supportive therapy that could act alone or in association with conventional treatment or with recently discovered neuroprotective or anti-inflammatory molecules to improve poor CM outcomes [63,64].

Supporting Information

Table S1

Found at: doi:10.1371/journal.pone.0003126.s001 (0.01 MB PDF)

Acknowledgments

Many thanks to Dr. Lindsay Ann Pirrit for revising the English, to Dr. Laurent Renia for critical reading of the manuscript and to Dr. Lúcio H. Freitas-Junior for delightful discussions.

Author Contributions

Conceived and designed the experiments: YCB UG WWAS FTMC. Performed the experiments: YCB ASF UG SCPL BOC. Analyzed the data: YCB ASF UG SCPL WWAS RA GW LMBS SG FTMC. Contributed reagents/materials/analysis tools: RA GW LMBS SG FTMC. Wrote the paper: FTMC.

References

1. Carter JA, Ross AJ, Neville BG, Obiero E, Katana K, et al. (2005) Developmental impairments following severe falciparum malaria in children. Trop Med Int Health 10: 3–10.
2. Newton CRJC, Krishna S (1998) Severe Falciparum malaria in children: current understanding of pathophysiology and supportive treatment. Pharmacol Ther 79: 1–53.
3. Newton CR, Peshu N, Kendall B, Kirkham FJ, Sowunmi A, et al. (1994) Brain swelling and ischaemia in Kenyans with cerebral malaria. Arch Dis Child 70: 281–287.
4. Newton CR, Marsh K, Peshu N, Kirkham FJ (1996) Perturbations of cerebral hemodynamics in Kenyans with cerebral malaria. Pediatr Neurol 15: 41–49.
5. Pongponratn E, Riganti M, Punpoowong B, Aikawa M (1991) Microvascular sequestration of parasitized erythrocytes in human falciparum malaria: a pathological study. Am J Trop Med Hyg 44: 168–175.
6. White NJ, Warrell DA, Looareesuwan S, Chanthavanich P, Phillips RE, et al. (1985) Pathophysiological and prognostic significance of cerebrospinal-fluid lactate in cerebral malaria. Lancet 1: 776–778.
7. Warrell DA, White NJ, Veall N, Looareesuwan S, Chanthavanich P, et al. (1988) Cerebral anaerobic glycolysis and reduced cerebral oxygen transport in human cerebral malaria. Lancet 2: 534–538.
8. Patankar TF, Karnad DR, Shetty PG, Desai AP, Prasad SR (2002) Adult cerebral malaria: prognostic importance of imaging findings and correlation with postmortem findings. Radiology 224: 811–816.
9. Medana IM, Turner GD (2006) Human cerebral malaria and the blood-brain barrier. Int J Parasitol 36: 555–568.
10. Hunt NH, Grau GE (2003) Cytokines: accelerators and brakes in the pathogenesis of cerebral malaria. Trends Immunol 24: 491–499.
11. Taylor TE, Fu WJ, Carr RA, Whitten RO, Mueller JS, et al. (2004) Differentiating the pathologies of cerebral malaria by postmortem parasite counts. Nat Med 10: 143–145.
12. Rudin W, Favre N, Bordmann G, Ryffel B (1997) Interferon-γ is essential for the development of cerebral malaria. Eur J Immunol 27: 810–815.
13. Hermsen CC, Crommert JV, Fredix H, Sauerwein RW, Eling WM (1997) Circulating tumour necrosis factor alpha is not involved in the development of cerebral malaria in Plasmodium berghei-infected C57BL mice. Parasite Immunol 19: 571–577.
14. Belnoue E, Kayibanda M, Vigario AM, Deschemin JC, van Rooijen N, et al. (2002) On the pathogenic role of brain-sequestered αβ $CD8^+$ T cells in experimental cerebral malaria. J Immunol 169: 6369–6375.
15. Nitcheu J, Bonduelle O, Combadiere C, Tefit M, Seilhean D, et al. (2003) Perforin-dependent brain-infiltrating cytotoxic $CD8^+$ T lymphocytes mediate experimental cerebral malaria pathogenesis. J Immunol 170: 2221–2228.
16. Prakash D, Fesel C, Jain R, Cazenave PA, Mishra GC, et al. (2006) Clusters of cytokines determine malaria severity in Plasmodium falciparum-infected patients from endemic areas of Central India. J Infect Dis 194: 198–207.
17. Gudewicz TM, Mader JT, Davis CP (1987) Combined effects of hyperbaric oxygen and antifungal agents on the growth of Candida albicans. Aviat Space Environ Med 58: 673–678.
18. Park MK, Myers RA, Marzella L (1992) Oxygen tensions and infections: modulation of microbial growth, activity of antimicrobial agents, and immunologic responses. Clin Infect Dis 14: 720–740.
19. Kaide CG, Khandelwal S (2008) Hyperbaric oxygen: applications in infectious disease. Emerg Med Clin North Am 26: 571–595.
20. Al-Waili NS, Butler GJ (2006) Effects of hyperbaric oxygen on inflammatory response to wound and trauma: possible mechanism of action. The Scientific World Journal 6: 425–441.
21. Zhang Q, Chang Q, Cox RA, Gong X, Gould LJ (2008) Hyperbaric oxygen attenuates apoptosis and decreases inflammation in an ischemic wound model. J Invest Dermatol 128: 2102–2112.
22. Lahat N, Bitterman H, Yaniv N, Kinarty A, Bitterman N (1995) Exposure to hyperbaric oxygen induces tumour necrosis factor-alpha (TNF-α) secretion from rat macrophages. Clin Exp Immum 102: 655–659.
23. Benson RM, Minter LM, Osborne BA, Granowitz EV (2003) Hyperbaric oxygen inhibits stimulus-induced proinflammatory cytokine synthesis by human blood-derived monocyte-macrophages. Clin Exp Immunol 134: 57–62.
24. Yang ZJ, Bosco G, Montante A, Ou XI, Camporesi EM (2001) Hyperbaric O_2 reduces intestinal ischemia-reperfusion-induced TNF-α production and lung neutrophils sequestration. Eur J Appl Physiol 85: 96–103.
25. Buras JA, Stahl GL, Svoboda KK, Reenstra WR (2000) Hyperbaric oxygen downregulates ICAM-1 expression induced by hypoxia and hypoglycemia: the role of NOS. Am J Physiol Cell Physiol 278: 292–302.
26. Yin W, Badr AE, Mychaskiw G, Zhang JH (2002) Down regulation of COX-2 is involved in hyperbaric oxygen treatment in a rat transient focal cerebral ischemia model. Brain Res 926: 165–171.
27. Li Y, Zhou C, Calvert JW, Colohan AR, Zhang JH (2005) Multiple effects of hyperbaric oxygen on the expression of HIF-1 alpha and apoptotic genes in a global ischemia-hypotension rat model. Exp Neurol 191: 198–210.

28. Al-Waili N, Butler GJ, Beale J, Abdullah MS, Hamilton RWB, et al. (2005) Hyperbaric oxygen in treatment of patients with cerebral stroke, brain trauma, and neurological disease. Adv Therapy 22: 659–678.
29. Thackham JA, McElwain DL, Long RJ (2008) The use of hyperbaric oxygen therapy to treat chronic wounds: A review. Wound Repair Regen 16: 321–330.
30. Rencricca NJ, Coleman RM, Altschule MD, Faletra PP, Gray AD, et al. (1981) Quantification of hyperbaric oxygen-induced toxicity utilizing a malarial system. Aviat Space Environ Med 52: 85–87.
31. Engwerda C, Belnoue E, Grüner AC, Renia L (2005) Experimental models of cerebral malaria. Curr Top Microbiol Immunol 297: 103–143.
32. Arrais-Silva WW, Collhone MC, Ayres DC, de Souza Souto PC, Giorgio S (2005) Effects of hyperbaric oxygen on Leishmania amazonensis promastigotes and amastigotes. Parasitol Int 54: 1–7.
33. Overbergh L, Giulietti A, Valckx D, Decallonne R, Bouillon R, Mathieu C (2003) The use of real-time reverse transcriptase PCR for the quantification of cytokine gene expression. J Biomol Tech 14: 33–43.
34. Irani DN, Griffin DE (1991) Isolation of brain parenchymal lymphocytes for flow cytometric analysis. Application to acute viral encephalitis. J Immunol Methods 139: 223–231.
35. Piguet PF, Kan CD, Vesin C, Rochat A, Donati Y, et al. (2001) Role of CD40-CVD40L in mouse severe malaria. Am J Pathol 159: 733–742.
36. Arrais-Silva WW, Pinto EF, Rossi-Bergmann B, Giorgio S (2006) Hyperbaric oxygen therapy reduces the size of Leishmania amazonensis-induced soft tissue lesions in mice. Acta Trop 98: 130–136.
37. Renia L, Potter SM, Mauduit M, Rosa DS, Kayibanda M, et al. (2006) Pathogenic T cells in cerebral malaria. Int J Parasitol 36: 547–554.
38. Lou M, Eschenfelder CC, Herdegen T, Brecht S, Deuschl G (2004) Therapeutic window for use of hyperbaric oxygenation in focal transient ischemia in rats. Stroke 35: 578–583.
39. Veltkamp R, Siebing DA, Heiland S, Schoenffeldt-Varas P, Veltkamp C, et al. (2005a) Hyperbaric oxygen induces rapid protection against focal cerebral ischemia. Brain Res 1037: 134–138.
40. Veltkamp R, Siebing DA, Sun L, Heiland S, Bieber K, et al. (2005b) Hyperbaric oxygen reduces blood-brain barrier damage and edema after transient focal cerebral ischemia. Stroke 36: 1679–1683.
41. Schabitz WR, Schade H, Heiland S, Kollmar R, Bardutzky J, et al. (2004) Neuroprotection by hyperbaric oxygenation after experimental focal cerebral ischemia monitored by MRI. Stroke 35: 1175–1179.
42. Yin D, Zhou C, Kusaka I, Calvert JW, Parent AD, et al. (2003) Inhibition of apoptosis by hyperbaric oxygen in a rat focal cerebral ischemic model. J Cereb Blood Flow Metab 23: 855–864.
43. Calvert JW, Yin W, Patel M, Badr A, Mychaskiw G, et al. (2002) Hyperbaric oxygenation prevented brain injury induced by hypoxia-ischemia in a neonatal rat model. Brain Res 951: 1–8.
44. Niklas A, Brock D, Schober R, Schulz A, Schneider D (2004) Continuous measurements of cerebral tissue oxygen pressure during hyperbaric oxygenation-HBO effects on brain edema and necrosis after severe brain trauma in rabbits. J Neurol Sci 219: 77–82.
45. Ostrowski RP, Colohan ART, Zhang JH (2005) Mechanisms of therapeutic of oxygen-induces neuroprotection in a rat model of subarachnoid hemorrhage. J Cereb Blood Flow Metab 25: 554–571.
46. Rockswold SB, Rockswold GL, Vargo JM, Erickson CA, Sutton RL, et al. (2001) Effects of hyperbaric oxygenation therapy on cerebral metabolism and intracranial pressure in severely brain injured patients. J Neurosurg 94: 403–411.
47. Kapp JP (1981) Neurological response to hyperbaric oxygen a criterion for cerebral revascularization. Surg Neurol 15: 43–46.
48. Jennings VM, Lal AA, Hunter RL (1998) Evidence for multiple pathologic and protective mechanisms of murine cerebral malaria. Infect Immun 66: 5972–5979.
49. Hink J, Jansen E (2001) Are superoxide and/or hydrogen peroxide responsible for some of the beneficial effects of hyperbaric oxygen therapy? Med Hypotheses 57: 764–769.
50. Reiner SL, Zheng S, Wang ZE, Stowring L, Locksley RM (1994) Leishmania promastigotes evade interleukin 12 (IL-12) induction by macrophages and stimulate a broad range of cytokines from CD4+ T cells during initiation of infection. J Exp Med 179: 447–456.
51. Sobolewski P, Gramaglia I, Frangos JA, Intaglietta M, van der Heyde H (2005) Plasmodium berghei resists killing by reactive oxygen species. Infect Immun 73: 6704–6710.
52. Gillman BM, Batchelder J, Flaherty P, Weidanz WP (2004) Suppression of Plasmodium chabaudi parasitemia is independent of the action of reactive oxygen intermediates and/or nitric oxide. Infect Immun 72: 6359–6366.
53. Medana IM, Hunt NH, Chaudhri G (1997) Tumor necrosis factor-alpha expression in the brain during fatal murine cerebral malaria: evidence for production by microglia and astrocytes. Am J Pathol 150: 1473–1486.
54. De Kossodo S, Grau GE (1993) Profiles of cytokine production in relation with susceptibility to cerebral malaria. J Immunol 151: 4811–4820.
55. Jennings VM, Actor JK, Lal AA, Hunter RL (1997) Cytokine profile suggesting that murine cerebral malaria is an encephalitis. Infect Immun 65: 4883–4887.
56. Day NP, Hien TT, Schollaardt T, Loc PP, Chuong LV, et al. (1999) The prognostic and pathophysiologic role of pro- and antiinflammatory cytokines in severe malaria. J Infect Dis 180: 1288–1297.
57. Gadd MA, McClellan DS, Neuman TS, Hansbrough JF (1990) Effect of hyperbaric oxygen on murine neutrophil and T-lymphocyte functions. Crit Care Med 18: 974–979.
58. Granowitz EV, Skulsky EJ, Benson RM, Wright J, Garb JL, et al. (2002) Exposure to increased pressure or hyperbaric oxygen suppresses interferon-gamma secretion in whole blood cultures of healthy humans. Undersea Hyperb Med 29: 216–225.
59. Lee CC, Chen SC, Tsai SC, Wang BW, Liu YC, et al. (2006) Hyperbaric oxygen induces VEGF expression through ERK, JNK and c-Jun/AP-1 activation in human umbilical vein endothelial cells. J Biomed Sci 13: 143–156.
60. Ohgami Y, Chung E, Shirachi DY, Quock RM (2008) The effect of hyperbaric oxygen on regional brain and spinal cord levels of nitric oxide metabolites in rat. Brain Res Bull 75: 668–73.
61. Gramaglia I, Sobolewski P, Meays D, Contreras R, Nolan JP, et al. (2006) Low nitric oxide bioavailability contributes to the genesis of experimental cerebral malaria. Nat Med 12: 1417–1422.
62. Idro R, Jenkins NE, Newton CRJ (2005) Pathogenesis, clinical features, and neurological outcomes of cerebral malaria. The Lancet 4: 827–840.
63. Kaiser K, Texier A, Ferrandiz J, Buguet A, Meiller A, et al. (2006) Recombinant human erythropoietin prevents the death of mice during cerebral malaria. J Infect Dis 193: 987–995.
64. Wassmer SC, Cianciolo GJ, Combes V, Grau GE (2005) Inhibition of endothelial activation: a new way to treat cerebral malaria? PloS Med 2: 245e.

Cellular Immunology 253 (2008) 1–4

Contents lists available at ScienceDirect

Cellular Immunology

journal homepage: www.elsevier.com/locate/ycimm

Rapid Communication

Thymic alterations in *Plasmodium berghei*-infected mice

C.F. Andrade [a,1], J. Gameiro [a,1], P.R.A. Nagib [a,1], B.O. Carvalho [b], R.L. Talaisys [b], F.T.M. Costa [b], L. Verinaud [a,*]

[a] Department of Microbiology and Immunology, Biology Institute, State University of Campinas, Campinas, São Paulo, Brazil
[b] Department of Parasitology, Biology Institute, State University of Campinas, Campinas, São Paulo, Brazil

ARTICLE INFO

Article history:
Received 9 April 2008
Accepted 4 June 2008
Available online 16 July 2008

Keywords:
Plasmodium berghei
Thymus
Thymic atrophy
T-cell generation

ABSTRACT

The primary function of the thymus is to develop immature T-cells into cells that further in the periphery will be able to carry out immune functions. The Literature has shown that thymus can be a target for many pathogens and severe structural alterations take place in this organ during infectious diseases. Here, we investigated if thymus is also a target organ during experimental malaria infection by analyzing the presence of parasites inside the organ and histological alterations in thymuses from *Plasmodium berghei* NK65-infected BALB/c. After 14 days of infection, parasites were found inside the thymus that presented a profound atrophy with total loss of its architecture. We propose that the presence of parasites in the thymus induces histological modifications that alter the microenvironment, impairing by consequence the successful T cell development. Additional studies are currently being developed in our laboratory to verify if such thymic alterations can influence the systemic immune response to the parasite.

1. Introduction

The complex molecular structure of *Plasmodium* sp., the etiological agent of malaria, stimulates multifaceted immune responses, including antibodies, NK and NKT cells, $CD4^+$ and $CD8^+$ T cells [1]. However, the precise mechanisms responsible for host protective immunity against the parasite have not been fully elucidated. Some experimental models have demonstrated that T cells play a major role in protection against *Plasmodium*. According to the literature, $CD4^+$ T cells stimulate $CD8^+$ T cell cytotoxic activity, inhibiting the development of liver stages and preventing the infection of red blood cells [2,3]. In a murine model of *Plasmodium berghei* NK 65 infection, the initial innate response to the intraerythrocytic stages of malaria parasites engages $CD4^+$ Th_1 cells illustrated by detection of serum IgG and IFNγ producing $CD4^+$ T cells [4].

Mature T cells are generated from marrow-derived T lymphocyte precursors that differentiate and maturate in the thymus through a complex process characterized by lymphocyte (or thymocytes while in the thymus) migration throughout the thymic microenvironment. Alongside the thymocytes, at different stages of maturation, the thymic microenvironment is formed by epithelial cells, which form a meshwork to provide mechanical support and stimuli for the proliferation and development of thymocytes and by macrophages, dendritic cells, fibroblasts and matrix molecules that provide mechanical support and molecular stimuli for complete T cell development [5,6].

It has been demonstrated that several pathogens, such as *Trypanosoma cruzi* [7,8], Human Immunodeficiency Virus [9,10] and *Paracoccidioides brasiliensis* [11,12], are able to invade the thymus causing severe atrophy and deep disorganization of thymic architecture [13]. Recently, Seixas et al. (2005) [14] have also observed thymic alterations in mice treated with non-lethal malaria model of *Plasmodium chabaudi*. In this paper, we reported thymic atrophy and histological alterations by using lethal murine malaria model of *P. berghei*. Besides, we demonstrate for the first time the presence of parasites inside thymus. We conjecture that such events may influence the process of intrathymic T cell differentiation impairing the normal development of T cells and, most probably, the peripheral immune response to the parasite.

2. Materials and methods

2.1. Animals

Specific pathogen-free BALB/c male mice, 5-week-old, were purchased from CEMIB/UNICAMP (Campinas, São Paulo, Brazil) and housed in microisolator cages with free access to water and food. All protocols were performed in accordance with the guidelines of the State University of Campinas Committee on the Use and Care of Animals.

* Corresponding author. Address: Departamento de Microbiologia e Imunologia–UNICAMP, Cidade Universitária Zeferino, Vaz s/n., CEP: 13084-970 Campinas–São Paulo, Brazil.
E-mail address: verinaud@unicamp.br (L. Verinaud).
[1] These authors contributed equally to this work.

0008-8749/$ - see front matter © 2008 Elsevier Inc. All rights reserved.
doi:10.1016/j.cellimm.2008.06.001

2.2. Infection of mice

Nine groups of five animals each were intraperitoneally infected with 5×10^6 parasitized red blood cells obtained from a source mouse or with saline (control group). Parasitemia was assessed daily by counting the number of infected erythrocytes in Giemsa-stained thin blood films. At days 3, 7 and 14 following infection, three groups of mice were sacrificed and their thymuses collected and analyzed by histological methods, Polymerase Chain Reaction (PCR) and Transmission Electron Microscopy (TEM).

2.3. Thymic index

The gross weight of each mouse was recorded on 3, 7 and 14 days of infection. The mice were then sacrificed and the thymus glands were collected and weighed. The thymic index was calculated as: organ weight (g)/body weight (g) × 100.

2.4. Histological analysis

For microscopic histological evaluation, thymuses were collected and fixed in a solution 2% paraformaldehyde for 12 h at room temperature. The specimens were submitted to diafanization with xylene, dehydrated by graded ethanol, embedded in paraffin and cut in 5-μm-thick sections. Histologic changes were evaluated on sections stained with hematoxylin and eosin (H&E).

2.5. Polymerase chain reaction

Detection of parasites inside thymus was assessed by PCR method. Briefly, thymuses were perfunded with ACK via the heart to prevent erythrocyte contamination and teased apart in 1 ml of digestion buffer with proteinase K for DNA extraction. DNA was purified by phenol/chloroform and precipitated in 100% ethanol and sodium acetate and then washed in 70% ethanol and resuspended in water. The control of PCR amplification was performed using oligonucleotides based on the sequence of the mouse β-actin gene (sense: BA1 5′-ATGGATGACGATATCGCT-3′ and the anti-sense: BA2 5′-ATGAGGTAGTCTGTCAGGT-3′). For PCR reaction based on the malaria ribosomal RNA gene, the following oligonucleotides were utilized as template: sense rPLU3 5′-TTTTTATAAGGATACGGAAAAGCTGT-3′ and anti-sense rPLU4 5′-TACCCGTCATAGCCATGTTAGGCCAATACC-3′ [15]. DNA amplification was made by technique of thermal denaturation with one cycle of 5 min at 94 °C, followed by 45 cycles of 1 min at 94 °C, 1 min 30 s at 63 °C and 1 min 30 s at 72 °C. PCR products were analyzed in a 2% agarose gel.

2.6. Transmission electron microscopy

For TEM studies, animals were perfunded via the heart with ACK and fixative solution containing glutaraldehyde and paraformaldehyde. Then, thymuses were collected, fixed by the same fixative solution, post fixed in 1% osmium tetroxide and embedded in resin (Epon 812). Ultrathin sections were double stained in uranyl acetate and lead citrate and examined in a LEO 906 transmission electron microscope (Zeiss, Oberkochen, Germany) operated at 60 kV.

2.7. Cytofluorometry

Thymuses were removed from infected (14 days of infection) and control animals. They were minced, washed and resuspended in PBS–FBS 5% for subsequent cellularity evaluation, which was followed by triple immunofluorescence staining. Appropriate dilutions of the following fluorochrome-labeled monoclonal antibodies (mAbs) were used: FITC/anti-CD4 (clone GK1.5), Alexa Fluor 647/anti-CD8 (clone 53–6.7) and PeCy-7/anti-CD3 (clone 145-2C11). These reagents were purchased from Pharmingen/Becton–Dickinson (South San Francisco, CA, USA). Fluorochrome-labeled isotype-matched negative controls for the specific mAbs were also Pharmingen products. Cells were staining for 20 min and then washed with PBS, fixed and analyzed by flow cytometry in a FACSaria® device (Becton Dickinson, San Jose, CA, USA) equipped with Diva software. Analyses were done after recording 10,000 events for each sample using FCS Express V3 software. Lymphocytes were gated based on forward and side scatter parameters, so as to avoid larger leukocytes such as macrophages and granulocytes.

2.8. Statistical analysis

Statistical evaluation of the results between control and infected mice was carried out by unpaired *t* test (GraphPad Prism 4.0 software). Results are presented as mean ± SE and *p* values equal or lower than 0.05 were considered significant.

3. Results

All mice infected with lethal murine malaria *P. berghei* NK65 developed high levels of parasitemia, which peaked on day 14 after parasite inoculation and 100% mortality until 15 days after infection (data not shown).

Severe thymic atrophy, with pronounced fall of thymus weight, was observed from 7 days of infection. This atrophy was progressive and reached its maximum value at 14 days post-infection, coinciding with the parasitemia peak. Before 3 days of infection, no thymic alterations could be detected (Fig. 1).

Atrophy was accompanied by histological alterations in thymus architecture with total loss of cortical-medullar delimitation at 14 days post-infection when compared to the control mice and/or to the infected mice on day 3 after infection (Fig. 2A–C). Furthermore, changes in the histological pattern of thymus were detected at 14 days after infection when higher atrophy levels were detected.

In order to investigate if histological alterations were associated with the presence of parasites inside the thymus, we have proceeded with transmission electron microscopy and PCR methods. Analysis of thymus by TEM has suggested the presence of parasites

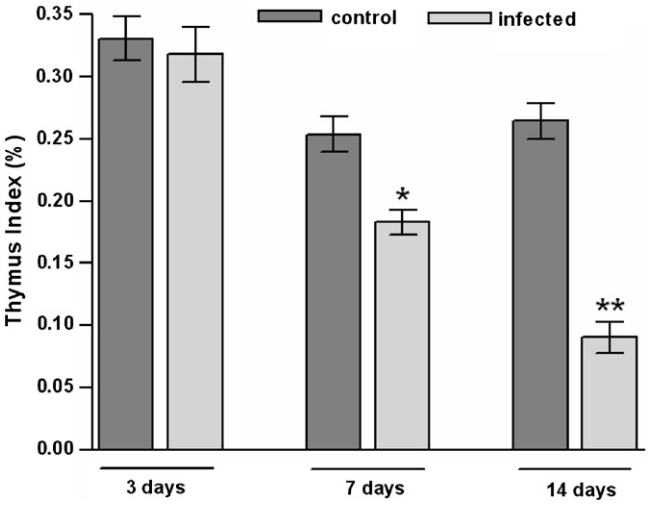

Fig. 1. Changes in thymus weight in *Plasmodium berghei*-infected BALB/c mice. Significant differences between control and infected mice were only observed on days 7 and 14 p.i., although such differences were more prominent at day 14 after infection. Asterisks indicate a statistically significant difference at $^{*}p < 0.05$ and $^{**}p < 0.001$. Results are representative of three similar experiments.

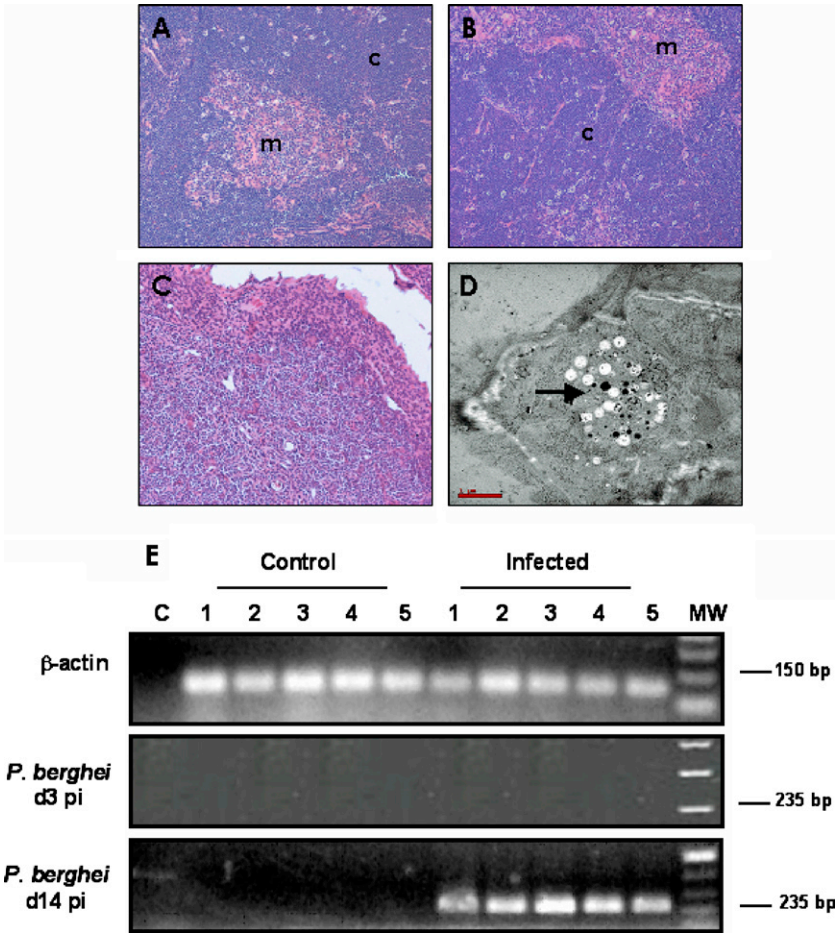

Fig. 2. (A–C) Histopathological analysis. Thymus from control mice and infected mice at 3 days post-infection showing preserved delimitation between cortical (c) and medullary zones (m) (A and B). Thymus from *Plasmodium berghei*-infected mice presenting total loss of corticalmedullary delimitation after 14 days p.i. (C). (D) Transmission Electron Microscopy. Thymus from *Plasmodium berghei*-infected mice showing evidences for the presence of haemozoin pigments (arrow) inside macrophage on day 14 p.i. (E) DNA amplification by Polymerase-Chain Reaction. No specific PCR products were detected in control mice or infected mice on day 3 after infection. Specific PCR products were detected at 14 days of infection in thymus from *Plasmodium berghei*-infected mice. All results are representative of three similar experiments.

in the organ based on the observation of *Plasmodium* hemozoin inside thymic macrophages (Fig. 2D). Amplification of *Plasmodium* parasite DNA fragments in thymus from experimental mice has confirmed this hypothesis. No specific PCR products could be detected in the thymus of control mice or infected mice at 3 days of infection. On the other hand, specific PCR products were only detected in thymus from *P. berghei*-infected animals on day 7 (data not shown) and at 14 days post-infection (Fig. 2E).

Next, cytofluorometry analysis of CD4 and CD8 expression on thymocytes was conducted. As expected, thymocytes from uninfected mice were mostly immature and cortical $CD4^+CD8^+$ cells. Around the day of peak parasitemia, infected mice showed low numbers of double negative ($CD4^-CD8^-$), double positive ($CD4^+CD8^+$) and single positive cell subsets ($CD4^+CD8^-$; $CD4^-CD8^+$). Somewhat impressing, immature $CD4^+CD8^+$ thymocyte subpopulation decreased sharply (about 50 times) in infected mice when compared to the control ones. Representative results obtained with thymic cells from control and infected mice are depicted in Fig. 3.

4. Discussion

Thymus is the central lymphoid organ that plays an important role in cellular immunity by generating circulating T lymphocytes. Although its function declines with age, the thymus remains indispensable to T-cell-repertoire reconstitution, which ensures immune reactions in various situations until late adulthood [16,17]. The T-cell development process in the thymus requires a complex structural organization formed by non-lymphoid cells and elements of extracellular matrix that provide a favorable microenvironment to interactions that are essential for the evolution of lymphocytes in different stages of maturation [18,19]. Thus, it is reasonable to suppose that insults to this organ can threaten its function since T-cell generation depends on the structural maintenance of its compartments, i.e., cortex, sub capsular cortex zone, cortico-medullary junction and thymic medulla.

It has long been known that the thymus is vulnerable to several infectious diseases [7–13]. Here, we demonstrated that murine malaria lethal strain *P. berghei* NK65 infection is also able to trigger severe thymic alterations. *Plasmodium berghei* NK65 infection in BALB/c mice induces high parasitemia and 100% lethality without the development of cerebral malaria [20]. Now, our results using this experimental model show a decrease in the total number of thymic cells observed from data of thymic index and total loss of delimitation among cortical and medullary zones. These findings suggest that the normal thymocytes maturation may be severely impaired given that the successful development of these cells into mature T cells depends on their ordered and constant migration through an organized thymic microenvironment. Similar results, i.e., thymic atrophy and histological disorganization with alteration of thymocyte migration, were already shown in experimental infections by *T. cruzi* [7,8] and *P. brasiliensis* [11,12]. The causes of thymic atrophy were not available here, however, accumulating

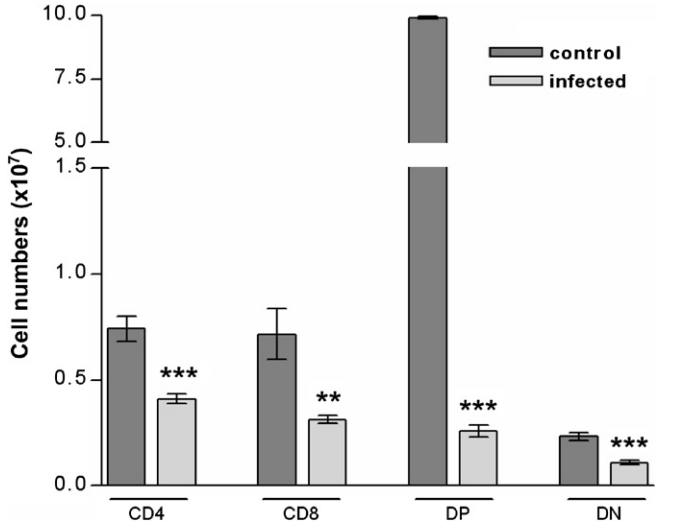

Fig. 3. Thymocytes subset variation in the thymus of control and *Plasmodium berghei*-infected mice. The figure shows absolute numbers of single-positive ($CD4^+CD8^-$ or $CD4^-CD8^+$) cells, double positive (DP/$CD4^+CD8^+$) and double negative (DN/$CD4^-CD8^-$) cells per group. Values expressed by mean ± S.E.; $n = 10–12$ animals per group, with infected animals being sacrificed on day 14 post-infection. $^{**}P < 0.001$ and $^{***}P < 0.0001$.

evidences from the literature have indicated that among them are apoptosis and precocious migration of immature thymocytes to the periphery [13]. Amplification of parasite-specific DNA in the peak of parasitemia (14th day post-infection) argues strongly in favor of the direct participation of *Plasmodium* in such thymic alterations, since it unequivocally demonstrates the presence of parasites inside the thymus. These data were obtained even when the organ was perfunded with hypotonic solution to exclude the possibility of contamination by cytoadherence of parasitized erythrocytes to microvascular endothelium, a common phenomenon observed in mature stages of *Plasmodium*-parasitized erythrocytes. Moreover, thymic atrophy could not be observed in the beginning of infection (3rd day post-infection); it was only noted 7 days after infection coinciding with the time when parasites were detected inside the thymus. It is important to highlight that the sequence utilized as primer for detection of the *Plasmodium* DNA only amplifies the genetic material of viable parasites [15], reinforcing our hypothesis of direct participation of the pathogen in thymic alterations.

We have also observed changes in thymocyte subsets that, most probably, are related to the structural thymic alterations reported here after *Plasmodium* infection since maintenance of thymus microenvironment is essential for T cell maturation. It is reasonable to suppose that both the presence of parasites inside the thymus and the histological alterations, with a severe depletion of thymocyte absolute numbers mainly in very immature DP cells, lead to functional alterations in this primary lymphoid organ. Alterations in thymus compartment and thymocyte subpopulations with changes in the peripheral T cell repertoire were already reported during *T. cruzi* infection [8]. We believe that alterations in secondary lymphoid organs are also present in our infection model and new experiments are being conducted to investigate such possibility. In any way, results presented here showing that the thymus is a target during *P. berghei* NK65 infection strongly suggest an important role for the organ in the immune response to malaria.

To the best of our knowledge, data presented here show for the first time a correlation between the presence of malaria parasites inside the thymus and parasitism with significant atrophy and histological alterations of this lymphoid organ. A fundamental question that remains open is whether such thymic insults during malaria infection are relevant for the peripheral immune response. We believe that future studies, from this and other laboratories, could elucidate the functional consequences of thymic alterations during *P. berghei* infection, opening up new possibilities for the understanding of immune response during malaria infections.

Acknowledgments

We thank Dr. Nobuko Yoshida from Department of Microbiology, Immunology and Parasitology, UNIFESP, São Paulo, SP, Brazil who kindly provided *P. berghei* NK65 parasites. This work was supported by grants from Fundação de Amparo à Pesquisa do Estado de São Paulo (#05/59774-9 & 04/03599-1) and Conselho Nacional de Desenvolvimento Científicoe Tecnológico (CNPq).

References

[1] M. Tsuji, F. Zavala, T cells as mediators of protective immunity against liver stages of *Plasmodium*, Trends Parasitol. 19 (2003) 88–93.
[2] L. Schofield, G.E. Grau, Immunological processes in malaria pathogenesis, Nat. Rev. Immunol. 5 (2005) 722–734.
[3] A. Morrot, F. Zavala, Regulation of the $CD8^+$ T cell response against *Plasmodium* liver stages in mice, Int. J. Parasitol. 34 (2004) 1529–1534.
[4] T.T.A. Long, S. Nakazawa, S. Onizuka, M.C. Huaman, H. Kanbara, Influence of $CD4^+$ $CD25^+$ T cells on *Plasmodium berghei* NK65 infection in BALB/c mice, Int. J. Parasitol. 33 (2003) 175–183.
[5] S. Suster, J. Rosai, Thymus, in: S.S. Sternberg (Ed.), Histology for Pathologists, Lippincott–Raven Publishers, Philadelphia, 1997, pp. 687–706.
[6] B.D. Jamieson, D.C. Douek, S. Killian, L.E. Hultin, D.D. Scripture-Adams, J.V. Giorgi, D. Marelli, R.A. Koup, J.A. Zack, Generation of functional thymocytes in the human adult, Immunity 10 (1999) 569–575.
[7] W. Savino, M.C. Leite-de Moraes, M. Hontebevrie-Joskowicz, M. Dardenne, Studies on the thymus in Chagas' disease. I. Changes in the thymic microenvironment in mice acutely infected with *Trypanosoma cruzi*, Eur. J. Immunol. 19 (1989) 1727–1733.
[8] V. Cotta-de-Alemida, A. Bonomo, D.A. Mendes-da-Cruz, I. Riederer, J. De Meis, K.R. Lima-Quaresma, A. Vieira-de-Abreu, D.M. Villa-Verde, W. Savino, *Trypanosoma cruzi* infection modulates intrathymic contents of extracellular matrix ligands and receptors and alters thymocyte migration, Eur. J. Immunol. 33 (2003) 2439–2448.
[9] W. Savino, M. Dardenne, C. Marche, D. Trophilme, J.M. Dupuy, D. Pekovic, N. Lapointe, J.F. Bach, Thymic epithelium in AIDS. An immunohistologic study, Am. J. Pathol. 122 (1986) 302–307.
[10] D.L. Sodora, J.M. Milush, F. Ware, A. Wozniakowski, L. Montgomery, H.M. McClure, A.A. Lackner, M. Marthas, V. Hirsch, R.P. Johnson, D.C. Douek, R.A. Koup, Decreased levels of recent thymic emigrants in peripheral blood of simian immunodeficiency virus-infected macaques correlate with alterations within the thymus, J. Virol. 76 (2002) 9981–9990.
[11] V.N. Brito, P.C.S. Souto, M.A. Cruz-Höfling, L.C. Ricci, L. Verinaud, Thymus invasion and atrophy induced by *Paracoccidioides brasiliensis* in BALB/c mice, Med. Mycol. 41 (2) (2003) 83–87.
[12] P.C.S. Souto, V.N. Brito, J. Gameiro, M.A. da Cruz Höfling, L. Verinaud, Programmed cell death in thymus during experimental paracoccidioidomycosis, Med. Microbiol. Immunol. 192 (2003) 225–229.
[13] W. Savino, The thymus is a common target organ in infectious diseases, PLoS Pathog. 6 (2006) 472–483.
[14] E. Seixas, D. Ostler, *Plasmodium chabaudi chabaudi* (AS): differential cellular responses to infection in resistant and susceptible mice, Exp. Parasitol. 110 (2005) 394–405.
[15] W. Jarra, G. Snounou, Only viable parasites are detected by PCR following clearance of rodent malarial infections by drug treatment or immune responses, Infect. Immun. 66 (1998) 3783–3787.
[16] R. Hong, The thymus: finally getting some respect, Chest. Surg. Clin. N. Am. 11 (2001) 295–310.
[17] A. Shanker, Is thymus redundant after adulthood?, Immunol. Lett. 91 (2004) 79–86.
[18] M. Ciofani, J.C. Zúñiga-Pflücker, The thymus as an inductive site for T lymphopoiesis, Annu. Rev. Cell. Dev. Biol. 23 (2007) 463–493.
[19] H.T. Petrie, J.C. Zúñiga-Pflücker, Zoned out: functional mapping of stromal signaling microenvironments in the thymus, Annu. Rev. Immunol. 25 (2007) 649–679.
[20] S. Nakazawa, *Plasmodium berghei* NK65: studies on the effect of treatment duration and inoculum size on recrudescence, Exp. Parasitol. 111 (1) (2005) 59–63.